Petrophysical characterization of sandstone reservoirs through boreholes E-S3, E-S5 and F-AH4 using multivariate statistical techniques and seismic facies in the Central Bredasdorp Basin


A Thesis in Petroleum Geosciences


By


HAAJIERAH MOSAVEL


Submitted in partial fulfillment of the requirements for the degree of Magister Scientiae in the Department of Earth Sciences, University of the Western Cape


MAY 2014


Supervised by Dr M. OPUWARI

Co-Supervised by Dr A. SIAD

# DECLARATION

I declare that Petrophysical characterization of sandstone reservoirs through boreholes E-S3, E-S5 and F-AH4 using multivariate statistical techniques and seismic facies in the Central Bredasdorp Basin is my own work, that it has not been submitted before for any degree or examination in any other university, and that all the sources I have used or quoted have been indicated and acknowledged by means of complete references.

Haajierah Mosavel
May 2014

_____
**Signature**

UNIVERSITY *of the*
WESTERN CAPE

**Petrophysical characterization of sandstone reservoirs through boreholes E-S3, E-S5 and F-AH4 using multivariate statistical techniques and seismic facies in the Central Bredasdorp Basin**

**Haajierah Mosavel**

# KEYWORDS

**Porosity**

**Permeability**

**Multivariate analysis**

**Factor analysis**

**Discriminant analysis**

**Cluster analysis**

UNIVERSITY *of the*
WESTERN CAPE

# ABSTRACT

The thesis aims to determine the depositional environments, rock types and petrophysical characteristics of the reservoirs in Wells E-S3, E-S5 and F-AH4 of Area X in the Bredasdorp Basin, offshore South Africa.

The three wells were studied using methods including core description, petrophysical analysis, seismic facies and multivariate statistics in order to evaluate their reservoir potential. The thesis includes digital wireline log signatures, 2D seismic data, well data and core analysis from selected depths.

Based on core description, five lithofacies were identified as claystone (HM1), fine to coarse grained sandstone (HM2), very fine to medium grained sandstone (HM3), fine to medium grained sandstone (HM4) and conglomerate (HM5). Deltaic and shallow marine depositional environments were also interpreted from the core description based on the sedimentary structures and ichnofossils.

The results obtained from the petrophysical analysis indicate that the sandstone reservoirs show a relatively fair to good porosity (range 13-20 %), water saturation (range 17-45 %) and a predicted permeability (range 4- 108 mD) for Wells E-S3, E-S5 andF-AH4.

The seismic facies model of the study area shows five seismic facies described as parallel, variable amplitude variable continuity, semi-continuous high amplitude, divergent variable amplitude and chaotic seismic facies as well as a probable shallow marine, deltaic and submarine fan depositional system. Linking lithofacies to seismic facies maps helped to understand and predict the distribution and quality of reservoir packages in the studied wells.

Multivariate statistical methods of factor, discriminant and cluster analysis were used. For Wells E-S3, E-S5 and F-AH4, two factors were derived from the wireline log data reflecting oil and non- oil bearing depths. Cluster analysis delineated oil and non-oil bearing groups with similar wireline properties.

This thesis demonstrates that the approach taken is useful because petrophysical analysis, seismic facies and multivariate statistics has provided useful information on reservoir quality such as net to gross, depths of hydrocarbon saturation and depositional environment.
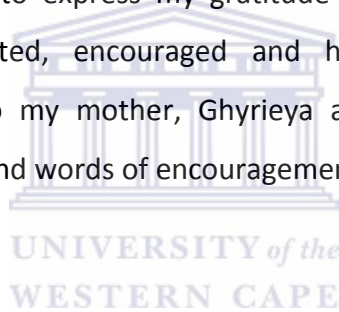
# ABBREVIATIONS AND ACRONYMS

**VSH OR VCLGR**      Volume of shale (%)

**GR**      Gamma ray log (API)

**RHOB**      Density log (g/c$^3$)

**NPHI**      Neutron log (dec)

**SW**      Water saturation (%)

**N/G**      Net over Gross

**m**      Meters

**SWSIM**      Simandoux water saturation

**SWJUH**      Juhasz water saturation

**PHIE**      Porosity (%)

**PREDICTED K**      Predicted Permeability (mD)

**T.D**      Total Depth

**SFLU**      Spherically Focused Log (ohm m$^2$/m)

**ILD**      Induction Log Deep (ohm m$^2$/m)

**MSFL**      Micro- Spherically Focused Log (ohm m$^2$/m)

**LLS**      Laterolog Shallow (ohm m$^2$/m)

**LLD**      Laterolog Deep (ohm m$^2$/m)

**SP**      Spontaneous Potential (mV)

# ACKNOWLEDGEMENT

# TABLE OF CONTENTS

# TABLE OF FIGURES

# LIST OF TABLES

UNIVERSITY *of the*

WESTERN CAPE

# CHAPTER 1

## 1.1 INTRODUCTION

The thesis comprises of three main parts, which is aimed at evaluating the reservoir potential of sandstone intervals of three wells in the Bredasdorp Basin using three different methods namely: petrophysical analysis, seismic facies and multivariate statistics. The interpretation of petrophysical parameters and seismic facies obtained from wireline logs and 2D seismic data respectively will predict the reservoir quality. Parameters such as volume of shale, porosity, water saturation, permeability and net to gross will be estimated using Interactive Petrophysics for selected reservoir intervals in all three wells. Wireline log data will be further used to identify oil and non-oil bearing depths from multivariate statistics using IBM SPSS Statistics.

The study area is in the Bredasdorp Basin (Fig.1.1), a rift sub-basin of the Outeniqua Basin located in the Indian Ocean offshore southern South Africa, southwest of Mossel Bay. Bredasdorp Basin covers about 18,000km$^2$ and contains a number of petroleum systems including the Oribi and Oryx oil fields, discovered by Petro SA in 1990 and 1988.

## 1.2 RESEARCH HYPOTHESIS

The purpose of this thesis is to verify that multivariate statistical analysis of petrophysical data, in combination with well data, is a useful tool for identifying reservoirs in the Bredasdorp Basin. Petroleum explorationists employ many tools including seismic and sequence stratigraphy, core analysis, 2D or 3D seismic, and petrophysical data to successfully identify prospective areas. This thesis will establish multivariate analyses of petrophysical data using cluster analysis, factor analysis and discriminant analysis to identify reservoirs as another useful tool for successful exploration programs. This is a first of its kind study in the Central Bredasdorp Basin, and the study is aimed to demonstrate that multivariate analytical approach can enable geoscientist to delineate reservoir potential contributing to a successful exploration program.
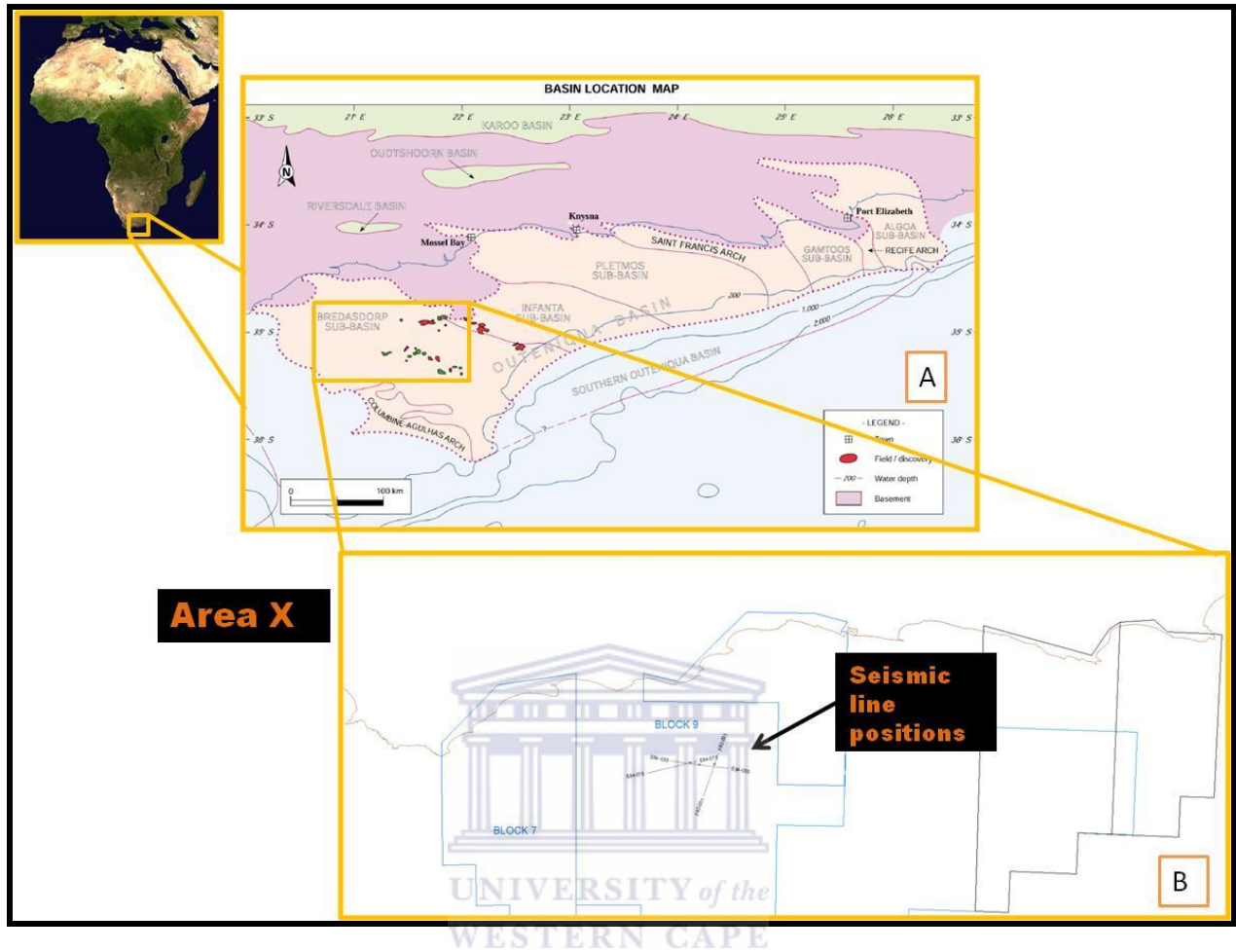
*Figure. 1.1. (A) Bredasdorp Basin location in the South Indian Ocean, offshore South Africa modified from IHS Energy (2010). (B) 2D seismic lines of the study area of Area-X used in this thesis.*

## 1.3 AIM & OBJECTIVES

This thesis has two main objectives. The first objective of the thesis is to determine the depositional environments and the different rock types present, through well log data and seismic facies. The second objective is to determine petrophysical characteristics of the reservoirs in the Bredasdorp Basin through wireline data, seismic facies and multivariate statistical analysis. Furthermore, the thesis aims to prove that multivariate statistical methods provides a quick, objective and reliable evaluation of logging units which should be considered for future studies and also that seismic facies has exploration significance for areas with no well controls.

# CHAPTER 2

## 2.1 GEOLOGICAL SETTING

Bredasdorp basin is one of a series of En echelon sub-basins of the Outeniqua Basin located off the southern coast of South Africa. It is bordered on the southwest and west by the Agulhas Arch and on the northeast by the Infanta Arch (Brown et al., 1995).

The southern offshore area indicates a strike slip movement during the Late Jurassic to Early Cretaceous breakup and separation of Gondwana (Petroleum Agency, 2010).
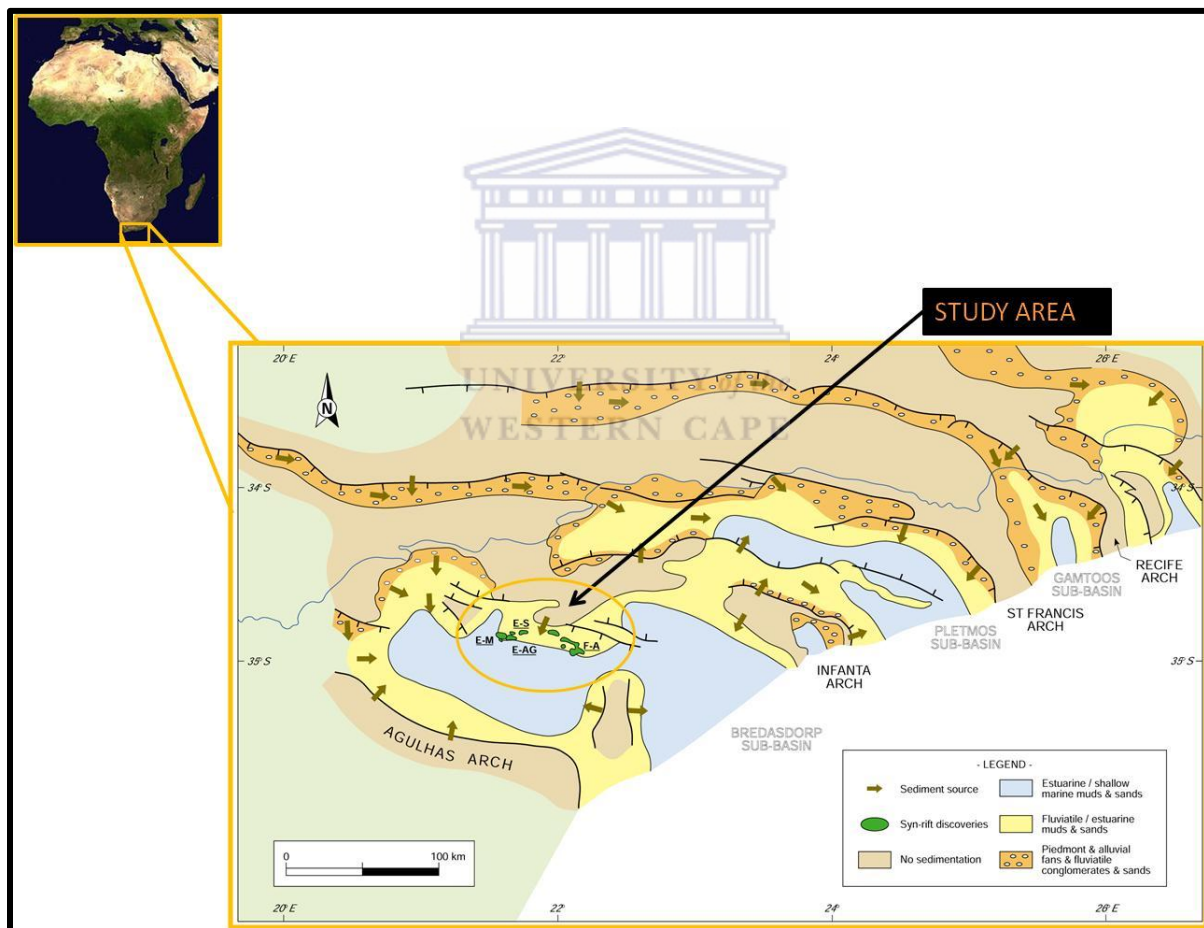


*Figure. 2.1. Map of study area in the Bredasdorp Basin on the South coast of South Africa (modified after IHS Energy (2010)).*

## 2.1.1 TECTONIC SETTING

Bredasdorp Basin is one of the rift sub- basins of the Outeniqua Basin, covering about 18,000km$^2$ and shows a south easterly trend rift. Three major tectonic stages can be recognized in the Bredasdorp Basin namely: Syn-Rift Stage, which comprises two Syn-rift episodes, Post-Rift/ Transitional Stage and Drift Stage (Broad et al., 2006).

The Syn-Rift Stage can be further divided into two phases; Syn-Rift I Stage and Syn- Rift II Stage.

Syn-Rift I Stage

Sedimentation started as early as Middle Jurassic and comprises four lithological units: the primary graben fill composed of claystone, conglomerates and sandstones deposited in alluvial fans and fluvial environments; Secondly the glauconitic fossiliferous sandstones of the lower shallow- marine unit which records the first transgression into the basin. Thirdly, the upper fluvial unit of meandering fluvial and alluvial floodplain deposits and the fourth unit with thick glauconitic fossiliferous sandstones of late Valanginian age (Broad et al., 2006) and shallow marine origin.
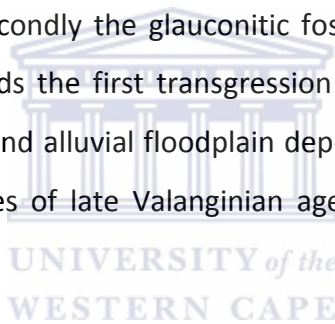
Syn-Rift II Stage

Comprises deep- water shales of Hauterivian age, which overlie tilted fault blocks and points out to a regional subsidence and widespread flooding (Broad et al., 2006).

Post-Rift/Transitional Stage

Sedimentation was affected by eustatic sea- level changes, tectonic events and thermal subsidence. The transitional phase is also described by episodes of aggradation and progradation. The transitional phase comprises of organic rich hydrocarbon source shales combined with porous and permeable sandstones (Broad et al., 2006).

Drift Stage

The drift phase is marked by the 14At1 mid- Albian unconformity. Deep- water submarine fan sandstones related with the 14At1 unconformity are important oil reservoirs. Sandstones of the 15At1 unconformity were the last sands deposited in the basin, with later sediments consisting of claystones and siltstones. During the Turonian a thin layer of organic- rich shales was deposited (Broad et al., 2006).
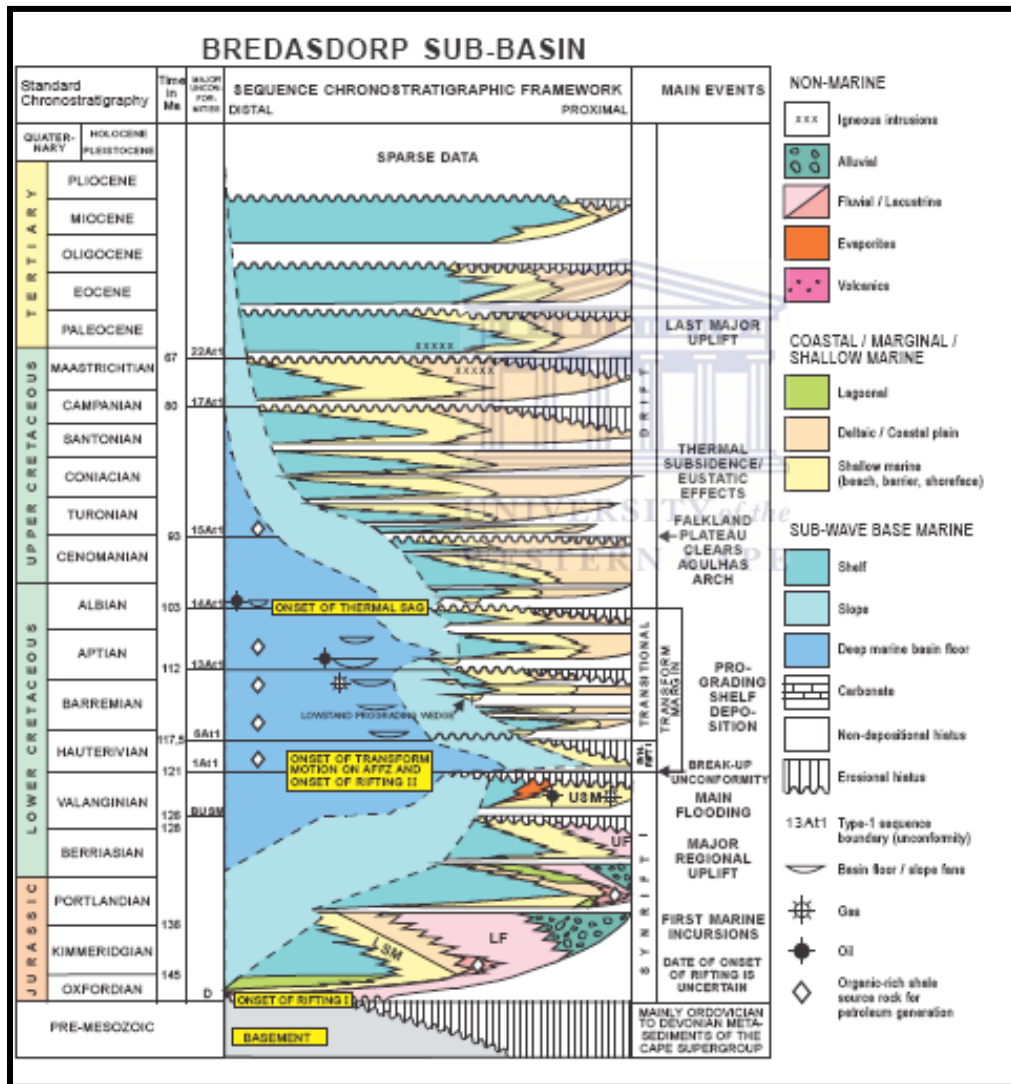


*Figure. 2.1.1.1. Chronostratigraphic and sequence stratigraphic diagram for the Bredasdorp Basin including supersequences and their corresponding ages (Petroleum Agency, 2010).*

## 2.1.2 DEPOSITIONAL SYSTEMS

The siliciclastic depositional environment of the Bredasdorp Basin developed from river dominated deltas and fan deltas to wave dominated deltas and related coastal systems. Simultaneously turbidite basin and slope systems to leveed slope and turbidite fans were formed. These changes occurred due to second order tectonic episodes, differences in sediment supply rates, accommodation rates plus increasing open- ocean processes. During the Barremian (117.5-112Ma) Age, river dominated deltaic and coastal systems prograded into the developed basin from north and northwest. After uplift and erosion occurred at 112Ma, the Bredasdorp Basin expanded during four succeeding Cretaceous subsidence events. The basin then became completely open to the circulation and wave energy of the Indian Ocean (Brown et al., 1995).
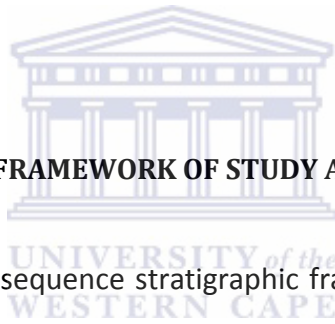
## 2.1.3 SEQUENCE STRATIGRAPHY FRAMEWORK OF STUDY AREA

Brown et al. (1995) established a sequence stratigraphic framework for the Bredasdorp Basin based on twenty-four basin wide sequence stratigraphic unconformities. The framework was made simpler considering six supersequences (Fig. 2.1.1.1&2.1.3.1) of third- and second-orders.
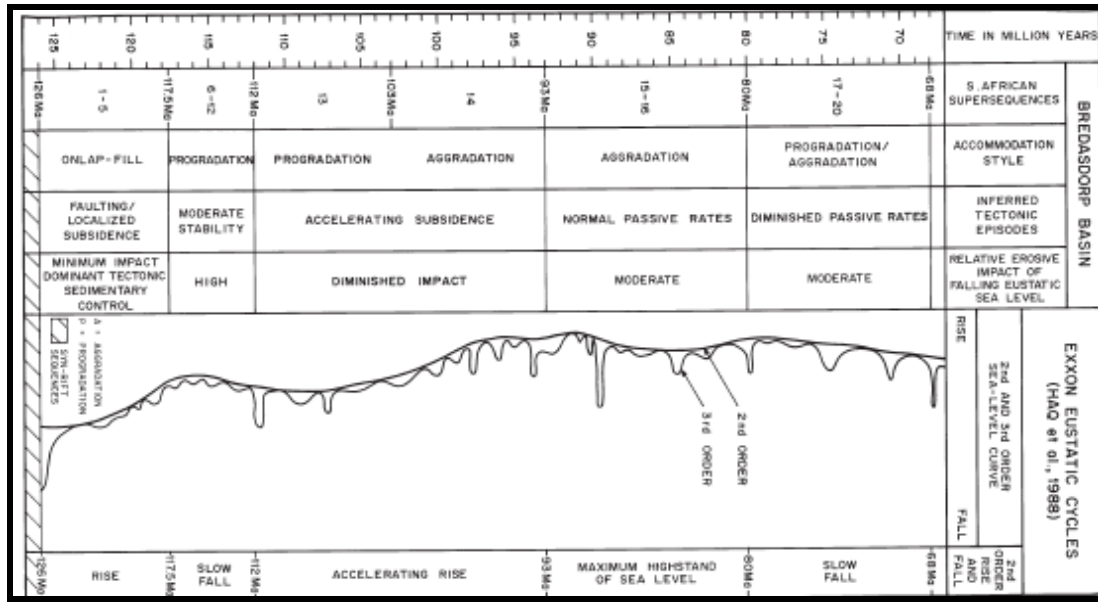
*Figure. 2.1.3.1. Six South African supersequences averaging ~10Ma duration each are bounded by type one unconformities. Exxon's supercycles (Haq et al., 1987, 1988) compared to the Post- rift Cretaceous history of Bredasdorp Basin.*

**Supersequence 1-5 (126- 117.5 Ma)**

Supersequence 1-5 (126–117.5 Ma) is described by sets of extremely aggradational third order composite sequences, which represent an older, incomplete supersequence set sitting on top of a rift to drift unconformity (Brown et al, 1995).

**Supersequence 6-12 (117.5- 112Ma)**

Supersequences 6-12 are described by sets of progradational third- order composite sequences, each consisting of progradational fourth- order sequence sets. Deposition occurred with fairly high subsidence that widen the basinal area and enhanced its contact with the proto- Indian Ocean. Deltaic systems prograded from the north across a fairly stable shelf to fault controlled hinge lines. Intensive erosion and deposition of well-developed lowstand systems resulted from lower subsidence rates of the third and fourth order cycles. Major uplift and severe erosion ended the supercycle (112Ma) (Brown et al., 1995).

**Supersequence 13 (112-103 Ma)**

The remaining third order sequence sets of the Cretaceous are Supersequences13, 14, 15-16 and 17-20. These third-order sequences are primary sequences composed of parasequence sets that indicate intensive erosion along second order type 1 unconformity 13At1 (112Ma), occurrence of a basin floor fan and slope fan within a lowstand depocenter (Brown et al., 1995).

**Supersequence 14 (103- 93Ma)**

During supersequence 14, deposition occurred during accelerating thermal decay subsidence rates. At this time (103-93Ma) the basin expanded and opened to the Indian Ocean in the southeast (Brown et al., 1995).

**Supersequence 15-16 (93-80Ma)**

The fifth post rift supersequence 15-16 was not studied in detail but some main deltaic systems shifted direction to enter the basin from the north and northeast (Brown et al., 1995).

**Supersequence 17-20 (80- 68Ma)**

According to Brown et al. (1995) supersequence 17-20 was not analyzed in the Bredasdorp Basin and is the lowest supersequence of an Upper Cretaceous lower Tertiary supersequence set.
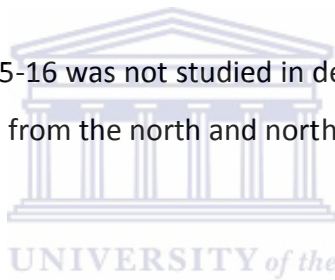
**2.1.4 HYDROCARBON COMPONENTS IN THE BREDASDORP BASIN**

<u>**Source rocks**</u>

Source rocks identified in the Bredasdorp Basin are of Aptian age, inside the Syn-rift and transitional rift- drift successions (Petroleum Agency SA, 2004/2005). The source rock is shale and deep marine sediments which can be more than 100m thick. Source rocks in the Bredasdorp Basin are mature over a large region.

**Reservoir rocks**

Reservoir rocks of Bredasdorp Basin are mainly shelf sandstones which are present in both the Syn-rift and drift stages. So the target areas, according to Broad (2004) include shallow marine to fluvial deposits, turbidite lobes and turbidite channels.

**Seal and traps**

Seal is an impermeable rock that blocks upward movement of oil and gas. Marine shales of the drift stage act as the main seals however Syn-rift seals also exist in the form of non-connecting faults of tilted and faulted blocks.

There are two types of oil and gas traps in the Bredasdorp Basin. Those controlled by geological structure as folding or faulting (structural traps) and those controlled by the stratigraphical position of the porous and non-porous sections (stratigraphical traps) (Lapidus, 2003). Structural traps, such as drape anticlines, tilted blocks and inversion related closures were common during the Syn-rift stage (Petroleum Agency of SA, 2004/2005). Stratigraphic traps include inversion closures and pinchouts (Petroleum Agency of SA, 2004/2005).
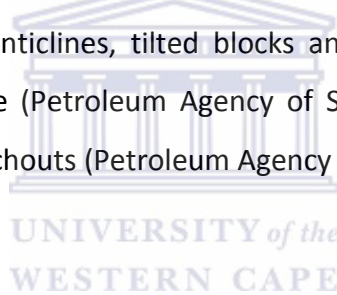
# CHAPTER 3

# METHODOLOGY

## 3.1 INTRODUCTION

Three techniques were used to characterize reservoir zones of Area X in the Bredasdorp Basin, which are outlined in this chapter with further details presented in the respective Appendices. Figure 3.1 presents the flow chart of the whole research process undertaken in this thesis. The software used for this thesis was Interactive Petrophysics, Kingdom Suite and IBM SPSS Statistics.

## 3.2 PETROPHYSICAL ANALYSIS

In order to assess the petrophysics of the study area, basic petrophysical parameters such as volume of shale, porosity, water saturation and predicted permeability were calculated for reservoirs identified using Interactive Petrophysics (IP) software. Depositional environments were interpreted for intervals of interest from the gamma ray log and from core data.

Conversion of digital logs to readable format, environmental correction, correlation of wells, porosity and water saturation are detailed in Appendix 1.

**Volume of shale**

Volume of shale (Vsh) was derived from the gamma ray log. The following linear equation was then used to determine the volume of shale:

$$Vsh = \frac{Grlog - Grmin}{Grmax - Grmin}$$

Where

Grlog= gamma ray reading for each zone (API)

Grmin and Grmax are the minimum (clean sand) and the maximum gamma ray value (shale)

If Vsh was less than 10% it would indicate a clean zone, if Vsh is from 10 to 35% it is a sandy shale zone and greater than 35% it is a shaley zone.

**Porosity**

Porosity of the selected reservoirs was determined from the density (RHOB) and neutron (NPHI) logs.

Porosity from density log (ΦD) is given as:

$$\frac{Pma - Pb}{Pma - Pf}$$

Where

$P_{ma}$= matrix density (g/cc)

Pb = fluid density of the mud filtrate (g/cc)

Pf = fluid density (g/cc); salt mud = 1.1 and fresh water = 1.0 g/cc
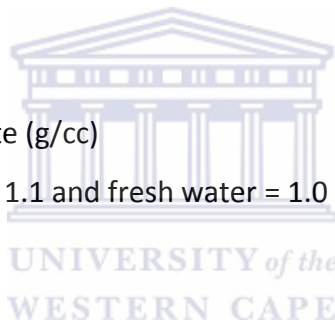
**Water saturation**

In a hydrocarbon bearing reservoir, the void spaces are partly occupied by formation water and remaining volume by hydrocarbon (Gluyas and Swarbrick, 2004). The resistivity of a hydrocarbon reservoir is a function of the formation factor (F), the Resistivity of formation water (Rw) and its water saturation (Sw).

Using Archie's equation, water saturation (Sw) for hydrocarbon bearing reservoir is defined as

Sw = [F * (Rw / Rt)] $^{0.5}$

Φ= A F $^{-M}$

Where

A= empirical constant specific to the rocks of the area of interest

M= cementation factor

Φ= porosity

**Predicted permeability**

To calculate the predicted permeability (K) a regression equation from core porosity and core permeability is required. A scatter plot of core porosity versus core permeability was generated to find the best regression equation, with $R^2$ close to one (Appendix 2).

**Net Pay**

A porosity cut- off of 10% (Appendix 7) was used along with a shale volume cut- off of 22.25% to define the reservoir quality. The water saturation cut- off value of 56.50% was used. Reservoirs were defined by the porosity greater than 10% and shale volume less than 22.25%. A reservoir was considered hydrocarbon rich, if the water saturation within the reservoir was less than 56.50%.

## 3.3 SEISMIC FACIES

2D seismic lines of the continental shelf of Bredasdorp Basin were used to identify seismic facies using SMT Kingdom software. The net to gross ratio (Appendix 3) was calculated for each seismic facies in order to identify intervals of interest and compare them with the petrophysical results.

Well log depth conversion to seismic data, horizons of interest and correlating well log with seismic facies, are detailed in Appendix 4. This section documents the reservoir patterns which were used to predict the distribution and quality of reservoir packages.

## 3.4 CORRELATION ANALYSIS

Correlation analysis estimates the range of the relationship between any pair of variables and displays them as a matrix. The relationship between the two variables is measured by the

covariance and determined by the variability of each of the two variables (Reimann et al., 2008). Covariance can take the form of any number however the strength of the relationship between the variables should be considered (i.e. + or -).

The linear relationship between two variables is measured by the correlation coefficient. The most common methods used to determine a correlation coefficient are the Kendall, Pearson and Spearman correlation (Galton, 1890; Kendal, 1938; Spearman, 1904). These methods conclude a number between -1 and +1 that indicates how close the variables are linked. The correlation coefficient is independent from the units of measurement. A value of the correlation coefficient near zero indicates little correlation between variables while a value near +1 or -1 indicates a high level of correlation (Reimann et al., 2008). This means when two variables have a positive correlation coefficient, an increase in the value of one variable indicates a likely increase in the value of the second variable while a negative correlation would mean the opposite. In the case where the correlation coefficient is 0, then the two variables are not correlated or no systematic relationship exists between the two variables.

Four variables (Gamma ray, Resistivity, Neutron and Density logs) from the wireline logs were analysed to determine if there is any significant relationship that exist using bivariate correlation method with Pearson correlation coefficient and a two-tailed test of significance in IBM SPSS Statistics 21 (IBM) whereby a similar approach was taken by Stuck et al (2013).

## 3.5 MULTIVARIATE STATISTICS

Two multivariate techniques namely Factor analysis with discriminant analysis and Cluster analysis with discriminant analysis were carried out in this thesis to determine oil bearing and non-oil bearing depths, to compare the results and determine which one is most efficient. The statistical methods were performed with IBM SPSS software version 21.0 (IBM SPSS Statistics, 2013).

### 3.5.1 FACTOR ANALYSIS

With factor analysis, interrelationships among a set of variables (GR, SFLU, SP, NPHI, RHOB, ILD and MSFL) were examined. This technique is used to derive a subset of uncorrelated variables called factors that explain the variance in the original observational data set without losing important information (Sharma et al., 2012). The analysis reveals structure in the data set by identifying which observations are mostly correlated.

With this analysis, the original data set is reduced, resulting in two or three factors that account for nearly all the variance in the original data set. Visualization of two or three factors is much simpler than visualization of the entire data set (Bucker et al., 2000).

A series of methods exist for carrying out factor analysis. Principal component analysis method was used to explain as much information contained in the data in as few components as possible (Reimann et al., 2008).The first principal component contains the maximum variability and the second principal component has to be orthogonal to the first component and will contain the maximum amount of remaining data (Reimann et al., 2008). The same principal is kept for the succeeding principal components, whereby they must be orthogonal to the previous component and contain the maximum of the remaining variability.

With factor analysis, the first step was to compute a correlation matrix. The second step was calculating factors and factor loadings from the standardized logging curves using principal component analysis. Varimax with Kaizer Normalization factor rotation (Davis, 1986) was applied because the matrix of factor loadings is often not unique or easily explained. The final step was interpreting factors by factor rotation. A factor is taken as being important for an underlying property, if its Eigen value is greater or equal to one. Factors with Eigen values less than one account for less variation than one of the initial variables (Bucker et al., 2000).

In this thesis, the factor scores were obtained using the regression method (Johnson & Wichern, 2007). The aim of factor analysis in the thesis was to spot intervals that are oil prone and to generate training depth samples for oil bearing and non-oil bearing depths which were characterized using discriminant analysis. (The interested reader can consult Appendix 5 for

further details).

## 3.5.2 CLUSTER ANALYSIS

Cluster analysis is an exploratory data analysis tool for organizing data into clusters or groups. The main aim of cluster analysis is to separate a number of observations or measured variables like resistivity or density into groups that are similar in their characteristic or behaviour (Reimann et al., 2008).

Cluster analysis differs from factor analysis in a way that the latter uses the correlation matrix (*see* section 3.*4 of this chapter*) for reducing the original data set while the former uses the distance measure to assign variables to a number of groups. Hence cluster analysis has no prior knowledge about which sample belongs to which group. Hierarchical Q mode clustering was applied in this thesis, with the use of Ward method together with Squared Euclidean distance (Ward, 1963). Hierarchical clustering is based on the idea of samples being more related to nearby samples than further away. This method connects samples to form clusters based on their distance. A cluster dendrogram is used to determine the number of groups or clusters as well as the memberships of the variables in those groups. In a dendrogram, the x-axis marks the distance at which the clusters merge, while the samples are placed along the y-axis such that the clusters don't mix. Squared Euclidean distance helps determine the best number of clusters compared to simple Euclidean distance in order to place weight on objects that are further apart.

The wireline log data were standardized (z scores) prior to clustering, which allows one to compare different variables expressed in different units of measurement, and the Ward Linkage was used as the hierarchic agglomerative cluster algorithm. (The interested reader can consult Appendix 6 for further details).

The groups created through Cluster Analysis were then verified and characterized using discriminant analysis. The combination of cluster and discriminant analyses depends upon

grouping samples data through cluster analysis and later characterizing them using discriminant analyses (Siad et al., 1994).

A similar approach was taken by Bucker et al (2000) using both factor and cluster analysis to identify chemical and physical properties of wireline logs.

### 3.5.3 DISCRIMINANT ANALYSIS

Discriminant analysis requires previous classification of data into relatively homogenous subgroups whose characteristics can be described by the statistical distributions of the grouping variables associated with each subgroup (Siad et al., 1994). The classification was performed by defining the distinct groups based on the unique characteristics of wireline log measurements such as water and oil bearing lithologies (Sharma et al., 2012). Due to the training dataset not being easily obtained, methods like factor analysis and cluster analysis were used to classify the training data set. In this study, a group of oil and none oil bearing functions were determined by distinct wireline logs defined in the model based on factor and cluster analysis using the created training dataset. The aim of using discriminant analysis was to verify and differentiate oil bearing from non-oil bearing training samples from Wells E-S3, E-S5 and F-AH4.

### 3.5.3.1 LINEAR DISCRIMINANT ANALYSIS

Linear discriminant analysis and the related Fisher's linear discriminant are methods used in statistics to find a linear combination of features which characterizes two or more classes of samples (Reimann et al., 2008). The resulting combination may be used for dimensionality reduction before later classification.

In this thesis, linear discriminant analysis uses previously defined training sets from both factor and cluster analysis, which represents oil and non-oil bearing groups. From the multivariate observations that make up these training sets, a number of discriminant functions are derived,

one per defined class. The discriminant function makes it possible to classify any new observation obtained either as oil bearing or non-oil bearing based on the wireline log properties. On the other hand, misclassifications are also possible yet discriminant analysis tries to keep the misclassifications low. The discriminant functions are defined as follows:

$$D = v_1 X_1 + v_2 X_2 + v_3 X_3 \ldots v_i X_i + a$$

Where

D = discriminate function

v = the discriminant coefficient or weight for that variable

X = respondent's score for that variable

a = a constant

i = the number of predictor variables

### 3.5.3.2 STEPWISE DISCRIMINANT ANALYSIS

Stepwise discriminant analysis selects the most important variables while retaining the highest discrimination power possible. When using this method variables are selected through Wilk's Lambda classification to determine the order in which they are included (entered/removed) in the analysis. At each step, the wireline log that yielded the best classification was entered.

The linear regression method followed whereby the highest correlated independent variable was added followed by successive variables to determine the percentage of group separation of oil and non- oil bearing depths. Once an independent variable is in the regression equation, a highly correlated variable assumes decreased significance and has only a minor effect on a multiple correlation coefficient (Siad et al., 1994).

The results for both statistical techniques (1- Factor analysis with discriminant analysis and 2- Cluster analysis with discriminant analysis) were then compared using scatter plots to check whether the results complement or contradict each other.
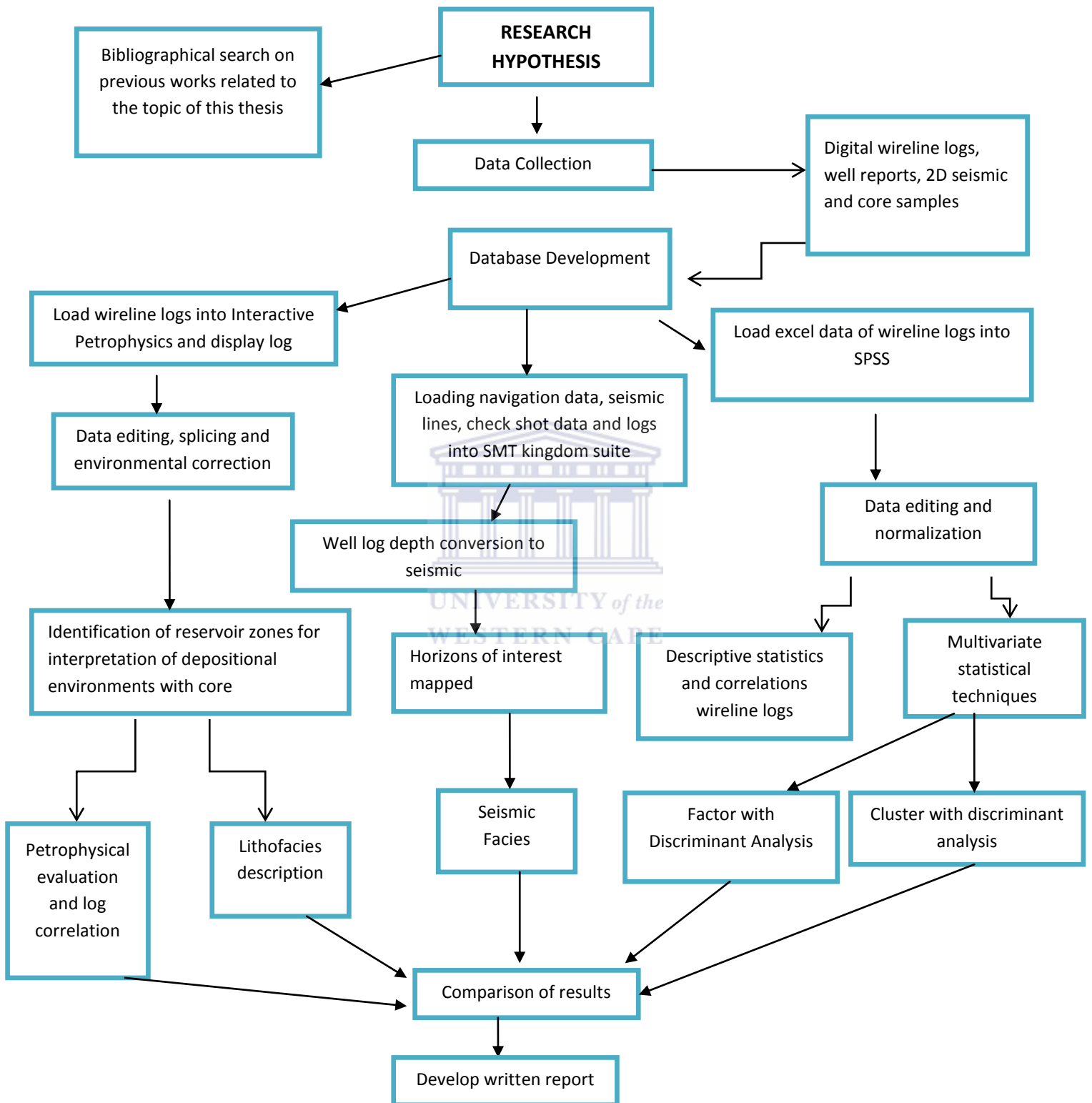
*Figure. 3.1. Flow chart of research methodology*

# CHAPTER 4

# RESULTS

## 4.1 DEPOSITIONAL ENVIRONMENTS FROM LOG SHAPES CORROBORATED WITH CORE DATA

The shape of well log curves are evidence of certain trends of the depositional environments the same way the vertical sedimentary sections do. The patterns include bell-shaped, funnel-shaped and cylindrical profiles. Shapes and descriptions were analyzed based on gamma ray log shapes.
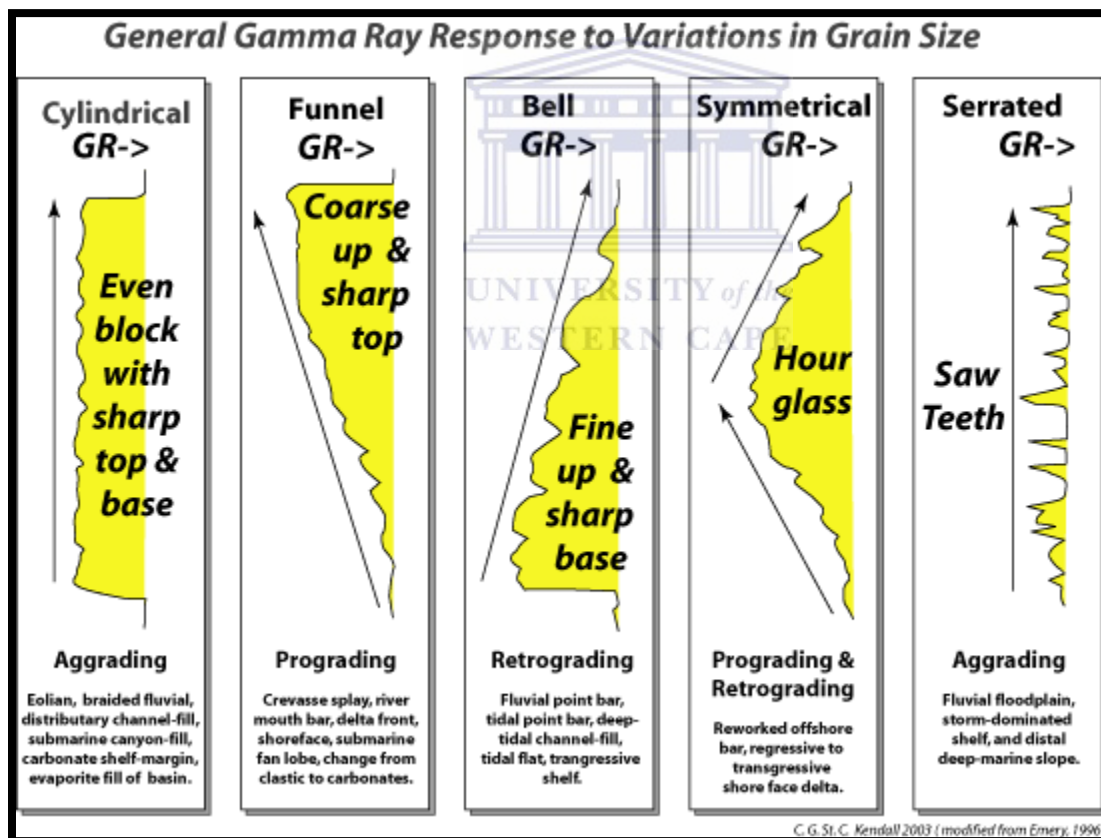


*Figure. 4.1.1.General gamma-ray response to variations in grain size (Ulasi et al., 2012)*

**WELL E-S3**

Depositional environments of areas of interest have been interpreted from core (Fig. 4.1.2) however, some areas had uncored well sections and were interpreted based on lithology descriptions, gamma ray log and shape profiles.
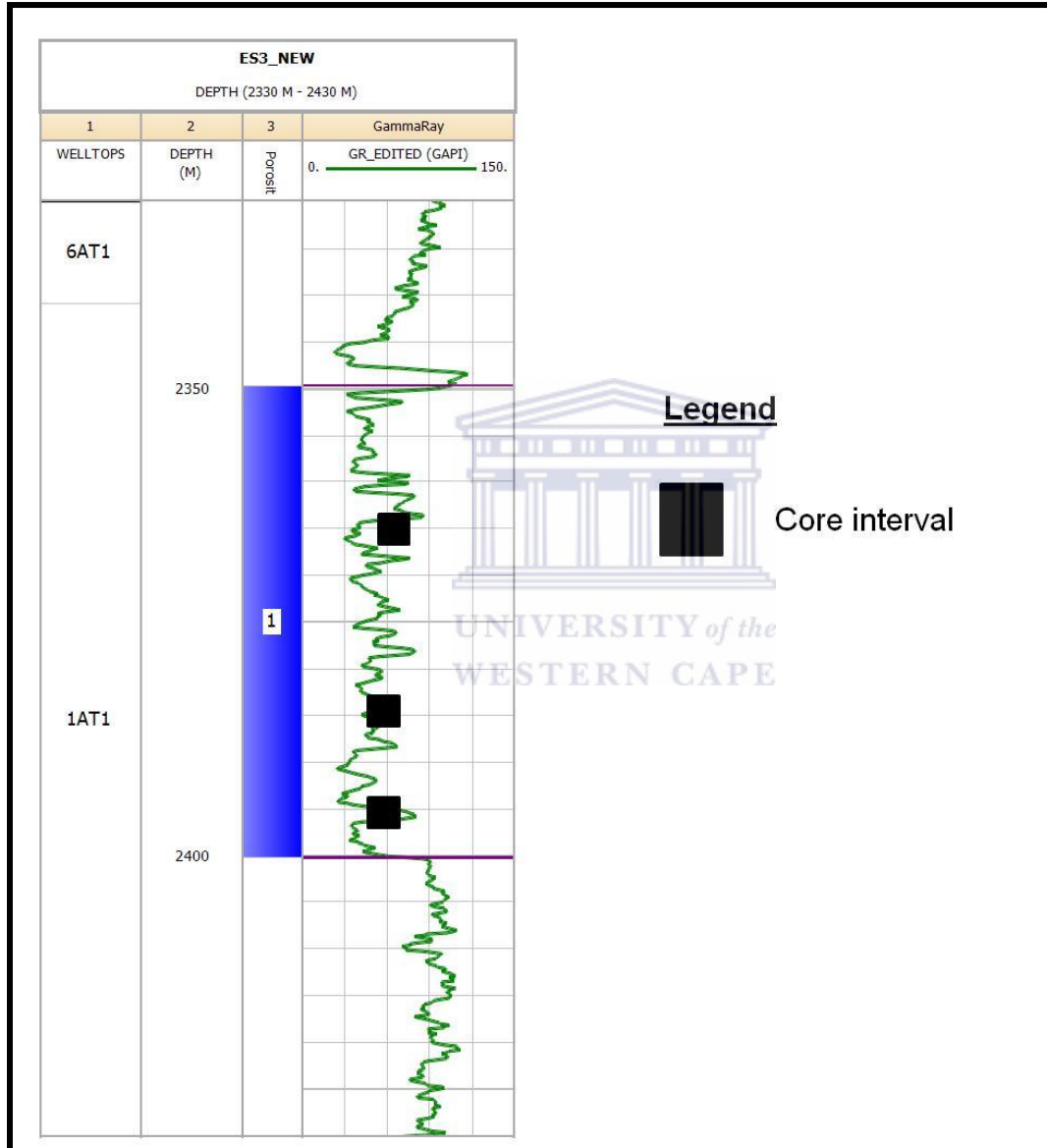


*Figure. 4.1.2.Well E-S3 (Gamma ray log, well top surfaces +core intervals).*

Core depth 2395.5 - 2394.5m (Fig.4.1.3) is an argillaceous 1m cross-bedded conglomerate layer containing pebbles of sandstone and claystone that are greenish grey in colour and well

rounded. This conglomerate is probably a deposit of a distributary channel cutting through the upper part of a delta front deposit.
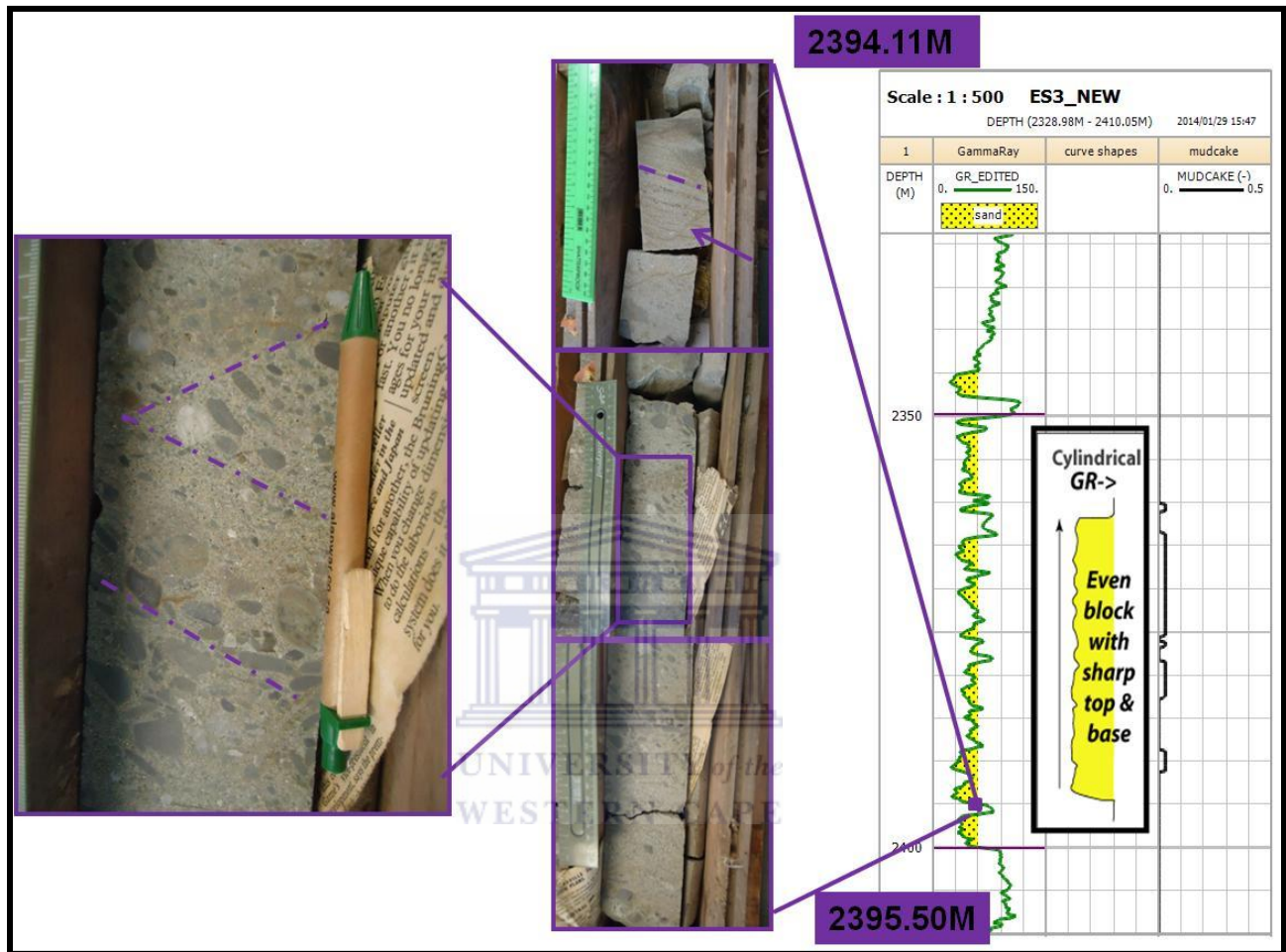


*Figure. 4.1.3. Illustration of core from depth 2395.5-2394.11m (pen=136mm). Syn-sedimentary fault (arrow) and trough cross- bedding (dash lines) appear.*

At 2391.73m (Fig.4.1.4), a syn-sedimentary normal fault is present possibly due to rapid deposition and instability in the sedimentary environment. At a depth of 2392.56 - 2391.0m (Fig.4.1.4) the sandstone is compacted, white to light greenish grey in colour and medium grained, well sorted and grains are rounded. Syn-sedimentary faults and trough cross- bedding are common in environments which have rapid deposition of high amount of sediment on top of the slope, such as deltas (particularly delta front).
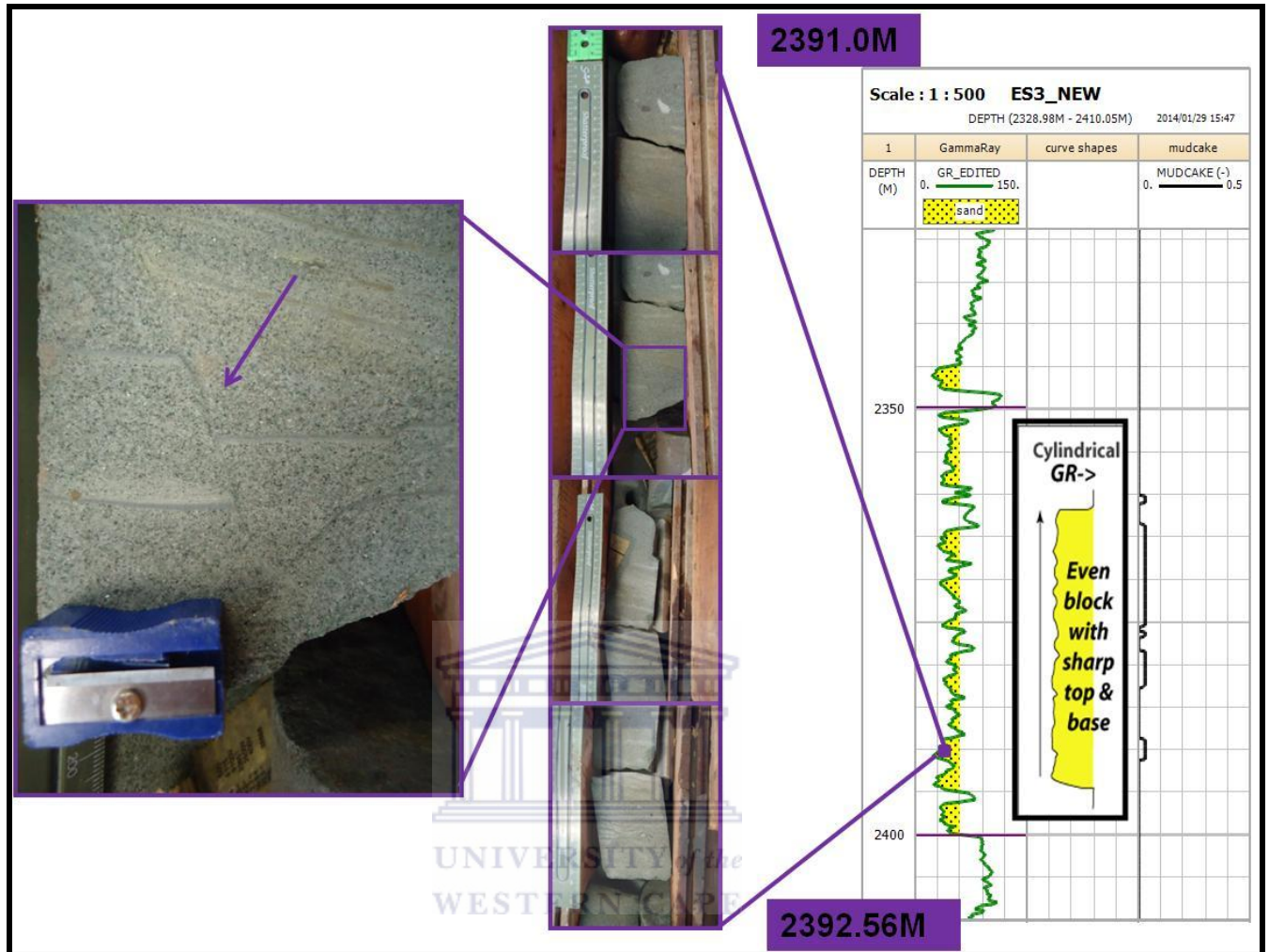
*Figure. 4.1.4. Illustration of core from depth 2392.56- 2391.0 (Sharpener= 26mm). Syn-sedimentary fault appear (arrow).*

Core depth 2384.90 – 2384m (Fig.4.1.5) interval comprised of sandstone that is well sorted, medium to fine grained, well rounded with cross-bedding. Core depth 2366.92 - 2366.45m (Fig.4.1.6) interval comprised of sandstone that is tight to slightly porous, very fine grained, very well sorted, well rounded grains and light grey in colour. The sandstone is apparently trough cross-bedded. Core depth 2366.45 - 2329.3m comprised of thick sandstone medium to coarse grained and slightly glauconitic.

The cylindrical shape indicated by the gamma ray log has a low reading with sharp borders and no internal change. Based on the gamma- ray log signature (cylindrical shape) as well as the

core study, a delta was identified. Friedman and Sanders (1978) stated that deltas are associated with subsiding regions, where rivers deposit their sediment load and thus may be able to aggrade as well as prograde depending on the accommodation space. Therefore core depth 2400 - 2350m suggests a possible fluvial deltaic environment and reservoir.
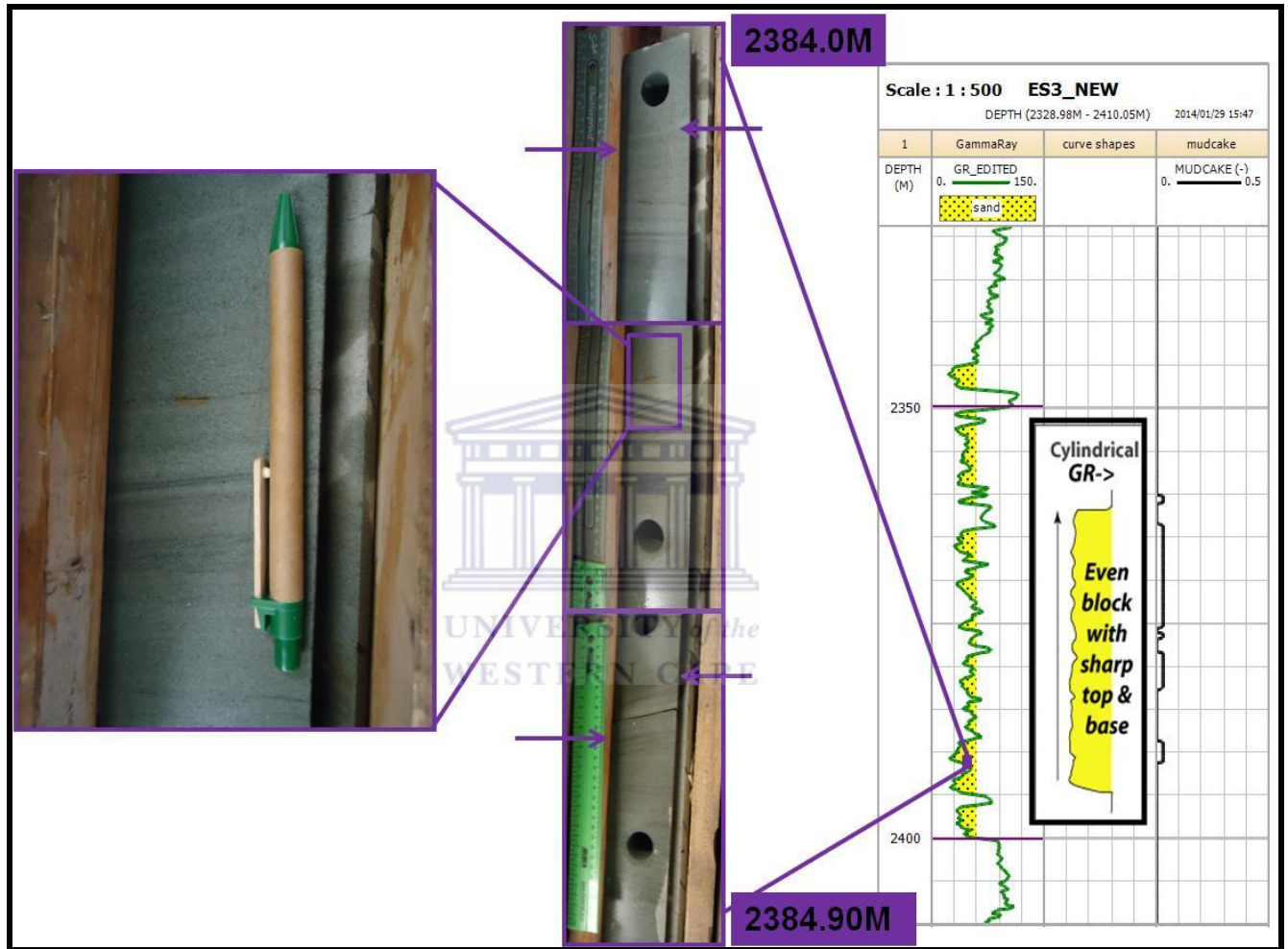


*Figure. 4.1.5. Illustration of core from depth 2384.9- 2384.0m (pen= 136mm). The arrow points out trough cross-bedding in medium to fine sandstone.*
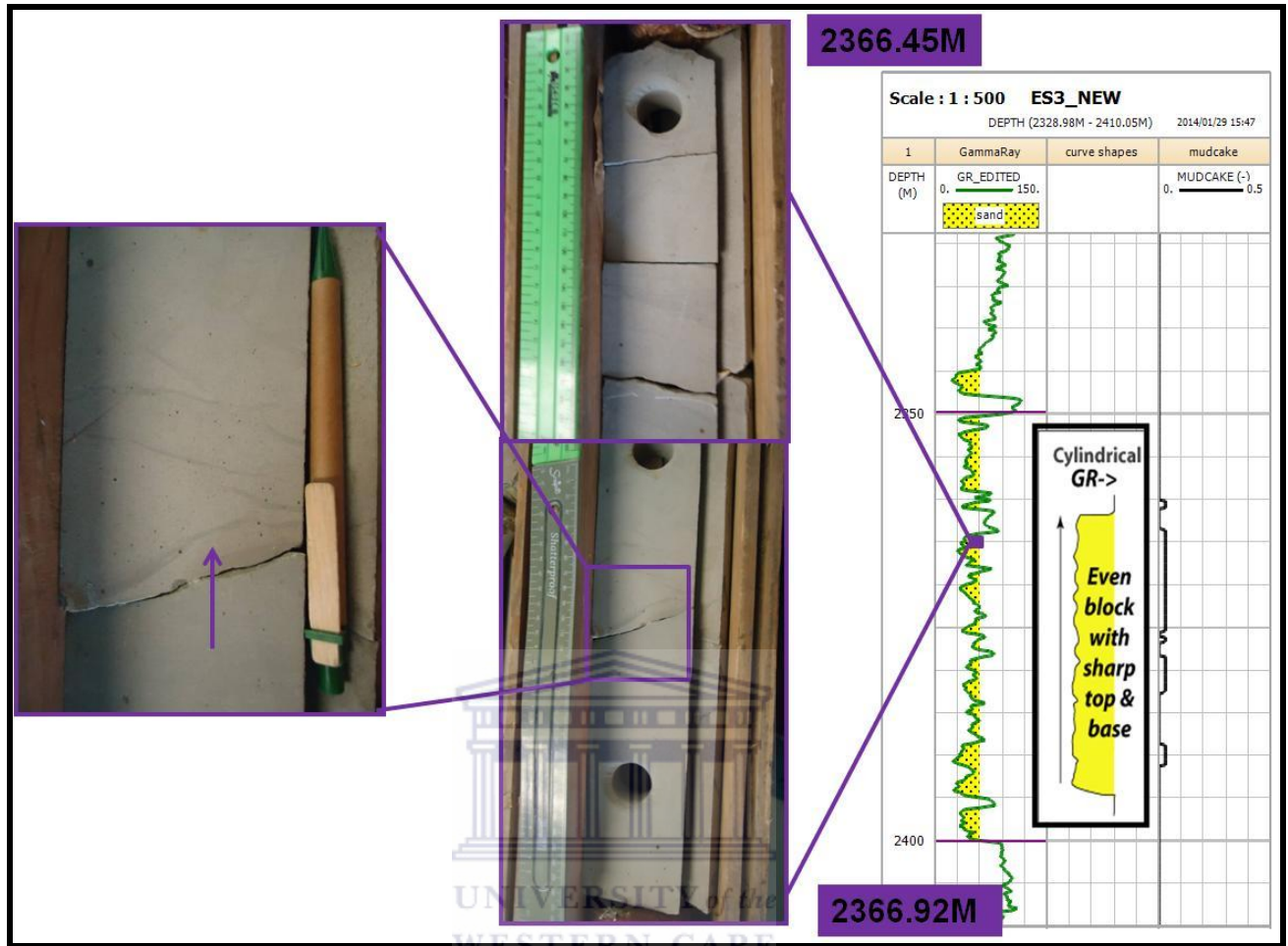
*Figure. 4.1.6. Illustration of core from depth 2366.92- 2366.45m (pen= 136mm), the arrow points trough cross- bedding in sandstone.*

Core depth 1933 - 1895m (Fig. 4.1.7) comprised of three coarsening- upwards sandstone bodies. Claystone, the first body (1933 - 1925m), was medium grey and dark grey in colour in the lower section. The dark grey claystones are very carbonaceous and showed no fluorescence, however they show a yellowish white crush cut. Core depth 1933 - 1925m displays a bell shape representing a gradual upward increase in gamma ray reading. This trend reflects an upward fining sequence, i.e. change from sand to shale indicating a decrease in depositional energy. In a shallow marine setting, this trend usually reflects an upward deepening and a decrease in depositional energy which could point out to a possible transgressive shelf environment.The second sandstone body (1915 - 1910m) was grading

upwards from claystone to siltstone that was medium light- grey in colour, calcareous, soft to firm and coarsening upwards to sandstone.
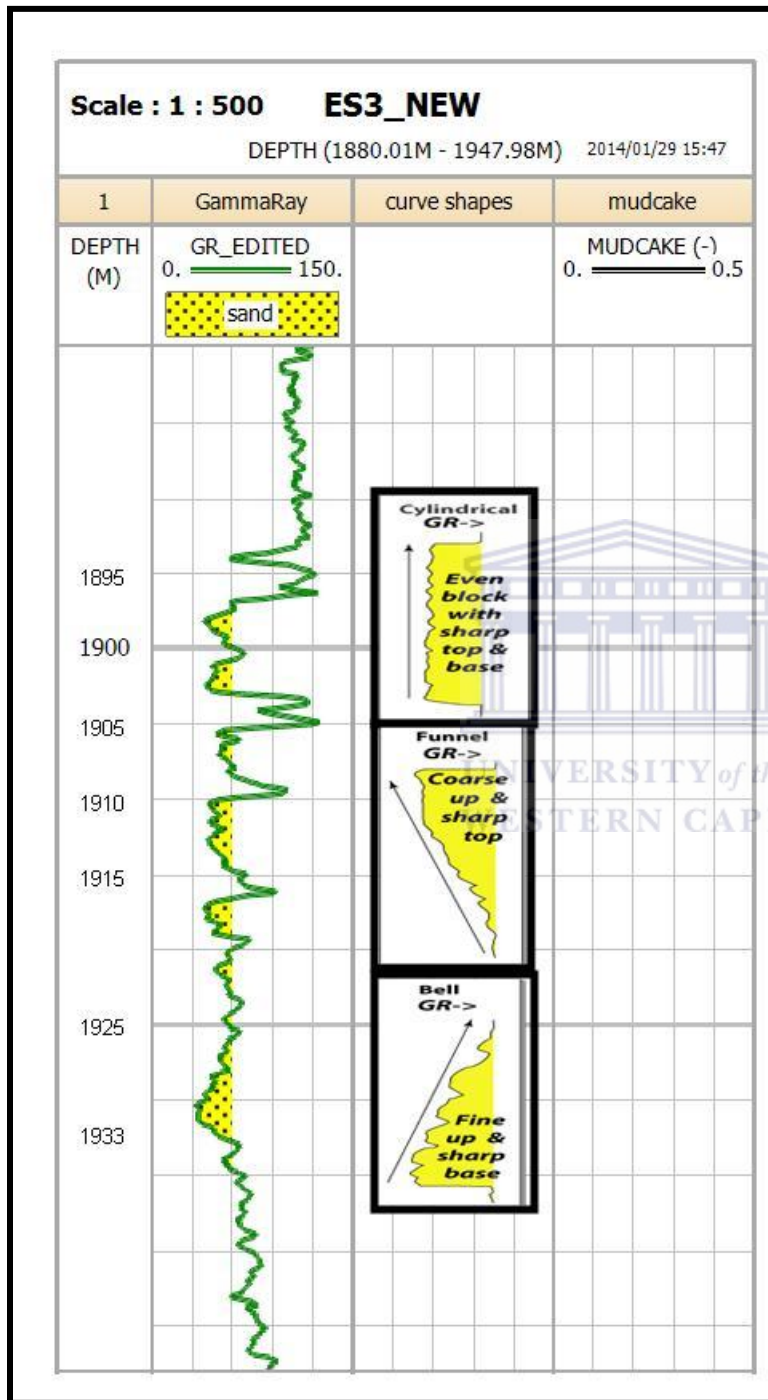


*Figure. 4.1.7.Illustration of gamma ray log from depth 1947.98-1880.01m.*

From a depth of 1915 - 1910m, the gamma ray displays a funnel shape indicating a coarsening-upwards trend (Fig.4.1.7). In a shallow marine environment, this trend reflects an upward increase in depositional energy probably due to the progradation of nearshore bars/ shallow marine deposits (Fig.4.1.8). The third sandstone body (1905 - 1895m) was tight to slightly porous, white to light grey in colour, very lignitic, fine to very fine grained and very well sorted. Core depth 1905 - 1895m shows a cylindrical shape, which signifies, that sands are aggrading. This trend together with the sedimentary facies point out to be possible shallow marine-foreshore to upper shoreface environment (Fig.4.1.8).Core was not available for depth 1933 - 1895m interval and is not a permeable zone as no mud cake is present and therefore not a possible reservoir. (*Core description courtesy of Petroleum Agency of SA*).
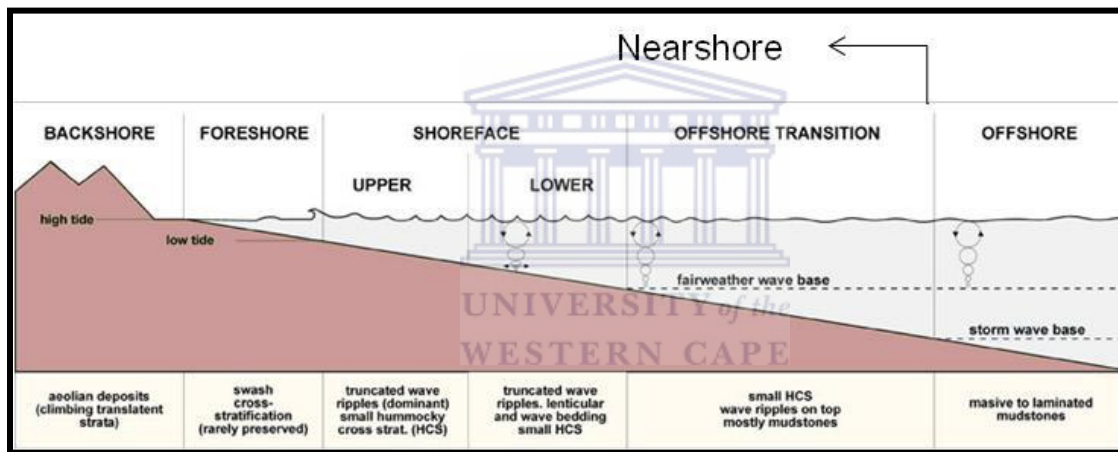


*Figure. 4.1.8. This is a typical shoreface profile (http://www.searchanddiscovery.com/abstracts/html).*

**WELL E-S5**

Depositional environments of areas of interest have been interpreted based on lithology descriptions, gamma ray log and shape profiles as no core was available for the area of interest identified. Core was only available from a depth of 2414m (Fig. 4.1.9) which ranged outside the area of interest.

*Figure. 4.1.9.Well E-S5 (Gamma ray log, well top surfaces +core interval).*

Core depth 2416.20 - 2415.37m (Fig.4.1.10) interval comprises of sandstone and conglomerate. The sandstone was grey in colour, poorly sorted, subrounded and very coarse grained. Core from depth 2416.20 - 2415.37m is interpreted as a channel deposit.
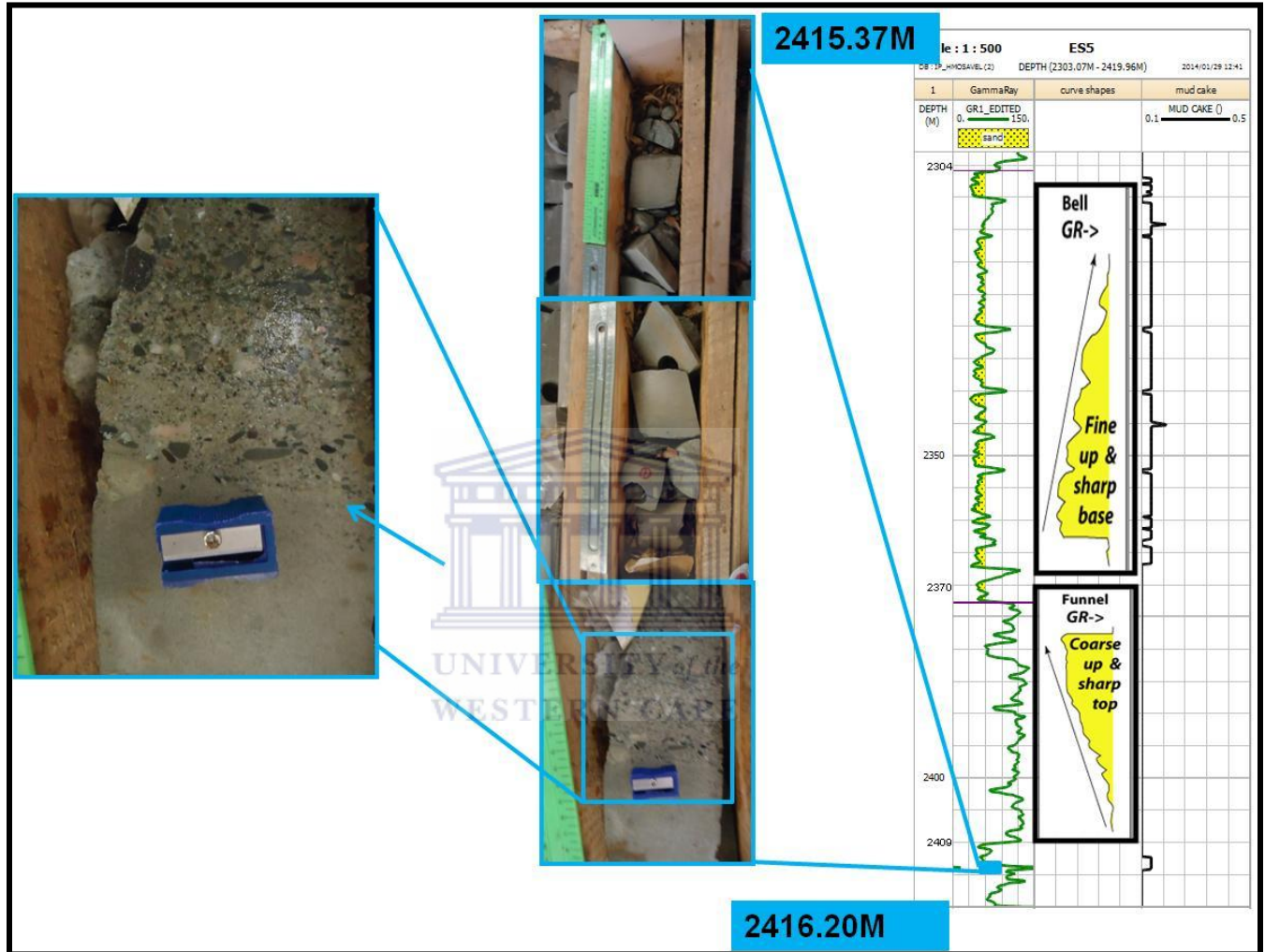


*Figure. 4.1.10. Illustration of core from depth 2416.20- 2415.37m (sharpener= 26mm). The arrow points the channel base.*

Core depth 2415.37 - 2414m (Fig.4.1.11) interval comprises of sandstone light grey in colour, medium grained, well rounded, very well sorted with convolute lamination. Convolute lamination can be related with deformation of water embedded sediment due to rapid deposition and compaction/overloading (S. Lanes, 2013, personal communication).
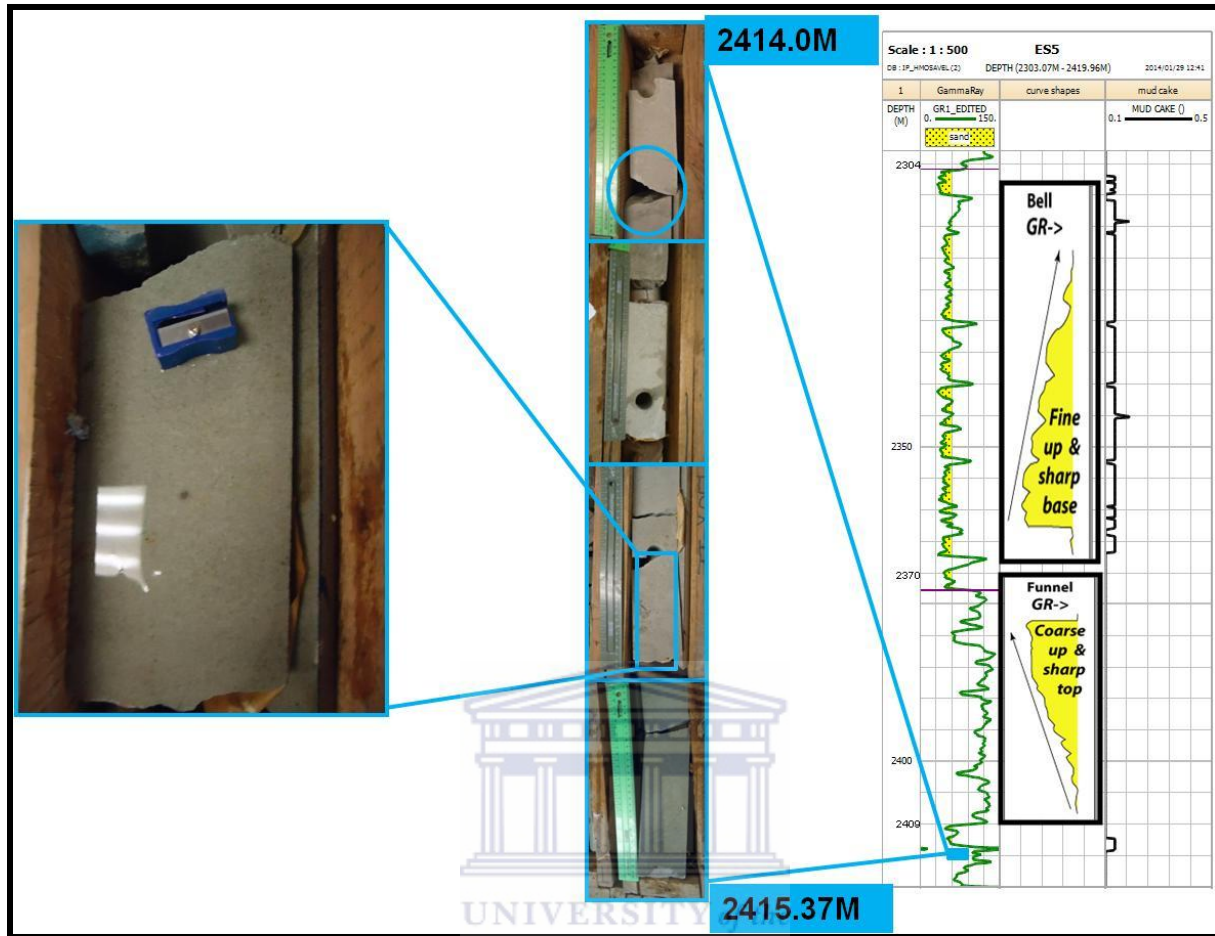
*Figure. 4.1.11. Illustration of core from depth 2415.37- 2414.0m (sharpener = 26mm). The oval shape points convolute lamination.*

Core depth 2409 - 2304m (Fig.4.1.11) is a continuous succession of claystone being silty at the base with minor traces of sandstone. The claystone ranged between dark grey, to brown and olive grey colour and slighlty carbonaceous and glauconitic. From a depth of 2409 - 2370m, thin beds of green claystone grades into sandstone indicating a coarsening- upwards trend (funnel shape). In a marine environment this trend reflects an upward increase in depostional energy probably due to the progradation of a delta front. Core depth 2370 - 2310m interval comprises of a 60m tight medium to fine grained sandstone bed with traces of green lithology in it grading to siltstone. The siltstone contains rare orange and green litholoclasts, which grades into claystone at depth 2304m indicating a fining- upwards interval (bell shape). In a marine setting,

this trend usually reflects an upward deepening and a decrease in depositional energy which could point out a possible channel.Core depth 2370 - 2305m depth is a possible reservoir as the presence of a mudcake indicates a permeable zone. (*Core description courtesy of Petroleum Agency of SA*).

Core depth 1930 - 1850m (Fig.4.1.12) the base comprised of 30 - 40m tight, very fine sandstone layer. Above this, a continuous medium grey soft, sticky claystone grading upwards into sandstone beds. Core depth 1915 - 1903m indicates a cylindrical shape, which has a low gamma ray reading with sharp borders and no internal change. Core depth 1889 - 1875m indicates a bell shape, which represents a gradual upward increase in gamma ray reading. This trend reflects an upward fining sequence, i.e. change from sand to shale indicating a decrease in depositional energy. In a shallow marine setting, this trend usually reflects an upward deepening and a decrease in depositional energy. Based on the literature review core depth 1915 - 1875m lies between supersequence 11At and 10At and due to core restrictions a possible deltaic environment could be placed forward. (*Core description courtesy of Petroleum Agency of SA*).
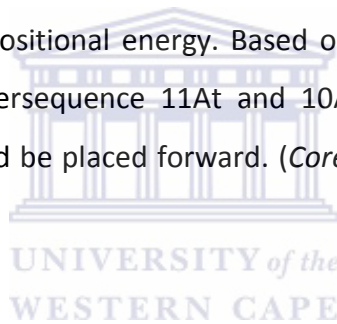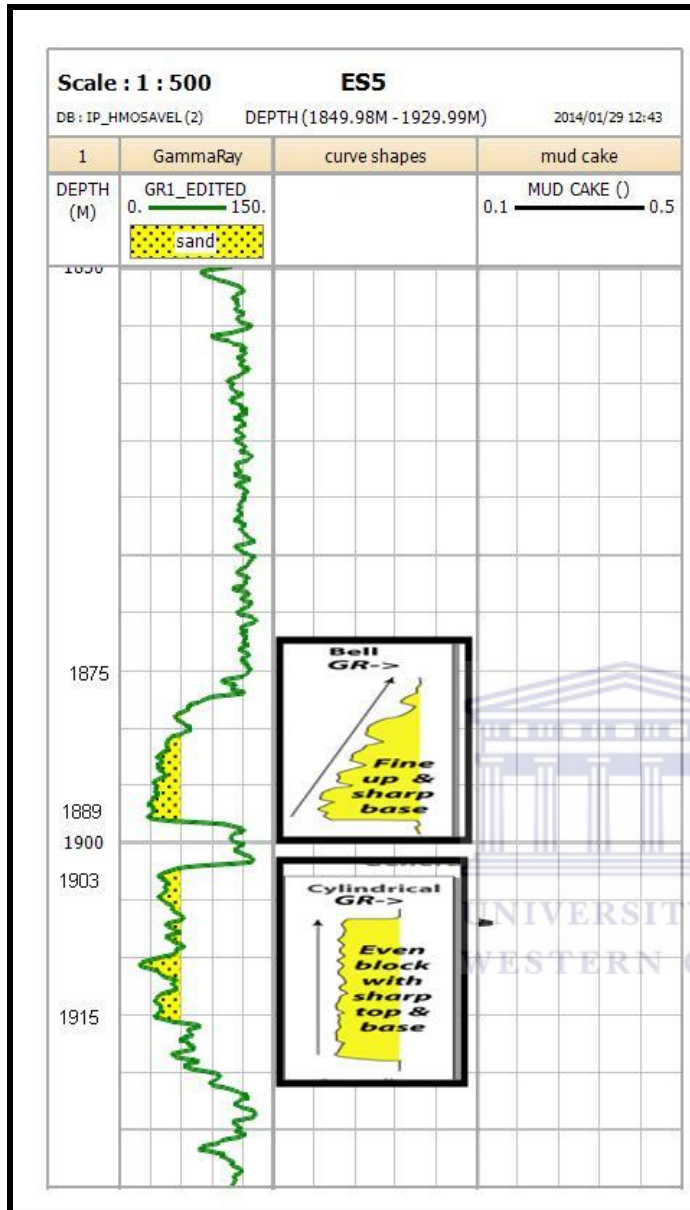
*Figure. 4.1.12. Illustration of gamma ray log from depth 1930.0- 1850.0m.*

Core depth 1775 - 1710m**:** comprised of a sequence of interbedded claystones and sandstones, with thin dolomite layers between 1760 - 1710m. From depth 1760 - 1742m claystone which is medium grey soft and sticky grades into sandstone beds. Above this layer, a 15m thick bed of coarse quartz sand (1742 - 1727m) followed by a 17m sandy claystone. Core depth 1775 - 1760m (Fig.4.1.13) displays a cylindrical shape with a low gamma ray reading with sharp

borders could indicate a possible foreshore to shore face environment. (*Core description courtesy of Petroleum Agency of SA*).
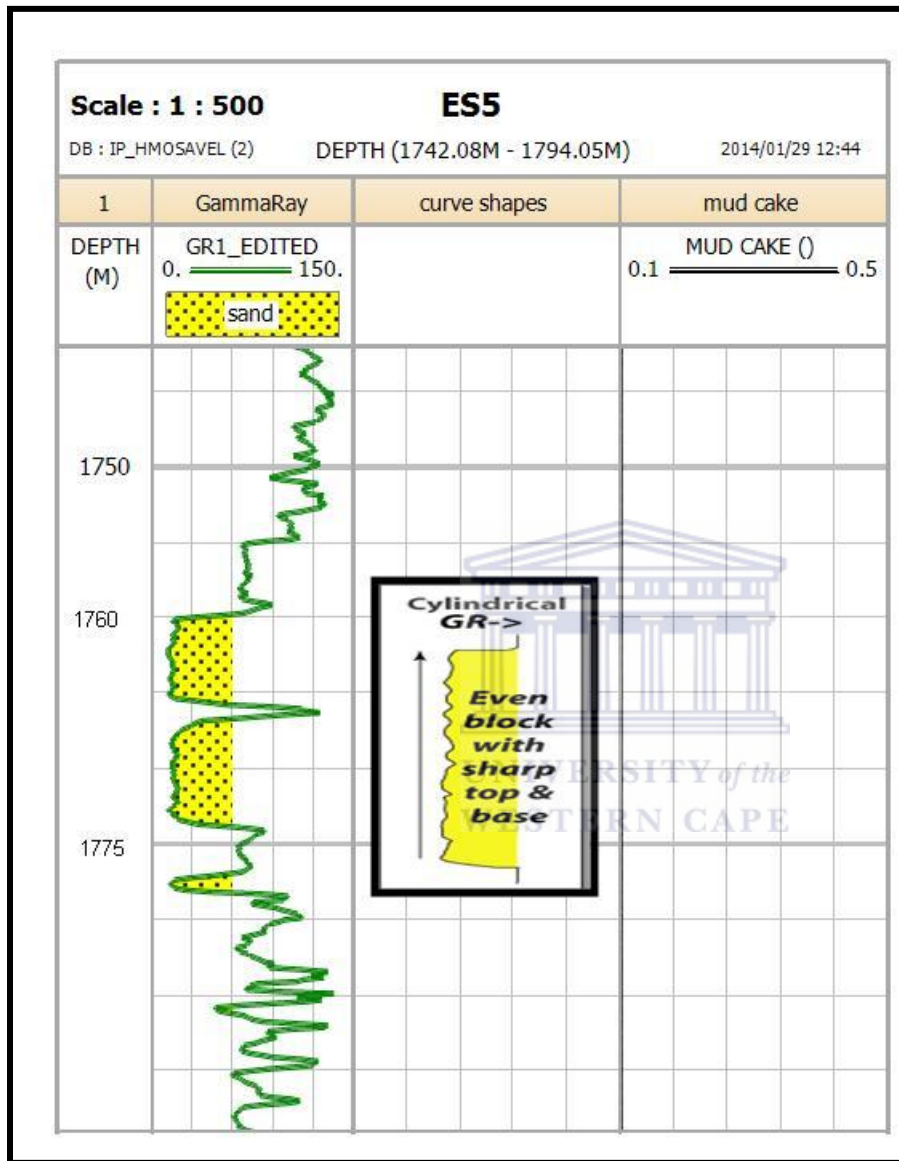


*Figure. 4.1.13. Illustration of gamma ray log from depth 1794.05- 1742.08m.*

**WELL F-AH4**

Depositional environments of areas of interest for Well F-AH4 have been interpreted from core (Fig. 4.1.14) however, some areas had uncored well sections and was interpreted based on lithology descriptions, gamma ray log and shape profiles.
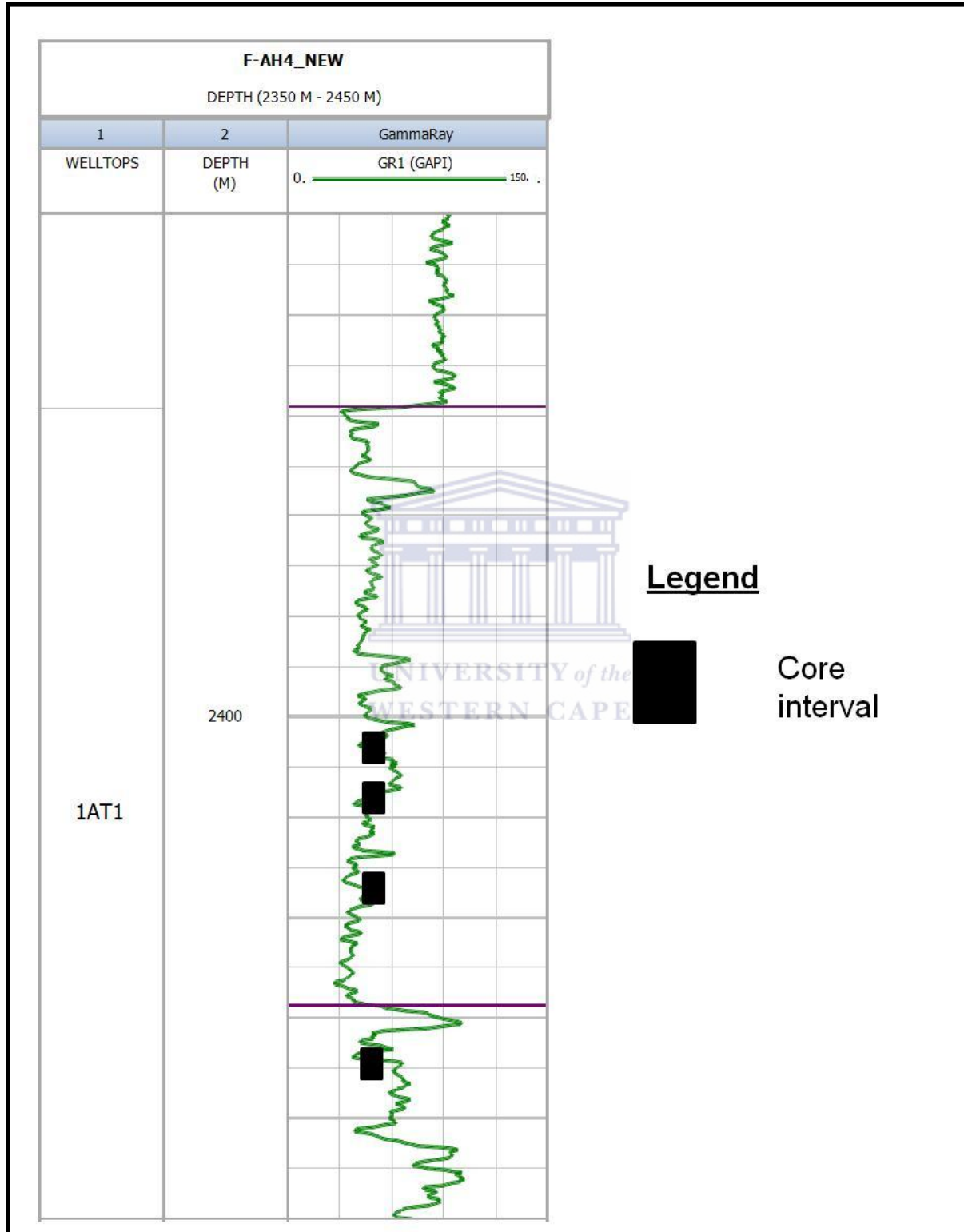
*Figure. 4.1.14. Well F-AH4 (Gamma ray log, well top surfaces +core interval).*

Green claystones at depth 2437.82 - 2436.86m (Fig.4.1.15) are non- calcareous, firm to moderately hard. The claystones comprise of *Chondrites* isp. (ichnofossil, bioturbation) made by detritivorous organisms that live in the bottom of marine environments and relatively dytoxic conditions (Fig.4.1.15).
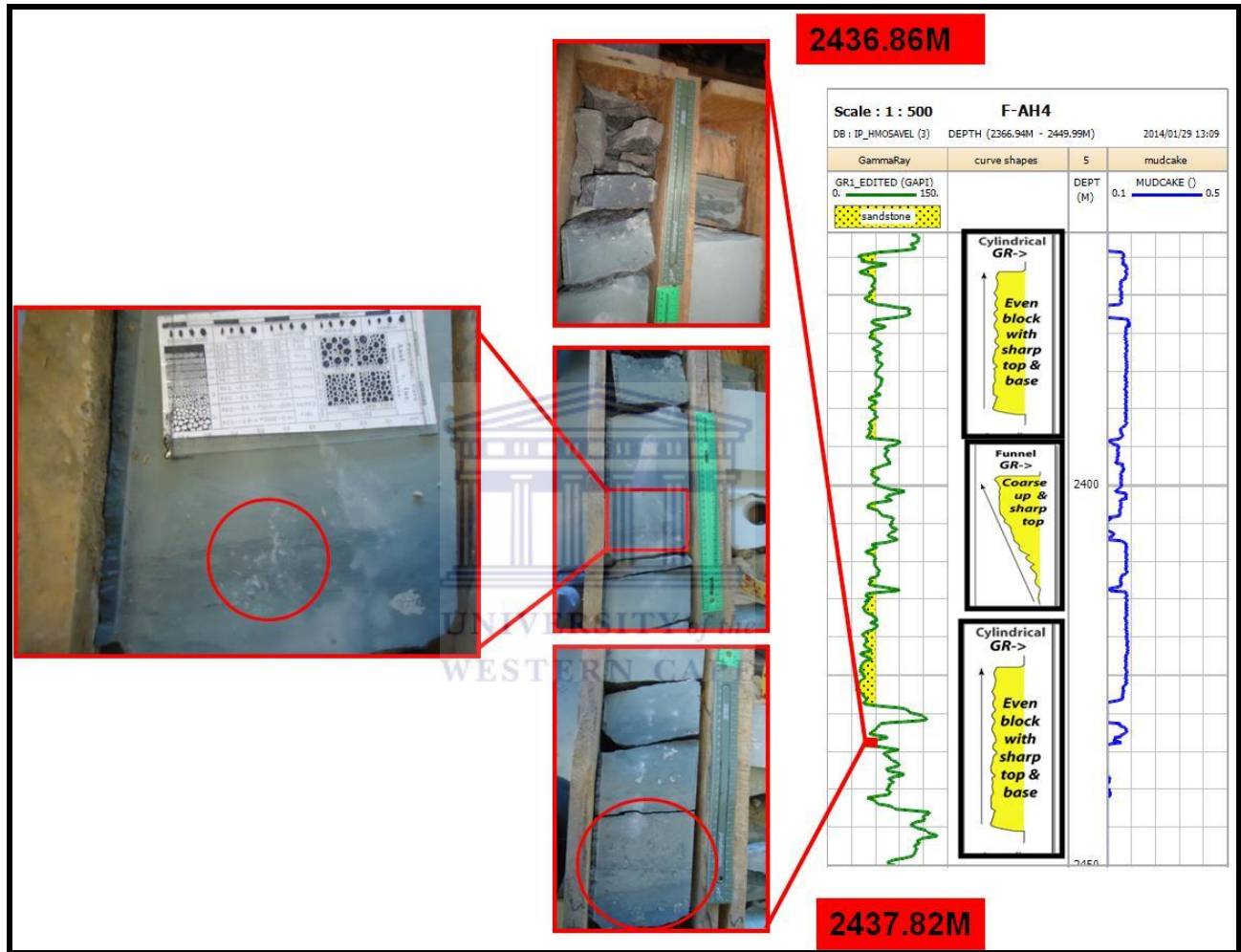


*Figure. 4.1.15. Illustration of core from depth 2437.82-2436.86m. Circle shape points out Chondrites isp. (Ichnofossil see text for description, page 49).*

At a depth of 2417.41m (Fig.4.1.16) conglomerate is present which was poorly sorted, slightly subangular and grey-white colour, grading into sandstone at a depth of 2416.94m which was grey in colour, well rounded, well sorted and coarse grained. The depth interval 2417.41 - 2416.19m of core is interpreted as a good example of a channel deposit composed by a finning-upwards succession of:

- Trough cross-bedded medium to fine grained sandstone.

- Trough cross-bedded gravelly coarse to medium sandstone.

- Trough cross bedded medium conglomerate containing mud clasts.
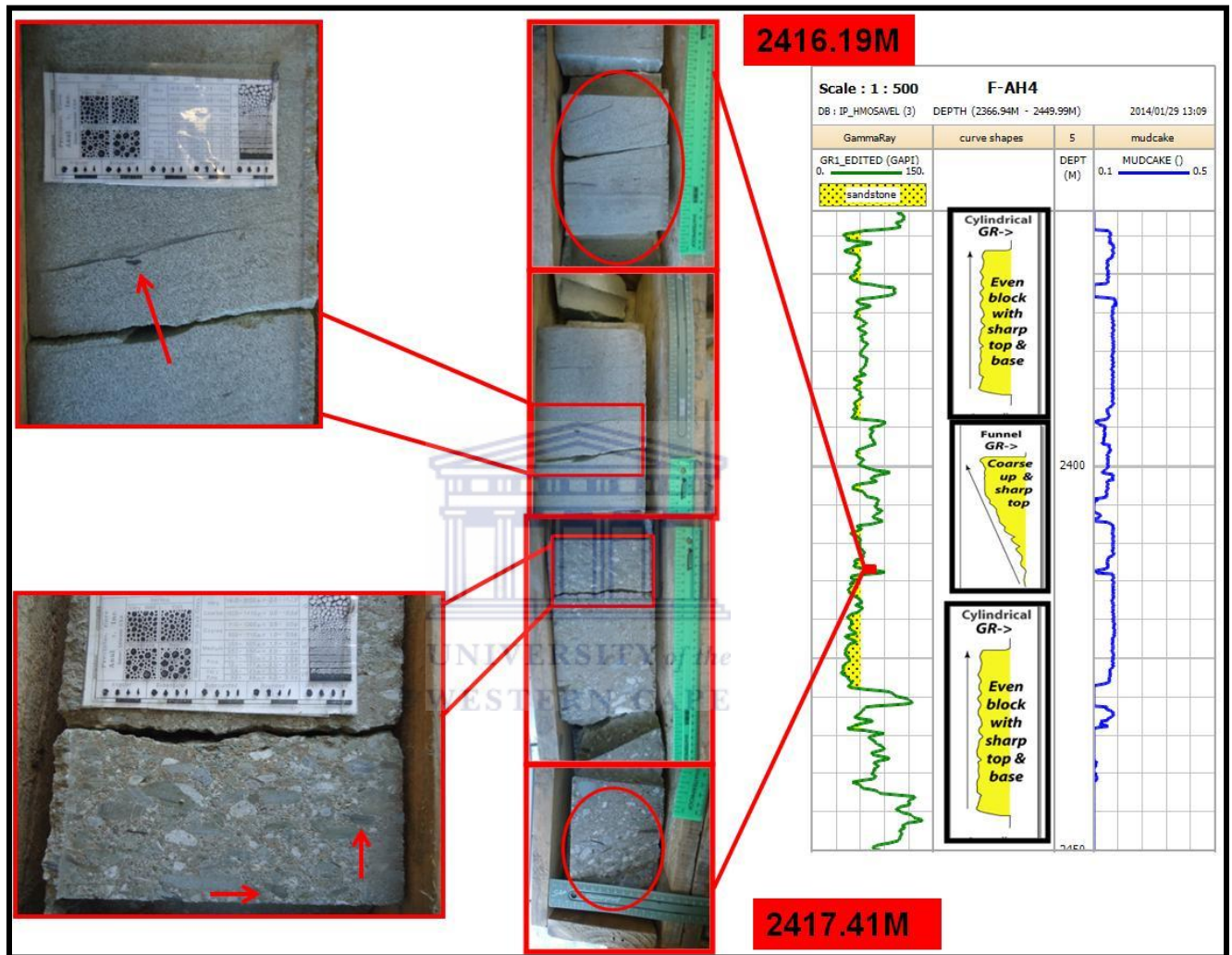


*Figure. 4.1.16. Illustration of core from depth -2417.41- 2416.19m. The arrow points out mud clast and the circle points out trough cross-bedded sandstone and conglomerate.*

From core depth 2410.19 - 2409.15m (Fig.4.1.17) the sandstone is tight to slightly porous, very fine grained, well sorted and well rounded with interbeds of claystone in places. In Figure 4.1.17, indicated by enlarged photo contains heterolithic wavy laminations and reflects an alternating influx of sand and mud to the environment which can occur in a delta.
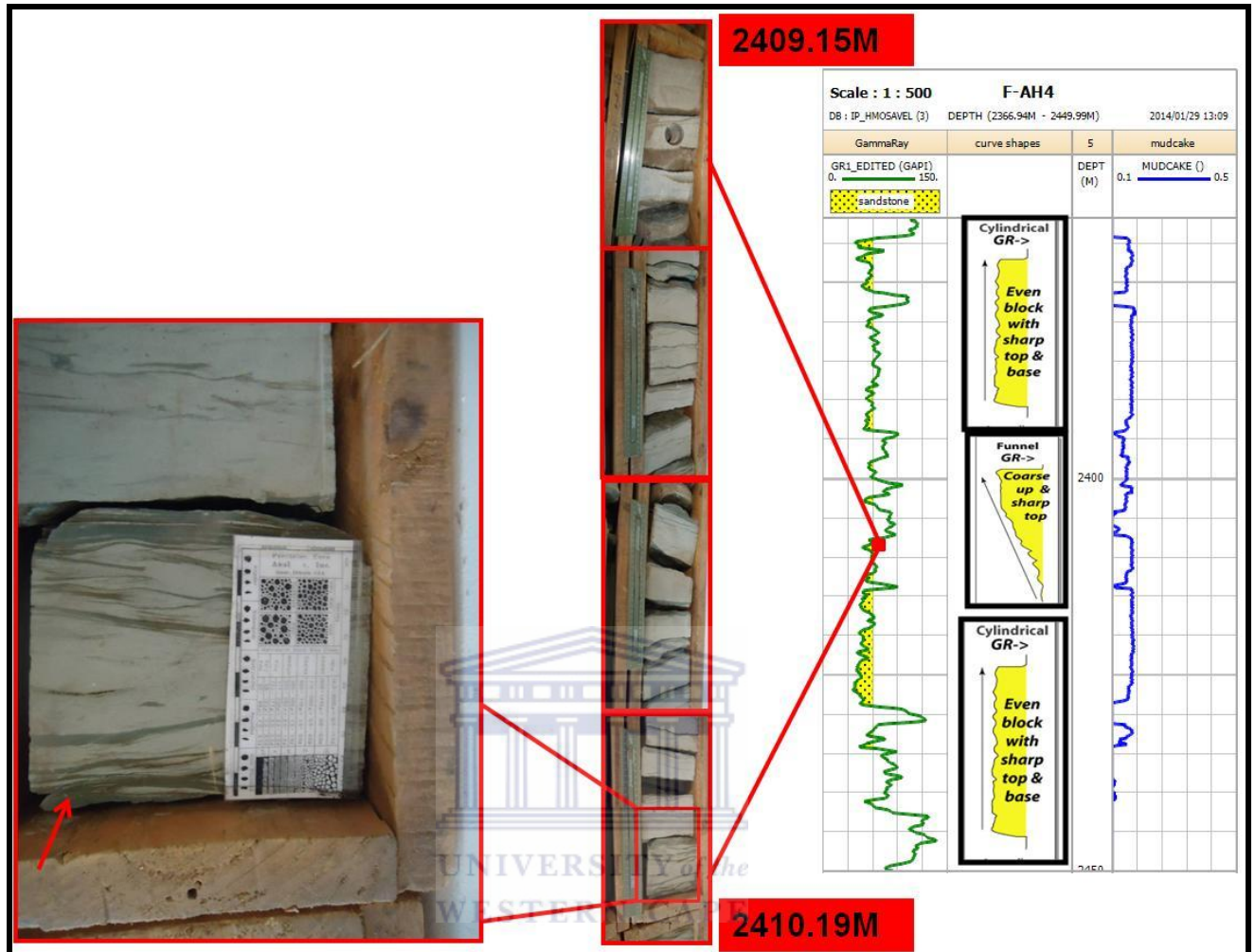
*Figure. 4.1.17. Illustration of core from depth 2410.19- 2409.15m. Heterolithic wavy laminations appear (arrow).*

From a depth of 2406.75 - 2405.52m (Fig.4.1.18) the interval comprised of interbedded trough-cross bedded channel conglomerate deposits with imbricated clasts at the bases. The channel conglomerates are grey in colour, subrounded and poorly sorted.
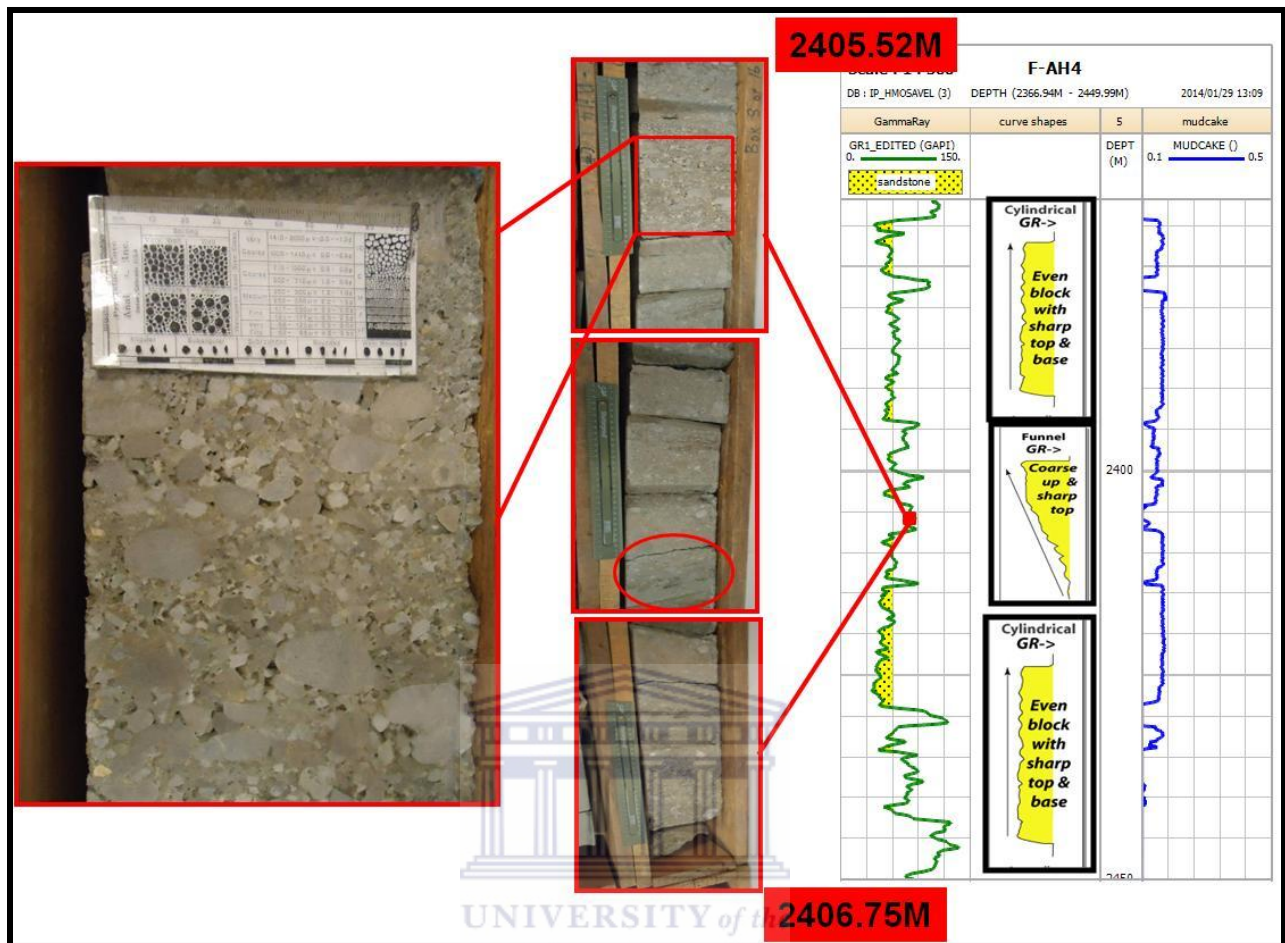
*Figure. 4.1.18. Illustration of core from depth 2406.75- 2405.52m. Trough cross-bedded conglomerate with imbricated clasts at the base (indicated by circle).*

Core depth 2404.39 - 2403.25m (Fig.4.1.19) comprises of a fined grained sandstone grey in colour with ichnofossils present, possibily *Thalassinoides* isp., *Planolites* isp. or *Teichichnus* isp. which are marine bioturbation and common in shoreface and shoreface- to- offshore transition zones in marine shelves. Core depth 2403.25 - 2367.05m, a shallow marine sandstone which is porous, fine to medium grained, round, grey coloured and rich in green lithoclasts.Core depth 2430 - 2367.05m displays a cylindrical and funnel shape, therefore a possible depositional environment suggests a distributary channel in a delta and a possible reservoir.
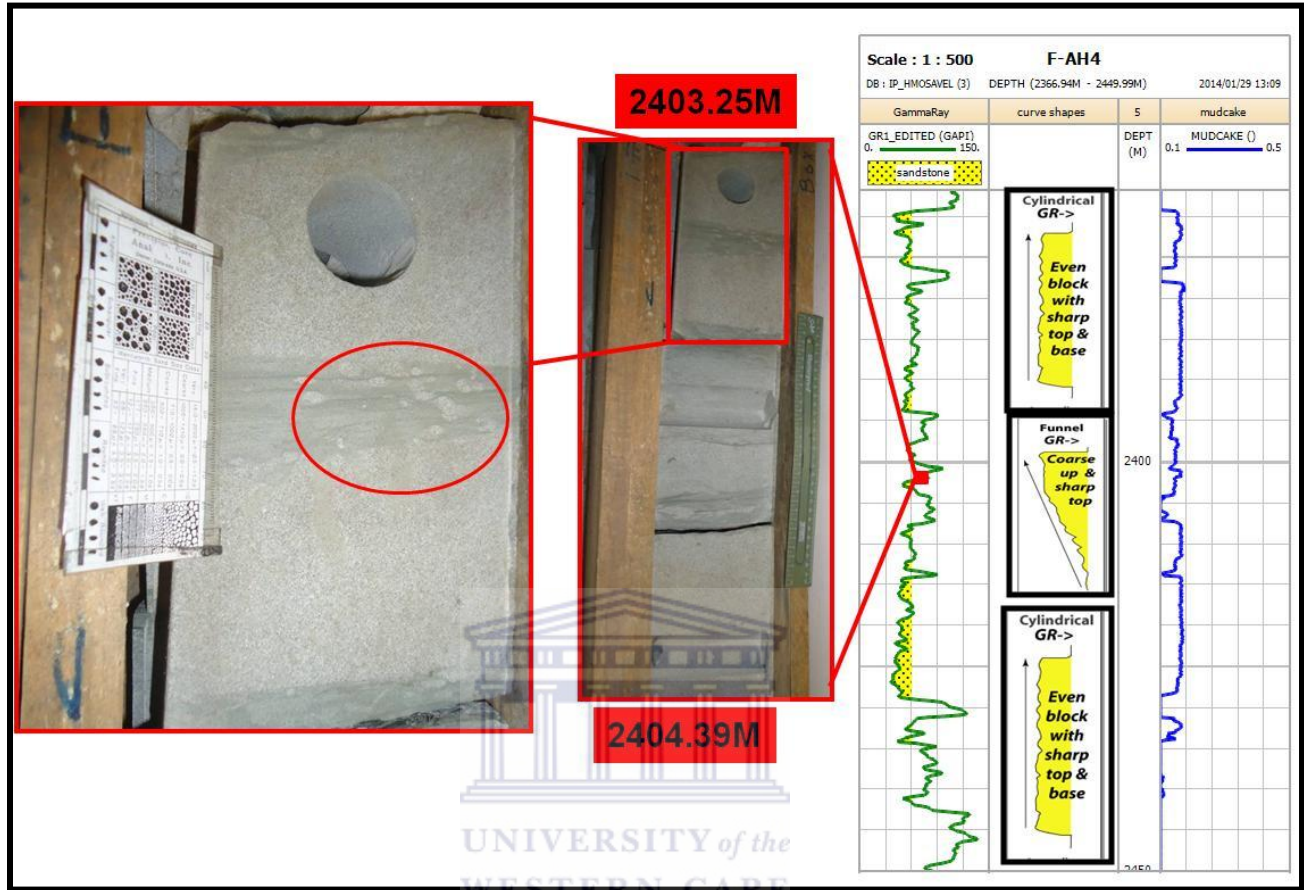
*Figure. 4.1.19. Illustration of core from depth 2404.39-2403.25m. Marine bioturbation appears (circle).*

Core depth 1899 - 1830m (Fig. 4.1.20) comprised of claystone and sandstone which was slightly porous, very fine to fine grained, subround and slightly glauconitic. Core depth 1899 - 1874m is an argillaceous interval of claystone interbedded with siltstone, greyish black colour. Claystone was dark grey in colour, noncalcareous and sandy in places. Bell shape from depth 1880 - 1855m represents a gradual upward increase in gamma ray reading. This trend reflects an upward fining sequence, i.e. change from sand to shale indicating a decrease in depositional energy. From depth 1874 - 1830m a substantial shallow marine sandstone interval. Near the base of depth 1874m the sandstone becomes finer grained and argillaceous. The sandstone was loose, medium and coarse grained in some places. Gamma ray logs show low values and a

cylindrical shape with sharp borders and no internal change from depth 1855 - 1830m. In a marine setting, cylindrical and bell shape point out to a possible rise in sea level. Sand body 1880-1830m could be a possible reservoir. *(Core description courtesy of Petroleum Agency of SA).*
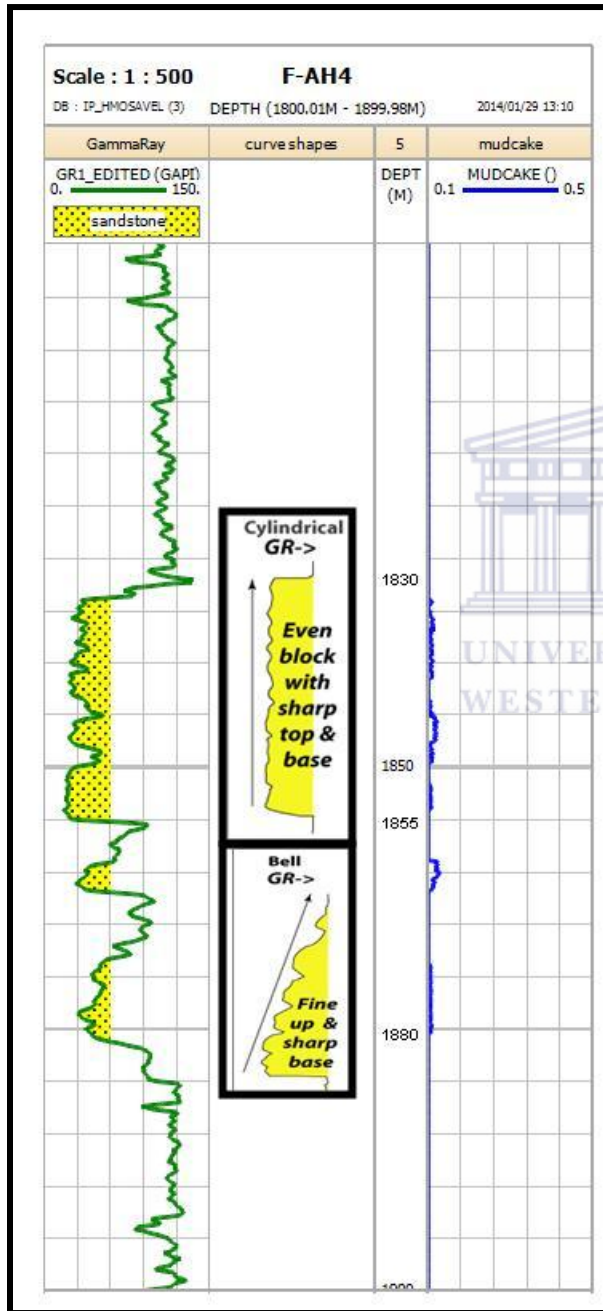


*Figure. 4.1.20.Illustration of gamma ray log from depth 1899.98- 1800.01m.*

## 4.1.1 CORRELATION

A correlation of a structural section through Wells E-S3, E-S5 and F-AH4 was constructed as shown in Figures 4.1.1.1 and 4.1.1.2, displaying the unconformity sequences in each well.
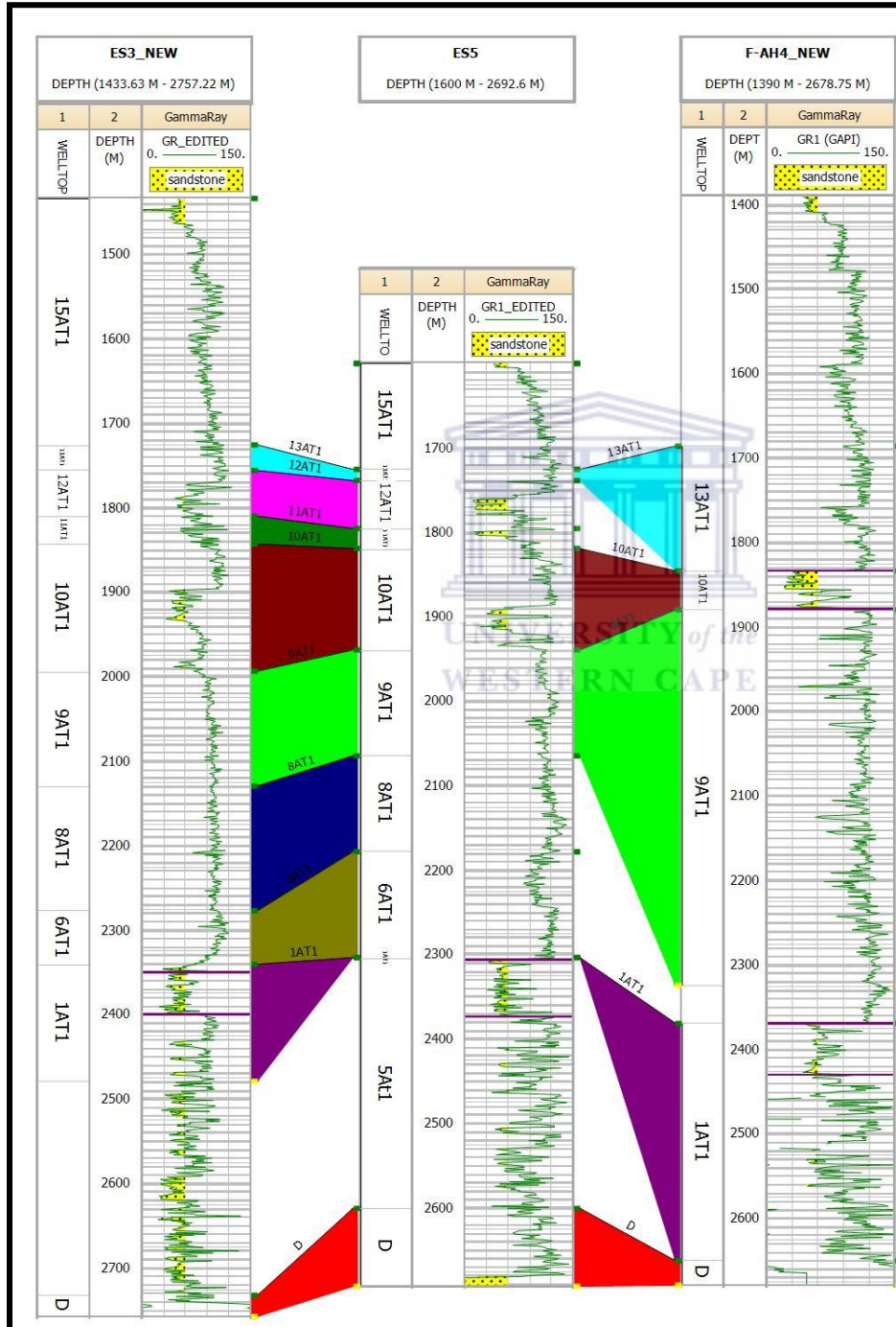


*Figure. 4.1.1.1.Well top correlation of Well E-S3, E-S5 and F-AH4.*
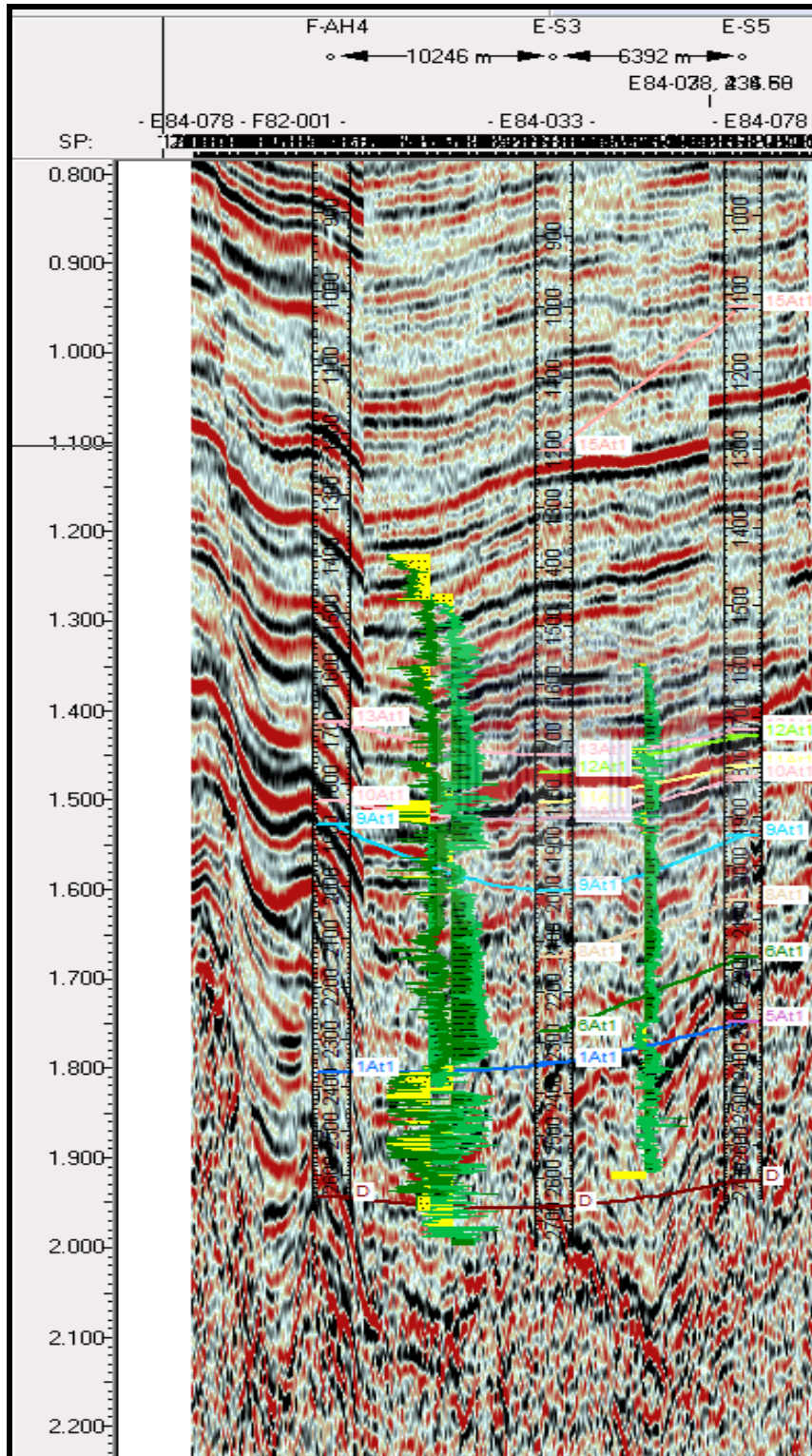
*Figure. 4.1.1.2. 2D seismic correlation of Wells E-S3, E-S5 and F-AH4 with well signatures for F-AH4, E-S5 and E-S3 superimposed.*

**4.1.2 FACIES**

According to Walker (1992) lithofacies is a rock body characterized by a particular combination of lithology, physical and biological structures that show an aspect different from the rock bodies above, below and laterally adjacent. Lithofacies reflect the sedimentary processes which formed that rock body and in order to determine the depositional environment where the, lithofacies were deposited, the lithofacies are grouped in "Facies associations" or groups of facies genetically related to one another and which have some environmental significance (Collinston, 1969). In general these facies associations (which some authors name as "Facies") represent parts of a sedimentary environment or "sub-environment. Five different lithofacies were classified as shown in Table 1.

TABLE. 1: Lithofacies description.

| Facies | Description | Reservoir quality | Facies photo |
|---|---|---|---|
| HM1 | Massive claystone, green-black colour. Contains*Planolites* isp. &*Chondrites* isp. ichnofossils | Non-reservoir |  |
| HM2 | Fine to coarse grained sandstone, subrounded grains, grey colour with trough cross-bedding | Moderate |  |

| HM3 | Very fine to medium grained sandstone, very well sorted, well rounded grains and grey in colour | Very good |  |
|------|------|------|------|
| HM4 | Fine to medium grained sandstone, light grey in colour, well rounded, well sorted with ripples. | Good |  |
| HM5 | Trough cross bedded conglomerate, light grey in colour, poorly sorted, sub-rounded grains | Good |  |

**Well E-S3 lithofacies**

Four lithofacies were identified from core of Well E-S3. They are facies HM2, HM3, HM4 and HM5 as seen in Figure 4.1.2.1 (B) below. Facies HM2 has a fair permeability value ranging between 1 - 10 mD, with a porosity between 10.8 - 20.6% (Fig. 4.1.2.1A). Facies HM3 has a poor permeability ranging between 0.1-1 mD, with a porosity between 1 and 10.8%. Facies HM4 has a similar permeability range as facies HM2 that being between 1 and 10 mD, with a porosity range being between 8% and 16.2%. Facies HM5 indicates a good reservoir quality with a good

permeability ranging between 10 - 100 mD and porosity values ranging between 10.8 - 20.6% (Fig. 4.1.2.1A).
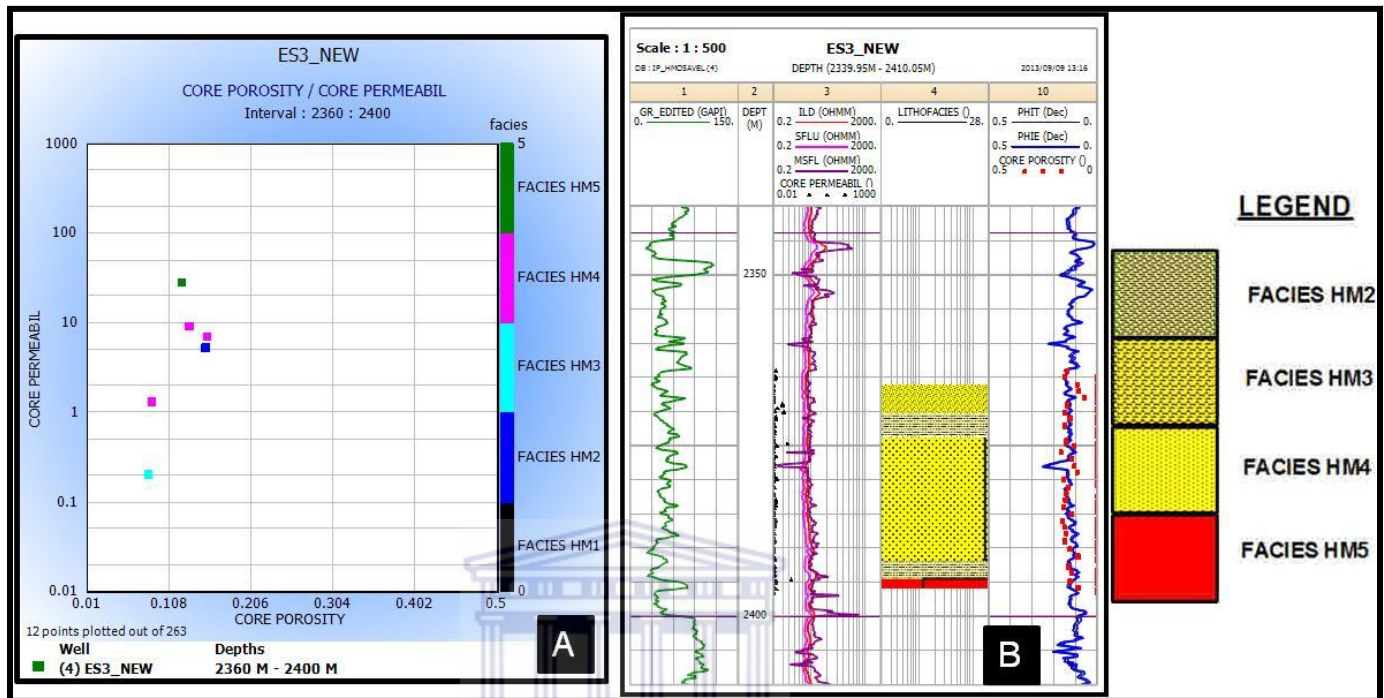


*Figure. 4.1.2.1. (A) Scatter plot of core porosity versus core permeability. (B) Core facies in track 4 of Well E-S3.*

**Well E-S5 lithofacies**

Two lithofacies were identified from core of Well E-S5. They are facies HM3 and HM5 as seen in Figure 4.1.2.2(B) below. Facies HM3 has a good reservoir quality with permeabilty values ranging between 0.7-100 mD and porosity between 9 - 20% (Fig. 4.1.2.2A). Facies HM5 has a poor reservoir quality with permeability values between 0.1 - 1 mD with porosity ranging from 0 - 10% (Fig. 4.1.2.2A).
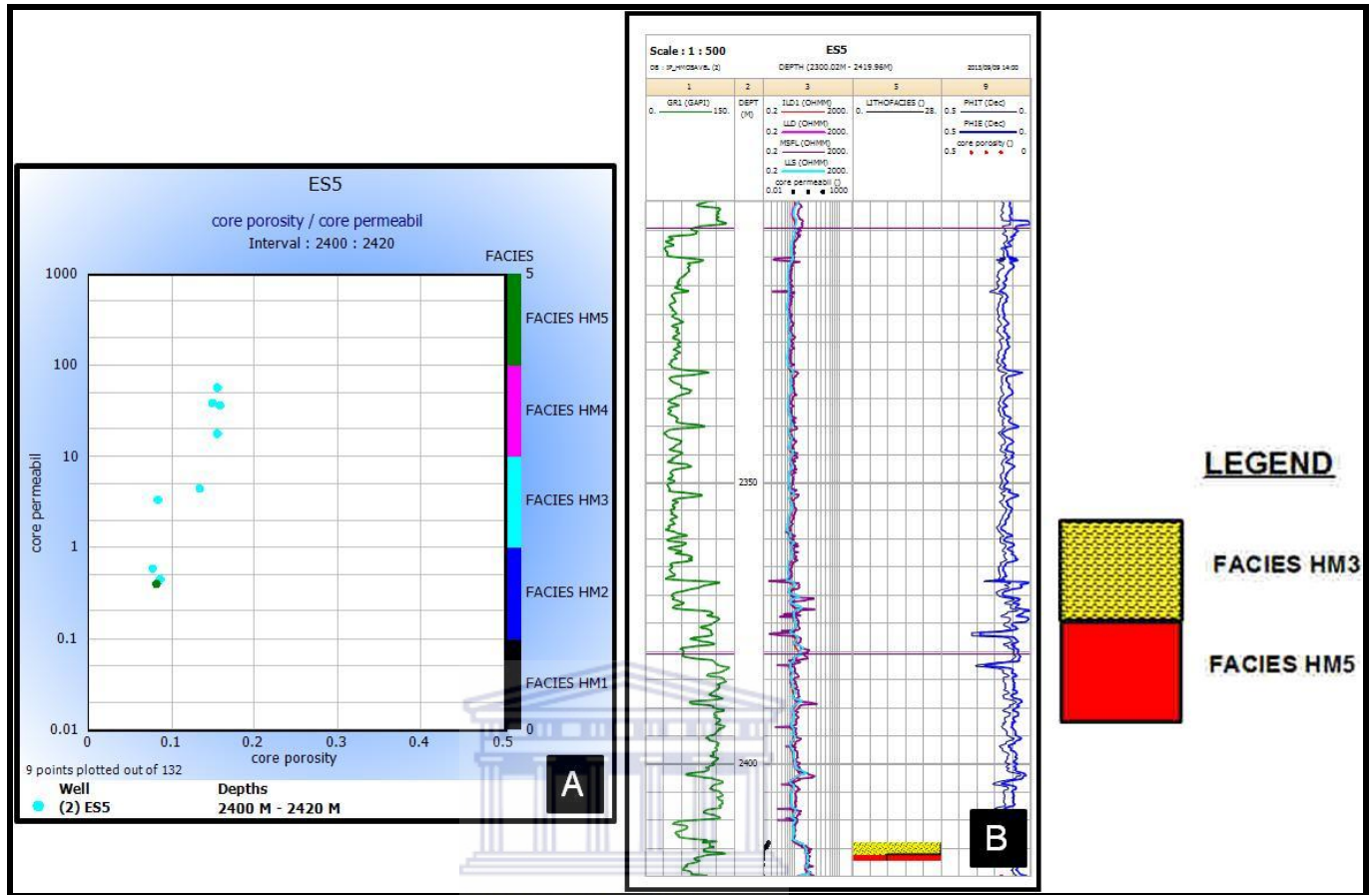
*Figure. 4.1.2.2. (A) Scatter plot of core porosity versus core permeability. (B) Core facies in track 5 of Well E-S5.*

**Well F-AH4 lithofacies**

Five lithofacies (facies HM1, HM2, HM3, HM4 and HM5) were identified from core of Well F-AH4 (Fig. 4.1.2.3B). Facies HM1 is classified as a non reservoir rock, facies HM3 has a good reservoir quality with permeability values between 10 and 150 mD and porosity of 10 - 20% . Facies HM4 and HM5 indicates a very good reservoir quality with permeability values between 100 - 1000 mD and porosity of 10 - 20% (Fig. 4.1.2.3A).
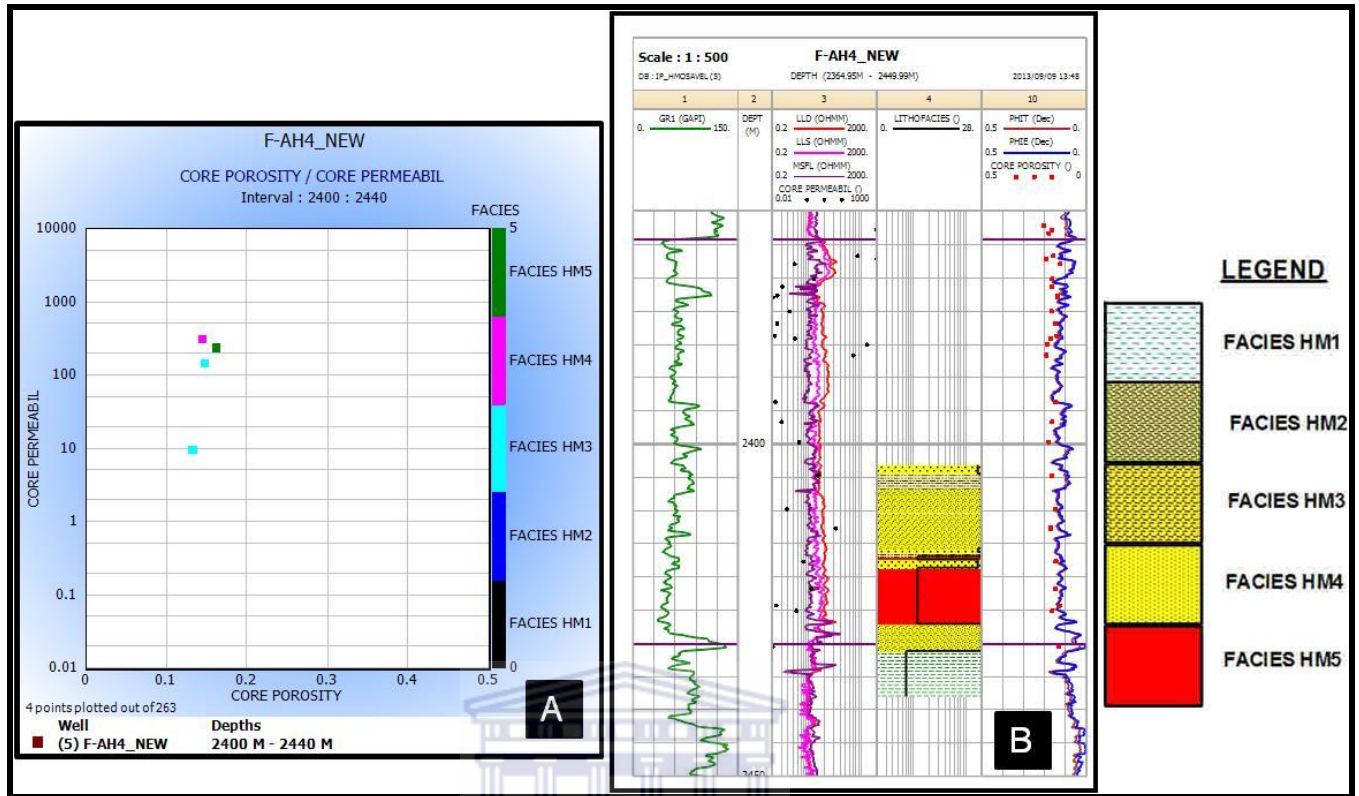
*Figure. 4.1.2.3. (A) Scatter plot of core porosity versus core permeability. (B) Core facies in track 4 of Well F-AH4.*

## 4.2 PETROPHYSICAL ANALYSIS OF VOLUME OF SHALE, POROSITY, WATER SATURATION AND PERMEABILITY FROM WIRELINE LOGS

Only certain depths of possible reservoirs were studied in each well based on the presence of a mud cake (which indicates a permeable zone), as seen from the logs in sub-section 4.1.

**WELL E-S3**

Interval 2350 - 2400m was divided into four sections to interpret the volume of shale, porosity, water saturation and predicted permeability based on the consistency of the gamma ray signature (Fig.4.2.1). The first division was from depth 2350.8 - 2359m with an average volume of shale of 26.43% indicating a sandy shale zone. From the comparison log, the Simandoux model is the best fit curve, having an average water saturation of 58.66% with a porosity of 11.79%. The average predicted permeability for the first division is 7.54mD, having a fair reservoir quality.

The second division from depth 2359 - 2364m had an average volume of shale of 38.93% indicating a shale zone with an average water saturation of 58.21%. The porosity is calculated to be 14.02% with a predicted permeability of 8.87mD. The third division from depth 2365 - 2388.9m had an average value of shale of 29.89% with a saturation value of 63.02%. The porosity was 14.20% with predicted permeability of 8.99mD. The fourth division from depth 2393.9 - 2399.2m had an average value of 24.94% for shale with an average water saturation value of 58.16%. The predicted permeability has an average of 7.46mD indicating a fair reservoir quality. The third division has the highest values for water saturation, porosity and permeability.
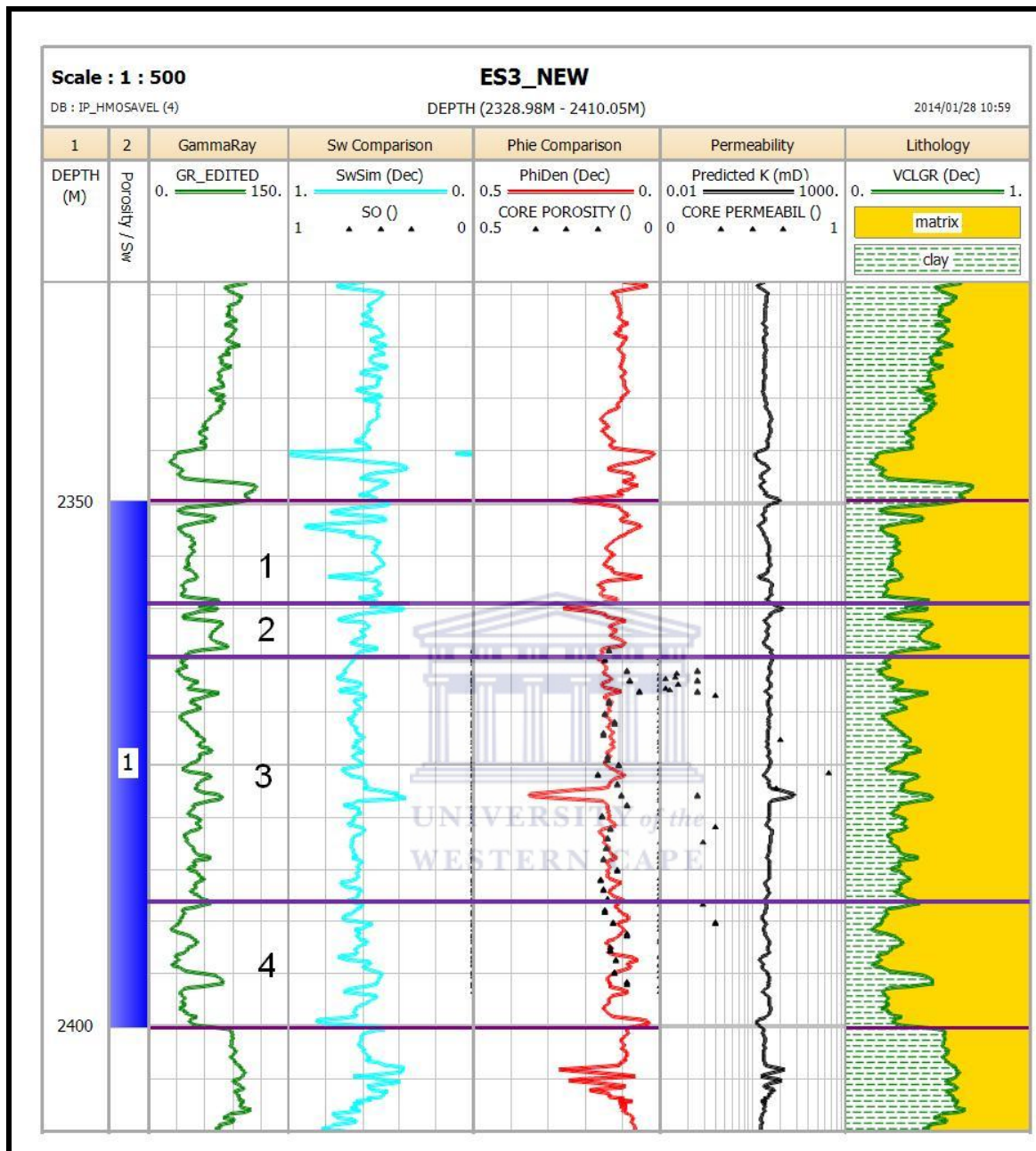
*Figure. 4.2.1. Comparison of core, water saturation, porosity models with volume of shale from 2350-2400m for Well E-S3*

**WELL E-S5**

Interval 2304 - 2374.85m was divided into three sections based on the changing gamma ray signature (Fig.4.2.2). The first division from depth 2304.4 - 2310.8m has an average volume of

shale 19.057% indicating a sandy shale zone. From the comparison log, the Juhasz model was the best fit curve compared to the core, having an average water saturation of 48.91% with a porosity of 12.59%. The average predicted permeability for the first division was 1.94mD, having a fair reservoir quality.

The second division from depth 2310.8 - 2329.4m had an average of 18.10% for the volume of shale with an average water saturation of 61.30%. The porosity was calculated to be 15.46% with a predicted permeability of 8.83mD having a fair reservoir quality. The third division from depth 2329.4 - 2374.85m had an average of 17.82% of shale indicating a sandy shale zone with a water saturation value of 60.08%. The calculated porosity for the third division was 13.79% with a predicted permeability of 3.66mD. The second division has the best values for a fair reservoir for Well E-S5.
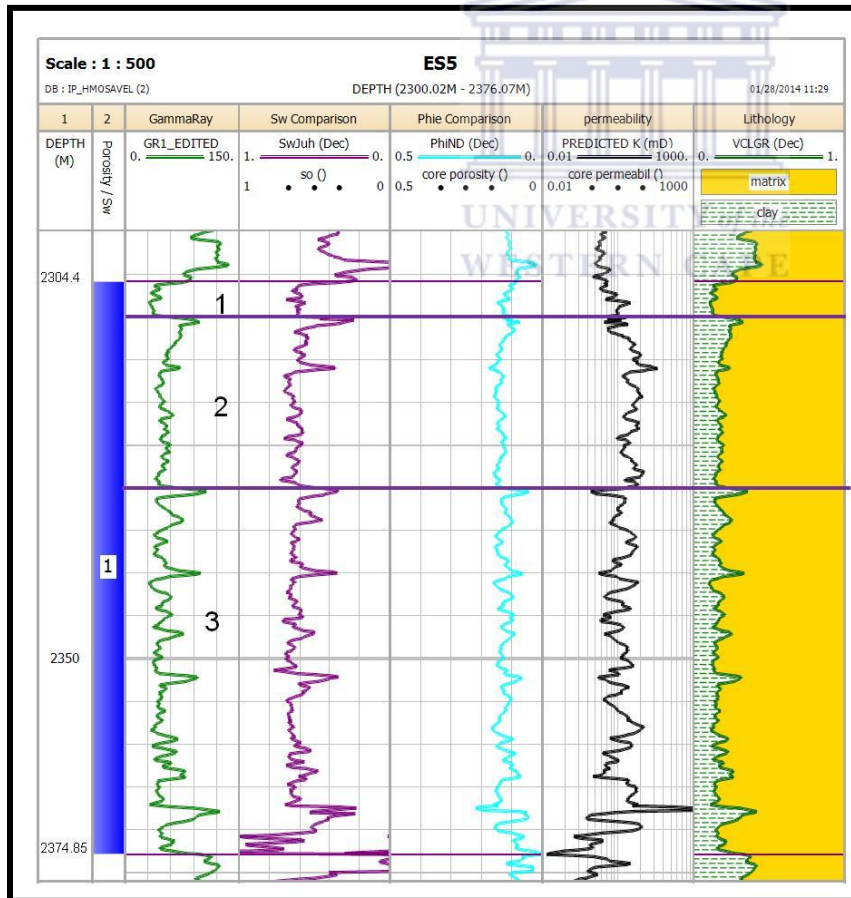


*Figure. 4.2.2. Comparison of water saturation, porosity models with volume of shale from 2304-2374.85m for Well E-S5.*

**WELL F-AH4**

Interval 1833 - 1877.58m was divided into three divisions based on the changing gamma ray signature (Fig.4.2.3). The first division from depth 1833.5 - 1854.7m has an average volume of shale 11.17% indicating a sandy shale zone with a porosity of 20.30% The Indonesian Model was used to calculate the water saturation, with an average of 68.61%. The average predicted permeability for the first division is 298.32mD, having a very good reservoir quality.

The second division from depth 1854.7 - 1861.4m had an average volume of shale of 24.72% and water saturation of 47.53%. The porosity calculated was 11.27% with a predicted permeability of 12.27mD having a moderate reservoir quality. The third division from depth 1861.4 - 1877.58m had an average water saturation of 42.13% and volume of shale of 29.18%. Predicted permeability had an average of 13.94 mD having a moderate reservoir quality. The first division has the highest permeability and porosity values and the best reservoir quality.
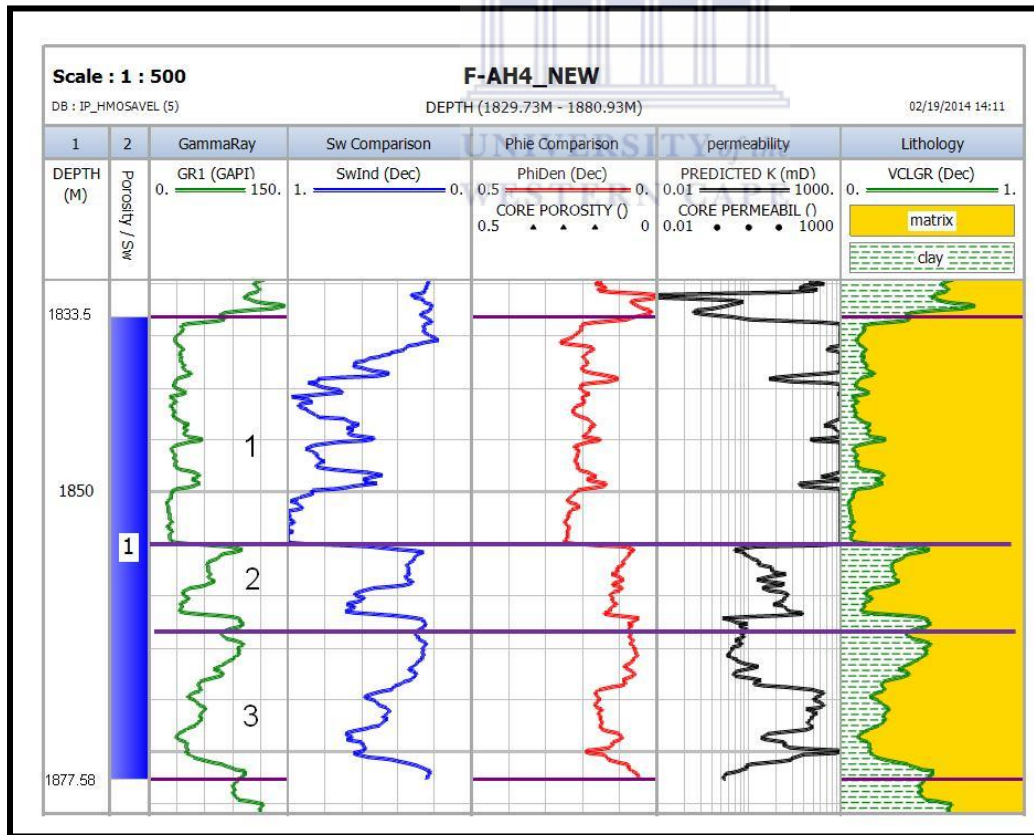


*Figure. 4.2.3. Comparison of water saturation, porosity models with volume of shale from 1833-1877.58m for Well F-AH4.*

Interval 2369.07 - 2430.18m was divided into four sections (Fig. 4.2.4). The first section from depth 2369.07 - 2376.0m and 2378.5 - 2393.9m has an average volume of shale of 28.01% and water saturation of 18.22%. The average porosity calculated was 15.61% with an average predicted permeability of 129.61mD. The second section from depth 2376.0.9 - 2378.5m had an average volume of shale of 40.82% indicating a shale zone, with an average water saturation of 18.36%. A porosity of 13.08% and predicted permeability of 52.18mD.The third section from depth 2393.9-2407.3m had an average volume of shale of 33.92% indicating a sandy shale zone and water saturation of 16.56%. Porosity of 13.67% and predicted permeability of 62.47mD show good reservoir quality. The fourth section from depth 2407.3 - 2430.18m had an average water saturation of 17.86% and a volume of shale being 22.75%.The porosity calculated for the third section was 14.38% and predicted permeability of 104.48mD. The first section has the highest predicted permeability and porosity values indicating a good reservoir quality.
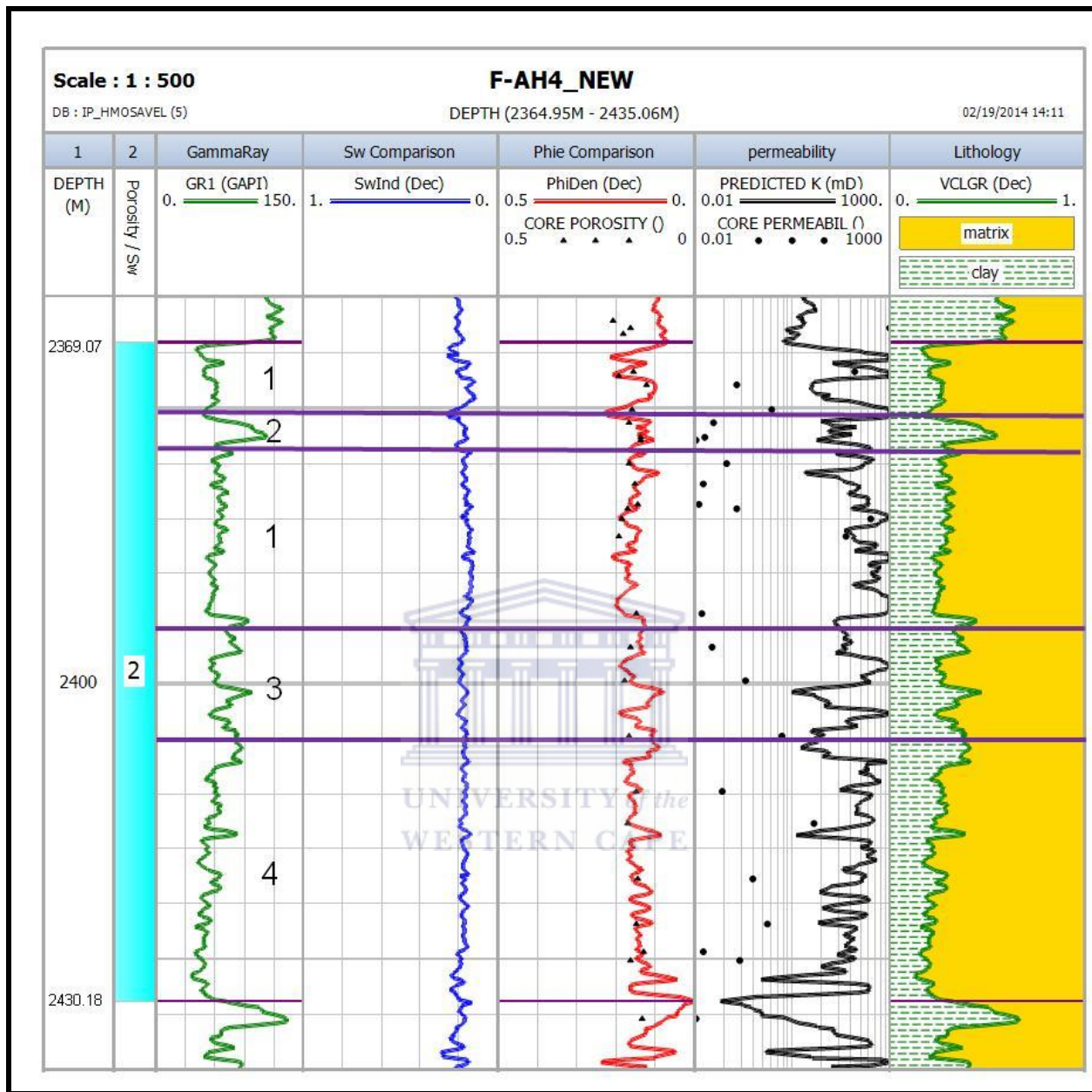
*Figure. 4.2.4. Comparison of core, water saturation, porosity models with volume of shale from 2369.07-2430.18m for Well F-AH4.*

**4.2.1 CUT-OFFS**

Cut- offs defines the net reservoir and net pay cut- off zones and calculate the average porosity, clay volume and water saturation for each zone of interest. Net reservoir is classified as a unit of rock that allows fluids to flow at commercially significant rates. Once the reservoir can produce hydrocarbons at an economical acceptable hydrocarbon/ water ratio, they are classified as net pay (Suzanne & Robert, 2004).

In order to determine net reservoir and net pay in this thesis volume of shale, porosity and water saturation cut- offs had to be validated using scatter plots and histograms to compute suitable cut-offs for areas of interest.

**Porosity Cut-offs**

A scatter plot of core porosity versus core permeability was used to define the porosity cut- off and minimum permeability considered capable of flowing hydrocarbons. Figure 4.2.1.1 below presents an example of Well E-S3 porosity- permeability scatter plot for cut-off determination (Appendix 7 has Well E-S5 and F-AH4 scatter plots).
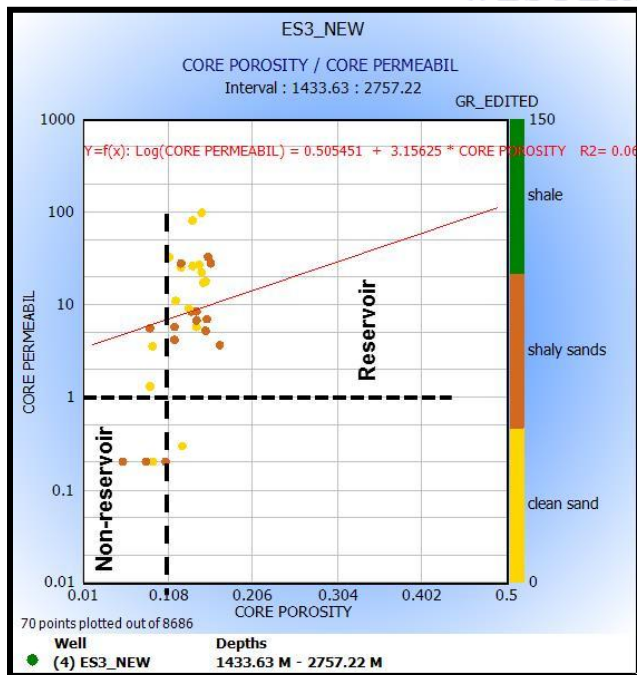


*Figure. 4.2.1.1 Scatter plot of core porosity versus core permeability of Well E-S3.*

**Volume of shale cut- offs**

Lithologies with low volume of shale (Vcl) have the capability to store hydrocarbons. Once the rock has a high volume of shale, it will be more difficult to store hydrocarbons or allow for migration of hydrocarbons to take place. This point was taken as the volume of shale cut-off for pay rocks determined from the scatter plot of volume of shale versus porosity and gamma ray. Figure 4.2.1.2 below presents the volume of shale cut-off for Well E-S3 (E-S5 and F-AH4 is in Appendix 8).
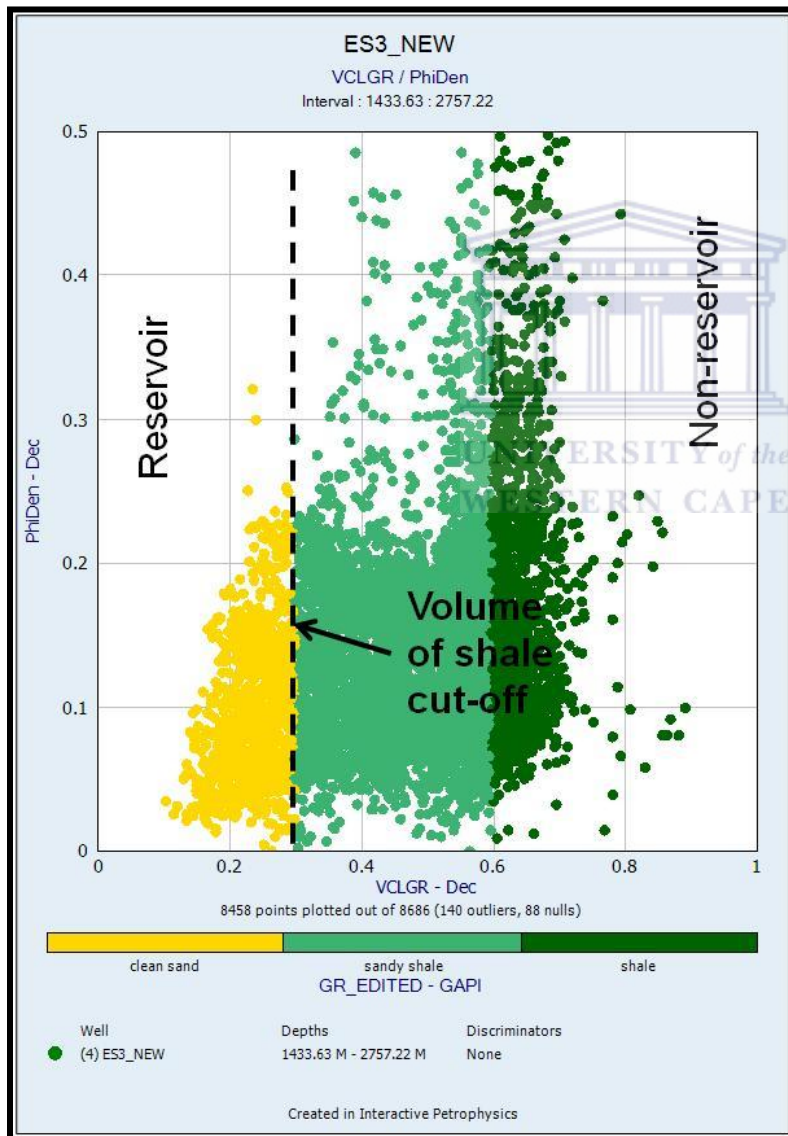


*Figure. 4.2.1.2. Scatter plot of volume of shale versus porosity and gamma ray of Well E-S3.*

Figure 4.2.1.2 above shows that the volume of shale cut- off was determined at 29.44%. Rocks with volume of shale greater than 29.44% was regarded as shale (non-reservoir) and those less than 29.44% are clean sand (reservoir rock).

**Water saturation cut- off**

Water saturation (Sw) cut-off separates hydrocarbon (productive) bearing intervals from water (wet) bearing intervals. Intervals that have water saturation greater than 59% were assumed to be wet intervals and those less than 59% were productive intervals.

A histogram together with a scatter plot was used to determine the water saturation cut-off in this study. Figure 4.2.1.3 below shows the water saturation frequency distribution histogram plot and scatter plot of water saturation versus porosity for Well E-S3 (Appendix 9 for Well E-S5 and F-AH4).
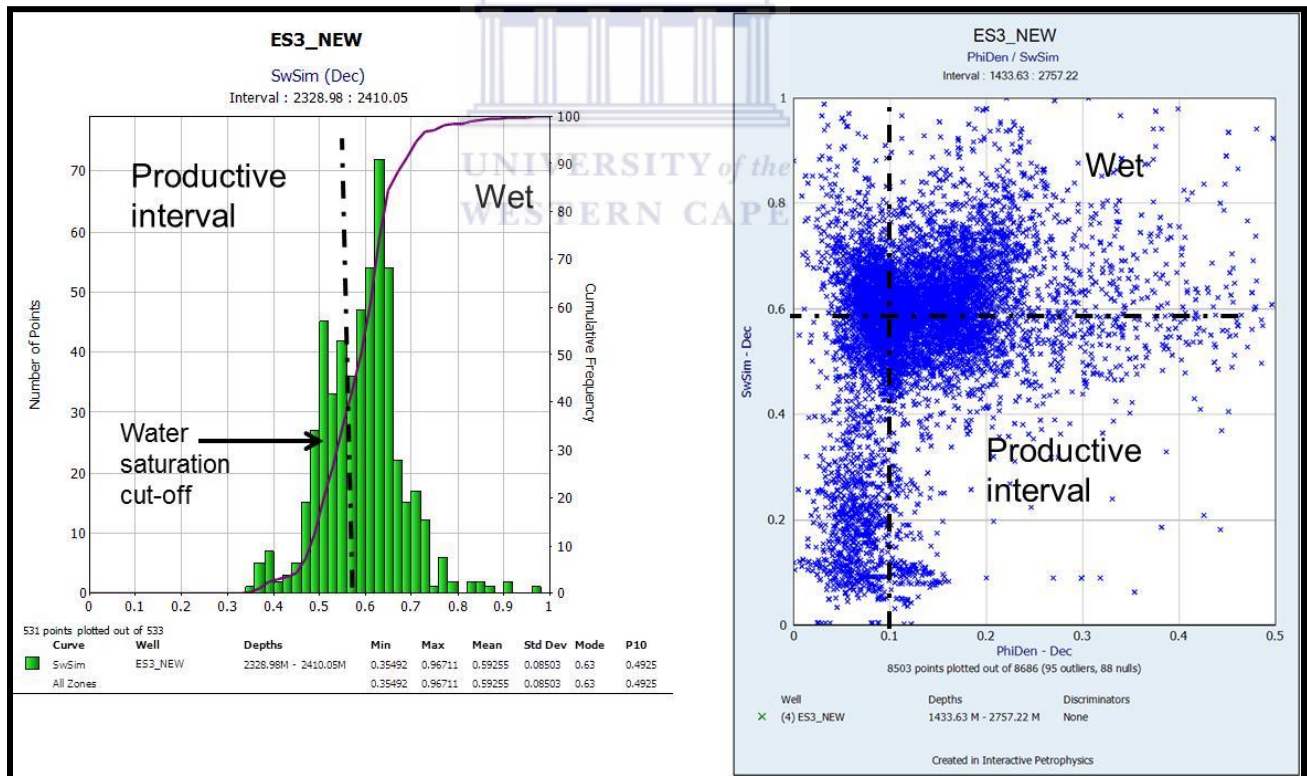


*Figure. 4.2.1.3. Histogram of water saturation and scatter plot of water saturation vs. porosity of Well E-S3.*

**WELL E-S3:**

Interval 2350 - 2400m of Well E-S3 seems to be a reservoir unit that is porous and permeable to store and transmit fluids. The reservoir has an average net pay of 3.51% and a gross of 50.60% having a poor to moderate quality and a poor to moderate connectivity. Interval 2350 - 2400m has an average porosity of 19.7%, 35.8% volume of shale and water saturation of 44.3% as presented in Table 2 and Figure 4.2.1.4.

TABLE. 2: Summary of calculated reservoir pay parameters for Well E-S3.

| Zone | Name | Top (m) | Bottom (m) | Gross | Net | N/G | Av Phi | Av Vcl | Av Sw |
|------|------|---------|------------|-------|------|-------|--------|--------|-------|
| 1 | Reservoir 1 | 2350 | 2400 | 50.60 | 3.51 | 0.069 | 0.197 | 0.358 | 0.443 |
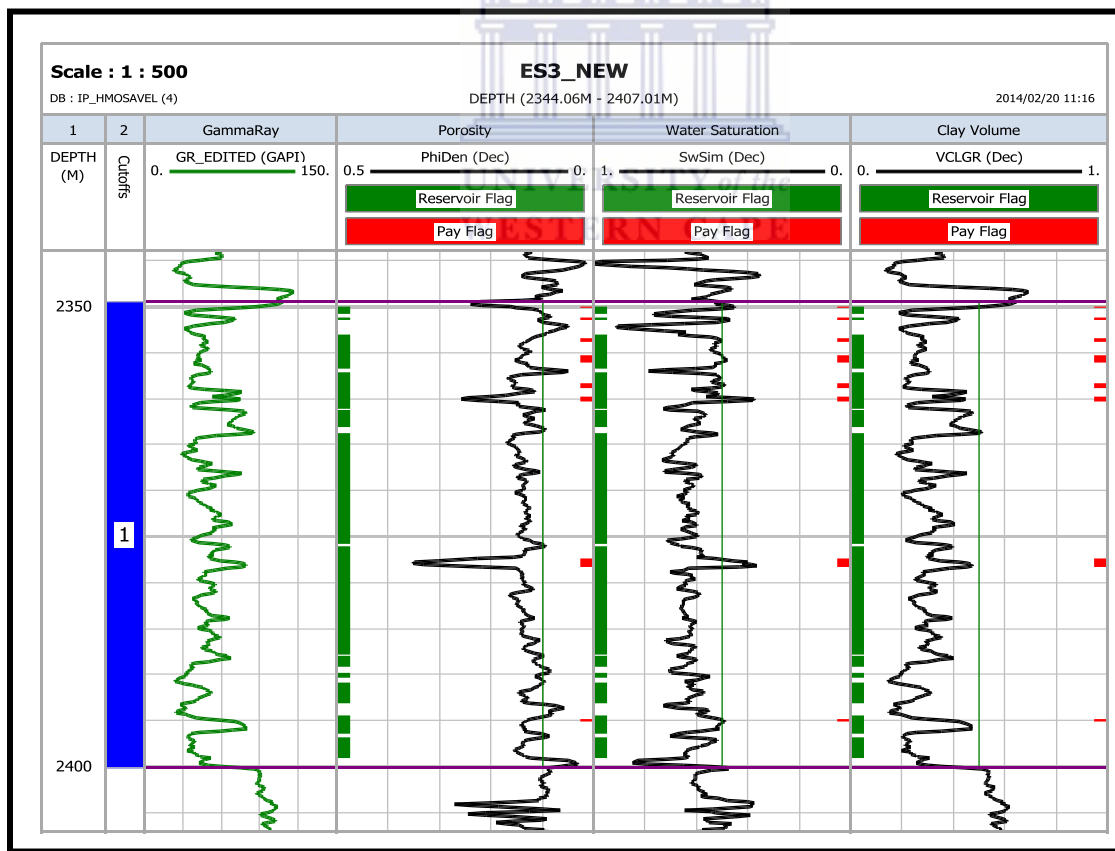


*Figure. 4.2.1.4. Well E-S3 showing calculated reservoir parameters and pay flags from 2350-2400m.*

**WELL E-S5:**

Interval 2303.53 - 2374.85m of Well E-S5 appears as a reservoir unit with an average net pay of 3.66% and a gross of 67.51% having a poor to moderate quality and a poor to moderate connectivity. Interval 2303.53 - 2374.85m has an average porosity of 13.8%, 23.8% volume of shale and water saturation of 41.5% as presented in Table 3 and Figure 4.2.1.5.Therefore, interval 2303.53-2374.85m unit of E-S5 has portions that contain hydrocarbons or pay flags as seen in Figure 4.2.1.5.

TABLE. 3: Summary of calculated reservoir pay parameters for Well E-S5.

| Zone | Name | Top (m) | Bottom (m) | Gross | Net | N/G | Av Phi | Av Vcl | Av Sw |
|------|------|---------|------------|-------|------|-------|--------|--------|-------|
| 1 | Reservoir 1 | 2303.53 | 2374.85 | 67.51 | 3.66 | 0.054 | 0.138 | 0.238 | 0.415 |
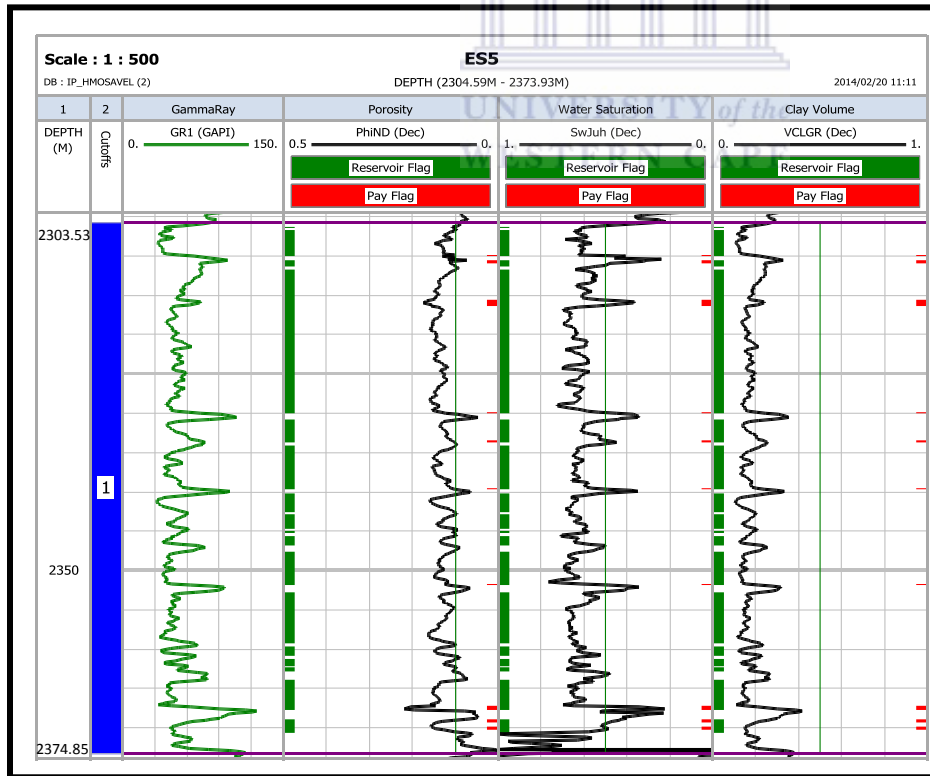


*Figure. 4.2.1.5. Well E-S5 showing calculated reservoir parameters and pay flags from 2303.59-2374.85m.*

**WELL F-AH4:**

Two reservoir units were encountered in Well F-AH4, in intervals 1833 - 1877.58m (reservoir one) and 2369.07 - 2430.18m (reservoir two). Reservoir one has an average net pay of 8.84% and a gross of 44.65% indicating a poor to moderate quality and connectivity. This reservoir also has an average porosity of 16.5%, water saturation of 36.3%, and 20.3% volume of shale as presented in Table 4 and Figure 4.2.1.6.

TABLE. 4: Summary of calculated reservoir pay parameters for Well F-AH4.

| Zone | Name | Top (m) | Bottom (m) | Gross | Net | N/G | Av Phi | Av Vcl | Av Sw |
|------|------|---------|-----------|-------|------|-------|--------|--------|-------|
| 1 | Reservoir 1 | 1833 | 1877.58 | 44.65 | 8.84 | 0.198 | 0.165 | 0.203 | 0.363 |
| 2 | Reservoir 2 | 2369.07 | 2430.18 | 59.89 | 55.47 | 0.926 | 0.151 | 0.270 | 0.174 |
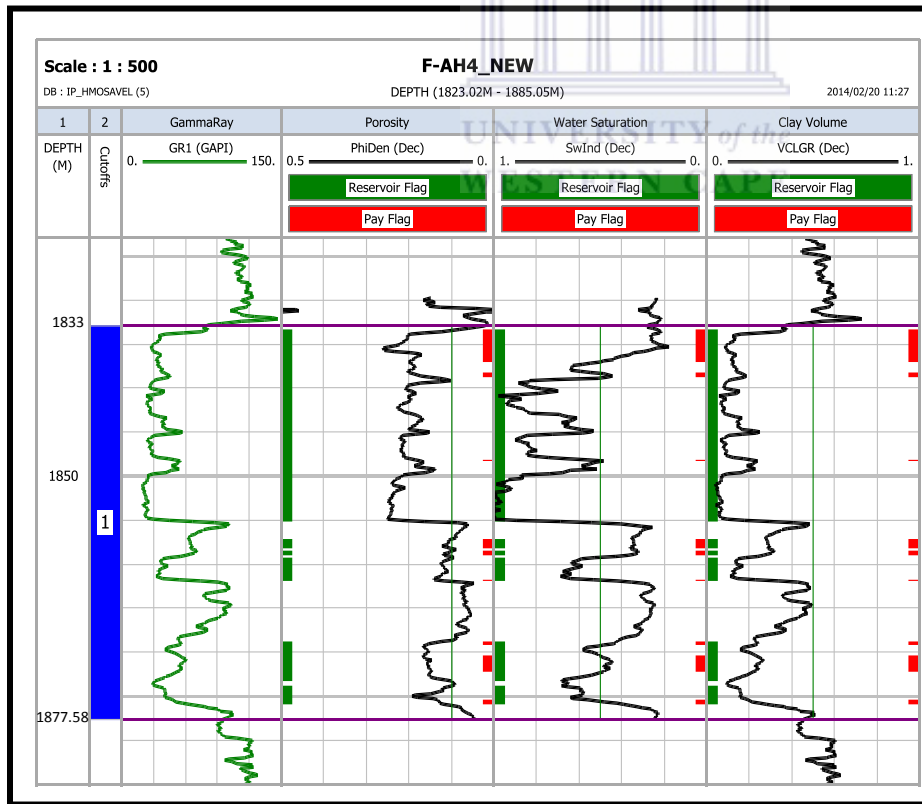


*Figure. 4.2.1.6. Well F-AH4 showing calculated reservoir parameters and pay flags from 1833-1877.58m.*

Reservoir two has an average net pay of 55.47% and a gross of 59.89% having a moderate to good reservoir quality with a moderate to good connectivity. This reservoir has an average porosity of 15.1%, 27.0% volume of shale and water saturation of 17.4% presented in Table 4 and Figure 4.2.1.7 below. Reservoir two also contains economically producible hydrocarbons based on the pay zone as seen in Figure 4.2.1.7.
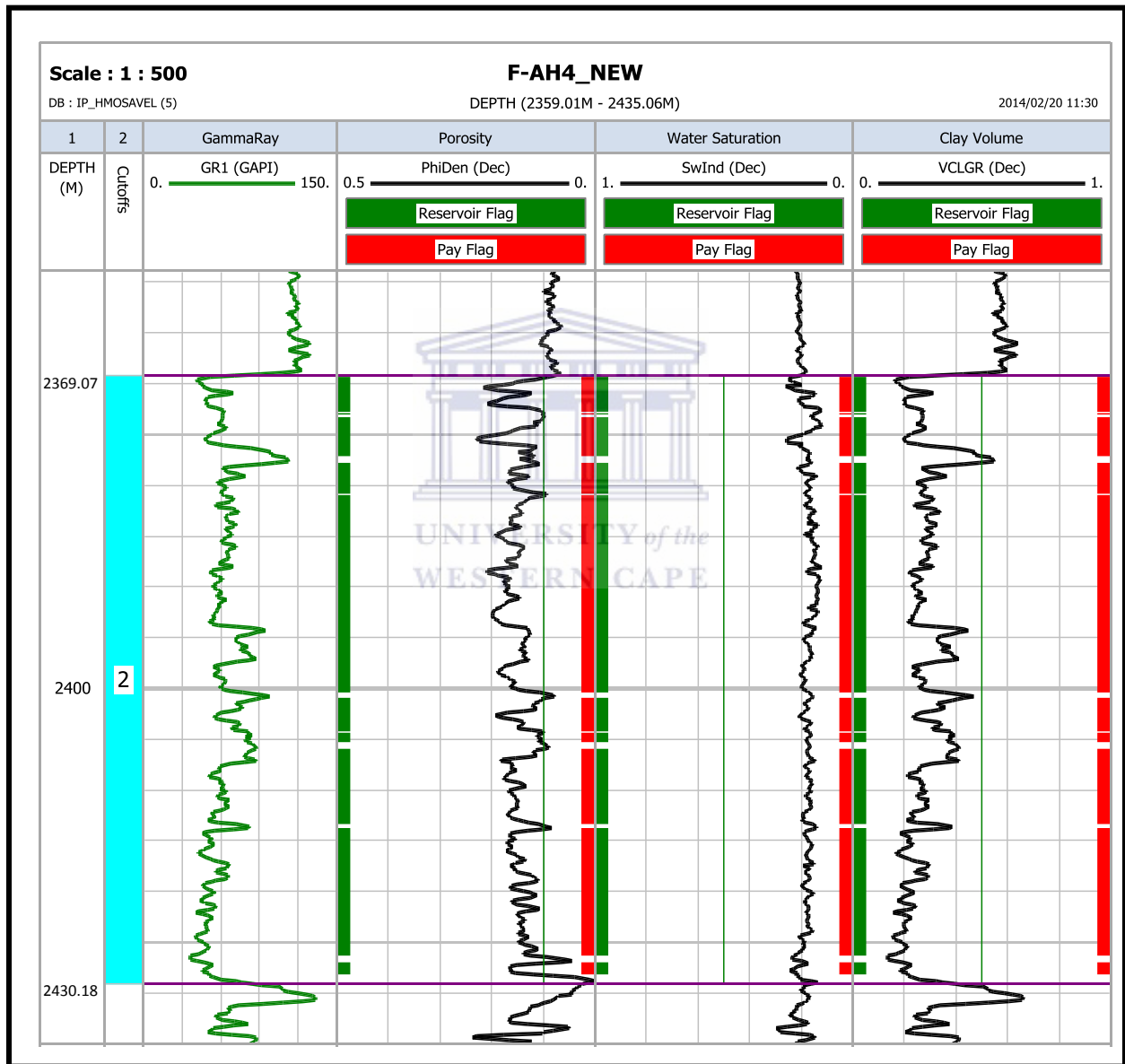


*Figure. 4.2.1.7. Well F-AH4 showing calculated reservoir parameters and pay flags from 2369.07-2430.18m.*

## 4.3 SEISMIC FACIES ANALYSIS

Seismic facies analysis interprets depositional sequences and lithologic features from seismic data (Mitchum et al., 1977). Seismic facies is a set of seismic reflections with features such as amplitude, continuity, configuration and interval velocity that distinguish them from neighbouring sets. The main seismic facies reflection configurations include prograding, variable continuity, divergent and chaotic patterns.

**Well E-S3**

Five different seismic facies were identified from the seafloor to total depth (T.D.) at 2,760m for Well E-S3 (Fig. 4.3.1).  Descriptions of the seismic facies in Figs. 4.3.2 – 4.3.6, give an indication of the prevailing geology, the facies occurrence within the basin, and the probable deposystem (Prather et al., 1998). Seismic facies analysis therefore provides very useful corroborative data in support of well log and core data in the thesis' objective to interpret the depositional environments of the study area.
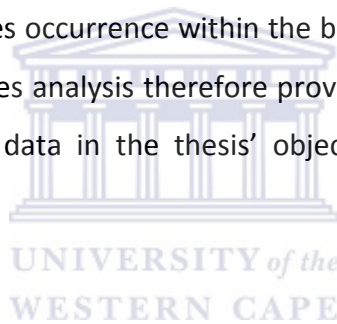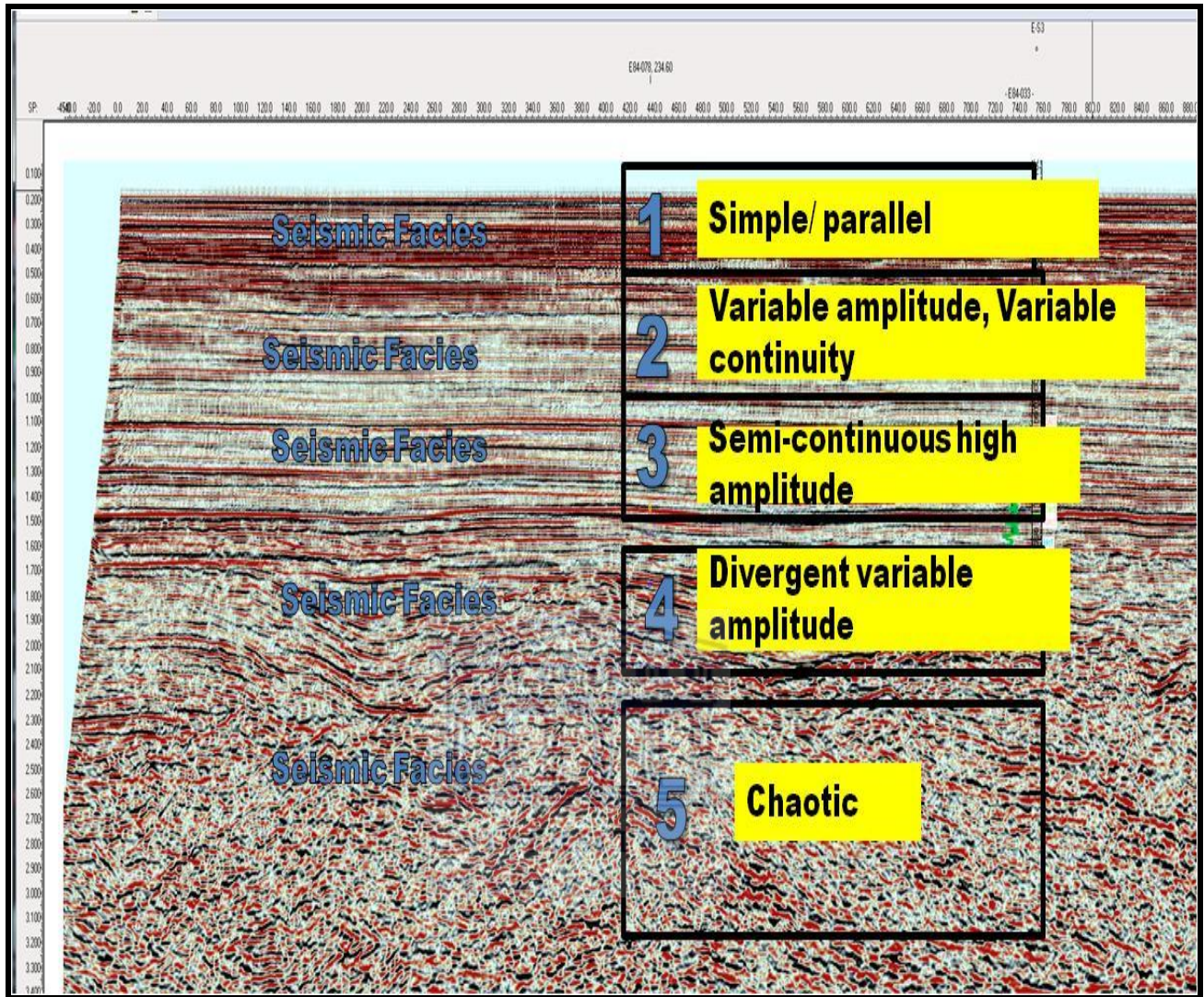
*Figure. 4.3.1. Five different seismic facies identified on 2D seismic data.*

**SEISMIC FACIES, SEISMIC FACIES DESCRIPTION and GEOLOGIC INTERPRETATION OF WELL E-S3 IN THE BREDASDORP BASIN**

Seismic Facies **1** Simple/ Parallel
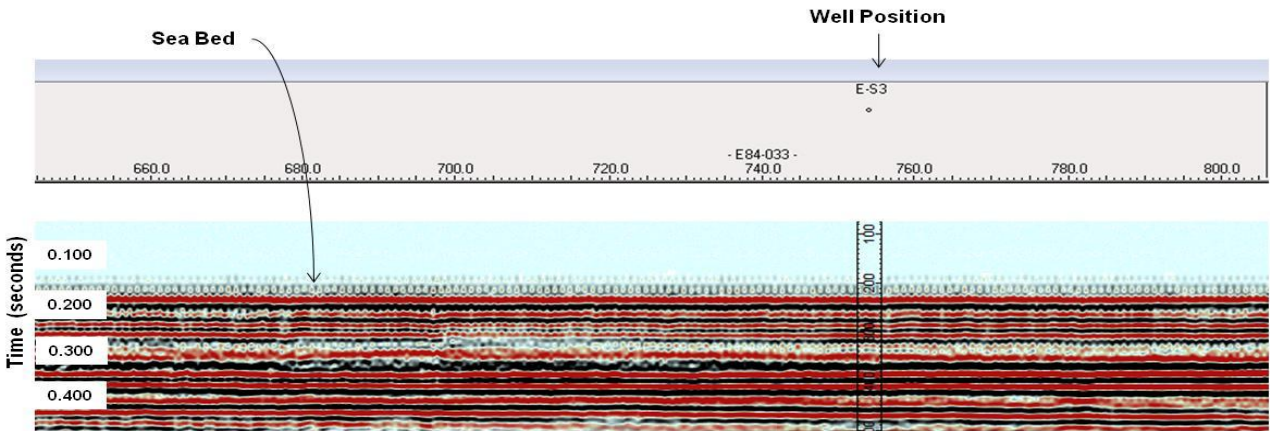
| Seismic Facies | Simple/ parallel |
| --- | --- |
| Seismic Facies Description | Basin aggradation reflection geometry. Change up dip and down dip into parallel high amplitude facies |
| Geologic Interpretation | Near shore sandy deposits |
| Occurrence in Offshore Basin | Mainly in near shoreface environment, representing continental topset deltaic sand sediments. |
| Deposystems | Mud-rich prograding sand lobes |

*Figure. 4.3.2. Parallel facies from 100m until 500m of Well E-S3.*

**SEISMIC FACIES, SEISMIC FACIES DESCRIPTION and GEOLOGIC INTERPRETATION OF WELL E-S3 IN THE BREDASDORP BASIN**

Seismic Facies **2** Variable amplitude, Variable continuity

Well Position

E-S3
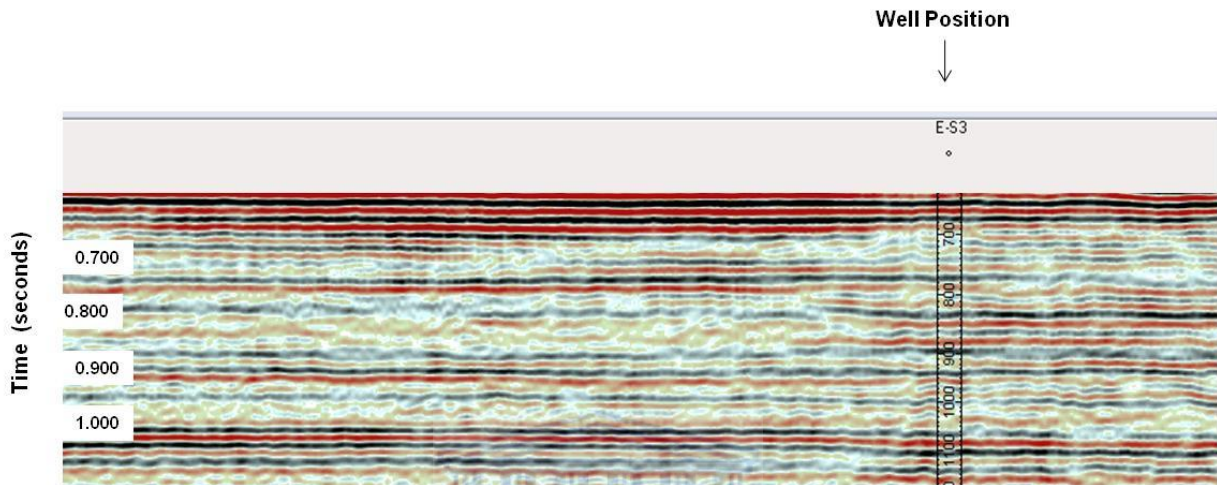
| Seismic Facies | Variable amplitude, Variable continuity |
|---|---|
| Seismic Facies Description | Lateral variation in both amplitude and continuity within a short distance Wedge shaped external configuration |
| Geologic Interpretation | Deltas |
| Occurrence in Offshore Basin | Mainly in more distal environment offshore, representing paralic foreset deltaic sand / shale sediments, including delta front successions |
| Deposystems | Delta |

*Figure. 4.3.3. Variable amplitude facies of 646m until 1149m of Well E-S3.*

SEISMIC FACIES, SEISMIC FACIES DESCRIPTION and GEOLOGIC INTERPRETATION
OF WELL E-S3 IN THE BREDASDORP BASIN

**Seismic Facies** **3** Semi-continuous high amplitude

Mapped Horizon 15At1
equivalent to 1203 m
well depth

Well Position

E-S3

Time (seconds)

1.100
1.200
1.300
1.400

Mapped Horizon 12At1
equivalent to 1756 m
well depth

Sand Bodies
(GR Interpretation)
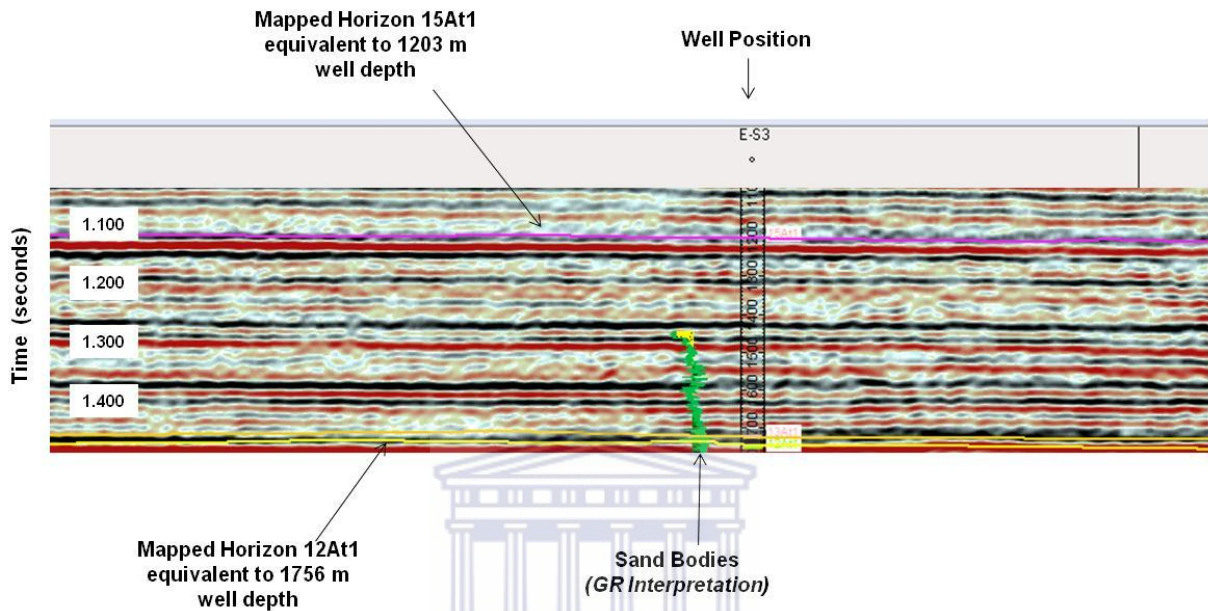
| Seismic Facies | Semi-continuous high amplitude |
|---|---|
| Seismic Facies Description | Sub parallel, semi-continuous high amplitude reflections Concave-up high amplitude reflections are dominant Wedge shaped external configuration |
| Geologic Interpretation | Sand-rich channel/ lobe complexes / Sandy lobe complexes/ claystone |
| Occurrence in Offshore Basin | Mostly in deepening part of basin, possibly near edge of continental shelf. Associated with depocenter. |
| Deposystems | Sand-rich turbiditic channel/lobe complexes/ floodplain |
| Net to Gross | Very poor to poor |
| Connectivity | Very poor to poor |

*Figure. 4.3.4. Semi- continuous facies of 1100m until 1776m of Well E-S3.*

**SEISMIC FACIES, SEISMIC FACIES DESCRIPTION and GEOLOGIC INTERPRETATION OF WELL E-S3 IN THE BREDASDORP BASIN**

Seismic Facies **4** **Divergent variable amplitude**

Mapped Horizon 10At1
equivalent to 1843 m
well depth

Well Position

E-S3

Pre-1At1= Syn rift deposits
Time (seconds)

1.500
1.600
1.700
1.800

Mapped Horizon 1At1
equivalent to 2341m
well depth

Sand Bodies
*(GR Interpretation)*
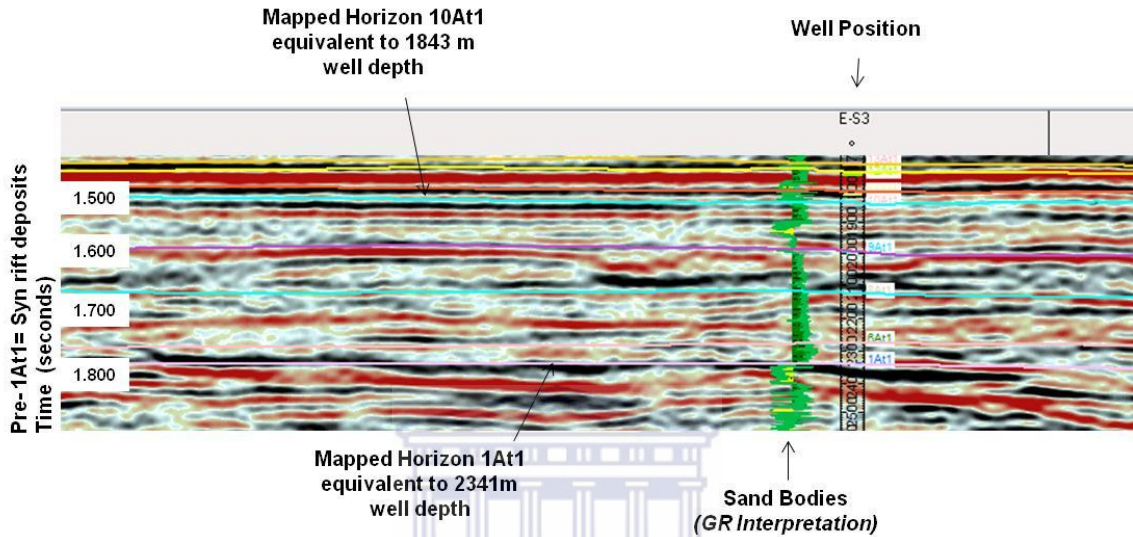
| Seismic Facies | **Divergent variable amplitude** |
|---|---|
| Seismic Facies Description | Wedge-shaped in dip view and mounded-shaped in strike view Sub parallel variable amplitude reflections |
| Geologic Interpretation | Channel/overbank –lobe complexes (fine to coarse sediments) |
| Occurrence in Offshore Basin | Mainly in more distal environment offshore, representing shale sediments |
| Deposystems | Channel/over bank-lobe complexes/ mass transport in turbidite systems |
| Net to Gross | Poor to moderate |
| Connectivity | Poor to moderate |

*Figure. 4.3.5. Divergent variable amplitude facies of 1697m until 2560m.*

SEISMIC FACIES, SEISMIC FACIES DESCRIPTION and GEOLOGIC INTERPRETATION
OF WELL E-S3 IN THE BREDASDORP BASIN

**Seismic Facies** **5** **Chaotic**

Mapped Horizon 6At1
equivalent to 2277 m
well depth

Well Position

E-S3

Mapped Horizon D
equivalent to 2732 m
well depth

Sand Bodies
*(GR Interpretation)*
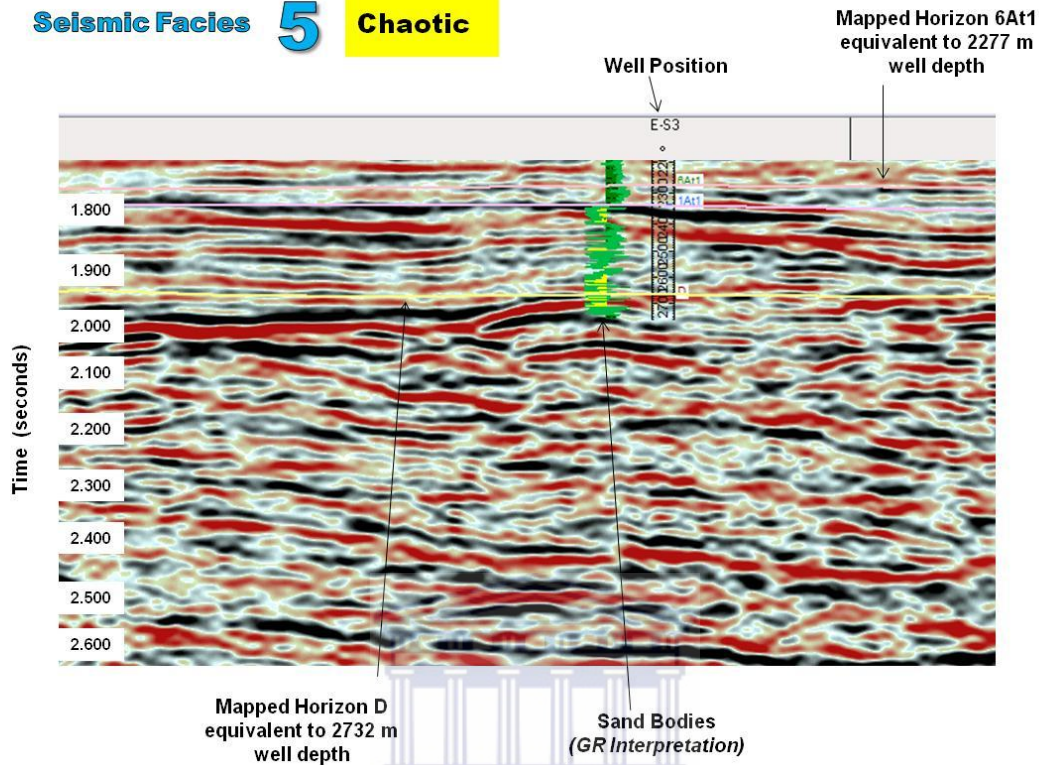
**Seismic Facies** **Chaotic**

| | |
|---|---|
| **Seismic Facies Description** | Disorganized, discontinuous, high or low amplitude reflections with mounded external configuration |
| **Geologic Interpretation** | Syn- rift deposits of the Basin pre- 1At1 (fine to coarse sediments) |
| **Occurrence in Offshore Basin** | In most distal part of study area during geological past. Deep basin margins or on flanks of submarine fans. |
| **Deposystems** | Slump, debris flow, creep, floodplain |
| **Net to Gross** | Poor to moderate |
| **Connectivity** | Poor to moderate |

*Figure. 4.3.6. Chaotic facies of 2191m until 2754m of Well E-S3.*

**Well E-S5**

Five different seismic facies were identified from the seafloor to T.D at 2,692m for Well E-S5 (Fig. 4.3.7). Descriptions of the seismic facies in Figs. 4.3.8 – 4.3.12, give an indication of the existing geology and the facies occurrence within the basin.
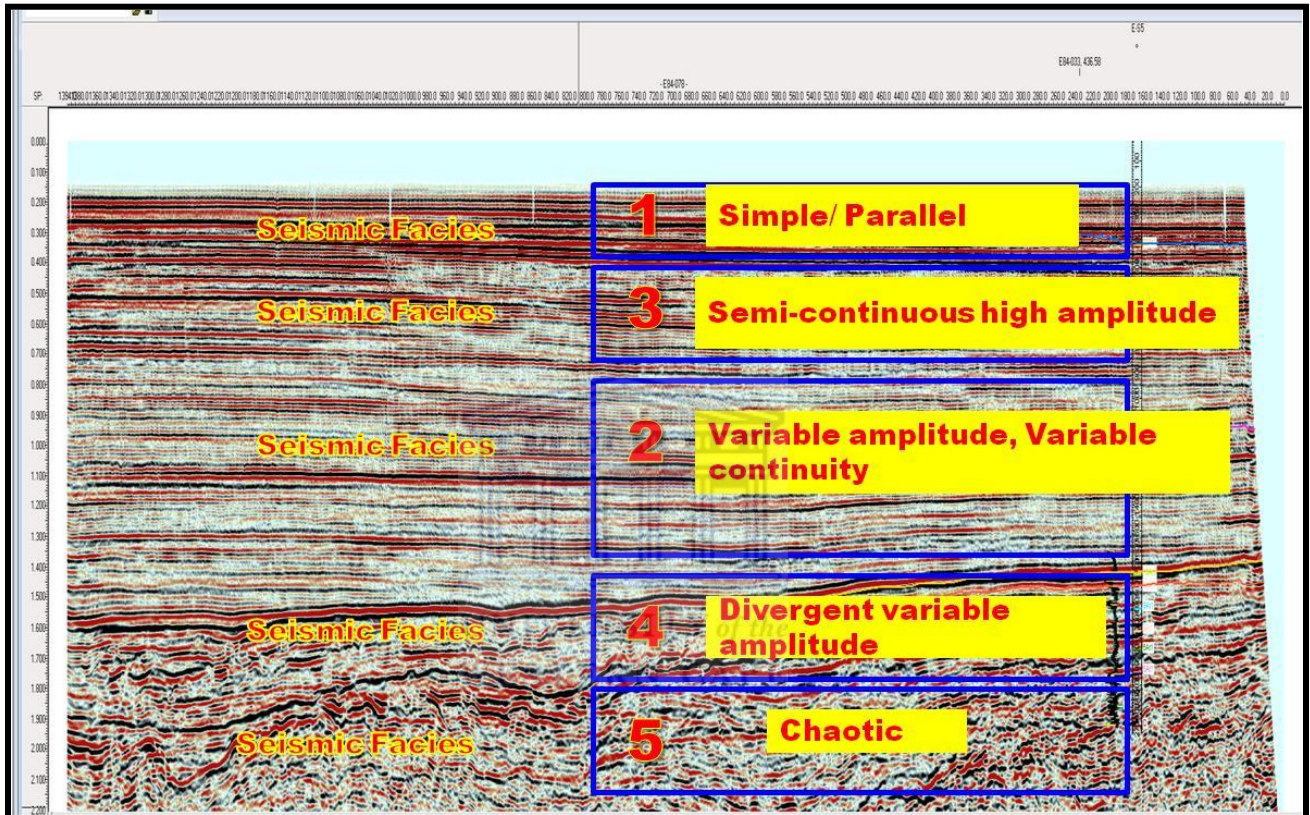


*Figure. 4.3.7. Five different seismic facies of Well E-S5 identified on 2D seismic data.*

## SEISMIC FACIES, SEISMIC FACIES DESCRIPTION and GEOLOGIC INTERPRETATION OF WELL E-S5 IN THE BREDASDORP BASIN

**Seismic Facies** **1** **Simple/ parallel**
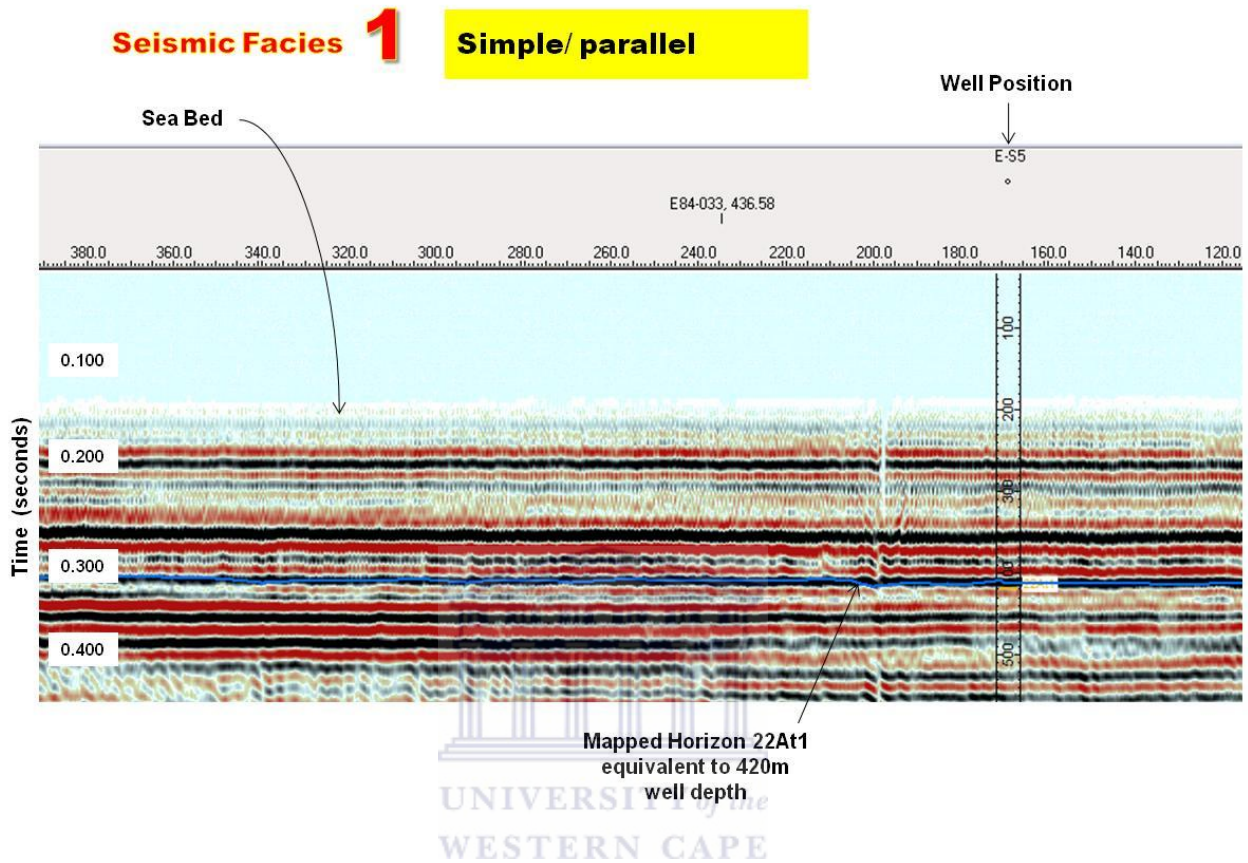


| Seismic Facies | Single/ parallel |
|---|---|
| Seismic Facies Description | Basin aggradation reflections geometry. Change up dip and down dip into parallel low amplitude facies |
| Geologic Interpretation | Near shore sandy deposits |
| Occurrence in Offshore Basin | Mainly in near shoreface environment, representing continental topset deltaic sand sediments. |
| Deposystems | Mud-rich prograding sand lobes |

*Figure. 4.3.8. Parallel facies from 100m until 636m of Well E-S5.*

**SEISMIC FACIES, SEISMIC FACIES DESCRIPTION and GEOLOGIC INTERPRETATION OF WELL E-S5 IN THE BREDASDORP BASIN**

Seismic Facies  **3**  Semi-continuous high amplitude

Well Position

E-S5

Mapped Horizon 22At1
equivalent to 420 m
well depth
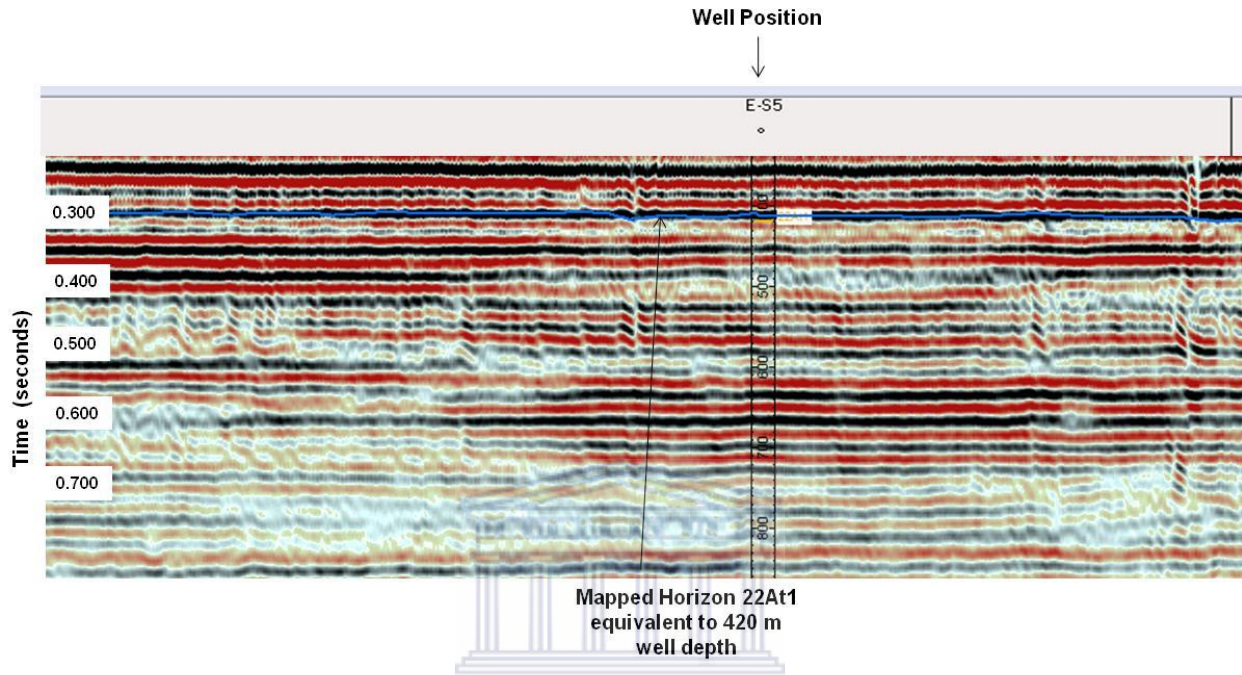
Seismic Facies    Semi-continuous high amplitude

| Seismic Facies Description | Sub parallel, semi-continuous high amplitude reflections Concave-up high amplitude reflections are dominant Wedge shaped external configuration |
| --- | --- |
| Geologic Interpretation | Sand-rich channel/ lobe complexes / Sandy lobe complexes/ delta systems |
| Occurrence in Offshore Basin | Mostly in deepening part of basin, possibly near edge of continental shelf. Associated with depocenter. |
| Deposystems | Sand-rich channel/lobe complexes/ delta systems |

*Figure. 4.3.9. Semi- continuous facies of 322m until 874m of Well E-S5.*

# SEISMIC FACIES, SEISMIC FACIES DESCRIPTION and GEOLOGIC INTERPRETATION OF WELL E-S5 IN THE BREDASDORP BASIN

**Seismic Facies** **2** **Variable amplitude, Variable continuity**
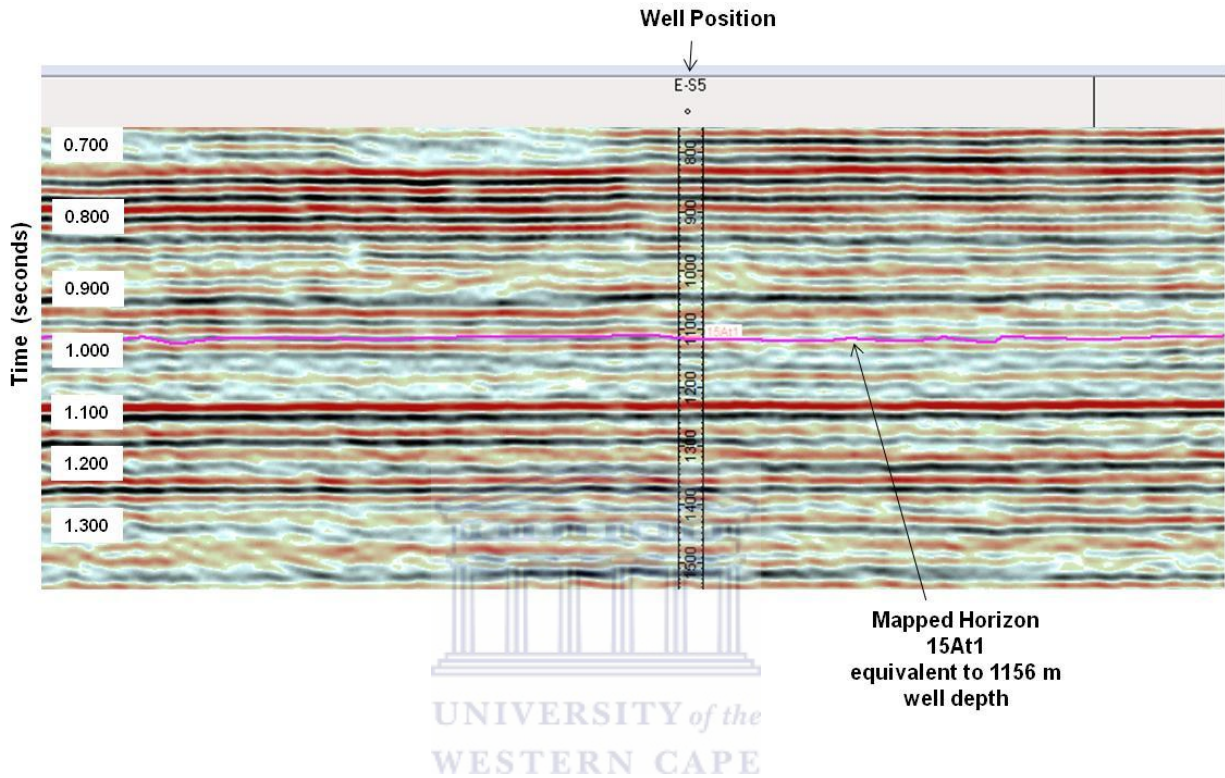


| Seismic Facies | Variable amplitude, Variable continuity |
|---|---|
| Seismic Facies Description | Lateral variation in both amplitude and continuity within a short distance Wedge shaped external configuration |
| Geologic Interpretation | Turbidite systems |
| Occurrence in Offshore Basin | Mainly in more distal environment offshore, representing paralic foreset deltaic sand / shale sediments. |
| Deposystems | Turbidite systems |

*Figure. 4.3.10. Variable amplitude facies of 733m until 1564m of Well E-S5.*

SEISMIC FACIES, SEISMIC FACIES DESCRIPTION and GEOLOGIC INTERPRETATION
OF WELL E-S5 IN THE BREDASDORP BASIN

**Seismic Facies** **4** Divergent variable amplitude

Mapped Horizon 12At1
equivalent to 1895 m
well depth

Well Position

E-S5

E84-033, 436.58

240.0    220.0    200.0    180.0    160.0

Time (seconds)
1.500
1.600
1.700

Sand Bodies
(GR Interpretation)

Mapped Horizon 6At1
equivalent to 2178m
well depth

UNIVERSITY of the
WESTERN CAPE
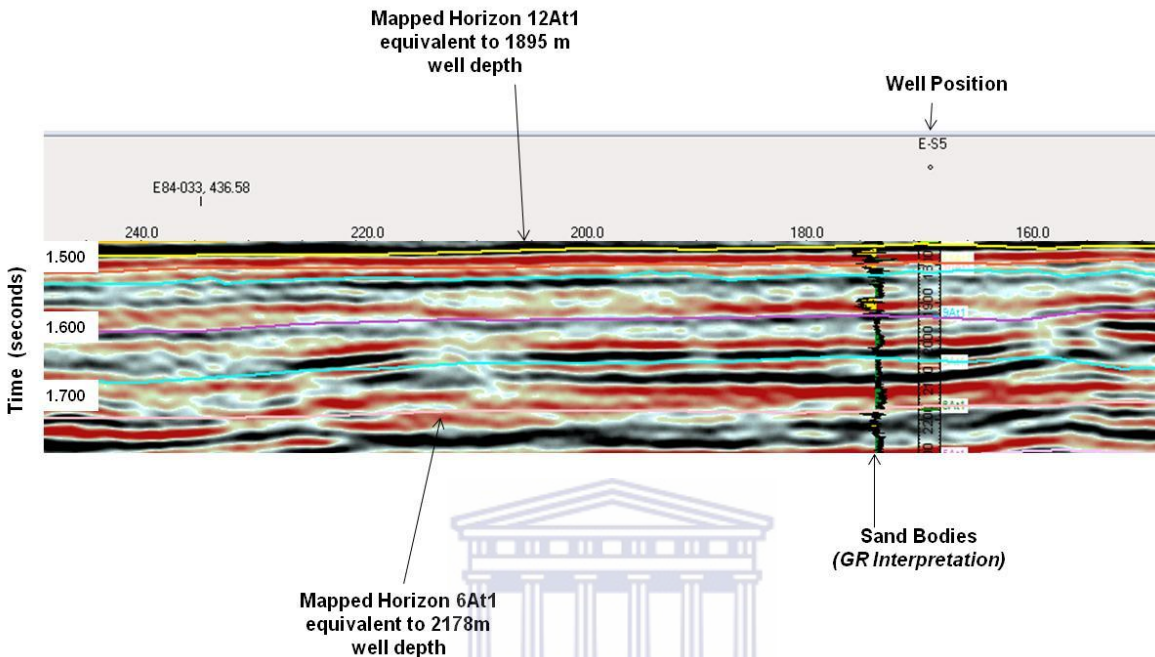
| Seismic Facies | Divergent variable amplitude |
|---|---|
| Seismic Facies Description | Wedge-shaped in dip view and mounded-shaped in strike view Sub parallel variable amplitude reflections |
| Geologic Interpretation | Heterolithic sheet turbidites |
| Occurrence in Offshore Basin | Along more distal parts of deep basin margins. Associated with depocenters |
| Deposystems | Heterolithic sheet turbidites |
| Net to Gross | Poor to moderate |
| Connectivity | Poor to moderate |

*Figure. 4.3.11. Divergent variable amplitude facies of 1732m until 2231m.*

# SEISMIC FACIES, SEISMIC FACIES DESCRIPTION and GEOLOGIC INTERPRETATION OF WELL E-S5 IN THE BREDASDORP BASIN

**Seismic Facies** **5** **Chaotic**



Mapped Horizon D equivalent to 2700 m well depth

Sand Bodies (GR Interpretation)
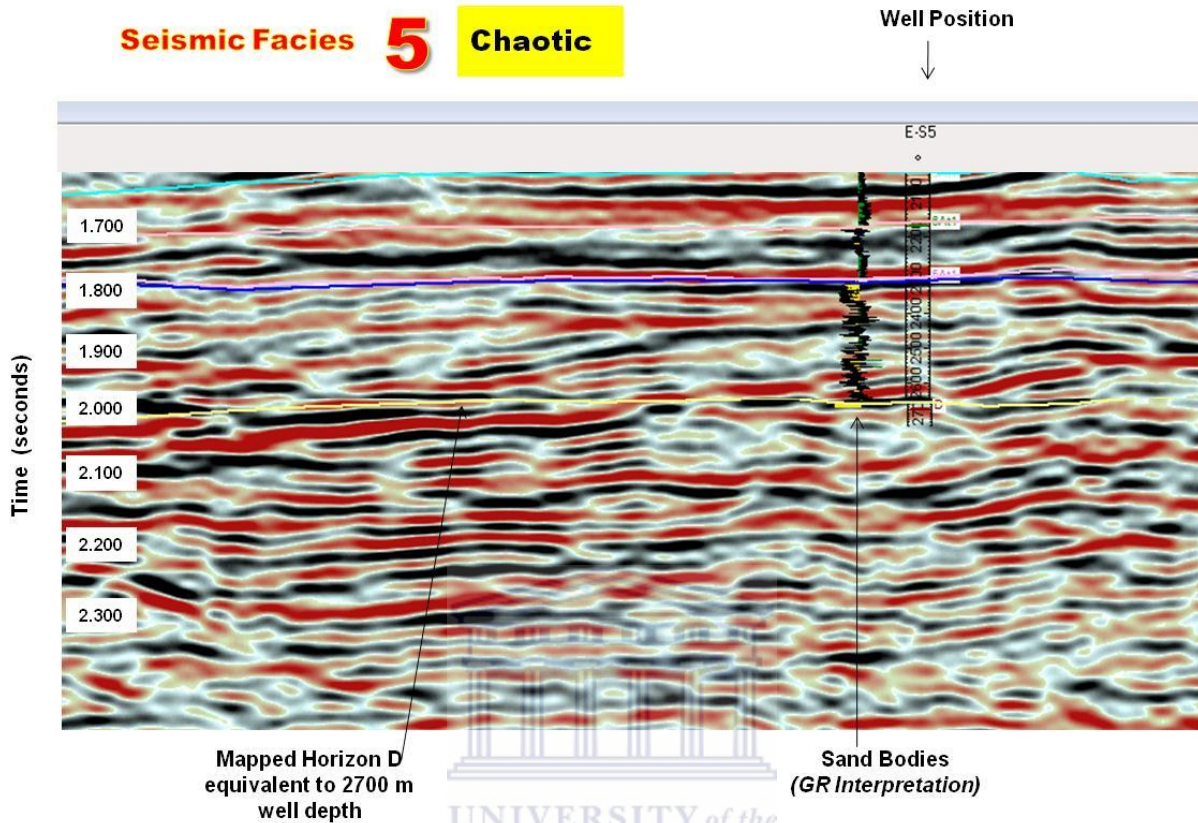
| Seismic Facies | Chaotic |
|---|---|
| Seismic Facies Description | Disorganized, discontinuous, high or low amplitude reflections with mounded external configuration |
| Geologic Interpretation | Slump, debris, flow, creep (very fine sediments) |
| Occurrence in Offshore Basin | In most distal part of study area during geological past. Deep basin margins or on flanks of submarine fans. Including Syn-rift deposits of the Basin. |
| Deposystems | Slump, debris flow, creep, floodplain |
| Net to Gross | Extremely poor |
| Connectivity | Extremely poor |

*Figure. 4.3.12. Chaotic facies of 1822m until 2751m of Well E-S5.*

**WELL F-AH4**

Five different seismic facies were identified from the seafloor to total depth (T.D.) at 2,670m for Well F-AH4 (Fig. 4.3.13). Descriptions of the seismic facies in Figs. 4.3.14 – 4.3.18, give an indication of the facies occurrence within the basin.
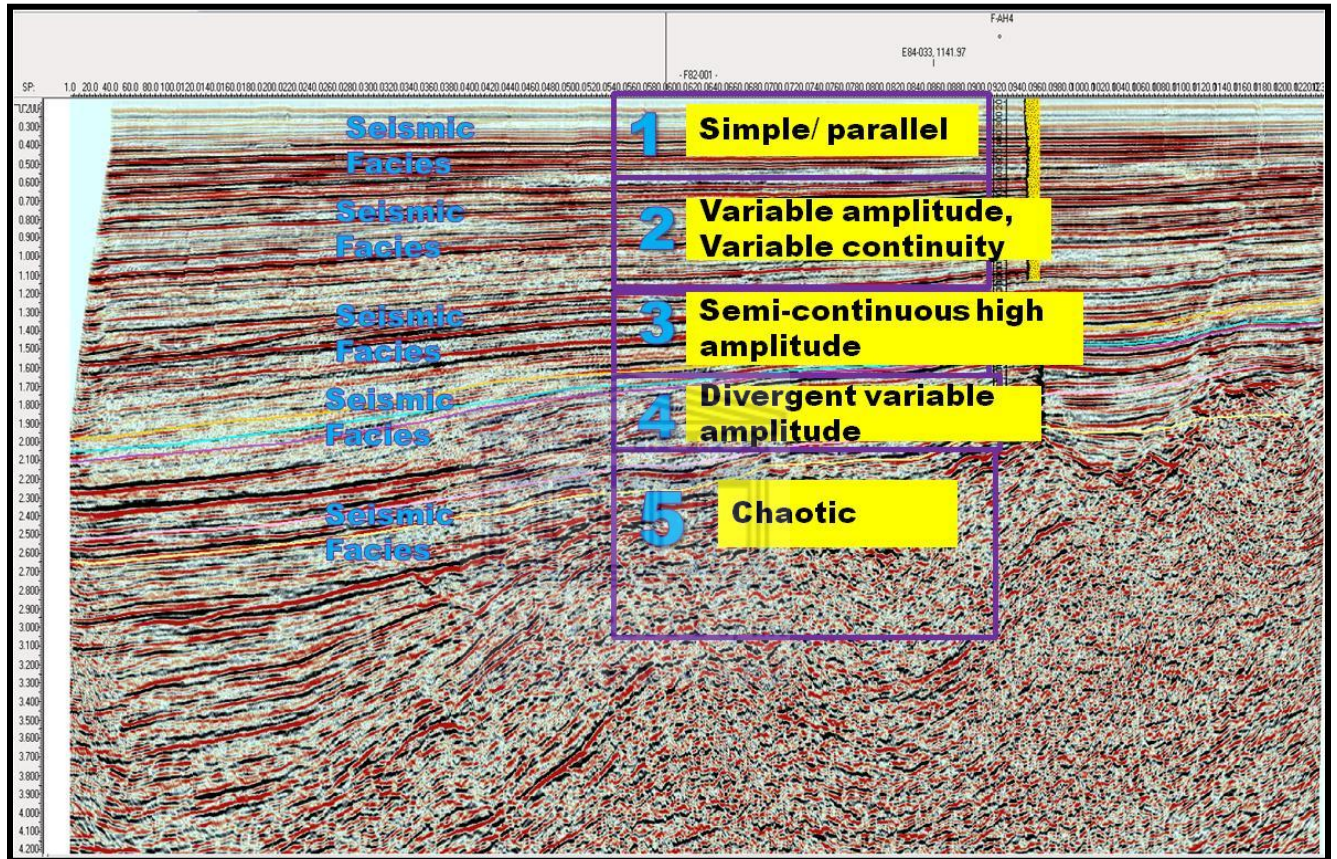


*Figure. 4.3.13. Five different seismic facies of Well F-AH4 identified on 2D seismic data.*

**SEISMIC FACIES, SEISMIC FACIES DESCRIPTION and GEOLOGIC INTERPRETATION OF WELL F-AH4 IN THE BREDASDORP BASIN**

Seismic Facies **1**  Simple/ parallel
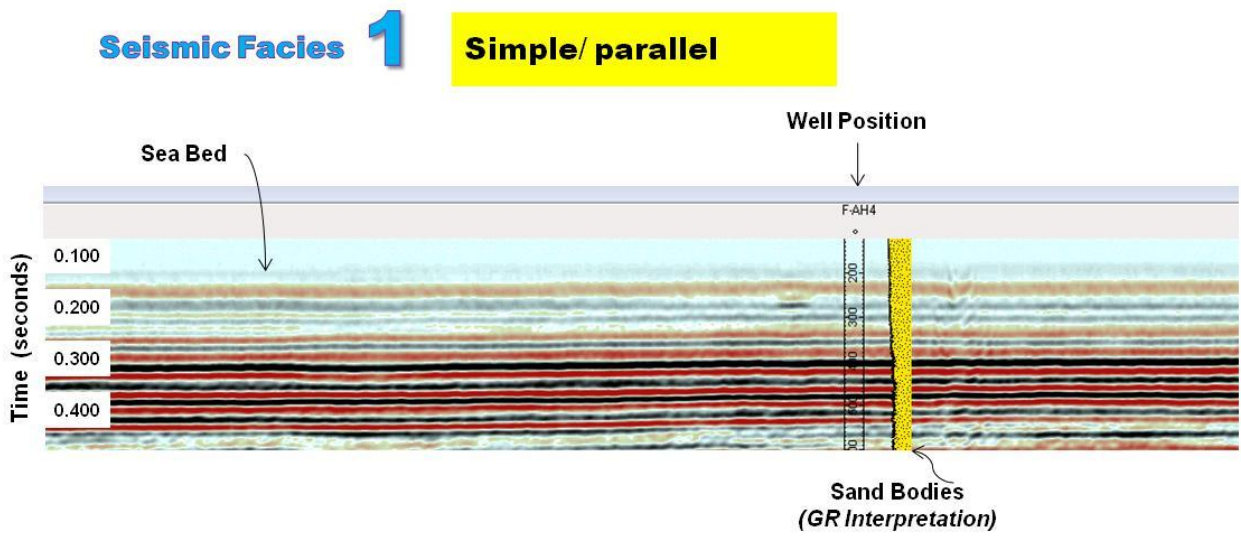
| Seismic Facies | Simple/ parallel |
|---|---|
| Seismic Facies Description | Basinward progradation reflections geometry. Change up dip and down dip into parallel low amplitude facies |
| Geologic Interpretation | Sand-rich prograding lobes. Near shore deposits |
| Occurrence in Offshore Basin | Mainly in near shoreface environment, representing continental topset deltaic sand sediments. |
| Deposystems | Mud-rich prograding sand lobes |

*Figure. 4.3.14. Parallel facies from 106m until 572m of Well F-AH4.*

## SEISMIC FACIES, SEISMIC FACIES DESCRIPTION and GEOLOGIC INTERPRETATION OF WELL F-AH4 IN THE BREDASDORP BASIN

**Seismic Facies** **2** Variable amplitude, Variable continuity
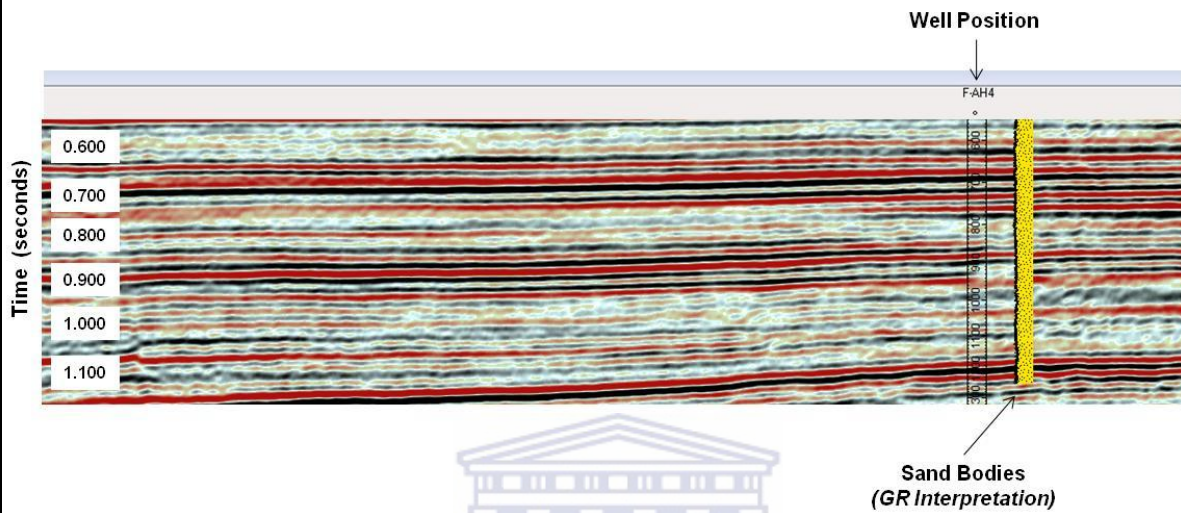


**Seismic Facies** Variable amplitude, Variable continuity

| | |
|---|---|
| **Seismic Facies Description** | Lateral variation in both amplitude and continuity within a short distance Wedge shaped external configuration |
| **Geologic Interpretation** | Channel/over bank- lobe complexes/ mass transport (fine to medium sediments) |
| **Occurrence in Offshore Basin** | Mainly in more distal environment offshore, representing paralic foreset deltaic sand / shale sediments. Including delta front. |
| **Deposystems** | Channel/over bank-lobe complexes/ mass transport . Probable delta systems |
| **Net to Gross** | Moderate to good |
| **Connectivity** | Moderate to good |

*Figure. 4.3.15. Variable amplitude facies of 558m until 1283m of Well F-AH4.*

**SEISMIC FACIES, SEISMIC FACIES DESCRIPTION and GEOLOGIC INTERPRETATION OF WELL F-AH4 IN THE BREDASDORP BASIN**

Seismic Facies **3** Semi-continuous high amplitude

Mapped Horizon 13At1 equivalent to 1685 m well depth

Well Position

F-AH4

Time (seconds)

1.300
0.400
1.500

Mapped Horizon 9At1 equivalent to 1880 m well depth

Sand Bodies *(GR Interpretation)*
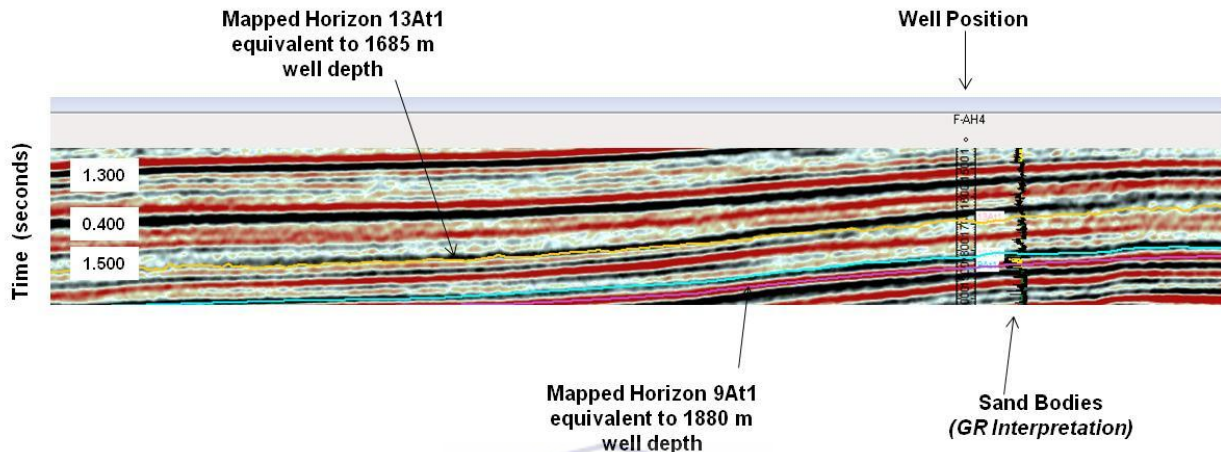
| Seismic Facies | Semi-continuous high amplitude |
| --- | --- |
| Seismic Facies Description | Sub parallel, semi-continuous high amplitude reflections Concave-up high amplitude reflections are dominant Wedge shaped external configuration |
| Geologic Interpretation | Sand-rich channel/ lobe complexes / Delta systems associated with the platform edge(fine to coarse sediments) |
| Occurrence in Offshore Basin | Mostly in deepening part of basin, possibly near edge of continental shelf. Associated with depocenter. |
| Deposystems | Sand-rich channel/lobe complexes |
| Net to Gross | Poor to moderate |
| Connectivity | Poor to moderate |

*Figure. 4.3.16. Semi- continuous facies of 1446m until 1952m of Well F-AH4.*

## SEISMIC FACIES, SEISMIC FACIES DESCRIPTION and GEOLOGIC INTERPRETATION OF WELL F-AH4 IN THE BREDASDORP BASIN

Seismic Facies **4** Divergent variable amplitude
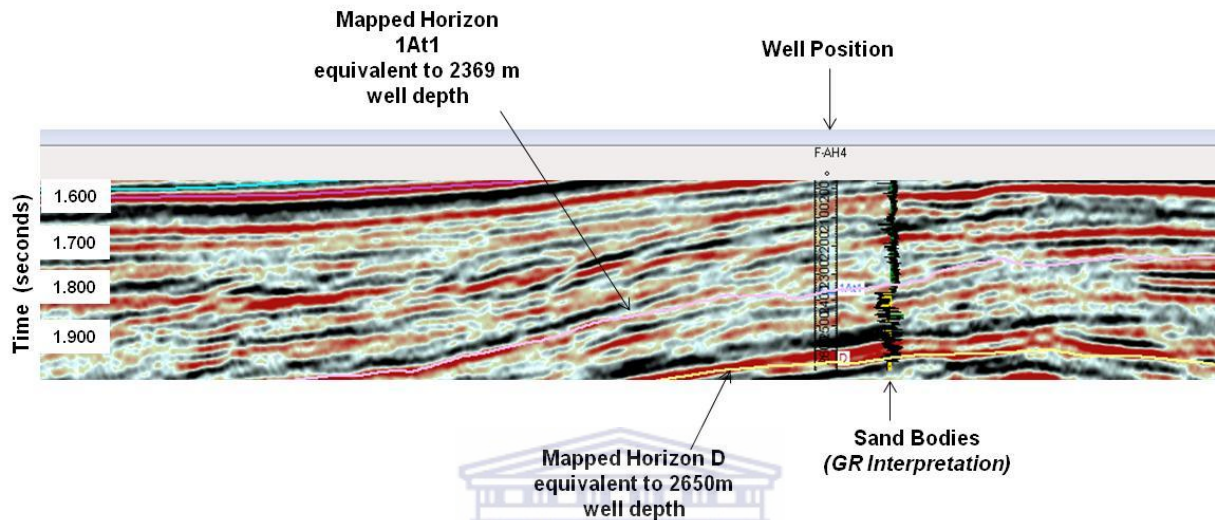


| Seismic Facies | Divergent variable amplitude |
|---|---|
| Seismic Facies Description | Wedge-shaped in dip view and mounded-shaped in strike view Sub parallel variable amplitude reflections |
| Geologic Interpretation | Heterolithic sheet turbidites (fine to medium sediments) |
| Occurrence in Offshore Basin | Along more distal parts of deep basin margins. Associated with depocenters |
| Deposystems | Heterolithic sheet turbidites |
| Net to Gross | Moderate to good |
| Connectivity | Moderate to good |

*Figure. 4.3.17. Divergent variable amplitude facies of 1962m until 2658m.*

# SEISMIC FACIES, SEISMIC FACIES DESCRIPTION and GEOLOGIC INTERPRETATION OF WELL F-AH4 IN THE BREDASDORP BASIN
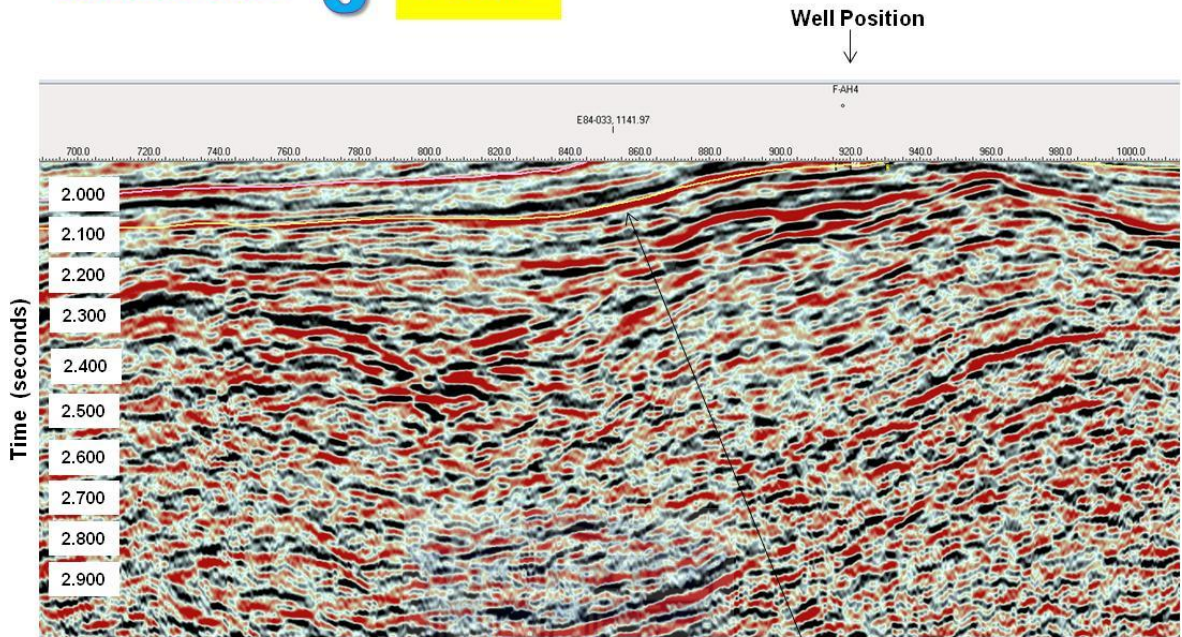
## Seismic Facies 5 — Chaotic



| Seismic Facies | Chaotic |
|---|---|
| Seismic Facies Description | Disorganized, discontinuous, high or low amplitude reflections with mounded external configuration |
| Geologic Interpretation | Slump, debris, flow, creep. Includes the Syn-rift deposits of the Basin (fine to coarse sediments) |
| Occurrence in Offshore Basin | In most distal part of study area during geological past. Deep basin margins or on flanks of submarine fans. |
| Deposystems | Slump, debris flow, creep |
| Net to Gross | Poor to moderate |
| Connectivity | Poor to moderate |

*Figure. 4.3.18. Chaotic facies of 2646m until 2675m of Well F-AH4.*

### 4.3.1 AMPLITUDE AND TIME MAPS

Amplitude and time maps were created for horizon 1At1 for Well E-S3, E-S5 and F-AH4. The maps represent an attribute over a wide area by taking widely spaced points and interpolating between them to fill in the area with no data (Kingdom, 2012).

According to Figure 4.1.1.1 the reservoirs of interest for the three wells fall within supersequence 1At1. High amplitudes indicate sandstone formations and low amplitudes indicate shaly formations as the horizon 1At1 was related to the gamma ray log of each well to indentify the lithology. High amplitudes are shown by the black colour on the seiemic amplitude map (Fig. 4.3.1.1A) for both reservoirs of Wells E-S3 (2350- 2400m) and F-AH4 (2369.07-2430.18m) pointing out sandstone formations. The reservoir of interest for Well E-S5 (2303.53-2374.85m) is situated in an area of low amplitude indicating a shaly formation.

A time map was contoured for horizon 1At1 to get a visual representation of the basin geometry as seen in Figure 4.3.1.1(B). The time map represents depth variation across the horizon pointing out that the basin deepens in a southward direction.
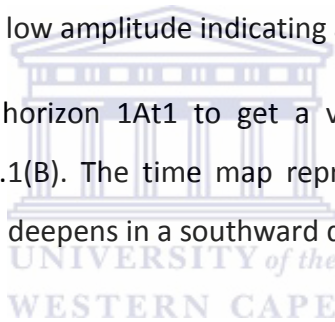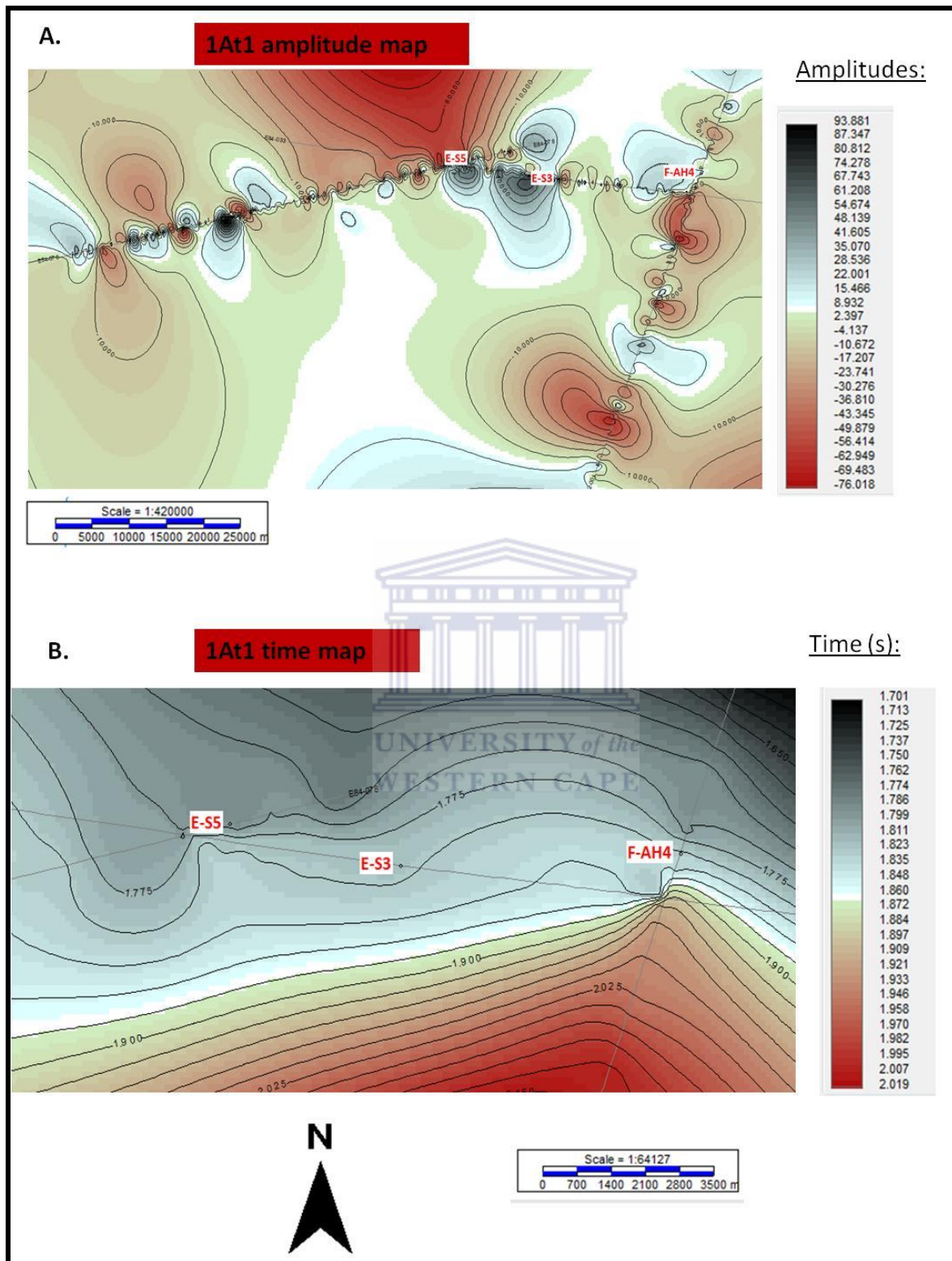
*Figure. 4.3.1.1: A- Generated amplitude map of horizon 1At1 and B- Generated time map of 1At1 horizon.*

Reservoir 1 (1833-1877.58m) of Well F-AH4 lies within supersequence 10At1 (Fig 4.1.1.1) hence an amplitude and time map was created for horizon 10At1. The amplitude map of horizon 10At1 represents the average amplitude values picked along the horizon on the seismic line and joined as a continuous surface interpreted by Kingdom Suite software. In Figure 4.3.1.2(A), Well F-AH4 is situated in the high amplitude area shown by the black colour representing a sandstone formation. Well E-S3 indicates a shaly formation shown by the colour red (low amplitude) and Well E-S5 a sandstone formation as seen in Figure 4.3.1.2(A).

In Figure 4.3.1.2(B) the time map indicates a deepening trend towards the South with sediments prograding basin ward in a southerly direction. Wells E-S3, E-S5 and F-AH4 could possibly be located on a slope of a delta.
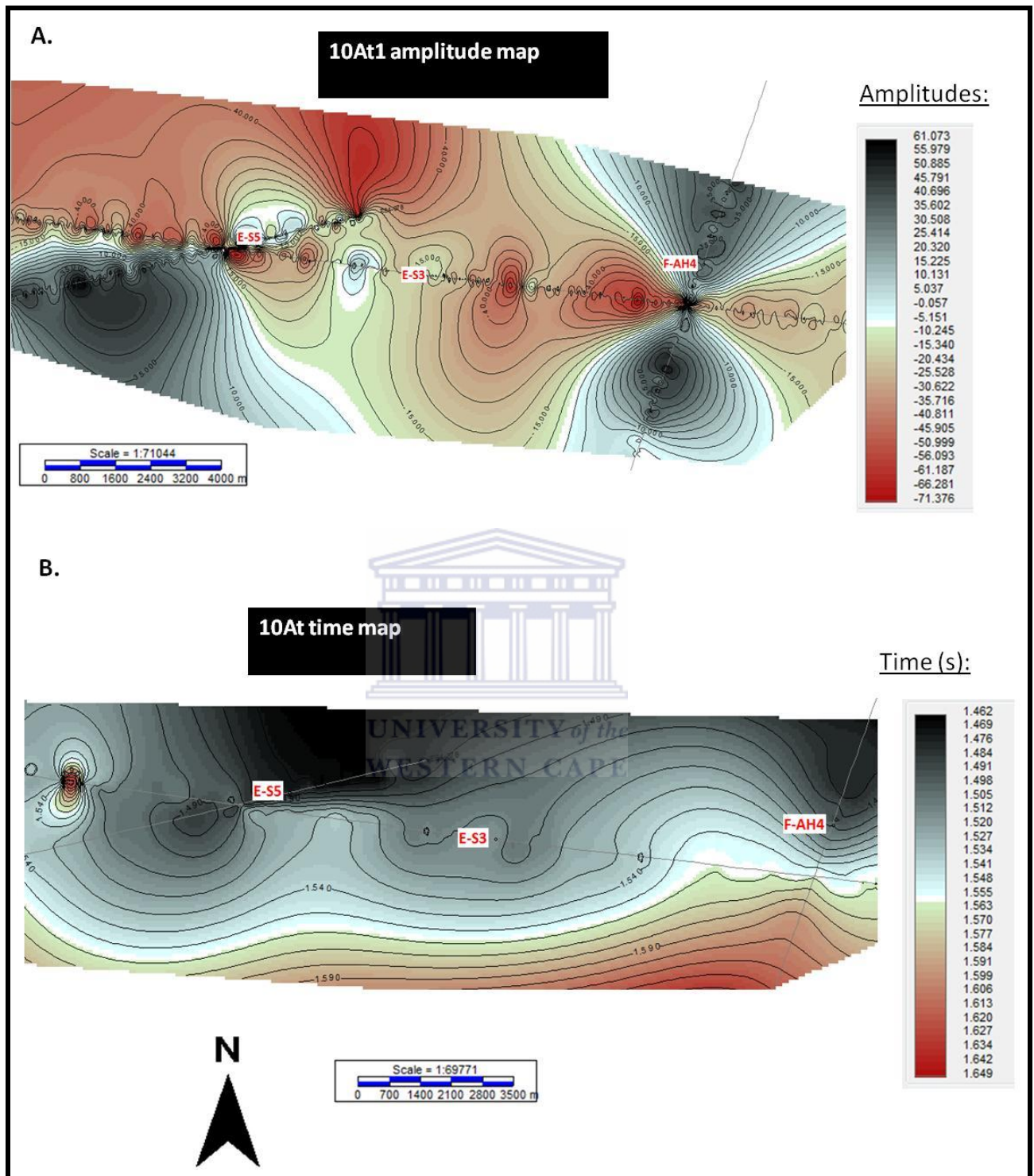
*Figure. 4.3.1.2: A- Generated amplitude map of horizon 10At1 and B- Generated time map of 10At1 horizon.*

## 4.4 CORRELATION ANALYSIS

Correlation analysis was done to see if there is any significant relationship between the wireline logs. The results of correlation analysis for the wireline logs are given in Tables 5, 6 and 7 below for the data of Wells E-S3, E-S5 and F-AH4 respectively. Five wireline logs were used in correlation analysis with a brief summary of each wireline log.

Spontaneous potential (SP) log measures the potential difference in millivolts (mV) between an electrode at the surface and an electrode in the borehole. The SP log points out permeability in a formation and calculates formation water resistivity (Rider, 1996).

The Gamma Ray (GR) log detects in API units radioactivity in a formation by the occurrence of uranium, thorium and potassium. GR is mainly used to identify shale lithologies but could also be used to correlate and identify facies (Rider, 1996).

Density (RHOB) logs measures the formation's bulk density in g/cm$^3$. Bulk density comprises of the density of a rock including the solid matrix as well as the pore fluid (Rider, 1996). Density logs measure porosity and in some way hydrocarbon density. Density logs identify certain minerals in a formation and are good lithology indicators (Rider, 1996).

Neutron (NPHI) log measures the formation's reaction to fast neutron bombardment in neutron porosity units (dec). Formations change neutrons swiftly when they contain many hydrogen nuclei i.e. water ($H_2O$). Thus, neutron logs measures the formation's water content, porosity, lithology and differentiates between oil and gas (Rider, 1996).

Resistivity (SFLU, ILD, MSFL, LLS and LLD) logs measure the formation's resistivity in ohms (ohm.m$^2$/m). Rock materials are mostly insulators and their surrounding fluids are conductors. Hydrocarbons are highly resistive therefore, the main use of resistivity logs is to detect for hydrocarbons.

- Laterolog shallow (LLS) and laterolog deep (LLD) are the laterologs which are the deepest resistivity logs and measures the virgin formation resistivity. Spherically focused log (SFLU) measures the shallower invaded zone resistivity. LLS, LLD and SFLU are best

used in holes drilled with salt muds compared to the induction tool, induction log deep (ILD), which is the only tool to measure resistivity in boreholes drilled with oil-based mud (Rider, 1996). Micro-spherically focused log (MSFL) measures the flushed zone resistivity and is only used in boreholes with salt muds.

Table 5 below represents the correlation analysis for Well E-S3. Results from this analysis show that the correlation coefficient between GR (gamma ray log) and NPHI (neutron log) is 0.574 indicating a positive relationship. ILD (Induction log deep) shows a high positive correlation with SFLU (spherically focused log) with a correlation coefficient of 0.961. This positive correlation implies that if ILD increases an increase in SFLU is likely. A strong negative relationship exists between NPHI and ILD as well as between NPHI and SFLU with a correlation coefficient of -0.702 and -0.675 respectively (Table. 5). This negative correlation implies that an increase in one variable tends to show a decrease in the other. GR has a negative correlation with ILD and SFLU with correlation coefficient values of -0.225 and -0.121 respectively. The correlation coefficient between NPHI and RHOB (density log) is -0.487, which means RHOB is negatively correlated with NPHI.
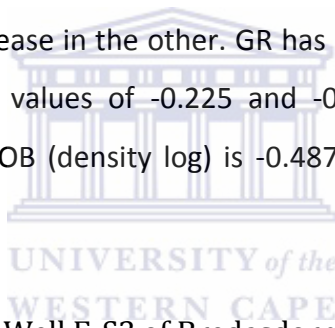
TABLE. 5: Correlation matrix for Well E-S3 of Bredasdorp Basin with units indicated (N=1050).

| Correlations | | | | | |
|---|---|---|---|---|---|
| | GR$^Z$ | ILD$^A$ | NPHI$^R$ | RHOB$^K$ | SFLU$^A$ |
| GR | 1 | | | | |
| ILD | -0.225$^{**}$ | 1 | | | |
| NPHI | 0.574$^{**}$ | -0.702$^{**}$ | 1 | | |
| RHOB | 0.081$^{**}$ | 0.506$^{**}$ | -0.487$^{**}$ | 1 | |
| SFLU | -0.121$^{**}$ | 0.961$^{**}$ | -0.675$^{**}$ | 0.597$^{**}$ | 1 |
| **. Correlation is significant at the 0.01 level (2-tailed). | | | | | |

$^Z$. API
$^A$. ohm m$^2$/m
$^R$. dec
$^K$. g/c$^3$

Table 6 below represents correlation results for Well E-S5. A significant positive relationship exists between GR, ILD, MSFL (micro-spherically focused log), RHOB and SFLU with correlation coefficient values of 0.648, 0.609, 0.729 and 0.715 respectively. ILD shows a positive relationship with MSFL, RHOB and SFLU with relative positive coefficient values of 0.704, 0.841 and 0.907 respectively (Table. 6). A negative relationship exists between ILD and NPHI with correlation coefficient value of -0.480. A negative correlation also exists between MSFL and NPHI with a correlation coefficient of -0.270.The correlation value between NPHI, RHOB and SFLU are -0.349 and -0.384 respectively. HOB shows a high positive relationship with SFLU with a correlation coefficient value of 0.863.

TABLE. 6: Correlation matrix for Well E-S5 of Bredasdorp Basin with units indicated (N=1082).

| Correlations | | | | | | |
|---|---|---|---|---|---|---|
| | $GR^Z$ | $ILD^A$ | $MSFL^A$ | $NPHI^R$ | $RHOB^K$ | $SFLU^A$ |
| GR | 1 | | | | | |
| ILD | 0.648** | 1 | | | | |
| MSFL | 0.609** | 0.704** | 1 | | | |
| NPHI | 0.073* | -0.480** | -0.270** | 1 | | |
| RHOB | 0.729** | 0.841** | 0.748** | -0.349** | 1 | |
| SFLU | 0.715** | 0.907** | 0.813** | -0.384** | 0.863** | 1 |
| **. Correlation is significant at the 0.01 level (2-tailed). | | | | | | |
| *. Correlation is significant at the 0.05 level (2-tailed). | | | | | | |
| $^Z$. API | | | | | | |
| $^A$. ohm m$^2$/m | | | | | | |
| $^R$. dec | | | | | | |
| $^K$. g/c$^3$ | | | | | | |

Table 7 below describes the strength of the relationship between the variables of Well F-AH4. A significant positive relationship exists between LLD (laterolog deep) and LLS (laterolog shallow) wireline logs with a correlation coefficient value of 0.915. GR log has a high positive relationship with NPHI and RHOB with correlation coefficient values of 0.904 and 0.955 respectively. This relationship indicates that if one variable increase then an increase of the other variables mentioned should be expected.

The linear relationship between wireline log variables considered significant for Well E-S3, E-S5 and F-AH4 is further discussed in Chapter 5.

TABLE. 7: Correlation matrix for Well F-AH4 of Bredasdorp Basin with units indicated (N=961).

| | GR$^Z$ | LLD$^A$ | LLS$^A$ | MSFL$^A$ | NPHI$^R$ | RHOB$^K$ |
|---|---|---|---|---|---|---|
| GR | 1 | | | | | |
| LLD | 0.061 | 1 | | | | |
| LLS | 0.017 | 0.915$^{**}$ | 1 | | | |
| MSFL | -0.082$^{*}$ | 0.223$^{**}$ | 0.375$^{**}$ | 1 | | |
| NPHI | 0.940$^{**}$ | 0.064$^{*}$ | 0.013 | -0.125$^{**}$ | 1 | |
| RHOB | 0.955$^{**}$ | 0.081$^{*}$ | 0.028 | -0.116$^{**}$ | 0.987$^{**}$ | 1 |
| *. Correlation is significant at the 0.05 level (2-tailed). | | | | | | |
| **. Correlation is significant at the 0.01 level (2-tailed). | | | | | | |
| $^Z$. API $^A$. ohm m$^2$/m $^R$. dec $^K$. g/c$^3$ | | | | | | |

## 4.5 MULTIVARIATE STATISTICAL ANALYSIS

Multivariate statistics was used to identify possible oil and non-oil bearing depths by the use of two different methods viz factor analysis with discriminant analysis and cluster analysis with discriminant analysis, determining the variables that best separate oil bearing from non-oil bearing depths and how the two methods compare to each other.

Wireline data used in this analyses were obtained from three wells (Well E-S3, E-S5 and F-AH4). Five logs were used with an average of 1031 sample data along with their corresponding depth for characterizing oil bearing groups and non- oil bearing groups. The well logs used were: Gamma ray (GR), resistivity (SFLU, ILD, MSFL, LLS, and LLD), neutron (NPHI), density (RHOB) and spontaneous potential (SP).

The gamma ray (GR) log detects the formation's radioactivity and the log is used to determine the shale volume. Resistivity (SFLU, ILD, MSFL, LLS, and LLD) logs measures the formation's resistivity, which is the resistance to the passage of an electric current. Resistivity tools as well as, induction and conductivity tools, measure a formation's ability to conduct an electric current and present the values in a logarithmic scale (Rider, 1996). Rocks are insulators and the fluids they contain are conductors. Hydrocarbons are highly resistive, while salt water has low resistivity (Rider, 1996). Resistivity logs are, therefore mainly used to determine hydrocarbon vs. water-bearing zones of a formation. The density log is used mainly to calculate porosity, acoustic impedance and hydrocarbon density. The neutron log is associated with the formation's hydrogen index, hence indicating the hydrogen content. Essentially the neutron log measures the formation's water content. SP logs can be used to calculate formation water resistivity and to specify permeability (Rider, 1996).

## 4.5.1 COMBINATION OF FACTOR ANALYSIS WITH DISCRIMINANT ANALYSIS (METHOD I)

Factor analysis was used to extract hydrocarbon related processes in order to create training samples that are either oil bearing or non- oil bearing samples using factor scores of wireline log data. While discriminant analysis is used to verify and characterize the training samples created through factor analysis and later group the ungrouped samples to their respective groups namely, oil bearing or non-oil bearing.

**WELL E-S3**

Factor analysis was done using five variables (NPHI, GR, ILD, SFLU and RHOB) for Well E-S3. Table 8 below describes the percent of variance of each factor and their Eigen values. Factors with Eigen values $\geq$ 1 were taken into account that resulted in two factors explaining 85.675% of the variance. Factor one is most dominant and describes 61.659% (Table. 8) of total data variability. This factor is highly positively loaded with ILD, SFLU and RHOB logs (Table. 9) and is considered as the oil bearing factor. Factor two describes 23.998% (Table. 8) of total data variability and is positively loaded with NPHI and GR logs and thus considered as non- oil bearing factor (Table 9). Data for the SP log contained negative values therefore was not included in the analysis as it would result in an incorrect interpretation.

TABLE. 8:  Total variance described by each factor for Well E-S3.

| Total Variance Explained | | | | | | | | |
|---|---|---|---|---|---|---|---|---|
| Component | Initial Eigen values | | | Extraction Sums of Squared Loadings | | | Rotation Sums of Squared Loadings | | |
| | Total | % of Variance | Cumulative % | Total | % of Variance | Cumulative % | Total | % of Variance | Cumulative % |
| 1 | 3.083 | 61.659 | 61.659 | 3.083 | 61.659 | 61.659 | 2.782 | 55.632 | 55.632 |
| 2 | 1.200 | 23.998 | 85.657 | 1.200 | 23.998 | 85.657 | 1.501 | 30.025 | 85.657 |
| 3 | 0.521 | 10.429 | 96.086 | | | | | | |
| 4 | 0.166 | 3.323 | 99.410 | | | | | | |
| 5 | 0.030 | 0.590 | 100.000 | | | | | | |

TABLE. 9:  Rotated component matrix of Well E-S3.

| Rotated component matrix | | |
|---|---|---|
| | Component | |
| | Factor one - Oil bearing | Factor two - Non-oil Bearing |
| SFLU | 0.939 | |
| ILD | 0.889 | |
| RHOB | 0.814 | |
| NPHI | -0.668 | 0.653 |
| GR | | 0.971 |

In order to differentiate oil bearing from non-oil bearing depths, box plots were used as shown in Figure 4.5.1.1. A base line at zero is established to distinguish between oil and non-oil bearing. All depths above the base line are considered as oil bearing with high positive loadings in SFLU, ILD and RHOB while all depths below the base line are considered as non- oil bearing with high positive loadings in NPHI and GR. The depth between intervals 2308.70 to 2339.18m and 2346.80 to 2430.32m is a possible reservoir for Well E-S3. According to the well description report of Well E-S3 depths between 2308.70 to 2339.18m relates to shallow marine sandstone bodies while depths between 2346.80 to 2430.32m relates to sandstone bodies with interbedded red claystone and green siltstone.
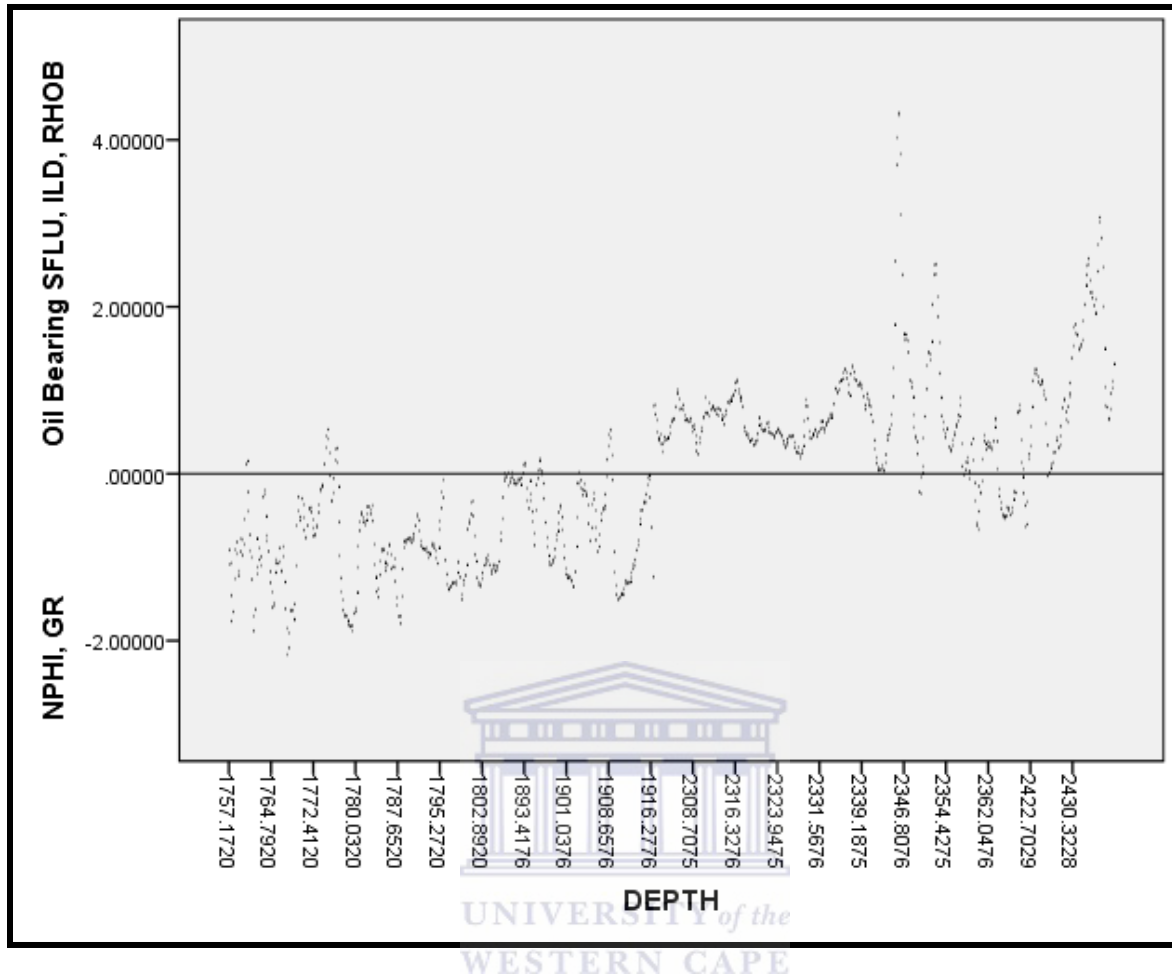
*Figure. 4.5.1.1.Box Plot of oil bearing depths for Well E-S3.*

**Linear discriminant analysis**

To verify and characterize the created training samples through factor analysis, discriminant analysis was carried out using the wireline log data. Since there are only two groups resulting from factor analysis, only one discriminant function was created (Table 10). Table 10 relates the wireline log variables to the discriminant function while Table 11 relates the possible oil and non-oil bearing depths to the discriminant function. Tables 10 and 11 were then used to differentiate the oil and non-oil bearing depths. The discriminant function has positive loadings for NPHI and GR with negative loadings for SFLU, ILD and RHOB that separates the oil bearing from the non- oil bearing depths. Oil bearing depths are highly negatively correlated with the

discriminant function, while the non-oil bearing depths or layers are positively correlated with the discriminant function (Table. 11).

TABLE. 10:  Structure matrix of Well E-S3.

| Structure Matrix | |
|---|---|
| | Function |
| | 1 |
| NPHI | 0.927 |
| GR | 0.504 |
| RHOB | -0.500 |
| SFLU | -0.463 |
| ILD | -0.390 |

TABLE. 11:  Functions at group centroids for Well E-S3.

| Functions at Group Centroids | |
|---|---|
| Depth types | Function |
| | 1 |
| Possible oil bearing | -1.537 |
| Possible non-oil bearing | 3.743 |

TABLE. 12: Classification of oil and non-oil groups of Well E-S3.

| Classification Results[a] | | | | | |
|---|---|---|---|---|---|
| | | Training depths | Predicted Group Membership | | Total |
| | | | Oil bearing | Non- oil bearing | |
| Original | Count | Oil bearing | 151 | 0 | 151 |
| | | Non- oil bearing | 0 | 62 | 62 |
| | | Ungrouped cases | 495 | 342 | 837 |
| | % | Oil bearing | 100.0 | 0.0 | 100.0 |
| | | Non- oil bearing | 0.0 | 100.0 | 100.0 |
| | | Ungrouped cases | 59.1 | 40.9 | 100.0 |
| [a]. 100.0% of original grouped cases correctly classified. | | | | | |

The training depths for oil and non-oil bearing depths were 100% correctly classified (Table. 12). Once the oil-bearing and non oil-bearing training depths were characterized, the remaining ungrouped depths were either grouped to oil-bearing or non oil-bearing depths or layers (Table. 12). In order to classify the ungrouped depths, the discriminant function created through the training depths using the wireline logs were used to classify the ungrouped depths either oil or non-oil bearing depths. Therefore according to the classification results, the depths were 96.7% correctly classified (Table. 13).

TABLE. 13: Classification results of samples containing oil or no oil from Well E-S3.

| Classification Results[a] | | | | | |
|---|---|---|---|---|---|
| | | Training depths | Predicted Group Membership | | Total |
| | | | Oil-bearing | Non- oil bearing | |
| Original | Count | Oil-bearing | 656 | 17 | 673 |
| | | Non-oil bearing | 18 | 359 | 377 |
| | % | Oil- bearing | 97.5 | 2.5 | 100.0 |
| | | Non-oil bearing | 4.8 | 95.2 | 100.0 |
| a. 96.7% of original grouped cases correctly classified. | | | | | |

The descriptive statistics of the oil and non-oil bearing depths in Table 14 shows that the oil bearing depth has the highest mean value of ILD and SFLU (4.31 and 3.38 ohm m$^2$/m respectively) and a low NPHI mean of 0.159 dec. The oil bearing depth has a low GR mean value indicating a sand body with low hydrocarbon density while the non- oil bearing depth has a high NPHI mean value of 0.241 dec in a sandy shale formation with a low density and porosity (Table.14). The non-oil bearing depths indicate that SFLU (3.118 ohm m$^2$/m) is higher than ILD (3.105 ohm m$^2$/m) which should be the case in non-oil bearing zones.

TABLE. 14: Descriptive statistics for oil and non-oil bearing functions of Well E-S3.

| STATISTICS | | | | | | | | |
|---|---|---|---|---|---|---|---|---|
| LOGS | OIL BEARING | | | | NON-OIL BEARING | | | |
| | Mean | Std. Deviation | minimum | maximum | Mean | Std. deviation | minimum | maximum |
| GR | 68.206 | 24.878 | 22.453 | 235.8750 | 99.422 | 22.776 | 45.218 | 241.750 |
| ILD | 4.3149 | 2.657 | 1.166 | 19.2188 | 3.1052 | 0.952 | 0.947 | 5.265 |
| NPHI | 0.1598 | 0.046 | 0.0142 | .2183 | 0.241 | 0.032 | 0.196 | 0.353 |
| RHOB | 2.471 | 0.0807 | 2.287 | 2.6602 | 2.426 | 0.144 | 1.891 | 2.640 |
| SFLU | 3.389 | 1.402 | 0.39 | 6.67 | 3.1182 | 1.784 | 0.35 | 8.29 |

**Stepwise discriminant analysis**

In order to find the best discriminating wireline log variable between the oil and non-oil bearing depths, stepwise discriminant analysis was considered. In Table15, NPHI and SFLU are the best discriminating wireline log variables between oil and non-oil bearing depths for Well E-S3. NPHI is the best discriminating wireline log variable classifying correctly up to 87.5% while SFLU improves the classification correctly up to 89.4% (Table.15).

TABLE. 15: Classification results of Predictors NPHI and SFLU.

| Variables | Classification |
|---|---|
| NPHI | 87.5% |
| SFLU | 89.4% |

**WELL E-S5**

Factor analysis was used to create training samples for oil and non- oil groups based on the wireline data. For Well E-S5 factor analysis was run on seven variables (SFLU, RHOB, ILD, MSFL, GR, NPHI and SP). Table 16 shows seven factors, their Eigen values and percent of variance for each factor. Factors with Eigen values $\geq 1$ were taken into account hence only two factors resulted in 82.730% of variance. In Table 16 below, factor one describes 60.712% of the total

data variability which is positively loaded with wireline logs SFLU, MSFL, ILD, RHOB and GR (Table. 17) and considered to indicate hydrocarbon. Factor two describes 22.018% (Table. 16) of the total data which is positively loaded with wireline logs NPHI and SP (Table. 17) which is regarded as the non- oil bearing indicator. Data for LLS and LLD logs were not included as the logs contained negative values, which cause the analysis to be incorrect. Once the factors were saved, graphs were selected with legacy dialogs and box plots. The factor variable oil was computed against depth to characterize the number of samples containing oil (Fig.4.5.1.2).

TABLE. 16: Total variance described by each factor of Well E-S5.

| Total Variance Explained | | | | | | | | | |
|---|---|---|---|---|---|---|---|---|---|
| Component | Initial Eigen values | | | Extraction Sums of Squared Loadings | | | Rotation Sums of Squared Loadings | | |
| | Total | % of Variance | Cumulative % | Total | % of Variance | Cumulative % | Total | % of Variance | Cumulative % |
| 1 | 4.250 | 60.712 | 60.712 | 4.250 | 60.712 | 60.712 | 3.964 | 56.629 | 56.629 |
| 2 | 1.541 | 22.018 | 82.730 | 1.541 | 22.018 | 82.730 | 1.827 | 26.101 | 82.730 |
| 3 | 0.569 | 8.122 | 90.852 | | | | | | |
| 4 | 0.256 | 3.661 | 94.513 | | | | | | |
| 5 | 0.171 | 2.444 | 96.958 | | | | | | |
| 6 | 0.153 | 2.179 | 99.136 | | | | | | |
| 7 | 0.060 | 0.864 | 100.000 | | | | | | |
| Extraction Method: Principal Component Analysis. | | | | | | | | | |

TABLE. 17: Rotated component matrix of Well E-S5.

| Rotated Component Matrix[a] | | |
|---|---|---|
| | Component | |
| | Factor 1- Oil Bearing | Factor 2- Non-oil Bearing |
| SFLU | 0.937 | |
| RHOB | 0.905 | |
| MSFL | 0.866 | |
| GR | 0.864 | |
| ILD | 0.858 | -0.402 |
| NPHI | | 0.879 |
| SP | | 0.865 |

Figure 4.5.1.2 indicates small possible oil bearing beds of less than 6m deep at depths of approximately 2302.00 to 2308.09m and 2424.68 to 2427.73m, however below approximately 2311.14m it can be seen that depths drop below the zero line which may be indicate a low hydrocarbon potential or high water content. Comparing the core and well description report of Well E-S5 to the possible oil bearing depths related to a claystone bed (between 2302 to 2308.09m) and a red- green claystone lithology with fine grained sandstone (2424.68 - 2427.73m).
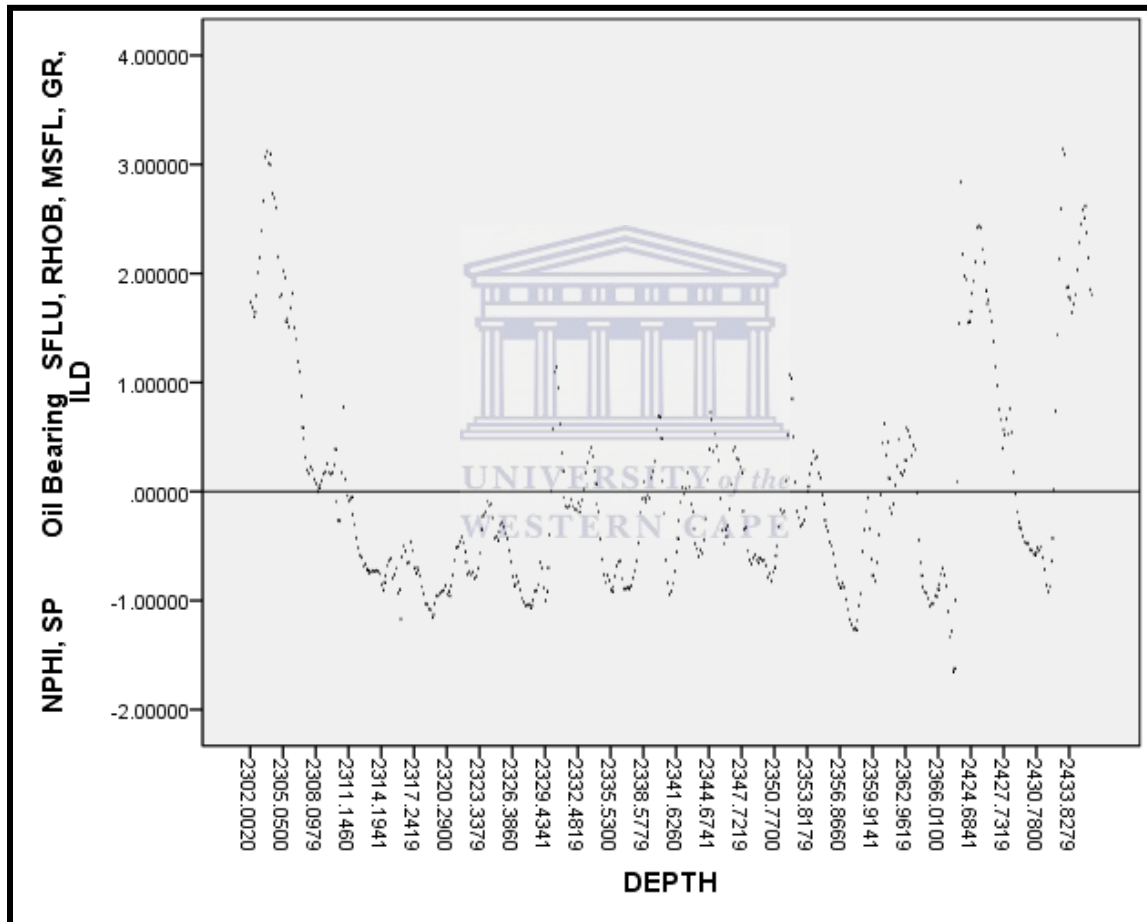


*Figure. 4.5.1.2. Box Plot of oil bearing depths of Well E-S5.*

**Linear discriminant analysis**

To verify and differentiate oil bearing from the non- oil bearing training depths, linear discriminant analysis was used. For the two groups a single discriminant function was extracted

based on the wireline logs. In Table 18, the structured matrix of the function is positively loaded with ILD, SFLU, RHOB, MSFL, and GR and was interpreted as the oil bearing depth, based on the training samples created with factor analysis. Negatively loaded components NPHI and SP (Table. 18) were grouped as non- oil bearing depths (Table. 19).

TABLE. 18: Structure matrix for Well E-S5.

| Structure Matrix | |
|---|---|
| | Function |
| | 1 |
| ILD | 0.812 |
| SFLU | 0.766 |
| RHOB | 0.667 |
| MSFL | 0.648 |
| GR | 0.422 |
| NPHI | -0.338 |
| SP | -0.292 |

TABLE. 19: Functions at group centroids for Well E-S5.

| Functions at Group Centroids | |
|---|---|
| Depth types | Function |
| | 1 |
| Possible oil bearing | 3.051 |
| Possible non-oil bearing | -2.480 |

A hundred and thirteen training samples for oil bearing and a hundred and thirty- nine for non-oil bearing depths or layers were created through factor analysis (Table. 20). Once the training samples were characterized, discriminant analysis was re-run in order to classify the ungrouped depths either oil bearing or non-oil bearing depths. The oil and non-oil bearing depths were 96.2% correctly classified as shown in Table 21.

TABLE. 20: Classification of oil and non- oil groups of Well ES-5.

| Classification Results[a] | | | | | |
|---|---|---|---|---|---|
| | | Training depths | Predicted Group Membership | | Total |
| | | | Oil bearing | Non-oil bearing | |
| Original | Count | Oil bearing | 113 | 0 | 113 |
| | | Non-oil bearing | 0 | 139 | 139 |
| | | Ungrouped cases | 570 | 260 | 830 |
| | % | Oil bearing | 100.0 | .0 | 100.0 |
| | | Non-oil bearing | 0.0 | 100.0 | 100.0 |
| | | Ungrouped cases | 68.7 | 31.3 | 100.0 |
| a. 100.0% of original grouped cases correctly classified. | | | | | |

TABLE. 21: Classification results of samples containing oil or no oil for Well E-S5.

| Classification Results[a] | | | | | |
|---|---|---|---|---|---|
| | | Training depths | Predicted Group Membership | | Total |
| | | | Oil bearing | Non-oil bearing | |
| Original | Count | Oil bearing | 643 | 40 | 683 |
| | | Non-oil bearing | 1 | 398 | 399 |
| | % | Oil bearing | 94.1 | 5.9 | 100.0 |
| | | Non-oil bearing | 0.3 | 99.7 | 100.0 |
| a. 96.2% of original grouped cases correctly classified. | | | | | |

According to the descriptive statistics in Table 22, the oil bearing group has the highest mean values of ILD, MSFL and SFLU (4.53, 6.77 and 3.29 ohm $m^2$/m) compared to the non- oil bearing group (3.11, 4.08 and 3.19 ohm $m^2$/m). The non-oil bearing group has a high mean value for NPHI (0.17 dec). Both oil and non-oil bearing groups show low mean GR values indicating sand bodies with high porosity (RHOB values) and low permeability (SP values).

TABLE. 22: Descriptive statistics for oil and non- oil bearing functions of Well E-S5.

| STATISTICS | | | | | | | | |
|---|---|---|---|---|---|---|---|---|
| LOGS | OIL BEARING | | | | NON-OIL BEARING | | | |
| | Mean | Std. Deviation | minimum | maximum | Mean | Std. deviation | minimum | maximum |
| GR | 87.241 | 29.891 | 34.281 | 158.125 | 50.056 | 10.164 | 32.031 | 125.312 |
| ILD | 4.532 | 0.759 | 3.089 | 7.507 | 3.117 | 0.456 | 2.371 | 4.617 |
| MSFL | 6.774 | 2.421 | 0.550 | 17.00 | 4.081 | 0.876 | 0.334 | 7.316 |
| NPHI | 0.166 | 0.034 | 0.078 | 0.283 | 0.175 | 0.022 | 0.130 | 0.355 |
| RHOB | 2.502 | 0.055 | 2.328 | 2.585 | 2.426 | 0.036 | 2.222 | 2.533 |
| SFLU | 3.299 | 1.174 | 0.98 | 6.09 | 3.191 | 1.026 | 1.02 | 5.84 |
| SP | -55.370 | 3.102 | -60.906 | -49.406 | -55.292 | 2.040 | -58.531 | -48.187 |

**Stepwise discriminant analysis**

In order to find out the best discriminating wireline log variables which separate oil from non-oil bearing depths, stepwise discriminant analysis was applied. As shown in Table 23 below SP, RHOB, GR and ILD are the best discriminating variables for the data from Well E-S5. SP separates the two groups up to 83.2% correctly (Table. 23) adding RHOB improves the classification correctly to 88.5% (Table. 23). Adding GR improves the classification to 94.3% while ILD improves the classification correctly up to 96.1%.

TABLE. 23: Classification results of Predictors.

| Variables | Classification |
|---|---|
| SP | 83.2% |
| RHOB | 88.5% |
| GR | 94.3% |
| ILD | 96.1% |

**WELL F-AH4**

Seven variables (RHOB, NPHI, GR, LLS, LLD, SP and MSFL) were used for Well F-AH4. In Table 24 two factors had Eigen values greater than 1, with factor one having an Eigen value of 3.014 and factor two 2.539. As seen in Table 24 below, factor one describes 43.056% of variance of total data which is positively loaded with wireline logs RHOB, NPHI and GR which is considered non-oil bearing (Table. 25). Factor two depicts 36.267% of the total data variability which is positively loaded with LLS, LLD, MSFL and SP logs which is regard as oil bearing (Table. 25). Based on the results found from Table 25, it can be seen that factor one is indicative of non-oil bearing samples whereas factor two indicates oil-bearing samples.

TABLE. 24: Total variance explained by each factor of Well F-AH4.

| Total Variance Explained | | | | | | | | | |
|---|---|---|---|---|---|---|---|---|---|
| Component | Initial Eigen values | | | Extraction Sums of Squared Loadings | | | Rotation Sums of Squared Loadings | | |
| | Total | % of Variance | Cumulative % | Total | % of Variance | Cumulative % | Total | % of Variance | Cumulative % |
| 1 | 3.014 | 43.056 | 43.056 | 3.014 | 43.056 | 43.056 | 2.972 | 42.462 | 42.462 |
| 2 | 2.539 | 36.267 | 79.324 | 2.539 | 36.267 | 79.324 | 2.580 | 36.862 | 79.324 |
| 3 | 0.849 | 12.132 | 91.456 | | | | | | |
| 4 | 0.457 | 6.535 | 97.991 | | | | | | |
| 5 | 0.066 | 0.941 | 98.933 | | | | | | |
| 6 | 0.063 | 0.897 | 99.829 | | | | | | |
| 7 | 0.012 | 0.171 | 100.000 | | | | | | |

TABLE. 25: Rotated component matrix of Well F-AH4.

| Rotated Component Matrix[a] | | |
|---|---|---|
| | Component | |
| | Factor 1- Non-oil Bearing | Factor 2- Oil Bearing |
| RHOB | 0.992 | |
| NPHI | 0.986 | |

| | | |
|---|---|---|
| GR | 0.973 | |
| LLS | | 0.935 |
| LLD | | 0.926 |
| SP | | 0.783 |
| MSFL | | 0.480 |

Figure 4.5.1.3 a display of depths containing oil and non-oil. Depths found above the zero line indicate the presence of oil with positive loadings in LLS, LLD, MSFL and SP whereas depths below the zero line are indicative of non-oil bearing depths having positive loadings of RHOB, NPHI and GR. Between depths 2364.48 and 2524.81m a possible hydrocarbon sandstone reservoir is present (Fig. 4.5.1.3).
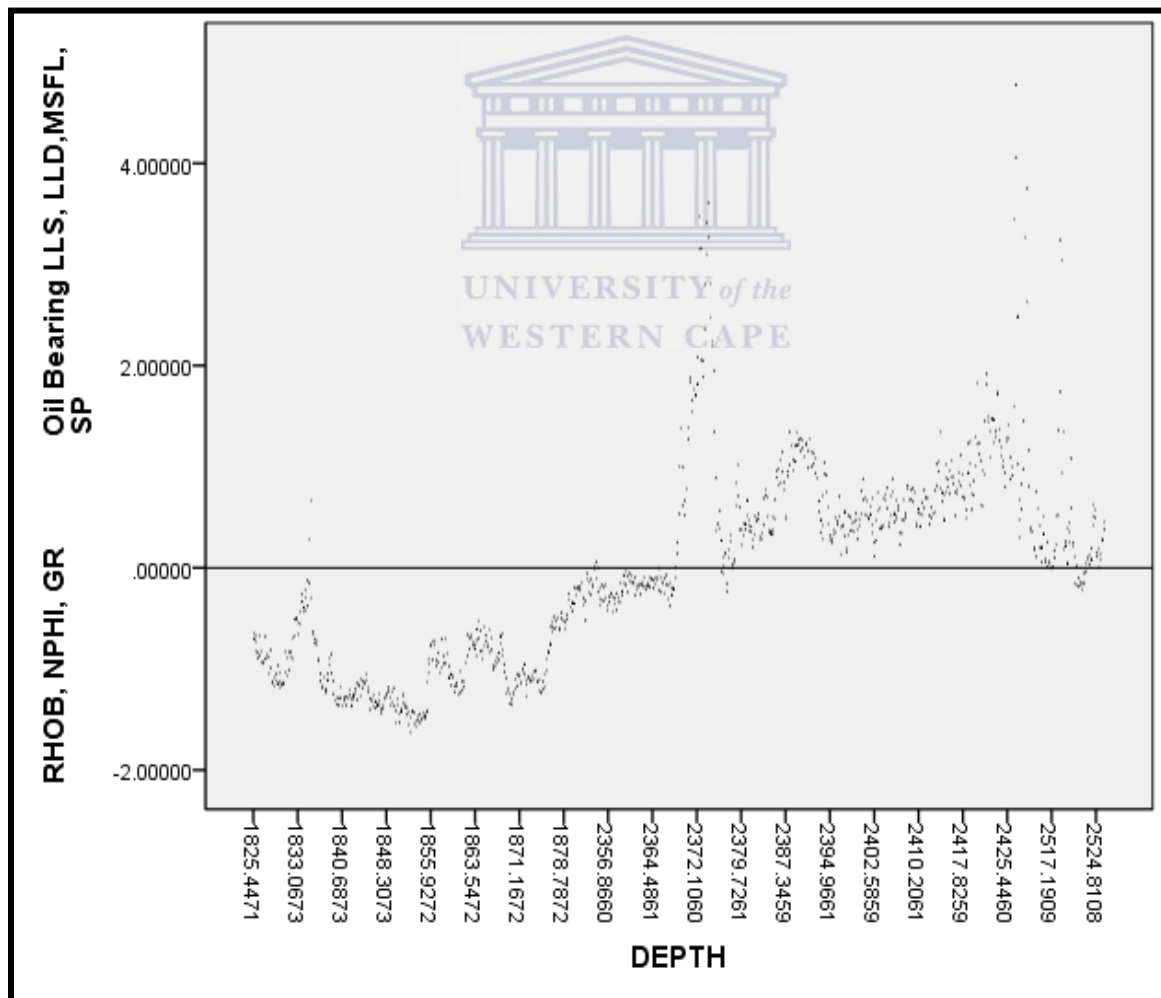


*Figure. 4.5.1.3. Box Plot of oil bearing depths of Well F-AH4.*

**Linear discriminant analysis**

Training samples created with factor analysis is characterized by linear discriminant analysis using the wireline log data. Given that there are only two groups (oil and non-oil bearing) one discriminant function was created (Table. 26). In Table 26, the discriminant function has positive loadings for SP, LLD, LLS, and MSFL characterized as oil bearing (Table. 27) with negative loadings for NPHI, RHOB and GR which points out the non- oil bearing depth as shown in Table 27.

TABLE. 26: Structure matrix for Well F-AH4.

| Structure Matrix | |
|---|---|
| | Function |
| | 1 |
| SP | 0.621 |
| LLD | 0.436 |
| LLS | 0.379 |
| MSFL | 0.098 |
| RHOB | -0.034 |
| NPHI | -0.033 |
| GR | -0.001 |

TABLE. 27: Functions at group centroids for Well F-AH4.

| Functions at Group Centroids | |
|---|---|
| Depth types | Function |
| | 1 |
| Non-oil bearing | -4.791 |
| Oil bearing | 5.043 |

Once the discriminant analysis was run only one hundred and twenty samples were classified as non- oil bearing and one hundred and fourteen as oil bearing (Table. 28). The training depths for oil and non-oil bearing depths were 100.0% correctly classified however in order to classify

the ungrouped cases, the discriminant function created was used to classify the ungrouped depths either oil or non-oil bearing. All the training depths were 95.7% correctly classified (Table. 29).

TABLE. 28: Classification results of oil and non-oil groups.

| Classification Results[a] | | | | | |
|---|---|---|---|---|---|
| | | Training depths | Predicted Group Membership | | Total |
| | | | Non-oil bearing | Oil- bearing | |
| Original | Count | Non-oil bearing | 120 | 0 | 120 |
| | | Oil- bearing | 0 | 114 | 114 |
| | | Ungrouped cases | 302 | 425 | 727 |
| | % | Non-oil bearing | 100.0 | .0 | 100.0 |
| | | Oil-bearing | 0.0 | 100.0 | 100.0 |
| | | Ungrouped cases | 41.5 | 58.5 | 100.0 |
| a. 100.0% of original grouped cases correctly classified. | | | | | |

TABLE. 29: Classification results of samples containing no oil and oil for Well F-AH4.

| Classification Results[a] | | | | | |
|---|---|---|---|---|---|
| | | Training depths | Predicted Group Membership | | Total |
| | | | Non-oil bearing | Oil- bearing | |
| Original | Count | Non-oil bearing | 381 | 41 | 422 |
| | | Oil-bearing | 0 | 539 | 539 |
| | % | Non-oil bearing | 90.3 | 9.7 | 100.0 |
| | | Oil-bearing | 0.0 | 100.0 | 100.0 |
| a. 95.7% of original grouped cases correctly classified. | | | | | |

In Table 30 below, the non- oil bearing group has a very high mean value for NPHI (21.956 dec) and very low in LLD, LLS and MSFL (3.58, 3.83 and 5.44 ohm $m^2$/m). The non- oil bearing group has a high GR mean value, pointing out shale with a high density. However the oil bearing group which is characterized by the resistivity wireline logs has high mean values in LLD, LLS and MSFL and extremely low mean value of NPHI in a sand body (Table. 30).

TABLE. 30: Descriptive statistics for oil and non-oil bearing functions of Well F-AH4.

| STATISTICS | | | | | | | | |
|---|---|---|---|---|---|---|---|---|
| LOGS | NON-OIL BEARING | | | | OIL BEARING | | | |
| | Mean | Std. Deviation | minimum | maximum | Mean | Std. deviation | minimum | maximum |
| GR | 69.456 | 36.475 | 19.684 | 146.558 | -14.441 | 291.017 | -999.00 | 131.374 |
| LLD | 3.584 | 2.284 | 0.5406 | 18.579 | 16.6594 | 9.029 | 4.257 | 57.846 |
| LLS | 3.834 | 2.328 | 0.1798 | 15.817 | 10.461 | 5.143 | 4.133 | 37.023 |
| MSFL | 5.444 | 3.149 | 0.8789 | 14.322 | 8.323 | 7.299 | 0.898 | 87.318 |
| NPHI | 21.956 | 3.314 | 15.703 | 36.692 | -62.156 | 269.190 | -999.00 | 193.20 |
| RHOB | 2.471 | 0.118 | 2.221 | 2.769 | -71.853 | 262.743 | -999.00 | 2.690 |
| SP | 174.16 | 3.081 | 169.00 | 181.375 | 184.434 | 2.055 | 180.00 | 187.937 |

**Stepwise discriminant analysis**

Stepwise was considered to find the best variable that separates the oil from non-oil bearing depths. In Table 31, SP indicates the best predictor for Well F-AH4. SP separates the groups 93.0% (Table. 31).

TABLE. 31: Classification results of Predictor SP.

| Variables | Classification |
|---|---|
| SP | 93.0% |

**4.5.2 COMBINATION OF CLUSTER ANALYSIS WITH DISCRIMINANT ANALYSIS (METHOD II)**

Cluster analysis was used to classify the available data from the three wells based on the wireline log data from each well. In Method II, hierarchical Q-mode cluster analysis was applied using Ward's method with squared Euclidean distance as a measure of distance. This approach helps to determine the best number of clusters to work with as a dendrogram.

**WELL E-S3**
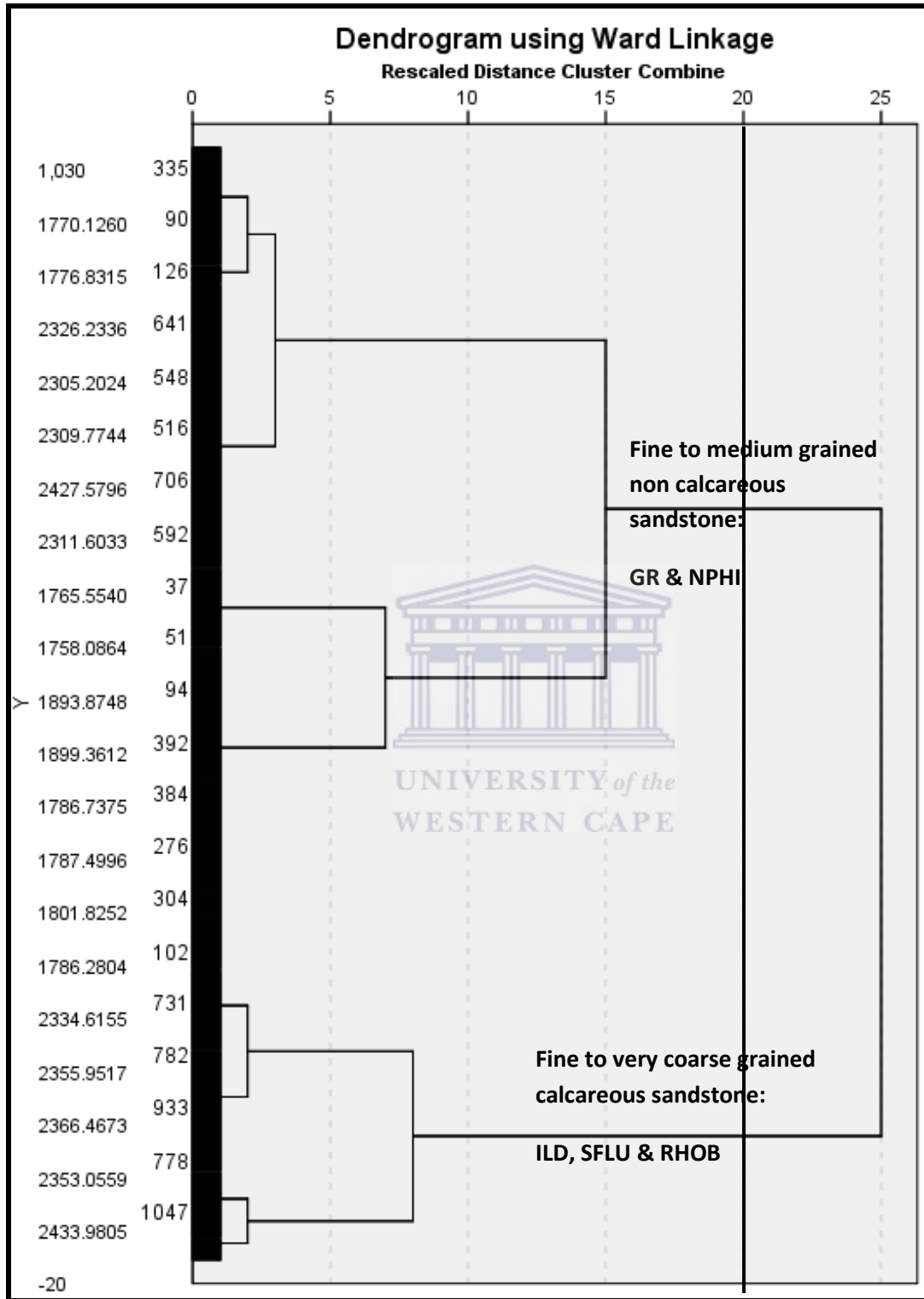
*Figure. 4.5.2.1. Dendrogram of Well E-S3.*

Using the above method at similarity level twenty, two major groups were achieved namely fine to medium grained non-calcareous sandstone and fine to very coarse grained calcareous sandstone for Well E-S3 as can be seen from the dendrogram (Fig. 4.5.2.1). The layer depths of each group was compared to the core and well description report of Well E-S3 and resulted in sandstone lithologies. In order to verify and characterize the two groups achieved through cluster analysis linear discriminant analysis was considered. Based on the two groups, one discriminant function resulted. Tables 32 and 33 show the structure matrix (relation between variables and discriminant function) and functions at group centroids (related to groups and discriminant functions). The function separates the fine to medium grained non-calcareous sandstone from the fine to very coarse grained calcareous sandstone and is highly positively loaded with NPHI and GR (Table. 32) and highly negatively loaded with ILD, SFLU and RHOB. GR and NPHI logs characterize the fine to medium grained non-calcareous sandstone group to be non-oil bearing (Table. 33). The fine to very coarse grained calcareous sandstone was classified as the oil bearing group and is characterized by ILD, SFLU and RHOB. Normally groups, which are highly negatively correlated to ILD and SFLU, are good interpreters of hydrocarbon.
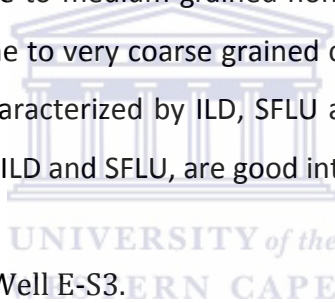
TABLE. 32: Structure matrix for Well E-S3.

| Structure Matrix | |
|---|---|
| | Function |
| | 1 |
| NPHI | 0.906 |
| ILD | -0.676 |
| SFLU | -0.605 |
| GR | 0.389 |
| RHOB | -0.252 |

TABLE. 33: Functions at group centroids for Well E-S3.

| Functions at Group Centroids | |
| --- | --- |
| Lithology groups | Function |
| | 1 |
| Fine to medium grained non-calcareous sandstone: non-oil bearing | 0.783 |
| Fine to very coarse grained calcareous sandstone: oil bearing | -2.218 |

Results show that 97.0% of the data has been correctly classified to their respective groups as shown in Table 34.

TABLE. 34: Classification of samples containing oil and no oil for Well E-S3.

| Classification Results[a] | | | Predicted Group Membership | | Total |
| --- | --- | --- | --- | --- | --- |
| | | Ward Method | Fine to medium grained non-calcareous sandstone | Fine to very coarse grained calcareous sandstone | |
| Original | Count | Fine to medium grained non-calcareous sandstone: non-oil bearing | 764 | 12 | 776 |
| | | Fine to very coarse grained calcareous sandstone: oil bearing | 20 | 254 | 274 |
| | % | Fine to medium grained non-calcareous sandstone: non-oil bearing | 98.5 | 1.5 | 100.0 |
| | | Fine to very coarse grained calcareous sandstone: oil bearing | 7.3 | 92.7 | 100.0 |
| [a]. 97.0% of original grouped cases correctly classified. | | | | | |

**Stepwise discriminant analysis**

Stepwise method was applied to the data to find out the relative influence of each wireline log on the overall data classification and which variable best separates the groups. In Table 35NPHI, ILD and RHOB were the best predictors for Well E-S3.NPHI has the highest influence in the data set of Well E-S3, which separates the groups 95.3% (Table. 35). Adding ILD separates the groups 96.4% correctly while RHOB improves the classification up to 96.9% (Table. 35).

TABLE. 35:  Classification results of all predicators.

| Variables | Classification |
|-----------|----------------|
| NPHI | 95.3 % |
| ILD | 96.4 % |
| RHOB | 96.9 % |

In Table 36 below, the oil bearing group (fine to very coarse grained calcareous sandstone) shows that the mean value of ILD (6.36 ohm $m^2$/m) and SFLU (3.31 ohm $m^2$/m) are the highest compared to the non-oil bearing group (fine to medium grained non-calcareous sandstone). The oil bearing group has the lowest NPHI mean value (0.11 dec) compared to the non-oil bearing group indicating a low porosity and water content. The oil bearing group (fine to very coarse grained calcareous sandstone) has a moderate GR value indicating a sandy shale formation with a bulk density of 2.51 g/$c^3$. The non-oil bearing group (fine to medium grained non-calcareous sandstone) has the highest NPHI mean value (0.21 dec) with a moderate GR value and high RHOB value (2.43 g/$c^3$) indicating a sandy shale formation with a possible gas effect (Rider, 1996).

TABLE. 36: Descriptive statistics of each group of Well E-S3.

| LOGS | Fine to medium grained sandstone Non-oil bearing | | | | Fine to very coarse grained sandstone Oil bearing | | | |
|---|---|---|---|---|---|---|---|---|
| | Mean | Std. Deviation | minimum | maximum | Mean | Std. deviation | minimum | maximum |
| GR | 87.940 | 27.216 | 38.718 | 241.750 | 58.341 | 19.043 | 22.453 | 100.00 |
| ILD | 2.961 | 1.023 | 0.947 | 0.121 | 6.362 | 2.793 | 2.451 | 19.218 |
| NPHI | 0.217 | 0.036 | 0.121 | 0.353 | 0.117 | 0.038 | 0.014 | 0.210 |
| RHOB | 2.433 | 0.119 | 1.891 | 2.660 | 2.513 | 0.055 | 2.398 | 2.646 |
| SFLU | 3.274 | 1.669 | 0.35 | 8.29 | 3.315 | 1.225 | 1.10 | 5.96 |

In Figure 4.5.2.2 below, the whisker box plot documents the distribution of oil bearing depths using the classification results. The whisker plots show two simultaneous comparisons where the fine to very coarse grained calcareous sandstone is oil prone according to the high median of ILD and the fine to medium grained non-calcareous sandstone has a low ILD median.



*Figure. 4.5.2.2. Whisker box plots of resistivity (ILD) ordered according to non-oil and oil bearing groups for Well E-S3.*

## WELL E-S5

Figure 4.5.2.3 below, is a depiction of the number of groups that has been characterized using cluster analysis. Based on the dendrogram in Figure 4.5.2.3 two major groups namely very fine grained sandstone and medium to fine grained sandstone with red claystone beds were established through cluster analysis. The layer depths of each group were compared to the core results and well report descriptions of Well E-S5 which related to sandstone and claystone lithologies. Each cluster has a different combination of wireline properties and can be considered as a statistically determined petrofacies (or "petrophysical facies") as defined by Serra (1986).
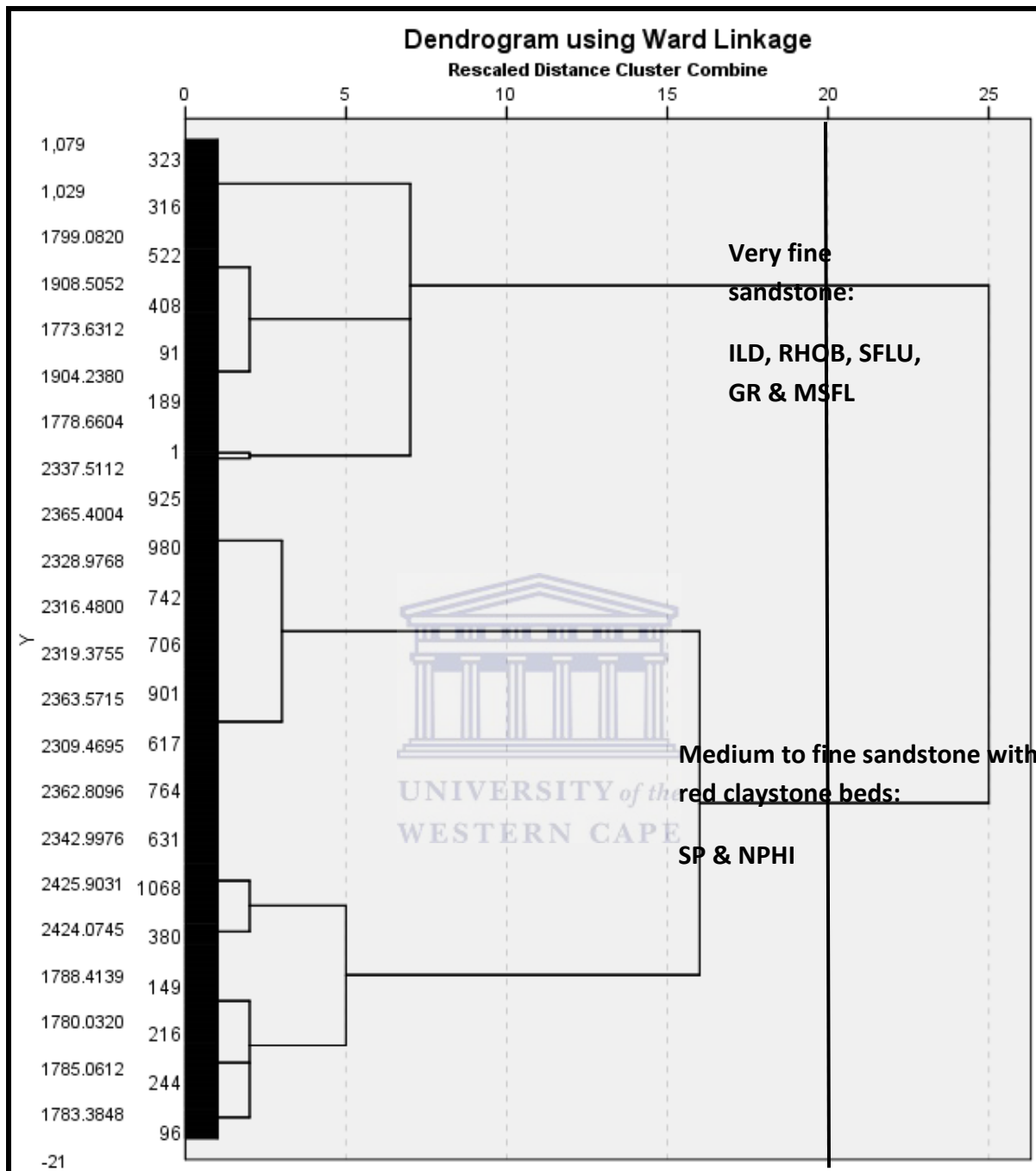
*Figure. 4.5.2.3. Dendrogram of Well E-S5.*

Linear discriminant analysis followed to verify and characterized the established sandstone and sandstone with claystone groups of Well E-S5. Since there were two groups, one discriminant function was extracted based on the wireline logs (Table. 37). The discriminant function is positively loaded with SP and NPHI and negatively loaded with ILD, RHOB, SFLU, GR and MSFL

(Table. 37). In Table 38 below, the very fine grained sandstone was characterized as the oil bearing group as ILD, SFLU and GR are good indictors of hydrocarbon in a highly porous formation on the basis of RHOB log. The medium to fine grained sandstone with red claystone beds were characterized as non- oil bearing on the bases of being highly loaded with NPHI and SP whereby NPHI indicates the formations water content and SP the formations water resistivity.

TABLE. 37: Structure matrix for Well E-S5.

| Structure Matrix | |
| --- | --- |
| | Function |
| | 1 |
| SP | 0.610 |
| ILD | -0.470 |
| RHOB | -0.419 |
| SFLU | -0.375 |
| NPHI | 0.304 |
| GR | -0.278 |
| MSFL | -0.270 |

TABLE. 38: Functions at group centroids for Well E-S5.

| Functions at Group Centroids | |
| --- | --- |
| Lithology groups | Function |
| | 1 |
| Very fine grained sandstone: oil bearing | -1.344 |
| Medium to fine grained sandstone with red claystone beds: non-oil bearing | 2.177 |

The two groups were verified and characterized to 94.4% through linear discriminant analysis (Table. 39). The very fine grained sandstone group comprises of five hundred and fifty oil

bearing depths while the medium to fine grained sandstone with red claystone beds group has four hundred and seventy-one non-oil bearing depths (Table. 39).

TABLE. 39: Classification results of samples containing oil and no oil for Well E-S5.

| Classification Results[a] | | | | | |
|---|---|---|---|---|---|
| | | Ward Method | Predicted Group Membership | | Total |
| | | | Very fine grained sandstone | Medium to fine grained sandstone with red claystone beds | |
| Original | Count | Very fine grained sandstone: oil bearing | 550 | 61 | 611 |
| | | Medium to fine grained sandstone with red claystone beds: non-oil bearing | 0 | 471 | 471 |
| | % | Very fine grained sandstone: oil bearing | 90.0 | 10.0 | 100.0 |
| | | Medium to fine grained sandstone with red claystone beds: non-oil bearing | 0.0 | 100.0 | 100.0 |
| a. 94.4% of original grouped cases correctly classified. | | | | | |

**Stepwise discriminant analysis**

The most significant variable was considered using stepwise discriminant analysis method which separates the oil bearing group from the non-oil bearing group. SP, MSFL and GR variables indicate the best set of predictors for Well E-S5 as shown in Table 40. SP separates the two groups that resulted from cluster and discriminant analysis up to 91.1% correctly (Table. 40). MSFL improves the classification to 92.5% with GR added it improves the classification to 93.3%.

TABLE. 40: Classification results of all predicators.

| Variables | Classification |
|---|---|
| SP | 91.1% |
| MSFL | 92.5% |
| GR | 93.3% |

The descriptive statistics of the oil and non-oil bearing groups in Table 41 shows that the very fine grained sandstone group has a low NPHI mean value (0.20 dec) compared to the medium to fine grained sandstone with red claystone bed group with low mean values of ILD (4.14 ohm $m^2$/m), MSFL (8.15 ohm $m^2$/m) and SFLU (3.52 ohm $m^2$ /m) which suggest a small indication of hydrocarbon but too low to be of economic value. The fine grained sandstone group has a moderate mean value of RHOB which possibly indicates a moderate porosity in a sandstone formation with a low SP value pointing out to low permeability. The medium to fine grained sandstone with red claystone bed group has a high mean value of NPHI (0.21 dec) in a sandbody (43.64 API) with a bulk density of 2.35 g/c$^3$. The medium to fine grained sandstone with red claystone bed group has low mean values of ILD, MSFL and SFLU respectively (Table. 44) whereby it could contain salt water (Rider, 1996).

TABLE. 41: Descriptive statistics of each cluster group of Well E-S5.

| LOGS | Very fine grained sandstone Oil bearing | | | | Medium to fine grained sandstone with claystone Non-oil bearing | | | |
|---|---|---|---|---|---|---|---|---|
| | Mean | Std. Deviation | minimum | maximum | Mean | Std. deviation | minimum | maximum |
| GR | 105.457 | 26.808 | 38.125 | 201.00 | 43.640 | 22.263 | 11.218 | 100.812 |
| ILD | 4.144 | 1.043 | 1.545 | 7.507 | 2.007 | 1.082 | 0.580 | 5.691 |
| MSFL | 8.150 | 2.966 | 1.068 | 28.312 | 3.381 | 1.694 | 1.236 | 10.328 |
| NPHI | 0.205 | 0.039 | 0.078 | 0.355 | 0.212 | 0.025 | 0.148 | 0.273 |
| RHOB | 2.516 | 0.062 | 2.271 | 2.650 | 2.356 | 0.089 | 2.199 | 2.537 |
| SFLU | 3.526 | 1.224 | 0.98 | 7.82 | 2.407 | 1.686 | 0.35 | 6.21 |
| SP | -47.967 | 21.142 | -60.656 | -0.239 | -8.363 | 1.980 | -12.625 | -3.209 |

In Figure 4.5.2.4 below, the whisker box plot document the distribution of oil bearing samples using the classification results. The fine grained sandstone group is more oil prone than the medium to fine grained sandstone with red claystone bed group having a higher median value for Well E-S5 (Fig. 4.5.2.4).
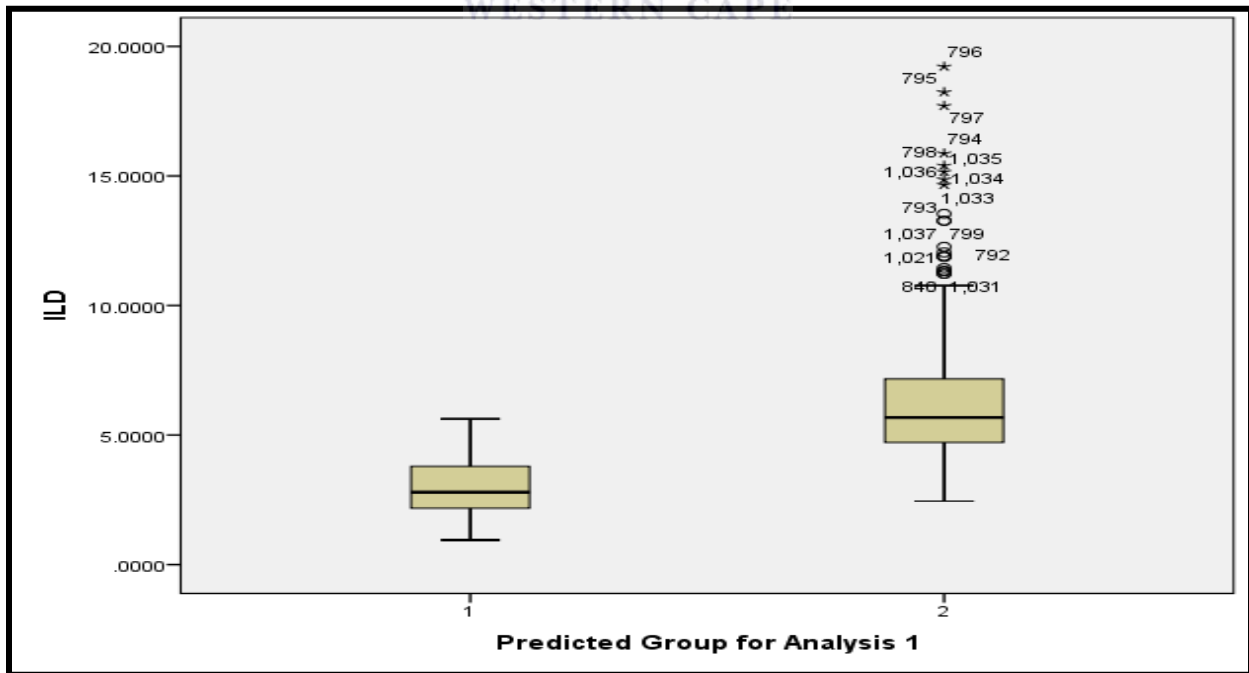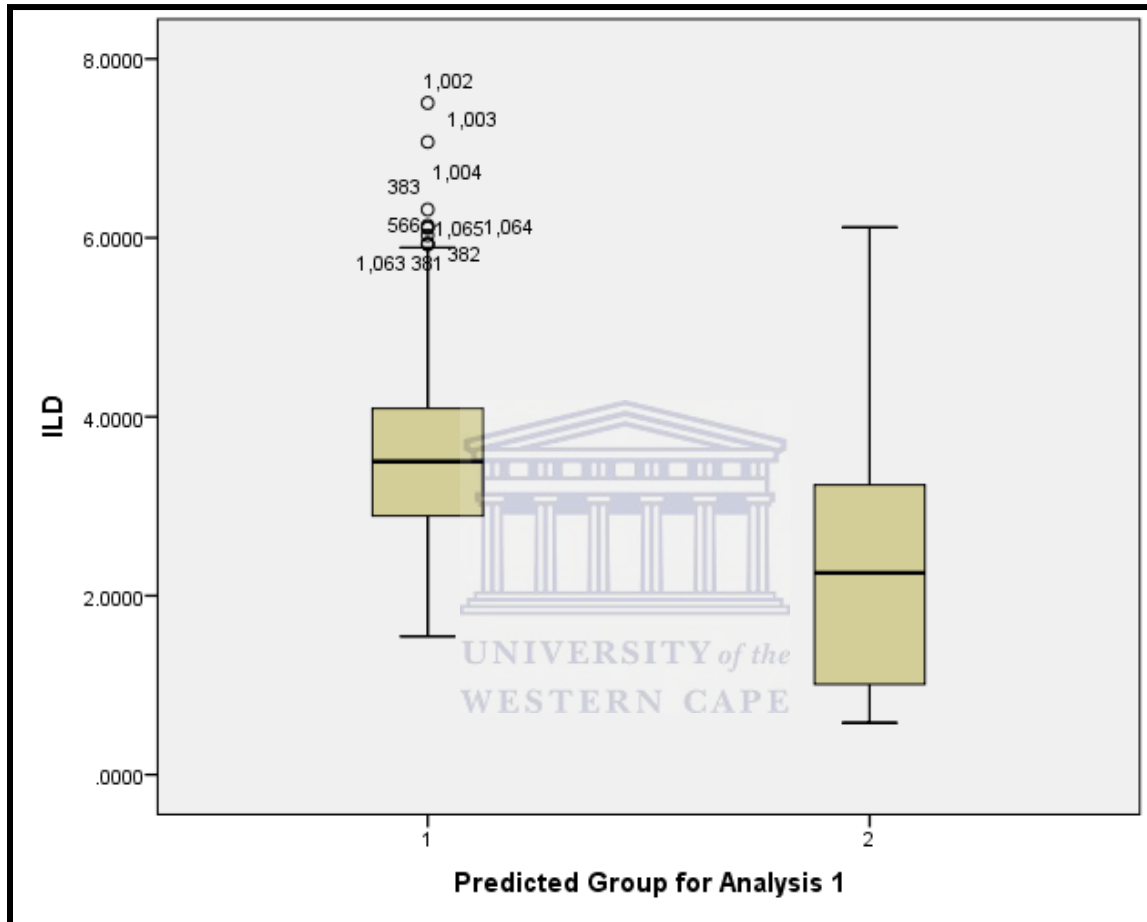


*Figure. 4.5.2.4. Whisker box plots of resistivity (ILD) ordered according to non-oil and oil bearing groups for Well E-S5.*

## WELL F-AH4

A cluster dendrogram and elbow criterion was used to decide how many clusters were significant and useful for Well F-AH4. In Figure 4.5.2.5 below, two distinct groups namely claystone interbedded with siltstone and fine-medium grained sandstone is shown based on the similarity line of twenty, for Well-F-AH4. Claystone interbedded with sandstone and fine-medium grained sandstone layer depths were compared to the well report descriptions of Well F-AH4 which related to the different lithologies.

**Dendrogram using Ward Linkage**

**Rescaled Distance Cluster Combine**

0    5    10    15    20    25

1850.5931
1854.8604    176
1840.8396
1850.2885    112
1843.2780
1840.5348    131
1869.4908
1872.8436    328
1873.6056
1829.4095    74
1870.7100
1858.0608
1857.2988    220
1859.1276
1863.0900    203
1865.9856
1832.7625    214
1836.2676
2428.7988    495
2374.5444
2516.2764
2517.6479    955
2357.9329
2363.4192    459
2358.9995
2353.2085    385
2363.5715
2352.2939    430
2360.6760
2422.7029    838
2389.6321
2392.0703
2390.3940    610
2414.9304
2405.1768    705
2406.7007
2519.0195    482
2378.5068
2395.4231    711
2399.8428
2370.1248    572
2379.5735
2411.2727
2384.6028    767
2414.1685
2416.7593    794
2414.0161
2521.3057    922
2515.9717
-19

Y

Claystone interbedded with sandstone:

NPHI, RHOB & GR

Fine- medium grained sandstone:

LLD, SP, LLS & MSFL

UNIVERSITY *of the* WESTERN CAPE

*Figure. 4.5.2.5. Dendrogram of Well F-AH4.*

131

**Linear discriminant analysis**

The two groups obtained in cluster analysis were then saved in order to be verified and characterized by linear discriminant analysis. Based on the two groups, a discriminant function was created. In Table 42, the discriminant function separates the two groups (1- claystone interbedded with sandstone and 2- fine-medium grained sandstone),which is highly positively loaded with LLD, SP, LLS and MSFL which separates the claystone interbedded with sandstone group from the fine-medium grained sandstone group. A high LLD, LLS and MSFL reading indicates a high resistivity reading with the possibility of hydrocarbons therefore the fine-medium grained sandstone group was classified as the oil bearing group. In Table 43, the claystone interbedded with sandstone group is highly negatively loaded with NPHI, RHOB and GR therefore classified as the non-oil bearing group because the neutron (NPHI) log measures the formation's water content hydrocarbon, the density (RHOB) log measures the bulk density (i.e. density of minerals forming the rock and the volume of free fluids in the rock) or the lithology based on the GR log (Rider, 1996).

TABLE. 42: Structure matrix of Well F-AH4.

| Structure Matrix | |
|---|---|
| | Function |
| | 1 |
| LLD | 0.627 |
| SP | 0.584 |
| LLS | 0.435 |
| NPHI | -0.304 |
| RHOB | -0.100 |
| MSFL | 0.059 |
| GR | -0.038 |

TABLE. 43: Functions at group centroids for Well F-AH4.

| Functions at Group Centroids | |
|---|---|
| Lithology groups | Function |
| | 1 |
| Claystone interbedded with sandstone: Non-oil bearing | -2.001 |
| Fine-medium grained sandstone: Oil bearing | 2.409 |

Since oil and non- oil bearing groups were identified from the structure matrix and functions at group centroids (Table. 42 and 43), groups were only classified based on the highest positively and highest negatively loaded functions. Once the linear discriminant analysis was run, 99.0% of the two groups were classified (Table. 44).

TABLE. 44: Classification results of samples containing oil and no oil for Well F-AH4.

| Classification Results[a] | | Ward Method | Predicted Group Membership | | Total |
|---|---|---|---|---|---|
| | | | Claystone interbedded with sandstone | Fine-medium grained sandstone | |
| Original | Count | Claystone interbedded with sandstone: Non-oil bearing | 489 | 7 | 496 |
| | | Fine-medium grained sandstone: Oil bearing | 2 | 421 | 423 |
| | % | Claystone interbedded with sandstone: Non-oil bearing | 98.6 | 1.4 | 100.0 |
| | | Fine-medium grained sandstone: Oil bearing | 0.5 | 99.5 | 100.0 |
| a. 99.0% of original grouped cases correctly classified. | | | | | |

**Stepwise discriminant analysis**

In order to find the best discriminating wireline log variables, stepwise discriminant analysis was applied. As shown in Table 45SP and LLD were the best discriminating variables for Well F-AH4.SP separates the two groups 85.0% correctly while adding LLD improves the classification correctly up to 98.4% (Table. 45).

TABLE. 45: Classification results of predicators.

| Variables | Classification |
|---|---|
| SP | 85.0 % |
| LLD | 98.4% |

In Table 46 below, the fine-medium grained sandstone group shows high mean values of LLD (19.489 ohm m$^2$/m), LLS (11.605 ohm m$^2$/m) and MSFL (7.792 ohm m$^2$/m) suggesting the presence of hydrocarbon. The fine-medium grained sandstone group has a mean SP value of

184.998 mV and GR of 60.420 API pointing out a permeable sandstone bed. The claystone interbedded with sandstone group comprises a small quantity of hydrocarbon due to the mean values of LLD, LLS and MSFL respectively as seen in Table 46. The claystone interbedded with sandstone group has a NPHI mean value of 22.177 dec suggesting the presence of water in a sandy-shale formation based on the GR log with a moderate density of 2.488 g/c$^3$.

TABLE. 46: Descriptive statistics of each cluster group of Well F-AH4.

| LOGS | Claystone interbedded with sandstone Non-oil bearing | | | | Fine-medium grained sandstone Oil bearing | | | |
|---|---|---|---|---|---|---|---|---|
| | Mean | Std. Deviation | minimum | maximum | Mean | Std. deviation | minimum | maximum |
| GR | 74.419 | 61.110 | -999.00 | 146.558 | 60.420 | 53.638 | -999.00 | 125.877 |
| LLD | 3.9222 | 2.205 | 0.5406 | 12.670 | 19.489 | 8.155 | 5.325 | 57.846 |
| LLS | 4.1513 | 2.262 | 0.1798 | 11.802 | 11.605 | 5.234 | 5.026 | 37.023 |
| MSFL | 6.1394 | 3.411 | 0.8789 | 14.771 | 7.7925 | 7.822 | 1.571 | 87.318 |
| NPHI | 22.177 | 8.323 | 13.2015 | 193.203 | 13.498 | 2.352 | 0.00 | 22.348 |
| RHOB | 2.488 | 0.1164 | 2.2214 | 2.7696 | 2.4510 | 0.069 | 2.240 | 2.690 |
| SP | 175.384 | 4.0944 | 169.00 | 187.375 | 184.75 | 2.026 | 175.687 | 187.937 |

A whisker box plot of the two groups versus LLD was created to show which group is highly oil prone based on the median of LLD. The fine-medium grained sandstone is highly oil prone having the highest LLD median while the claystone interbedded with sandstone group has the lowest median (Fig. 4.5.2.6).
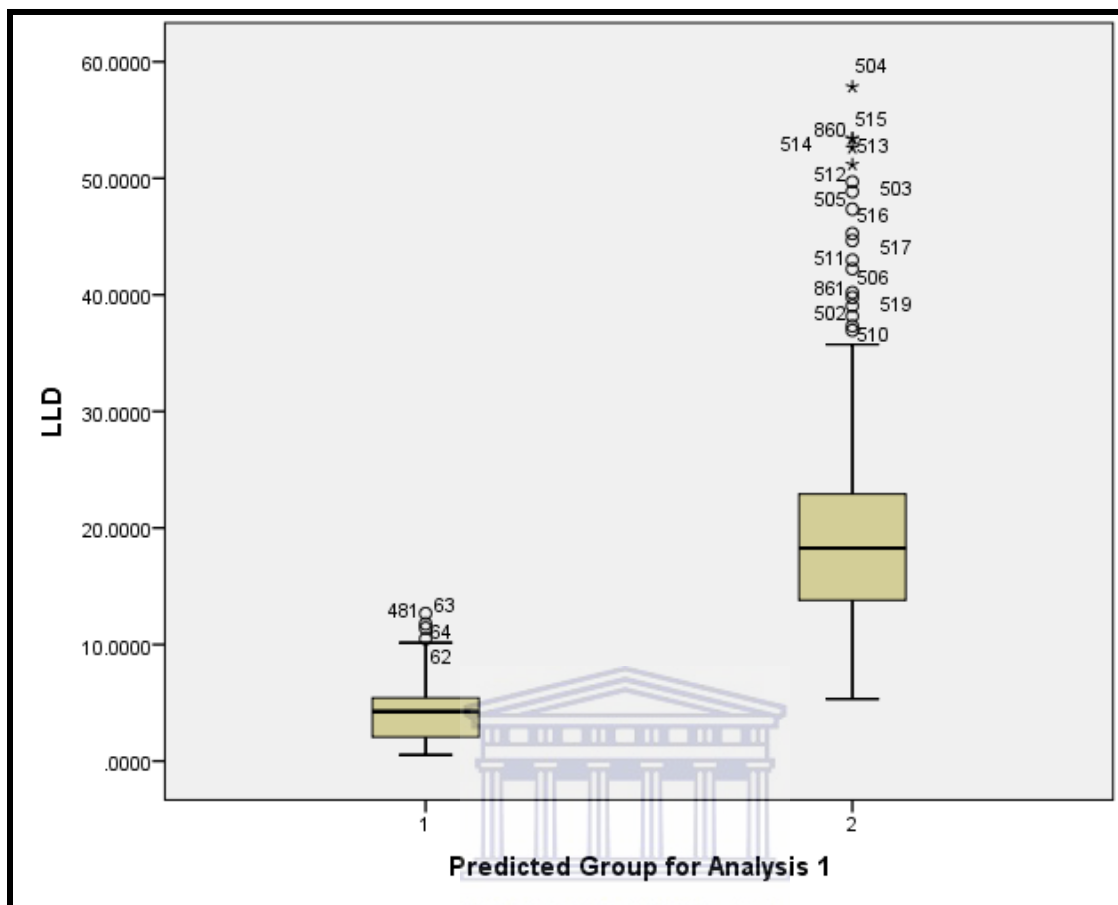
*Figure. 4.5.2.6. Whisker box plots of resistivity (LLD) ordered according to non-oil and oil bearing groups for Well F-AH4.*

**4.5.3 COMPARISON BETWEEN METHOD I & METHOD II**

**WELL E-S3**

In order to compare the results of factor and cluster analysis, two groups were selected namely oil and non-oil bearing depth groups. According to the cluster analysis two major groups were identified, firstly the fine to medium grained non-calcareous sandstone which was characterized as the non-oil bearing group and secondly the fine to very coarse grained calcareous sandstone the oil bearing group. The fine to medium grained non- calcareous sandstone group could further be subdivided in two sandstone lithology groups being non-oil bearing. In Figure 4.5.3.1 below, a scatter plot was created to examine the possible relationship between the results of factor and cluster analyses. The scatter plot confirms the results of both cluster and factor analyses. The fine to very coarse grained calcareous sandstone group is mainly oil prone and correlates with the oil bearing depths of factor analysis, showing that everything above the zero line is oil bearing (Fig.4.5.3.1) and the fine to medium grained non-calcareous sandstone group is non- oil prone and correlates to the non-oil bearing depths of factor analysis.
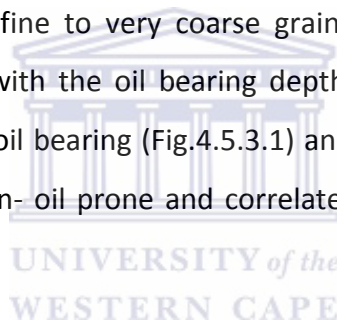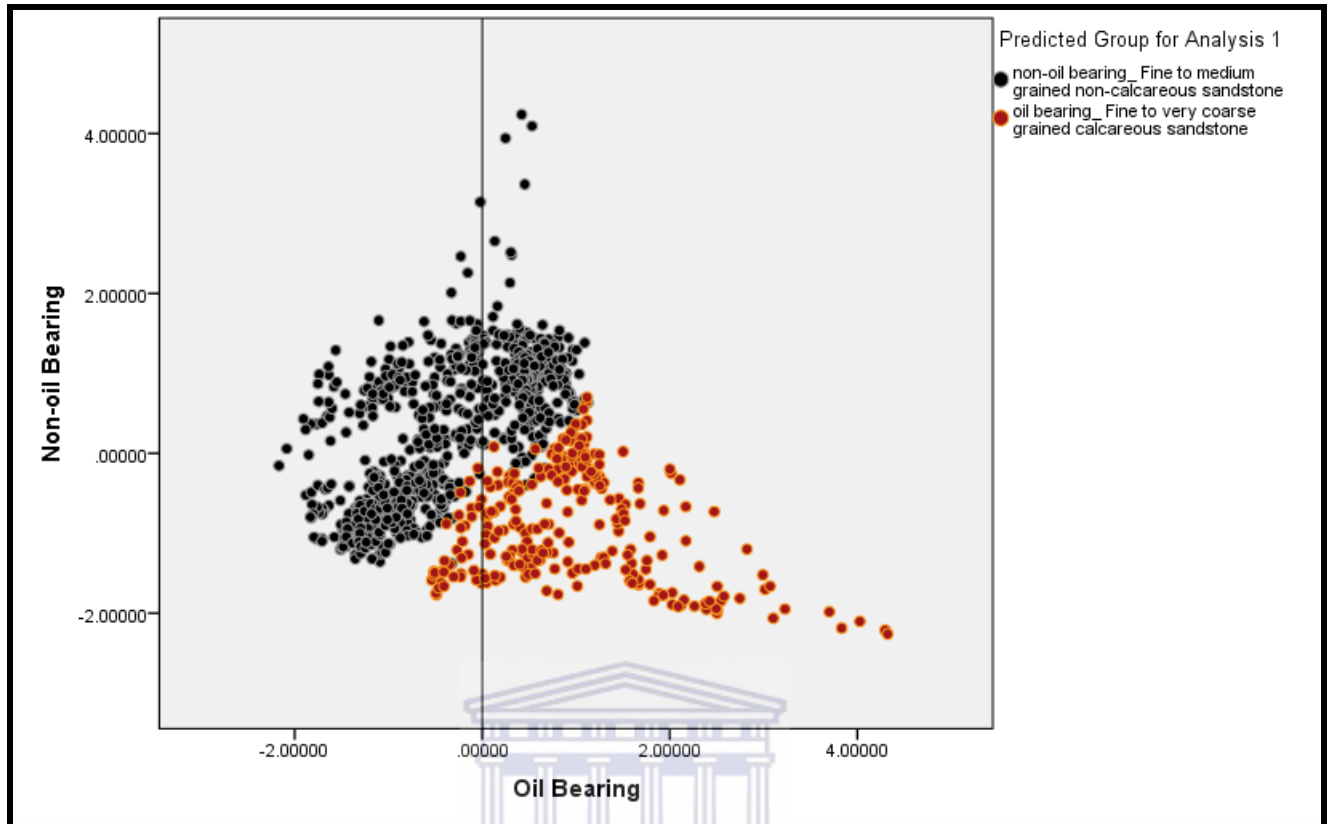
*Figure. 4.5.3.1. Scatter plot of factor analysis functions vs. cluster analysis predicted groups for Well E-S3.*

**WELL E-S5**

In Method I, factor analysis summarized the data set into two group types as oil- bearing and non- oil bearing depths. With cluster analysis, two major groups were identified as very fine grained sandstone group, which was oil bearing and medium to fine grained sandstone with red claystone beds as non- oil bearing. The medium to fine grained sandstone with red claystone could be further subdivided into two groups of different lithology (sandstone and claystone lithology). The very fine grained sandstone group was mainly oil bearing and correlates with the oil bearing depths (x-axis) (Fig.4.5.3.2). The medium to fine grained sandstone with red claystone bed group of the cluster analysis was characterized as non-oil bearing which correlates to the non-oil bearing depths of factor analysis.
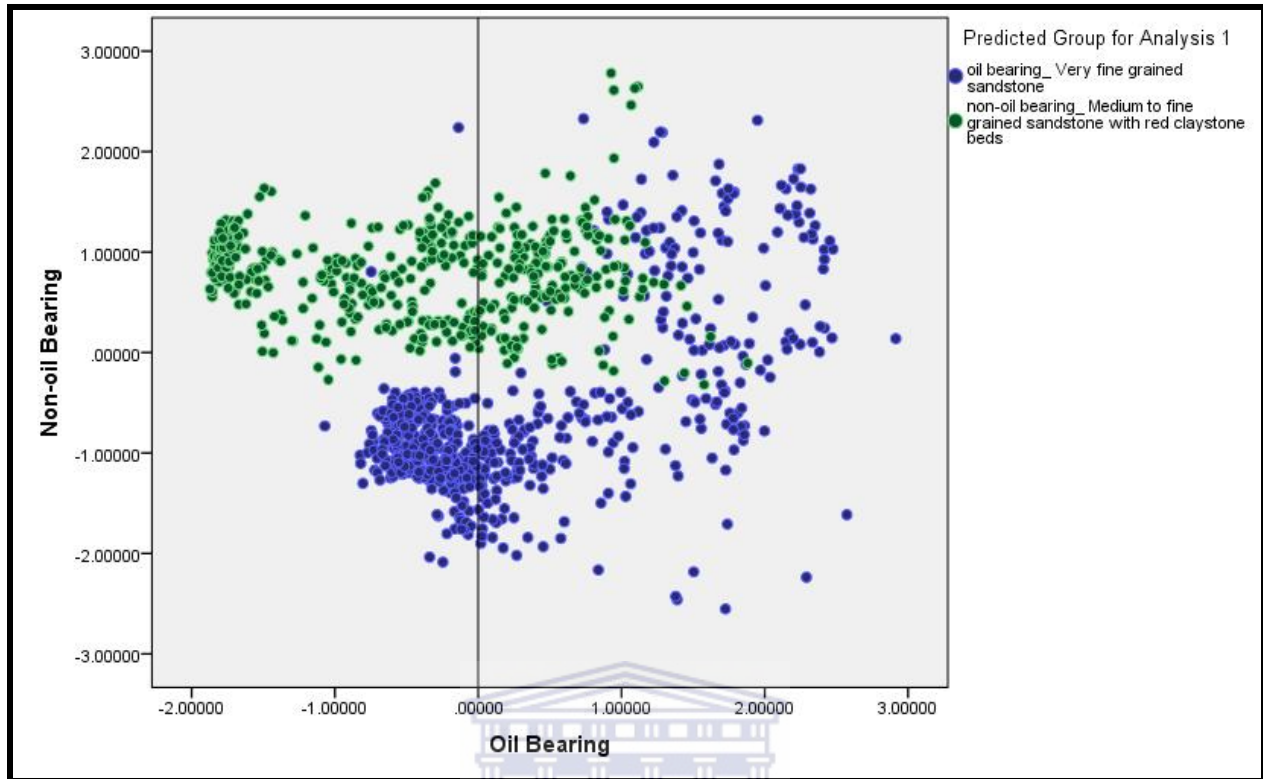
*Figure. 4.5.3.2. Scatter plot of factor analysis functions vs. cluster analysis predicted groups for Well E-S5.*

**WELL F-AH4**

With factor analysis two group types (the oil-bearing and non- oil bearing depths) were identified. Through cluster analysis two main groups were identified. The non-oil bearing group of cluster analysis can be further subdivided into two groups of sandstone lithology (very fine grained sandstone and fine to medium grained sandstone). In Figure 4.5.3.3 below, a scatter plot was created to show the relationship between the results of factor and cluster analyses. The scatter plot indicates that the fine-medium grained sandstone group from the cluster analysis is highly oil prone and positively correlates to the y-axis of factor analysis, showing group depths above the zero line as oil bearing (Fig.4.5.3.3) while the claystone interbedded with sandstone group highly correlates with the non-oil bearing depths of factor analysis displaying group depths below the zero line as non- oil shows.
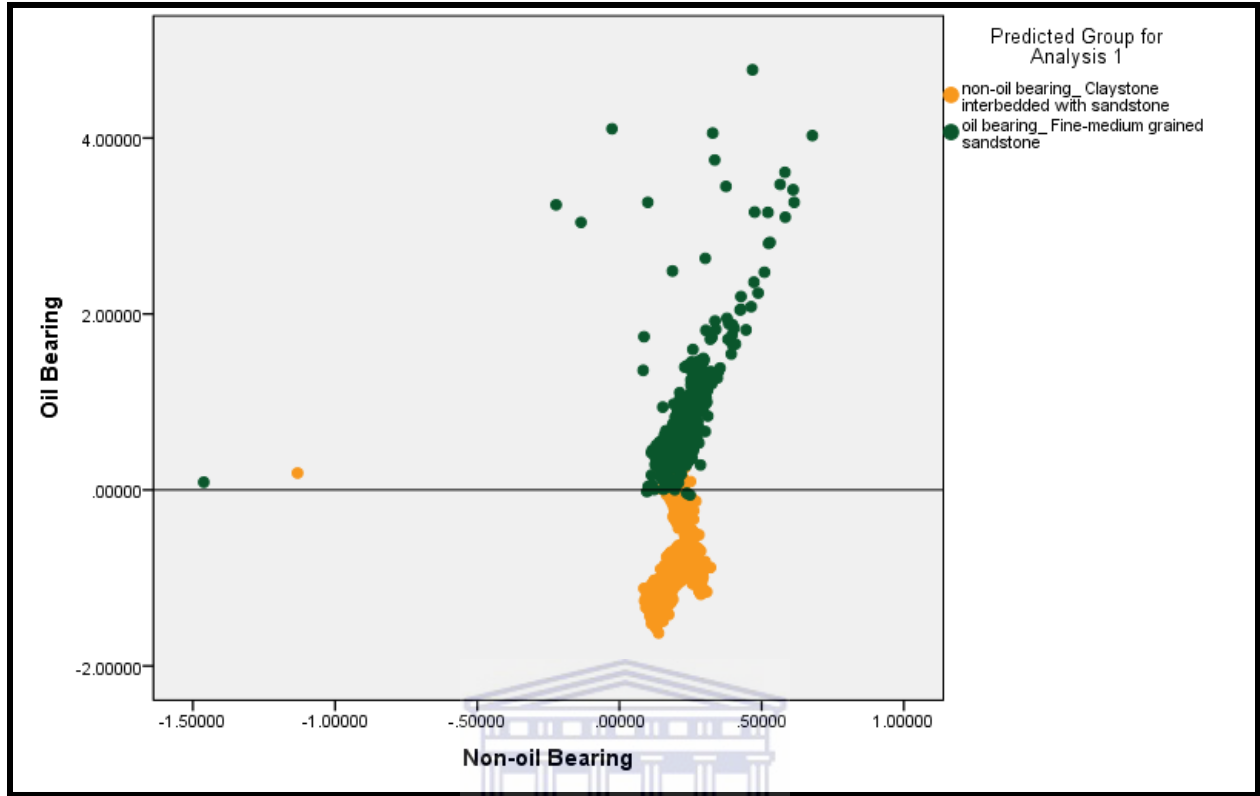
138

*Figure. 4.5.5.3. Scatter plot of factor analysis functions vs. cluster analysis predicted groups for Well F-AH4.*

# CHAPTER 5

## DISCUSSION

The sandstone reservoir units identified in the three wells were investigated using various methods namely petrophysical evaluation, seismic facies and multivariate statistics.

### Petrophysical Analysis

The petrophysical evaluation summarizes reservoir and pay flags parameters. Reservoir 1 of Well E-S3 had a net to gross value of 3.51/50.60 having a poor to moderate quality and connectivity. The cut-off parameters indicate that Reservoir 1 is a good reservoir to store hydrocarbons between depths 2350 - 2360m and between 2377 - 2378m pay flags as indicated (Fig. 4.2.1.4). These pay flags indicate that these specific depths or portions of the reservoir contains economical producible hydrocarbons. Nonetheless, these hydrocarbon indications are insufficient to be drilled. In Well E-S5 one reservoir was identified from a depth of 2303.53 - 2374.85m. The reservoir for Well E-S5 had a net to gross value of 3.66/67.51 indicating a poor to moderate quality and connectivity. Based on the cut-off parameters, pay flags (Fig. 4.2.1.5) are present in Well E-S5 at depths of 2309.9m, 2315.6 and 2368.9m therefore the reservoir contains hydrocarbons and is porous as well as permeable to store and transmit fluids. However, the hydrocarbon present in Well E-S5 is not economically valuable to be drilled.

In Well F-AH4, two reservoirs were identified. The first reservoir, Reservoir 1 at a depth of 1833 - 1877.58m indicated a pay flag portion in the reservoir, which is four meters thick (1833 - 1836m) (Fig. 4.2.1.6). Between depths 1857- 1873m of Reservoir 1, pay flags are also present. The net to gross values for Reservoir 1 of Well F-AH4 is 8.84/44.65 having a poor to moderate quality and connectivity. The second reservoir, Reservoir 2 of Well F-AH4 range between depth 2430.18 - 2369.07m and showed pay flags throughout the entire reservoir (Fig. 4.2.1.7). The net to gross for Reservoir 2 of Well F-AH4 was 55.47/59.89 having a moderate to good quality and connectivity for the reservoir. From the petrophysical aspect, Well F-AH4 is a good prospect for hydrocarbons and to test for oil.

**Seismic Facies**

The chaotic seismic facies of Well E-S3 (Fig. 4.3.6) from depth 2191 - 2754m includes the depth range of Reservoir 1 identified in the petrophysical analysis. The chaotic seismic facies indicates a poor to moderate net to gross quality as well as connectivity being fine to coarse grained. Therefore the results of the seismic facies correspond to the net to gross aspect for Well E-S3 and possibly related to Facies HM1 (claystone) or HM2 (fine to coarse grained sandstone) (Table 1). The chaotic seismic facies of Well E-S5 (Fig.4.3.12) from depth 1822 - 2751m comprises of the reservoir (2303.53 - 2374.85m) identified from the petrophysical evaluation. The chaotic seismic facies of Well E-S5 point out to an extremely poor connectivity and quality suggesting a claystone or shale lithology. Slumping (depositional environment) or a geological structure could have also caused the chaotic seismic facies. As a result, the seismic facies does not correspond with the net to gross petrophysical aspect of Well E-S5 and could be related to Facies HM1. Furthermore the petrophysical parameters can change locally within each individual rock (Stuck et al., 2013), probably due to being in the more distal part of the delta front and the timing of migration of hydrocarbons therefore it is less permeable and not a good reservoir. This could possibly have affected the results calculated for the reservoir in Well E-S5.

Semi- continuous high amplitude, seismic facies of Well F-AH4 (Fig. 4.3.16) ranging from 1446 - 1952m encompasses Reservoir 1 identified from the petrophysical analysis. The net to gross is poor to moderate for the semi- continuous high amplitude seismic facies (Seismic facies 3). Seismic facies 3, having a poor to moderate net to gross is fine to coarse grained and therefore possibly related to Facies HM1 or HM2. The divergent variable amplitude seismic facies (Seismic facies 4) of Well F-AH4 (Fig.4.3.17) from 1962 - 2658m includes Reservoir 2 and it indicates a moderate to good quality and connectivity. Seismic facies 4, with a moderate to good net to gross is fine to medium grained and is possibly related to lithofacies HM4 or HM5. Both semi-continuous and divergent variable amplitude seismic facies of Well F-AH4 correspond to the petrophysical results of net to gross.

Most of the seismic facies could be correlated with the petrophysical evaluation results, but some could not in the case of Well E-S5. Reservoirs are heterogeneous and multiple parameters

such as porosity, compaction and cementation can affect the petrophysical results obtained for Well E-S5, which could have affected the migration and storage of hydrocarbons.

## Correlation Analysis

For Well E-S3 a positive correlation exists between ILD and SFLU (Table. 5). ILD and SFLU measures resistivity of a rock but at different depths inside the rock body therefore should be correlated in a positive way. A negative correlation exists between GR, ILD and SFLU (Table. 5) because of the impossibility of shales being invaded 'because of their' low permeability. A negative correlation also exists between NPHI and RHOB. A cross plot of density versus neutron log (Appendix 10) demonstrates the negative correlation between NPHI and RHOB. A negative correlation can exist between NPHI and RHOB, when gas is detected (high density porosity and low neutron porosity).

In Well E-S5 there is a very high positive correlation between the resistivity logs (ILD, MSFL and SFLU) and RHOB as well as a negative correlation with NPHI. Resistivity logs measure hydrocarbons present in a rock body therefore gas or light hydrocarbons cause the porosity from the density log to increase and porosity from the neutron log to decrease (Schlumberger, 1989). As a result, resistivity logs can have a positive relationship with density logs while NPHI (neutron) has a negative correlation with RHOB and resistivity logs (ILD, MSFL and SFLU). A positive relationship also exists between GR, ILD, MSFL and SFLU, which could indicate a possible source rock comprising organic material or hydrocarbons.

In Well F-AH4 there is a positive relationship between LLS and LLD. LLD and LLS measure the same feature in a rock but at different depths inside the rock body therefore should have a positive correlation. A positive relationship also exists between GR, NPHI and RHOB, which could point out a shale body comprising of water, which has a higher density than oil.

## Multivariate statistics

The multivariate statistical technique was used to determine oil and non- oil bearing depths based on the available wireline log data. Multivariate statistical analysis compares numbers expressing geological attributes. Multivariate statistics results were compared to petrophysical

and seismic facies results. Factor and cluster analysis were used for selecting the best-related parameters with reservoir properties. In Well E-S3, both factor and cluster analysis indicated that between 2362m and 2422m deep, possible oil is present (Fig.4.5.1.1). The pay flag of Reservoir 1 in Well E-S3 indicates that oil is present between depths 2350 - 2360m and 2377 - 2378m (Fig. 4.2.1.4) in a fluvial deltaic environment. It seems reasonable to compare the multivariate statistics results with the petrophysical aspect. Oil shows between depths 2362 to 2422m and relates to seismic facies 5 (Chaotic) of Well E-S3 pointing out fine to coarse grained sediments with a poor to moderate net to gross and connectivity (Fig.4.3.6).

In Well E-S5, factor analysis shows that oil is present between depths 2302.00 - 2308.093m and 2424.68 - 2433.82m (Fig. 4.5.1.2) but is a very limited reservoir as the thickness of oil bearing depth is too small to be considered a prospective well. Pay flags are present in the reservoir (2303.53 - 2374.85m) of Well E-S5 however; the thickness of the pay flags is too small to be considered economically producible. In Well E-S5, the reservoir does not have good petrophysical properties where by the average porosity is 13.8%, volume of shale being 23.8% and water saturation of 41.5% (Table 3). It could be a local difference that has affected the properties due to a difference in the reservoir quality or in the geological structure of the area. Another reason could be a local variation in the depositional environment. Chaotic seismic facies of Well E-S5 (Fig.4.3.12) relates to the oil depth intervals of 2302.00 - 2308.093m and 2424.68 - 2433.82m of factor analysis indicating extremely poor net to gross and connectivity, implying a poor reservoir.

For Well F-AH4, factor analysis indicates that oil is present at depth 1833.06m while between depths 1836 - 1878.78m there is no oil present (Fig.4.5.1.3). The statistical results of both factor and cluster analysis are comparable to the petrophysical results for Reservoir 1 as well as the seismic facies of Well F-AH4 (1833 - 1877.58m), as the pay flag present between depth 1833 - 1836m indicates hydrocarbon and the semi-continuous high amplitude seismic facies indicate poor to moderate connectivity. Both factor and cluster analysis shows that oil is present from depth 2372.10 to 2524.81m in a distributary channel of a deltaic environment and justifies the results for Reservoir 2 (2369.07 - 2430.18m) in Well F-AH4. Hydrocarbon intervals between

depth 2372.10 - 2524.81m relates to both divergent variable amplitude and chaotic seismic facies having fine to medium grained sediments with varying deposystems.

In summary, it seems reasonable to compare the seismic facies and multivariate statistics results with the petrophysical evaluation. The seismic facies approach taken in this thesis never considered petrophysical properties, therefore a petrophysical model based on seismic facies could not be constructed. However, seismic facies can help to confirm some features of the depositional systems in absence of enough cores. It should also be pointed out that seismic facies is blind to specific reservoir depths but considers the entire net to gross of a particular facies. Multivariate statistics is a laborious but effective method and probably best used for big sets of data, but among the pitfalls of the method, it should be taken into account the fact that the method cannot be applied blindly. The logs and properties must be carefully chosen because they will be the criteria of discrimination.

# CHAPTER 6

## CONCLUSION

This thesis has addressed the depositional environment and petrophysical evaluation of four reservoirs in three wells of the Bredasdorp Basin. The depositional environments were interpreted based on core samples, gamma ray log, lithological description and seismic facies. Though at some depths core samples were not available and well reports were used to arrive at the necessary conclusion for the well bores. In Well E-S3 the depositional environment for reservoir (2350 - 2400m) was interpreted as fluvial deltaic of sequence 1At1 based on core samples, gamma ray log signatures and lithological descriptions. Reservoir (2304.59 - 2373.93m) of Well E-S5 points out to a channel deposit ranging between sequence 1At1 and 5At1 due to lithological descriptions and gamma ray signatures. Reservoir 1 of Well F-AH4 (1833 - 1877.58m) has been interpreted as a possible rise in sea level of sequence 10At1 based on seismic facies, lithological descriptions and gamma ray log signatures. Reservoir 2 of Well F-AH4 (2430.18 - 2369.07m) concluded a distributary channel in a delta of sequence 1At1 based on core samples, seismic facies, lithological descriptions and gamma ray signatures. The gamma ray log signature indicates that reservoirs are sealed by prodelta shales. Well tops reveal that the three wells studied (E-S3, E-S5 and F-AH4) span between 126 and 93 Ma in the Cretaceous Period.

Petrophysical evaluation results of the three studied wells reveals a water saturation range of 17 - 45% within the reservoir intervals. Wireline logs indicate a porosity range of 13 - 20% and predicted permeability range of 4 - 108 mD in Wells E-S3, E-S5 and F-AH4. The results suggest a fair to good reservoir quality for the study area.

Five distinct units were interpreted in each seismic section, characterized by different seismic facies. Well control was essential to calculate net to gross values, to identify reservoir areas and hydrocarbon prediction. Chaotic (Wells E-S3 and E-S5), semi-continuous high amplitude and divergent variable amplitude (Well F-AH4) seismic facies indicate reservoir areas.

Factor analysis and cluster analysis were performed to extract petrophysical properties from wireline logging data of the three wells, as the numbers have meaning. Both factor and cluster analyses indicate that possible hydrocarbon is present in Wells E-S3, E-S5 and F-AH4 at depths 2362 - 2422m, 2302 - 2308.09m, 1833.06m and 2372.10 - 2425.44m respectively. Giving a reliable estimate for hydrocarbon saturation by factor analysis, one can decrease the level of uncertainty of the petrophysical evaluation results. Having more data for the rest of the petrophysical uncertainties, a more accurate estimate for the petrophysical evaluation can be made. It is therefore concluded that factor analysis is processing orientated and cluster analysis is grouping orientated and not a good method to distinguish cases. Multivariate statistics is best used with more data, example 6-10 wells.

In this thesis all three methods, petrophysical evaluation, seismic facies, and multivariate statistics were applied to log data to predict hydrocarbon saturation. The results show that the petrophysical evaluation and multivariate analysis perform better than the seismic facies model. However, seismic facies is a good technique, if used properly and enough data is available for hydrocarbon prediction.
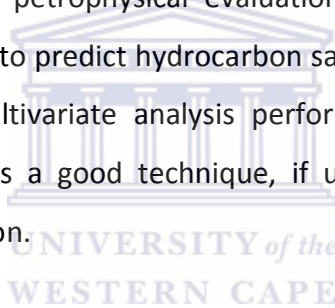
**From the thesis, the following deductions can be made and believe that future work should:**

- Incorporate both wireline logs and core samples to provide a strong mechanism for interpretation and determination of depositional environments and facies. Wireline logs also provide a continuous vertical profile of the well bore, which may be lost by incomplete recovery of core.

- Apply seismic facies classification techniques as a standard procedure during the exploration and production stage, but with the knowledge of the advantages (and limitations) of the seismic classification using 3D seismic data.

- Optimize conventional methods using multivariate statistical techniques as a first approach to differentiate between poor and good reservoirs, which makes quick reliable reservoir estimation and can be used as a powerful tool for reservoir properties from wireline logs in the petroleum industry. The technique provides a cost effective method

to interpret reservoirs and cannot be applied blindly. The benefits of the technique are: it will confirm or bring new information about the depths of hydrocarbon saturation estimated from different wireline logs; derived quantities of porosity, permeability, density and lithological characteristics because the information of all wireline logs available is used simultaneously. The disadvantage is that it cannot explain local attributes.

# REFERENCES

Broad 2004. South Africa Activities and Opportunities. An Unpublished Power Point Presentation to PetroChina.

Broad, D.S., Jungslager, E.H.A., McLachlan, I.R., Roux, J., 2006. Offshore Mesozoic Basins. In: M.R. Johnson, C.R., Anhaeusser, R. J. Thomas (Eds.), The geology of South Africa (Ed. By M.R. Johnson, C.R Anhaeusser, R.J. Thomas), pp. 553-571. Geological Society of South Africa, Johannesburg, Council for Geoscience, Pretoria, Johannesburg, Pretoria.

Brown, L.F., Brown Jr., L.F., Benson, J.M., Brink, G.J., Doherty, S., Jollands, A., Jungslager, E.H.A., Keenan, J.H.G., Muntingh, A., Van Wyk, N.J.S., 1995. Sequence stratigraphy in offshore South African divergent basins: an Atlas on Exploration for Cretaceous Lowstand Traps by SOEKOR Limited. AAPG Studies. Geol. 41, p 83–137 (SOEKOR (Pty) Ltd.).

Bucker C.J., Jarrard R.D., Wonik T., Brink J.O., 2000. Downhole Logging Data Analysis of Cape Roberts Drillhole CRP-2A: a Multivariate Statistical Approach. Terra Antartica, 7. 299-310.

Collimsom, J.D. 1969. The sedimentology of the Grindslow Shales and the Kindirsout Grit: a deltaic complex in the Narnuirian of northern England. Journal of Sedimentology Petrology 39. 194-221.

Davis, J.C. 1986. Statistics and Data Analysis in Geology, 2$^{nd}$ edn. Wiley, New York, 646p

Friedman, G.M. & Sanders, J.E. 1978. Principles of Sedimentology. New York: John Wiley & Sons, pp 495-508.

Galton, F (1890). Kinship and correlation. North American Review, 150:419-431.

Gluyas, J., Swarbrick, R. (2004). Petroleum Geoscience. Blackwell Science Ltd. Oxford, UK. p3-4

Haq, B. U., J. Hardenbol, and P. R. Vail, 1987, Chronology of fluctuating sea level since the Triassic: Science, v. 235, p. 1156–1166.

Haq, B., J. Hardenbol, and P. R. Vail, 1988, Mesozoic and Cenozoic chronostratigraphy and eustatic cycles of sea-level change, in C. K. Wilgus et al., eds., Sea-level change: an integrated approach: SEPM Special Publication42, p. 71–108.

IBM SPSS Statistics (2013). IBM ® SPSS ® Statistics 21. ©Copyright IBM Corporation 1989, 2012.

IHS Energy (2010). Outeniqua Basin, South Africa. Basin Monitor.

Interactive Petrophysics (2013). Interactive petrophysical™ software version 4.1.2012.275. Copyright © 2012 Senergy Software Ltd.

Johnson, R.A., Wichern, D. W (1992), Applied Multivariate Statistical Methods 6th edn. Prentice Hall, Upper Saddle River, New Jersey. p 516-519

Kendal, M (1938). A new measure of rank correlation. Biometrika, 30:81-89.

Kingdom (2012). Kingdom ™ geological software version 8.7. HIS Global Inc. Houston Texas

Lapidus, D.F., 2003. Collins internet- linked dictionary of Geology. Bishopbriggs, Glasgow. P 170,380.

Mitchum Jr. R. M., Vail. P. R., Sangree. J. B. (1977). Seismic Stratigraphy and Global Changes of Sea Level: Part 6. Stratigraphic Interpretation of Seismic Reflection Patterns in Depositional Sequences: Section 2. Application of Seismic Reflection Configuration to Stratigraphic Interpretation. In: M 26: Seismic Stratigraphy--Applications to Hydrocarbon Exploration, pp. 117-133. AAPG Memoir.

Petroleum Agency SA, (2004/2005). Petroleum Exploration Information and
Opportunities: Petroleum Agency SA Brochure, 2004/2005, p16-18.

Petroleum Agency SA, (2010). Petroleum Exploration in South Africa information and opportunities, 32p published by South African Agency for Promotion of Petroleum Exploration and Exploitation, Parow, Cape Town.

Petroleum Agency of SA, (2013). Well completion report E-S3 Bredasdorp Basin South Coast RSA, compiled by Gearhart Geodata Services Ltd. for Soeker.pp 06-07

Petroleum Agency of SA, (2013). Well completion report E-S5 Bredasdorp Basin South Coast RSA, compiled by Gearhart Geodata Services Ltd. for Soeker.pp 14-15

Petroleum Agency of SA, (2013). Well completion report F-AH4 Bredasdorp Basin South Coast RSA, compiled by Halliburton Energy Services, Drilling Services SLD for Soeker.pp 18-19

Prather, B., Booth, J., Steffens, G., and Craig, P., (1998). Global Seismic Facies.  AAPG Bull.V. 82, No. 5A, pp 701-728.

Reimann, C., Filzmoser, P., Garrett, R.G., Dutter, R (2008). Statistical Data Analysis Explained: Applied Environmental Statistics with R. John Wiley & Sons, Ltd. 181-270

Rider, M., 1996. The Geological Interpretation of Well Logs. Second Edition revised 2002, Whittles Publishing, Sutherland, Scotland. 33-134.

Schlumberger,1989. Log Interpretation Principles/ Applications. Schlumberger Educational Services. Houston, Texas. 5-9, 6-1, 6-2, 6-5p.

Serra, O. 1986. Fundamentals of Well log Interpretation (Vol.2): The interpretation of Logging Data. Division Petroleum Sciences. 15B, 371p.

Sharma, P., Mamgain, G., Bahuguna, V.K., Lal, C., 2012. Improved permeability estimates in carbonate reservoirs using electrofacies characterization: A case study of Mumbai high south. Search and discovery Article #41069

Siad, A., Matheis, G., Utke, A., Burger, H., (1994). Discriminant analysis as a geochemical mapping technique for lateritic covered area of South Western and Central Nigeria. ITC Journal 1994-1, Special CODATA Issue, 7-12 Enschede.

Spearman, C.E (1904). "General Intelligence" objectively determined and measured. American Journal of Psychology, 15:201-293.

Stuck, H., Koch, R., Siegesmund (2013). Petrographical and Petrophysical properties of sandstones: statistical analysis as an approach to predict material behavior and construction suitability. Environ Earth Sci (2013) 69: 1299-1332.

Suzanne, G.C., Robert, M.C (2004): Petrophysics of the Lance Sandstone Reservoirs in Jonah Field, Sublette County, Wyoming. AAPG Studies in Geology 52 and Rocky Mountain Association of Geologists 2004 Guidebook; 226-227.

Ulasi, A. I., Onvekuru, S. O., Iwuagwu, C.J., 2012. Petrophysical evaluation of uzek well using well log and core data, Offshore Depobelt, Niger Delta, Nigeria. Advances in Applied Science Research, 3 (5):2966-2991.

Walker, R.G.1992. Facies, Facies Models and Modern stratigraphic concepts. In Walker, R.G & James, N.P (eds): Facies Models: response to sea level change, Geological Society of Canada, Ontario. 1-13

Ward, J.H. (1963). Hierarchical grouping to optimize an objective function. Journal of the American Statistical Association 58 (301), 236-244.

**Electronic references**
(http://www.searchanddiscovery.com/abstracts/html/2008/hedberg_argentina/extended/gamero/images/fig01.jpg

# APPENDICES

## APPENDIX 1: PETROPHYSICS

### CONVERSION OF DIGITAL LOG TO READABLE FORMAT

Data from Wells E-S3, E-S5 and F-AH4 drilled inside the area of focus was obtained in digital format (LAS format), and converted into a readable format using InteractivePetrophysics software. Log traces were displayed in a composite log. The panel consists of log tracks, which are assigned a track location and width based on the scale. Log tracks, such as gamma ray, neutron, density, resistivity and sonic were displayed.
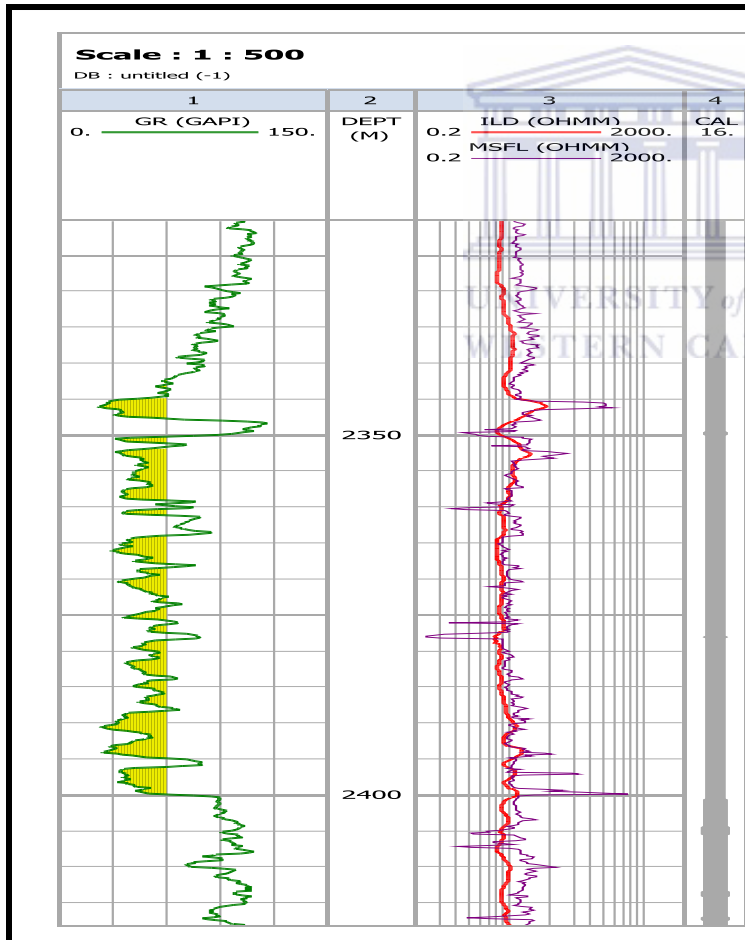


A.1.1. Example of a digital log track of a gamma ray and resistivity log (Interactive Petrophysics, 2013)

From the LAS/LBS load setting tab, six curve tracks were selected to be displayed (A.1. 2). The depth track was activated as well. All log curves were edited manually for environmental corrections and in some cases spliced if gaps were present. Histograms of each well were viewed in order to identify the value of the base line of the gamma ray log from the median and histograms of any other curves can also be used to change parameters interactively.
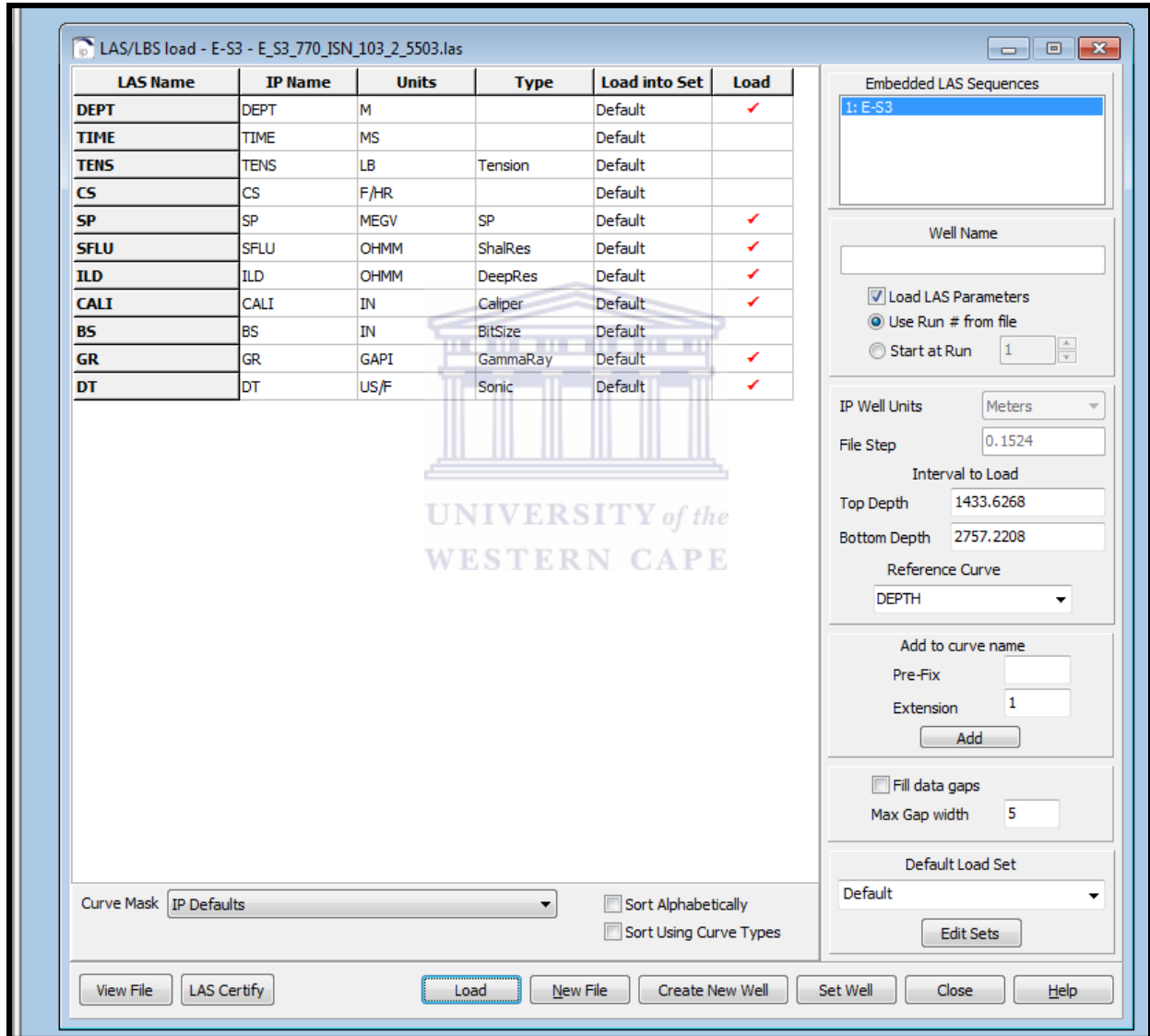


A.1.2. LAS/LBS settings dialog with define curve track (Interactive Petrophysics, 2013).

## ENVIRONMENTAL CORRECTION

Basic log analysis was done to determine different parameters (Table.A1) quick and easily. Clay volume was calculated from the gamma ray log as an input curve and the gamma ray histogram. Porosity was determined from either the density or the neutron / density cross plot. To display the neutron/density cross plot porosity, both the neutron and density curves had to be entered. The neutron porosity curve needs to be defined in limestone decimal units. If the neutron curve was in sandstone units then it should be converted into limestone units using the environmental correction tab. The output curve would be a porosity (PHI) curve calculated from the density or neutron/density logs. Water saturations were calculated using either the basic Archie equation, Indonesian equation or the Simandoux equation. The resistivity curve is used to calculate water saturation, with an output of a pickett plot. A pickett plot allows for the position of the wet line curve to select the Rw (formation water resistivity) and m (cementation factor) value interactively. Rw should be adjusted to the correct value from the wet line curve of the pickett plot based on the clustered points. Once all the parameters were determined and entered into the basic log analysis the analysis was ran.

Table. A1. Clay volume parameters obtained from basic log analysis

| WELL | GR CLEAN | GR CLAY | RHOB CLAY | NPHI CLAY | DT CLAY |
|------|----------|---------|-----------|-----------|---------|
| E-S5 | 11.2188 | 149.5 | 2.557 | 0.246 | 87 |
| E-S3 | 11.3594 | 168 | 2.7221 | 0.4082 | 125.1875 |
| F-AH4 | 11.8962 | 149.68 | 2.516 | 0.272 | 90 |

The mud cake was calculated to identify permeable zones by using the equation in A. 1.3.Once completed, all the settings were done so that it was automatically saved and the specific depths identified as permeable zones were exported as a clipboard file to be opened in Microsoft word in readable format.
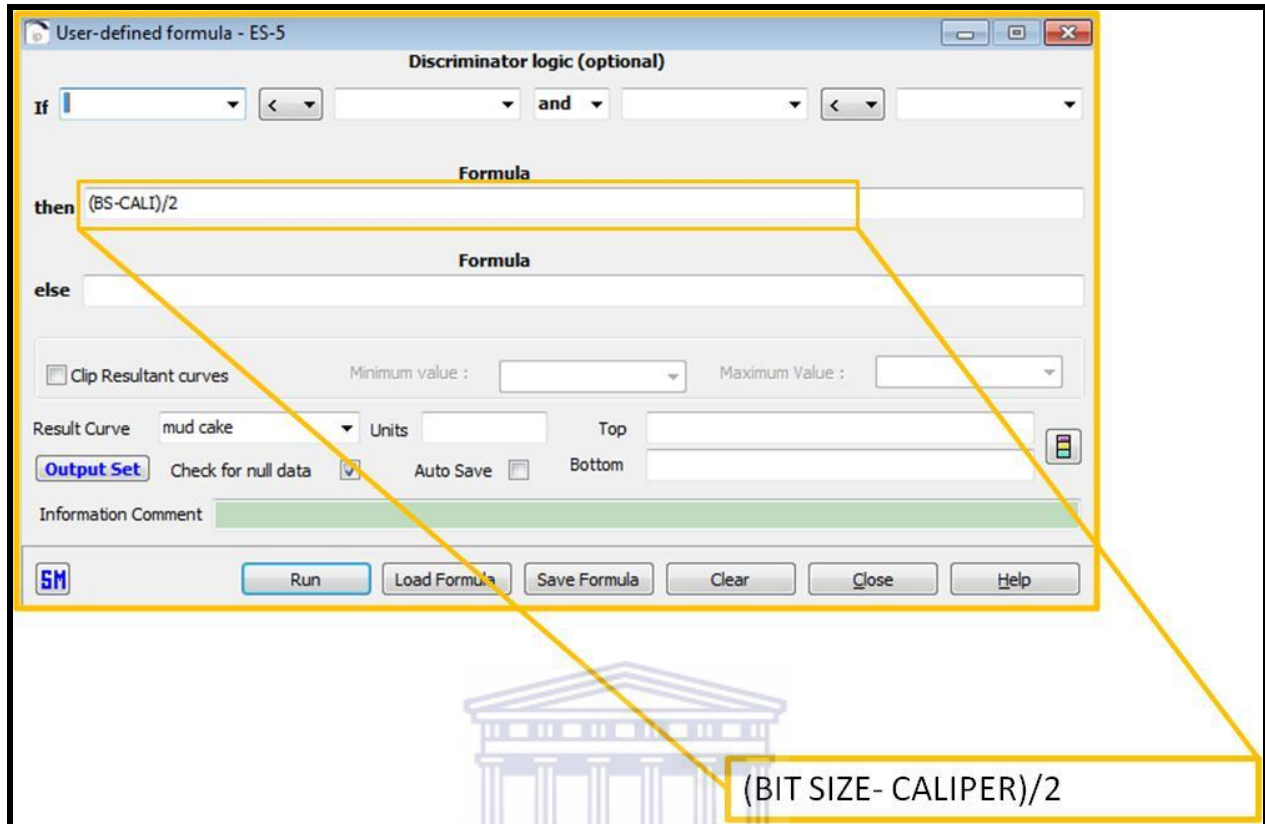
A .1.3. Calculation of mud cake computed using Interactive petrophysics software.

## Correlation of wells

Well correlation was done with interactive petrophysical software, which allows for multiple wells to be brought up in a well section and create correlation lines between wells (A.1.4). Multi-well correlation viewer was opened, followed by clicking the wells that would be used for correlating i.e. Well E-S3, E-S5 and F-AH4, in the input window. Once the wells are activated, new well tops were inserted manually via well manage zones/tops (A.1.4). Once the well tops were complete and activated the wells were correlated. Multi-well plots were saved into the database directory and exported as a clipboard file for pasting into word documents.
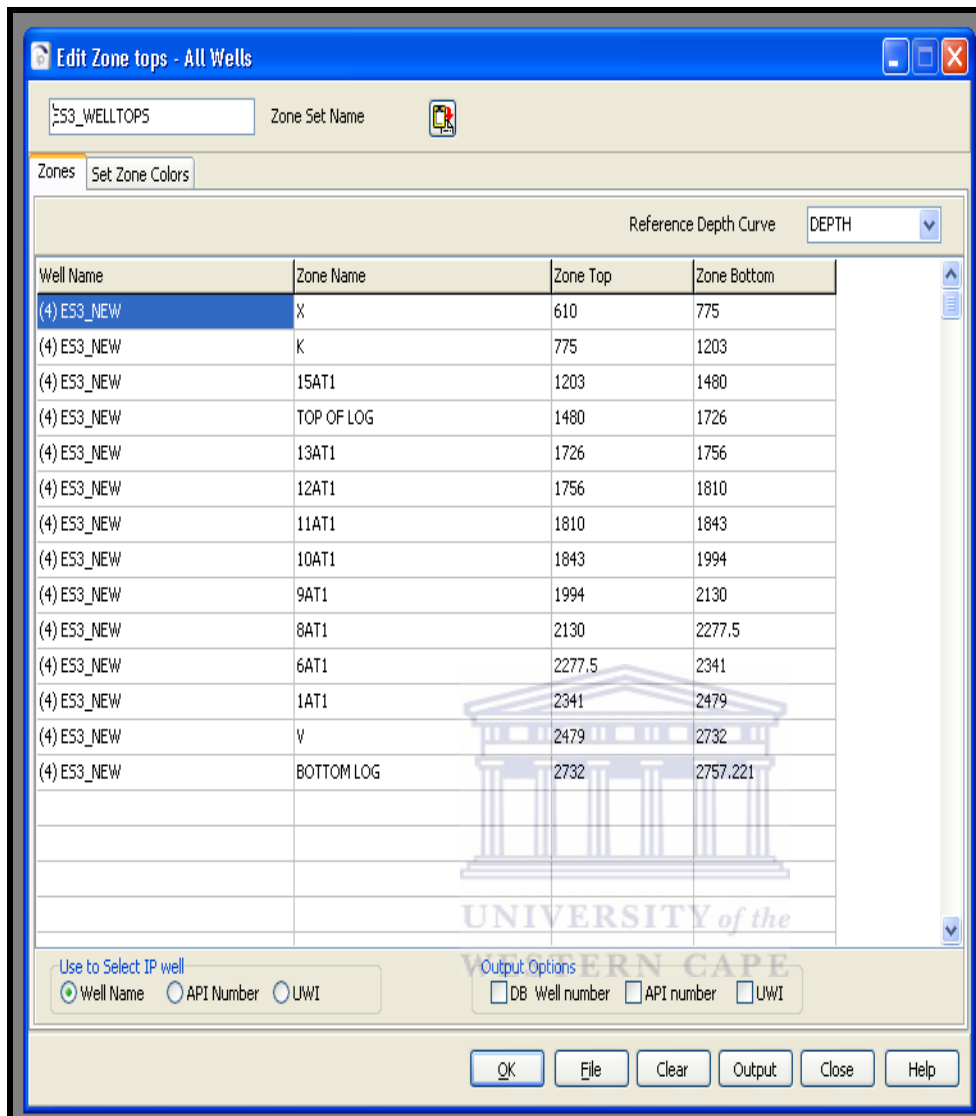
A.1.4. New well tops window displaying zone names and depth (Interactive Petrophysics, 2013).

## Porosity and water saturation

Porosity and water saturation analysis were used to calculate porosity (PHI) and water saturation (Sw) to compare different methods of obtaining porosity and water saturation. The number and type of output curves depends on the porosity model chosen and the logic selected. The temperature is an important controlling factor so its curve was calculated and used as an input for this analysis. The temperature curve was calculated using the temperature gradient tab and choosing the temperature units as degree Celsius.

Once the core permeability and core porosity curves are added to both water saturation and porosity comparison, the correct water saturation and porosity curve can be interpreted.

UNIVERSITY *of the*
WESTERN CAPE

**APPENDIX 2: SCATTER PLOTS OF CORE POROSITY VS. CORE PERMEABILITY**
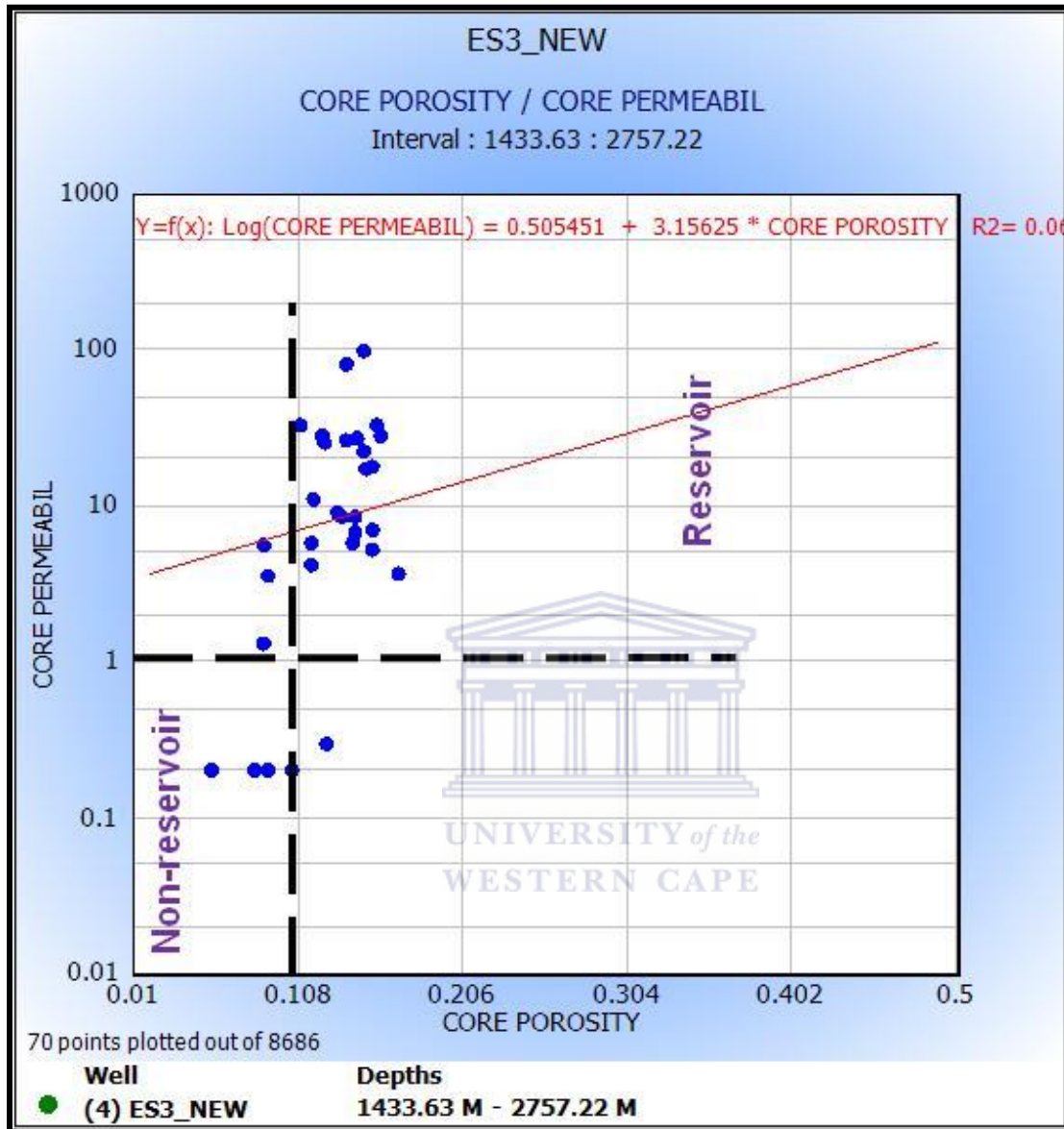
ES5

core porosity / core permeabil
Interval : 1598.07 : 2692.6

Y=f(x): Log(core permeabil) = -2.59422 + 22.8979 * core porosity   R2= 0.64343

Reservoir

Non-reservoir

UNIVERSITY of the
WESTERN CAPE
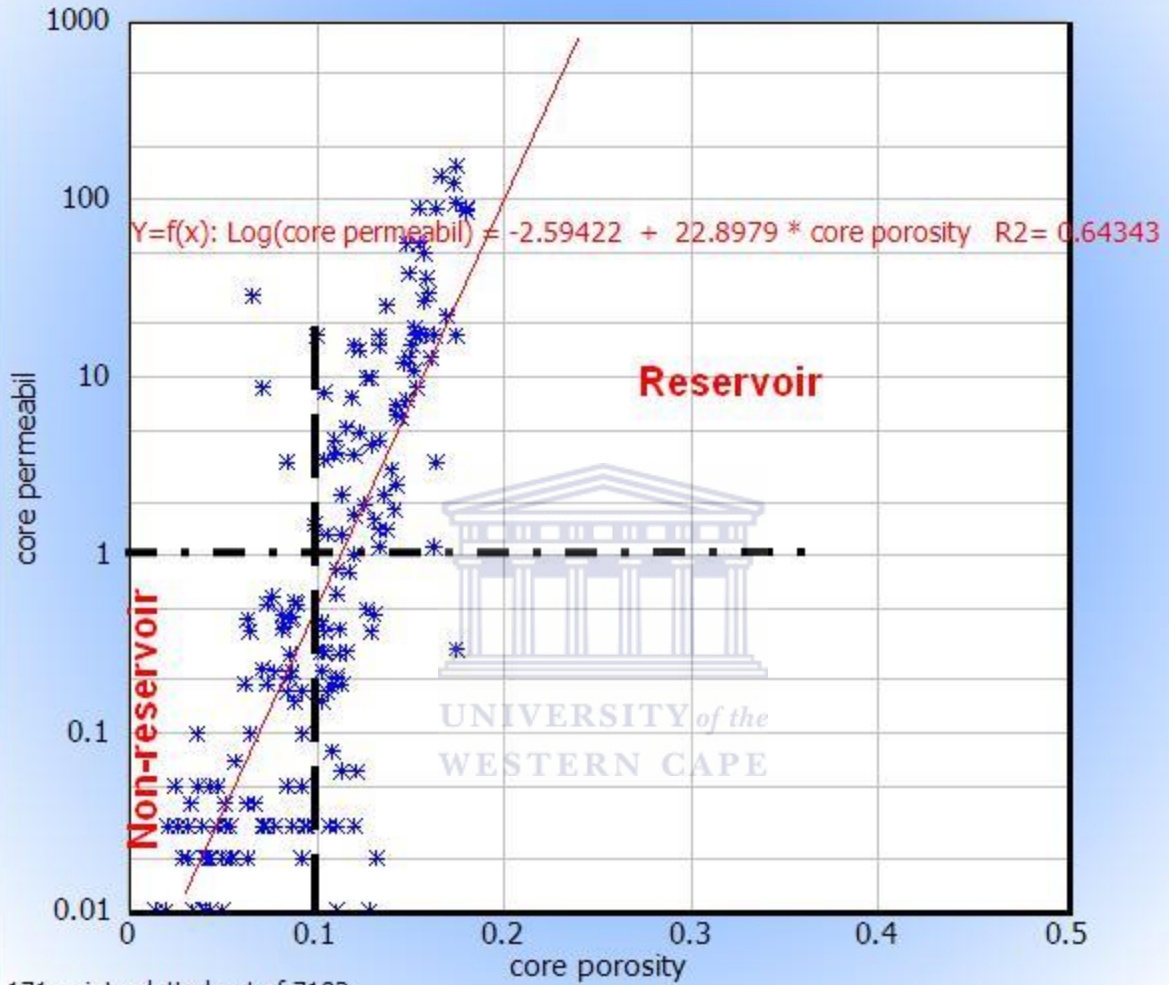
171 points plotted out of 7183

| Well | Depths |
|------|--------|
| (2) ES5 | 1598.07 M - 2692.6 M |

F-AH4_NEW

CORE POROSITY / CORE PERMEABIL
Interval : 122.24 : 2678.75

Y=f(x): Log(CORE PERMEABIL) = -1.41973 + 23.2128 * CORE POROSITY    R2= 0.54

27 points plotted out of 16776

| Well | Depths |
|---|---|
| (5) F-AH4_NEW | 122.24 M - 2678.75 M |
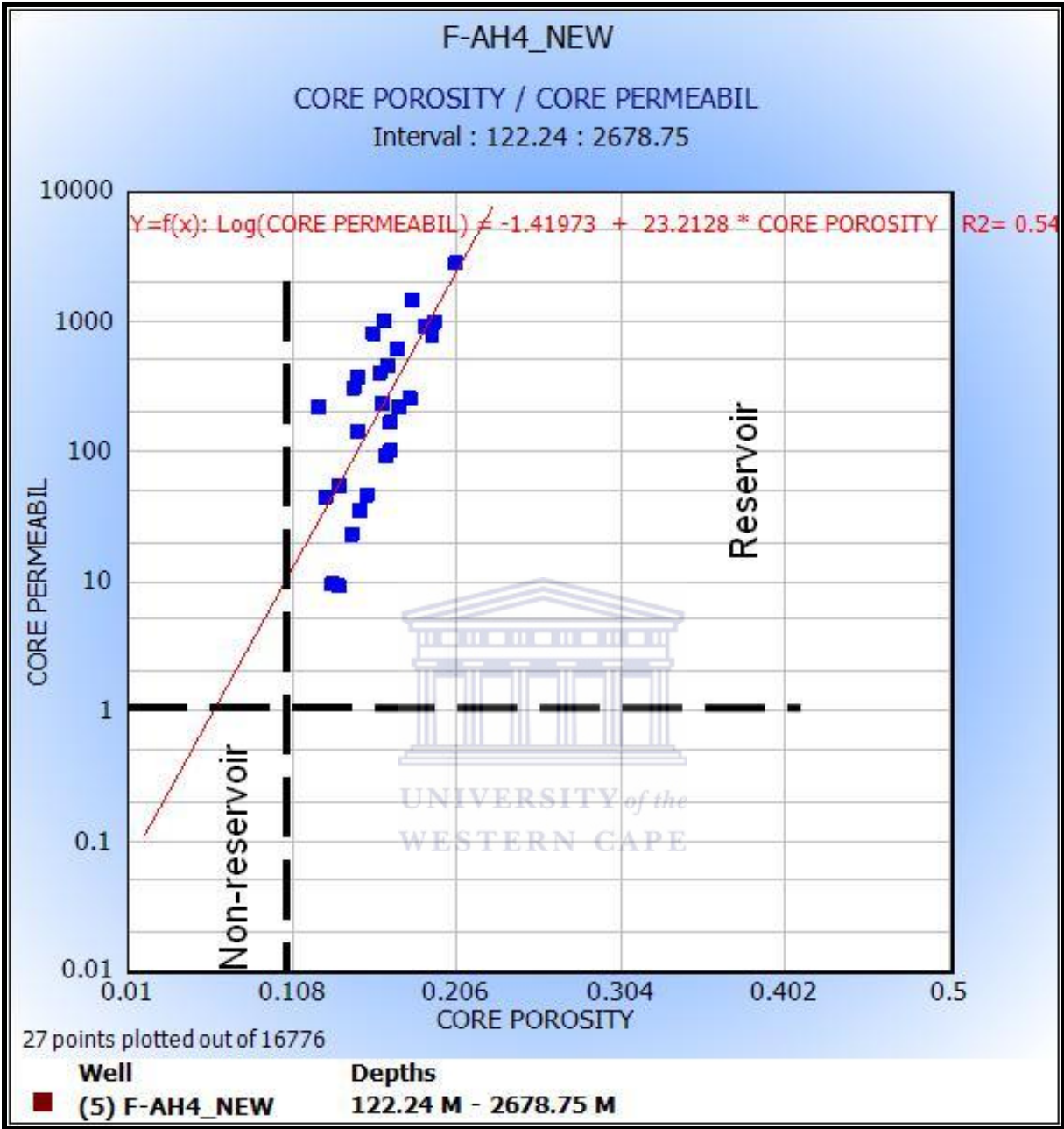
# APPENDIX 3: NET TO GROSS DETERMINATION
## NET/GROSS DETERMINATION METHOD

The gamma ray log may often be used quantitatively. Although the gamma ray value for shales varies enormously in any area or well, the values for pure shales tend to be constant (A. 3.1). Thus if one considers the maximum average gamma ray log value to be pure 100% shale (i.e., shale line, A. 3.1) and the lowest value to indicate no shale at all (i.e., sand line, A.3.1), a scale from 0 – 100% shale can be constructed.
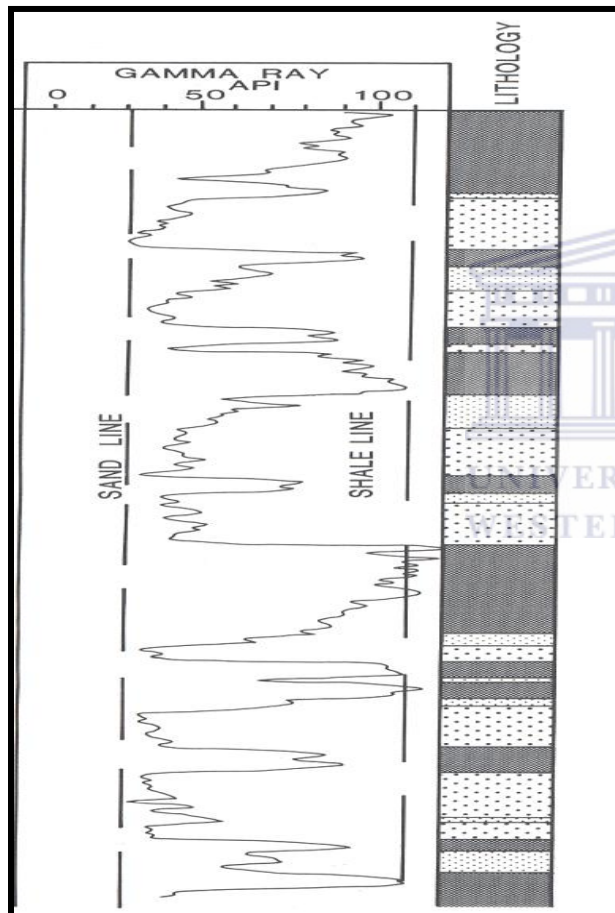


A.3. 1. Sand line and shale line defined on a gamma ray log. These 'baselines' are for the quantitative use of the log, and may be reasonably constant in one zone (After Rider, 1996).

According to Rider, 1996, if the scale is considered to be linear, any value (GR) of the gamma ray log will give the volume of shale from the simple calculation:

$$\text{Volume of shale \%} = \frac{GRvalue(\text{LOG}) - GR(MIN)}{GR(MAX) - GR(MIN)}$$

*GR (MAX) = 100% shale, GR (MIN) = 0% shale, i.e. cleans formation.*

Generally the value is not very accurate and tends to give an upper limit to the volume of shale (Vsh). Moreover, there is no scientific basis for assuming that the relationship between gamma ray value and shale volume should be linear. Thus a modification of the simple linear relationship used above has been proposed as a result of empirical correlation (A.3.2).

---

**For pre- Tertiary (consolidated) rocks,**

$VV_{SH} = 0.33(2^{2VsH} - 1)$

**For Tertiary (unconsolidated) rocks,**

$VV_{SH} = 0.083(2^{3.7VSH} - 1)$

Where $V_{SH}$ = shale volume from these formulae

$VV_{SH} = \frac{GR - GR(MIN)}{GR(MAX) - GR(MIN)}$

---

A.3.2. The relationship changes between younger (unconsolidated) rocks and older (consolidated) rocks.
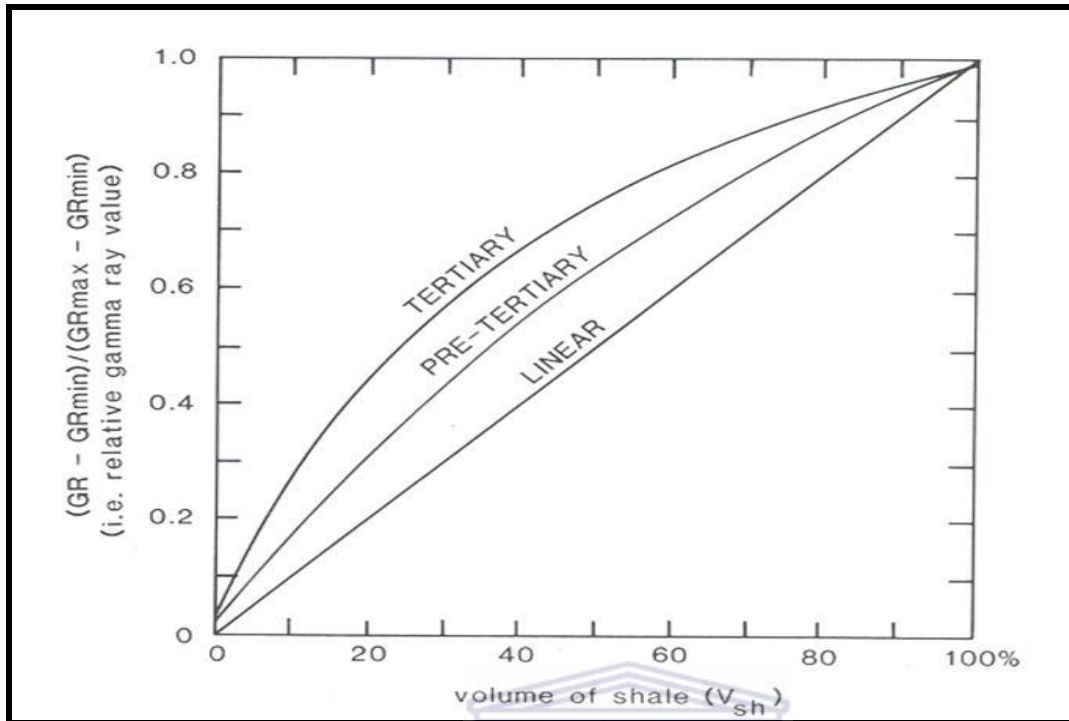
A. 3.3. Graphical representation of the relationship between relative gamma ray deflection and shale volume (from Dresser Atlas, 1982, seen in Rider, 1996).

As a first indicator of lithology, the gamma ray log is extremely useful as it suggests where shale may be expected. Moreover, as shown above, the higher the gamma ray value, the higher percentage of shale (A.3.3). But the log is only a first indicator. Radioactivity of some other lithologies shows that any lithology indicated by the simple gamma ray log must be confirmed by other logs.

**A QUICK LOOK METHOD FOR N/G**

A quick look method for estimating net over gross for exploration purposes does exist. As mentioned above, amongst the various applications of the gamma ray log is its application as a general lithology indicator. In this regard, the log signature can be used to discriminate between a reservoir and a non-reservoir (Net/Gross). After the baselines have been established (A.3.4), one can count the squares of the log paper under the log signature above the 50% shale line as constituting the Net, and the squares between the 50% shale line and the 100% shale line as constituting the rest of the Gross rock volume. Both values should be converted into percentages to give the Net/Gross ratio.

163
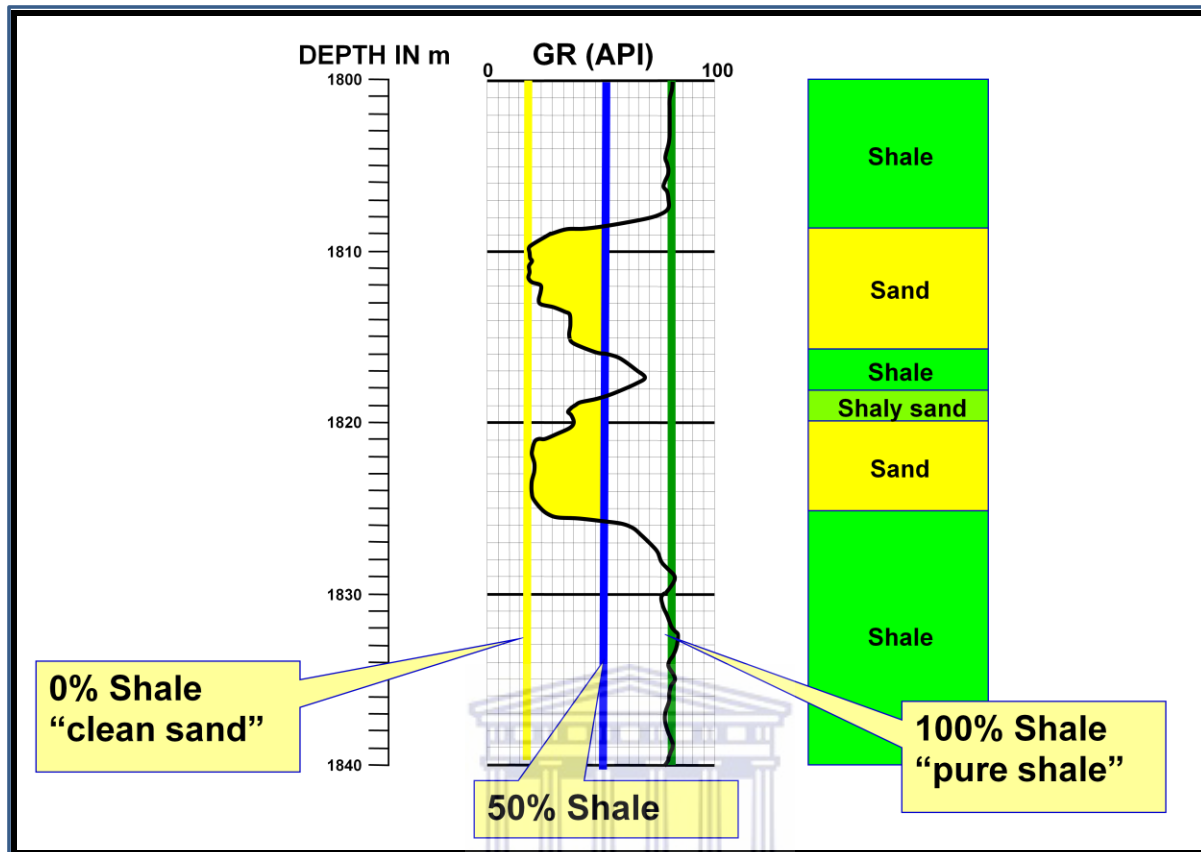
A. 3.4. Sand line and shale line defined on a gamma ray log. These 'baselines' are for the quantitative use of the log, and may be reasonably constant in one zone (Braide, 2012, Personal Communication).

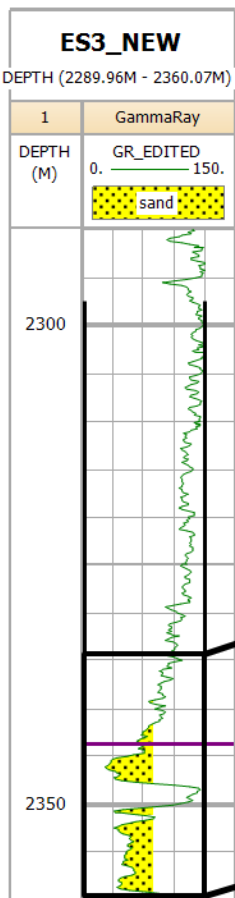## Net to Gross values for Well E-S3 (Appendix 3 continued)



**1575-1605m**
**1 blocks of sandstone**
**19 blocks of shale**
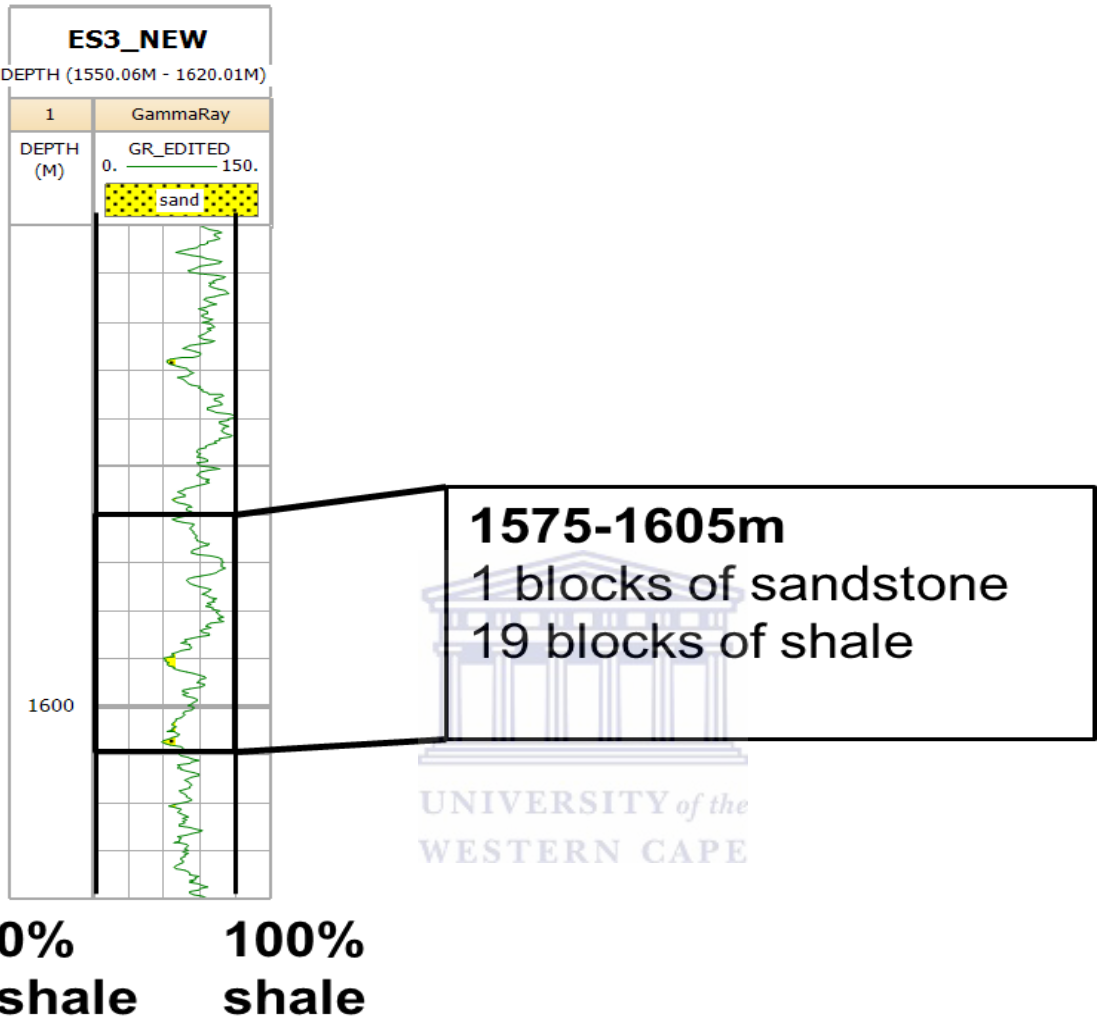
**DEPTH 1575-1605m**

Total squares= 20 blocks

Net=$\frac{1}{20} \times 100 = 5\%$

Gross=$\frac{19}{20} \times 100 = 95\%$

N/G= 5: 95

N/G: very poor to poor

Connectivity: very poor to poor

ES3_NEW
DEPTH (2289.96M - 2360.07M)

2335-2360m
3 blocks of sandstone
21 blocks of shale

0% shale    100% shale

**DEPTH 2335-2360m**

Total squares= 24 blocks

Net= $\frac{3}{24} \times 100 = 13\%$

Gross= $\frac{21}{24} \times 100 = 87\%$

N/G= 13: 87

N/G: poor to moderate

Connectivity:  poor to moderate

**DEPTH 2425-2445m**

Total squares= 16 blocks

Net= $\frac{2}{16} \times 100 = 13\%$

Gross= $\frac{14}{16} \times 100 = 87\%$

N/G= 13: 87

N/G: poor to moderate

Connectivity: poor to moderate

**Net to Gross values of Well E-S5 (Appendix 3 continued)**
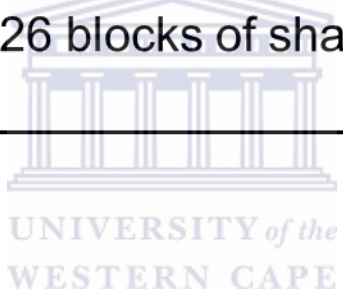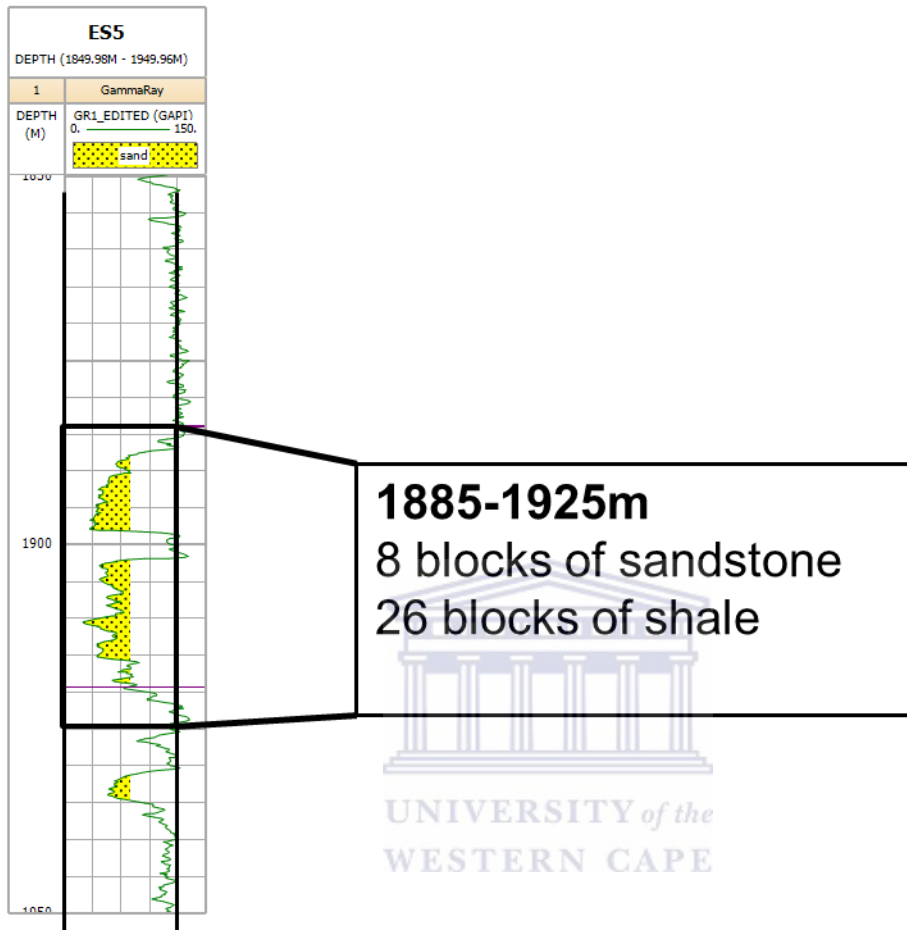


**DEPTH 1885-1925m**

Total squares= 34 blocks

Net= $\frac{8}{34} \times 100 = 24\%$

Gross= $\frac{26}{34} \times 100 = 76\%$

N/G= 24: 76

N/G: poor to moderate

Connectivity: poor to moderate

**ES5**

DEPTH (2200.05M - 2250.03M)

| 1 | GammaRay |
|---|---|
| DEPTH (M) | GR1_EDITED (GAPI) 0. ———— 150. |

2220-2240m
0 blocks of sandstone
16 blocks of shale

0% shale    100% shale
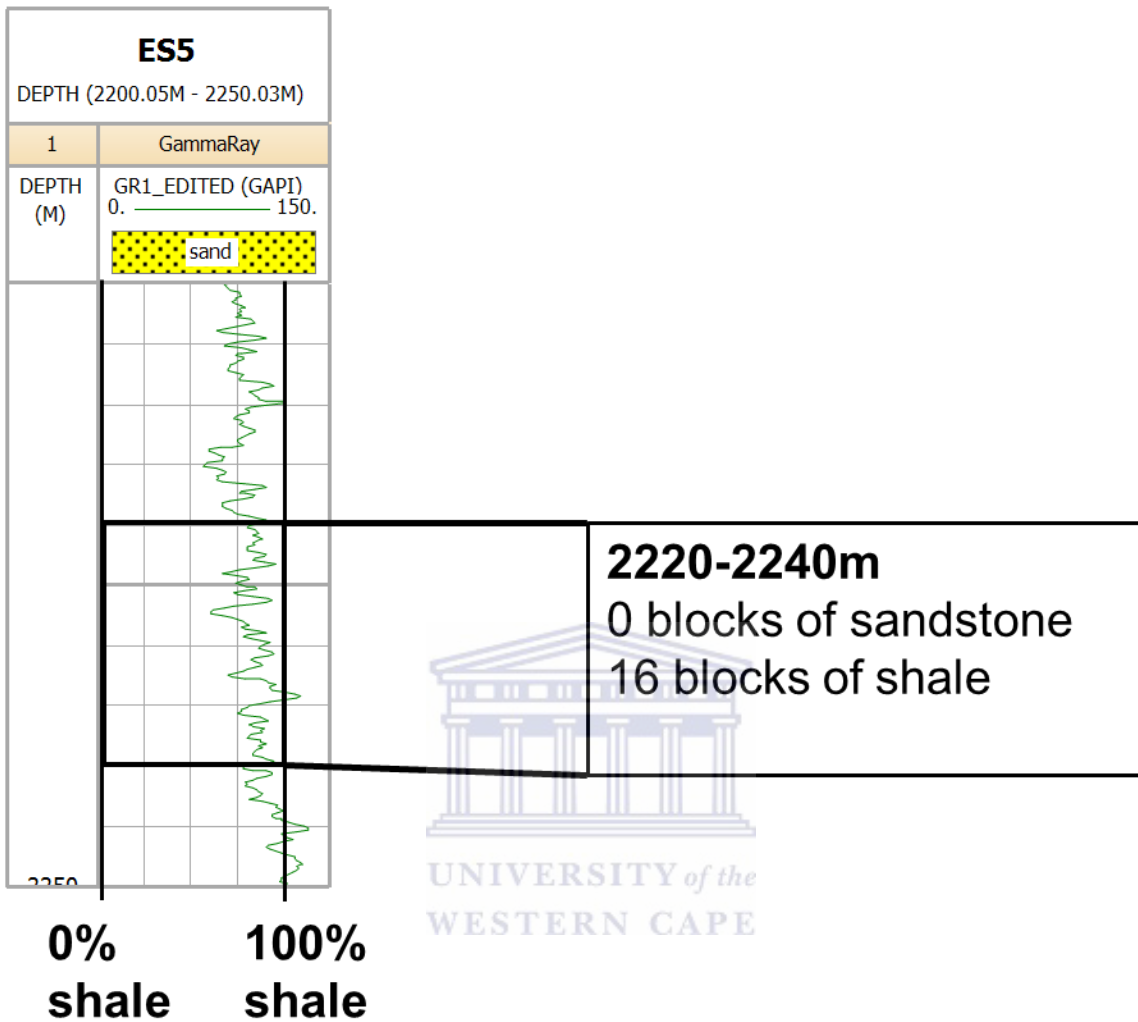
**DEPTH 2220-2240m**

Total squares= 16 blocks

Net= $\frac{0}{16} \times 100 = 0\%$

Gross= $\frac{0}{16} \times 100 = 100\%$

N/G= 0: 100

N/G:  extremely poor

Connectivity:  extremely poor

**Net to Gross values of Well F-AH4 (Appendix 3 continued)**
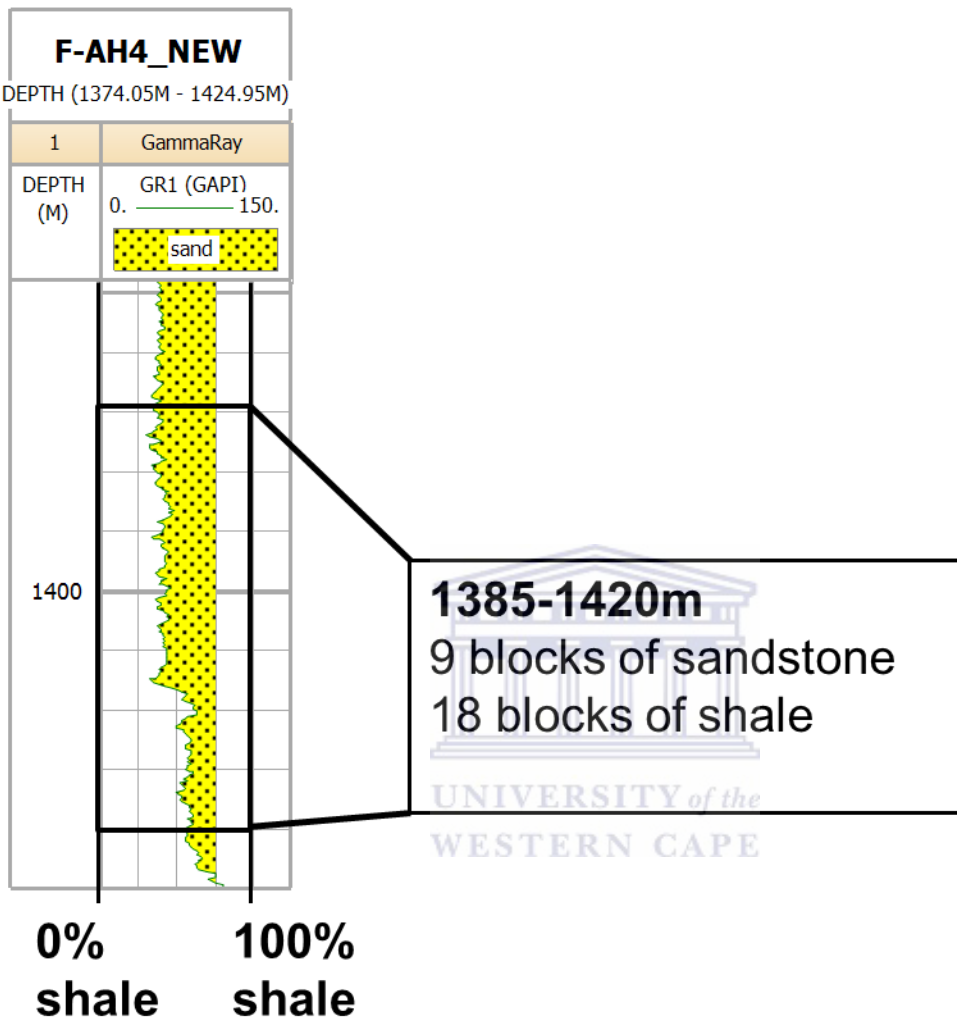


**DEPTH 1385-1420m**

Total squares= 27 blocks

Net= $\frac{9}{27} \times 100 = 33\%$

Gross= $\frac{18}{27} \times 100 = 67\%$

N/G= 19:81

N/G: moderate to good

Connectivity: moderate to good

**F-AH4_NEW**

DEPTH (1750.02M - 1800.01M)
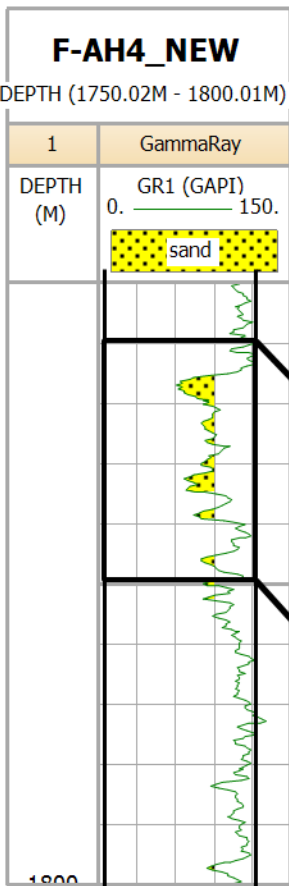
1765-1775m
2 blocks of sandstone
14 blocks of shale

0% shale    100% shale

**DEPTH 1765-1775m**

Total squares= 16 blocks

Net= $\frac{2}{16} \times 100 = 12\%$

Gross= $\frac{14}{16} \times 100 = 88\%$

N/G= 12: 88

N/G:  poor to moderate

Connectivity: poor to moderate

**F-AH4_NEW**

DEPTH (2375.01M - 2410.07M)

2380-2405m
5 blocks of sandstone
15 blocks of shale
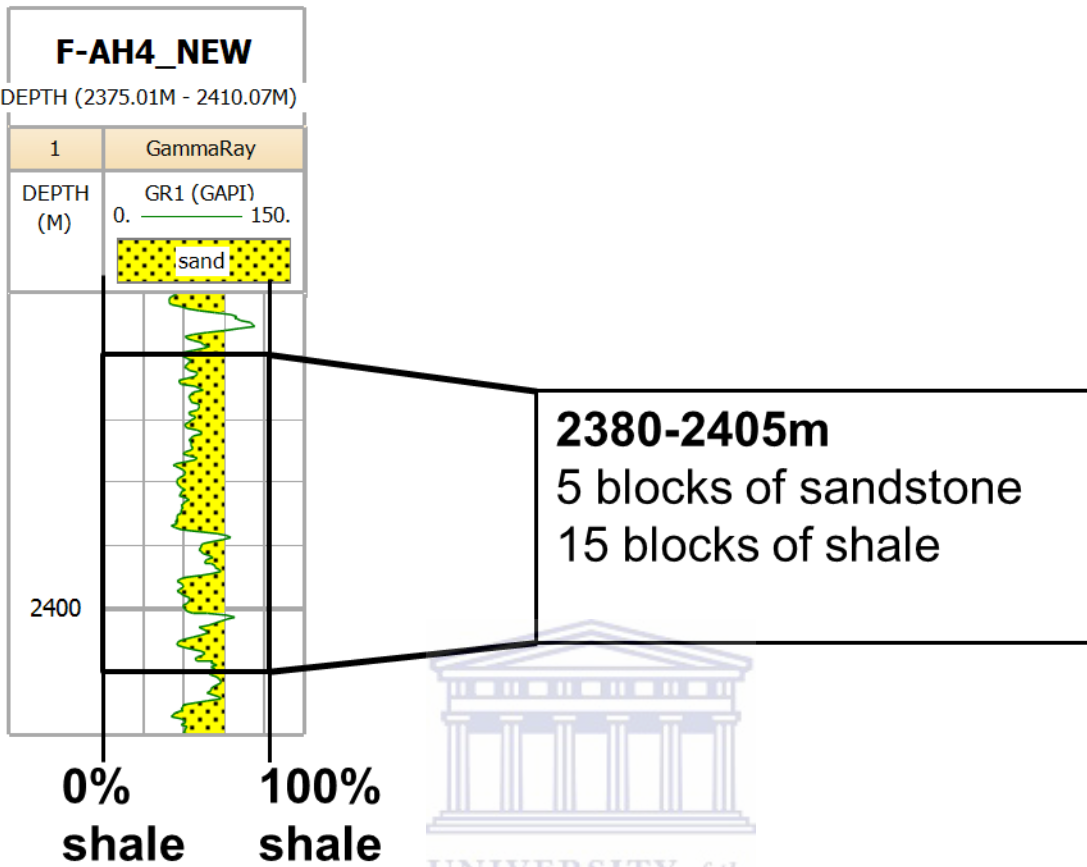
0% shale    100% shale

**DEPTH 2380-2405m**

Total squares= 20 blocks

Net= $\frac{5}{20} \times 100 = 25\%$

Gross= $\frac{15}{20} \times 100 = 75\%$

N/G= 25: 75

N/G:  moderate to good
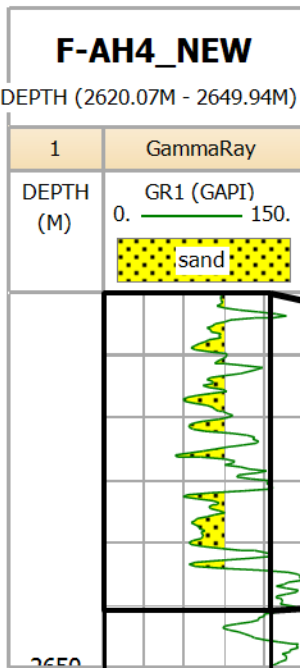
Connectivity: moderate to good

**DEPTH 2620.07-2645m**

Total squares= 21 blocks

Net= $\frac{4}{21} \times 100 = 19\%$

Gross= $\frac{17}{21} \times 100 = 81\%$

N/G= 19: 81

N/G: poor to moderate

Connectivity: poor to moderate

# APPENDIX 4: SEISMICS

**WELL LOG DEPTH CONVERSION TO SEISMIC DATA**

The seismic volume is in time and the logs are in depth, therefore a time- depth relationship was established using a check shot survey. This allows the log curve to be displayed on the seismic section as shown in A.4.1. Well tops at specific depth intervals (Table A4) were selected from the gamma ray log which was superimposed on the seismic data. Once the log was superimposed on the seismic line the exact time interval corresponding to each depth interval could be identified (A. 4.1). The time intervals were required for horizon mapping of the specific depths indicated.

Table A4. Time values and corresponding depth values of well tops

| Well tops | Depth (m) | | | Time (seconds) | | |
|---|---|---|---|---|---|---|
| | Well E-S3 | WELL E-S5 | WELL F-AH4 | Well E-S3 | WELL E-S5 | WELL F-AH4 |
| 1At1 | 2341 | 2304 | 2369.2 | 1.953 | 1.744 | 1.797 |
| 5At1 | | 2304.1 | | | 1.747 | |
| 6At1 | 2277.5 | 2178 | | 1.758 | 1.677 | |
| 8At1 | 2130 | 2065 | | 1.669 | 1.611 | |
| 9At1 | 1994 | 1940 | 1880 | 1.597 | 1.539 | 1.520 |
| 10At1 | 1843 | 1820 | 1833 | 1.521 | 1.474 | 1.488 |
| 11At1 | 1810 | 1796.5 | | 1.506 | 1.458 | |
| 12At1 | 1756 | 1739 | | 1.465 | 1.433 | |
| 13At1 | 1726 | 1726 | 1685 | 1.445 | 1.420 | 1.414 |
| 15At1 | 1203 | 1156 | | 1.104 | 0.951 | |
| 22At1 | | 420 | | | 0.331 | |
| Base of log | 2732 | 2700 | 2650 | 1.953 | 1.927 | 1.939 |
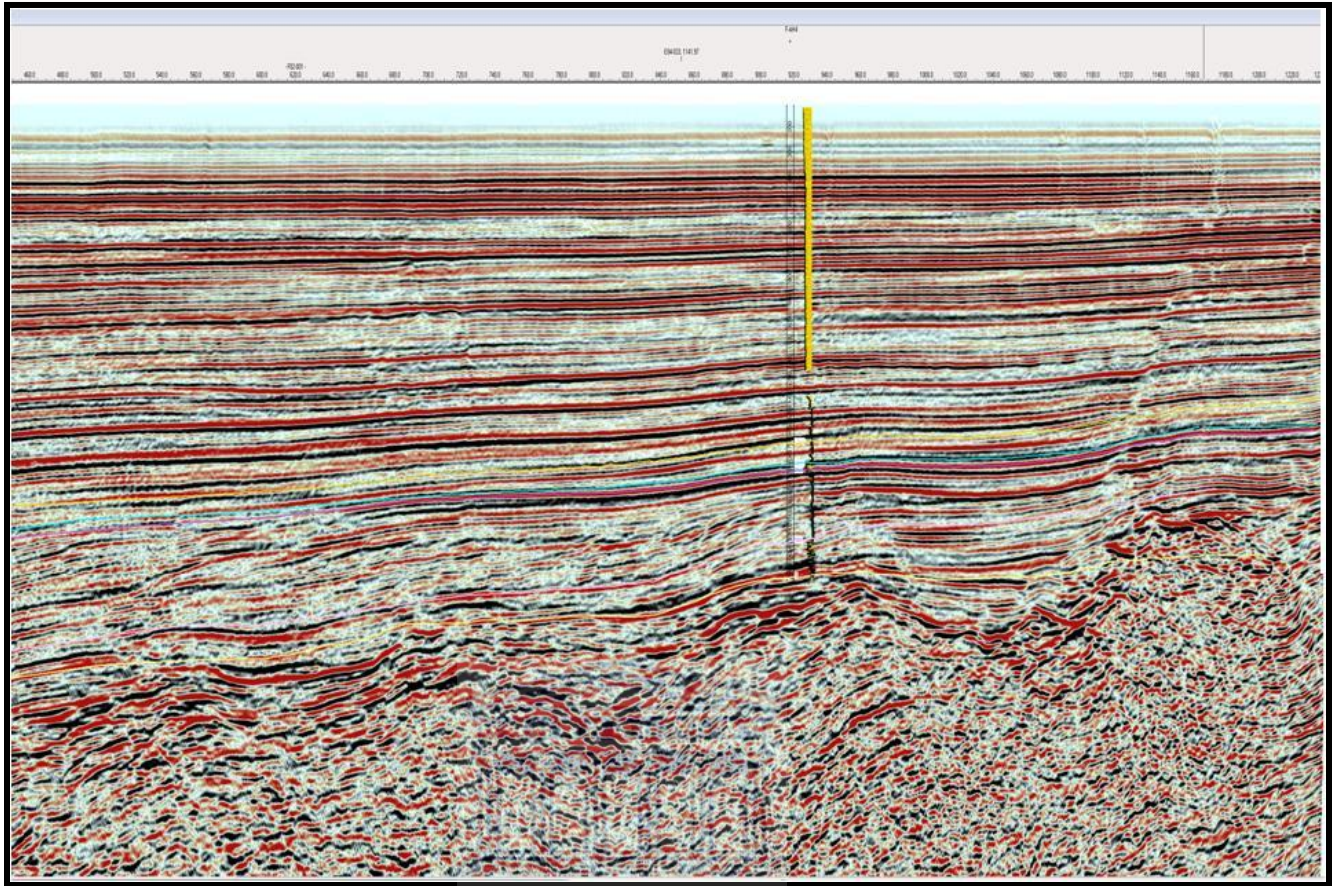
A. 4.1. Gamma ray log superimposed on seismic data.

**HORIZONS OF INTEREST MAPPED**

Horizons were created in a Kingdom Suite interpretation module called 2d- 3d Pak, where the horizon management dialog box was opened and a new horizon name was created (e.g. Horizon 1At1) and a colour was selected for the horizon of interest. Horizon picking followed, which was done manually by clicking the event that matches the base of the well tops which had to be interpreted. The event could be a trough or a peak. The base of the well tops was chosen to observe how events changes through time with the reservoirs of interest. Once the horizon has been mapped it will show on the base map (A.4.2). From the Kingdom main menu, the horizons picking toolbar was selected to change from one horizon interpretation to another.
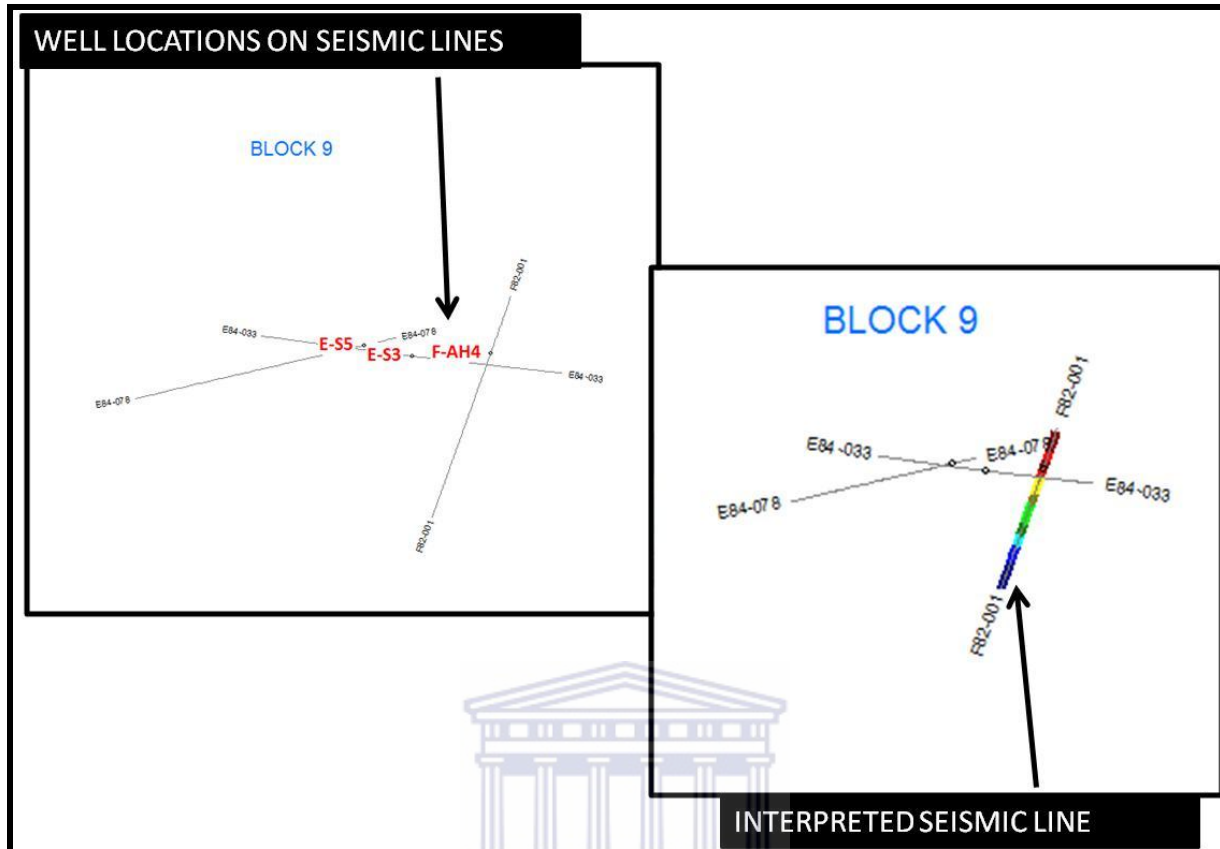
A. 4.2. Two dimensional seismic lines and Well positions in the Bredasdorp Basin.

## CORRELATING WELL LOG WITH SEISMIC FACIES

Due to a number of exploratory successes on the slope of the Gulf of Mexico by Shell Oil Company, it was soon realized that a particular reservoir pattern could be recognized on the seismic lines (Braide, 2012, personal communication). This pattern can be used to map and predict the distribution and quality of reservoir (and seal) packages, through the definition of a facies scheme based on seismic characteristics and geometries (seismic facies). Later this method was applied in oil fields outside the Gulf of Mexico. Seismic facies are identified largely based on the character and geometry of packages of seismic loops, e.g. amplitude, chaotic, parallel, base lapping to thinning. Local calibration is essential to make the seismic facies interpretation reliable (Prather et al. 1998).

**SEISMIC FACIES CONCEPT**

Seismic facies are defined based on a number of features such as:

-   Data Type: Seismic Facies of

    -   Acoustic Impedance Loop

    -   Single Loop

    -   Loopset

    -   Petrophysical Net/Gross

    -   SWC (Side Wall Core)

-   Slope Type: Graded Slope, Above Grade Ponded, Above Grade Stepped

-   Slope Classes: Mud Rich, Sand Rich, Mixed

-   Slope Position: Upper Slope, Middle Slope, Toe of Slope, Basin

-   Seismic Facies: Mounded, Convergent, Base lapping, Draping etc.

-   Petrophysical Net/Gross

All these parameters need to be classified and captured for a proper calibration. Only then we can expect to extract some meaningful statistical reservoir data from the seismic facies (Prather et al. 1998).

In this study, a sufficient number of the features above have been determined to give us some confidence in using seismic facies to interpret the geology in the study area, and make some inferences about the reservoir quality.

## APPENDIX 5: METHOD I: FACTOR ANALYSIS USED WITH DISCRIMINANT ANALYSIS

**Multivariate analysis:**

Excel data of the wireline logs were imported into the SPSS software. The data was first analyzed using factor analysis in order to create groups using the rotated matrix (A.5.1).
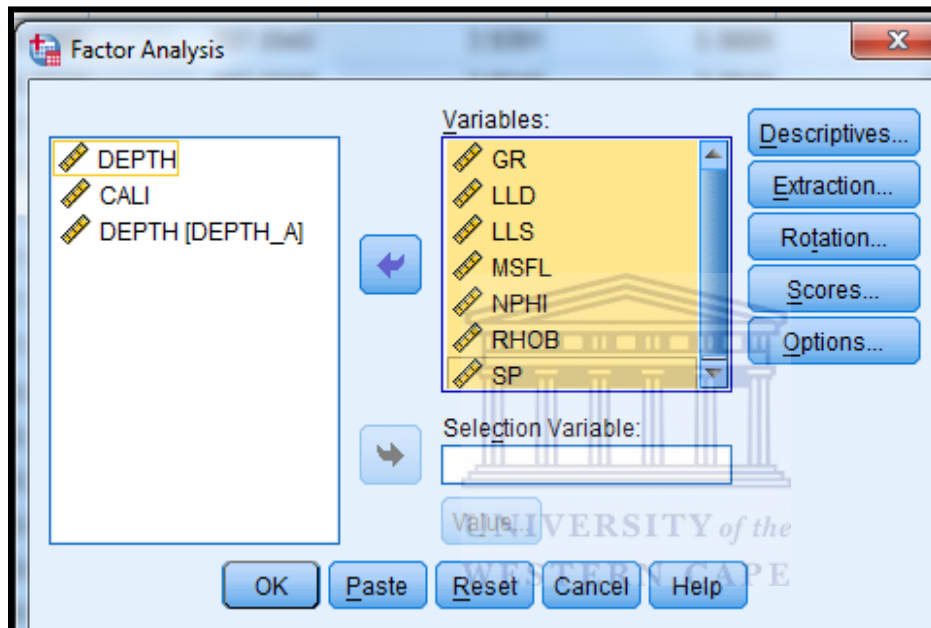


A. 6.1. Factor analysis dialog box

Once completed, two factors were saved based on the Eigen value greater than one. In the data view window a variable column was inserted to characterize the factors into two groups (1-oil and 2-non oil) which was identified from the rotated component matrix.

Discriminant analysis followed factor analysis by using the inserted variable column as the grouping variable and the wireline logs as the independents. The analysis was classified based on a summary table and combined groups (A. 5.2).
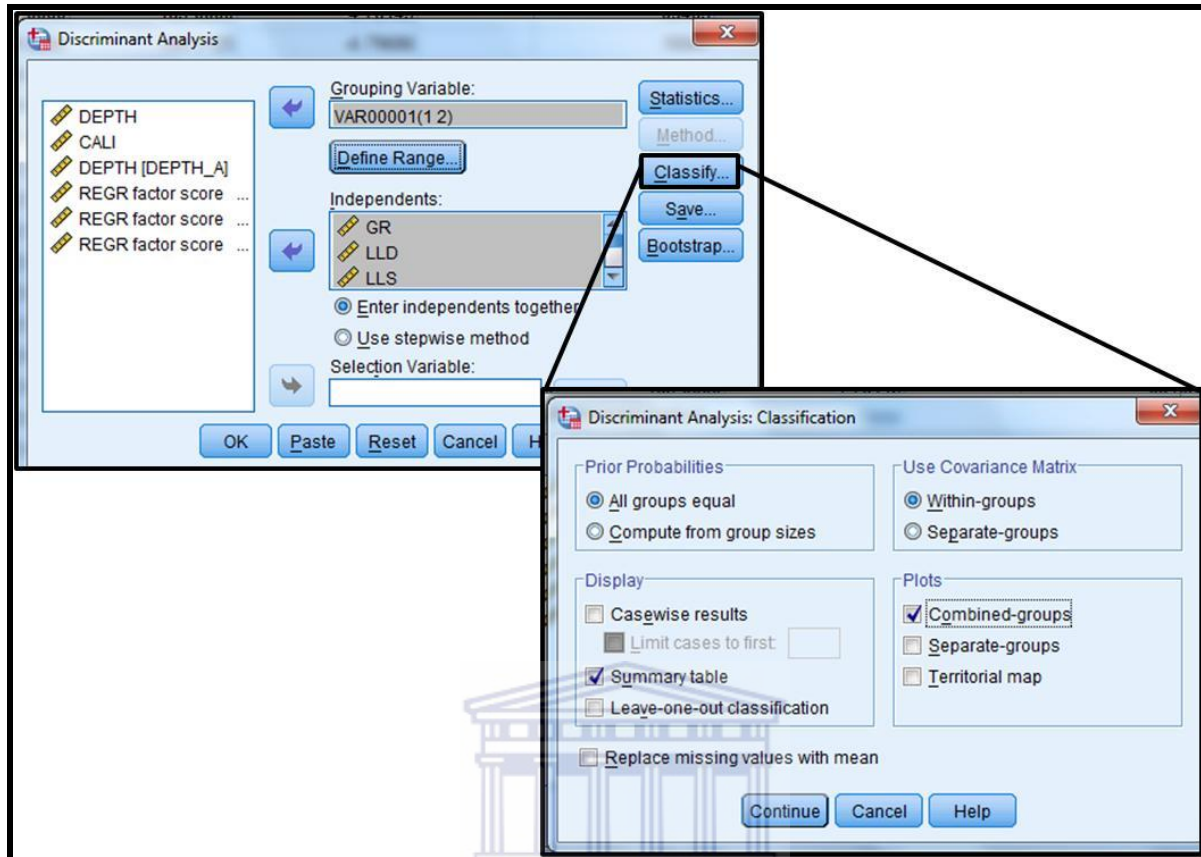
A. 5.2. Discriminant analysis classification dialogue box displaying summary table and combined groups.

Discriminant was used to predict an outcome, to distinguish the number of depths in each group either oil bearing or no oil bearing. The discriminant variables were saved to predict the unknown depths as a predicted group membership. Discriminant analysis was run again using the predicted group as the grouping variable to have 100% of the original grouped cases correctly classified with no ungrouped cases.

# APPENDIX 6: METHOD II: CLUSTER TOGETHER WITH DISCRIMINANT ANALYSIS

Cluster analysis creates groups if training samples are not available, which was done in this case by classifying it under hierarchical cluster analysis. Variables (wireline data in excel format) were then selected by using the Ward's Method and normalizing the data by Z scores (A.6.1). Dendrogram was selected as an output to identify the number of groups.
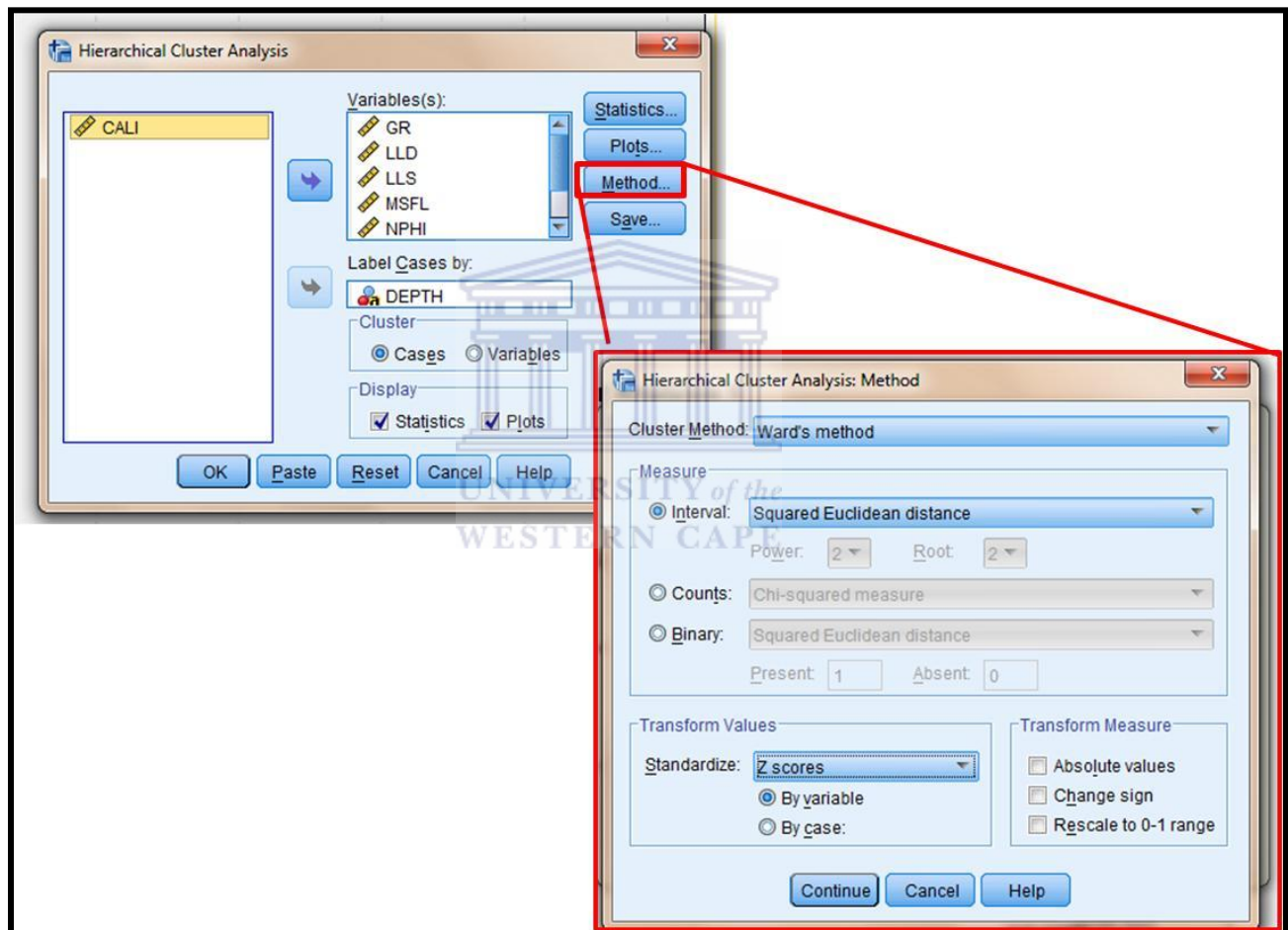


A. 6.1. Hierarchical cluster analysis using Ward's method and Z scores.

## Discriminant analysis

The groups that were saved in cluster analysis were used in discriminant analysis based on the Ward's Method. A range was defined by having a minimum of one and a maximum of five depending on the number of groups. The initial variables were chosen as the independents. The variables were then classified according to a summary table of the combined groups. Once the analysis was completed the results were displayed statistically in the form of structure matrix, functions at group centroids and classification tables.
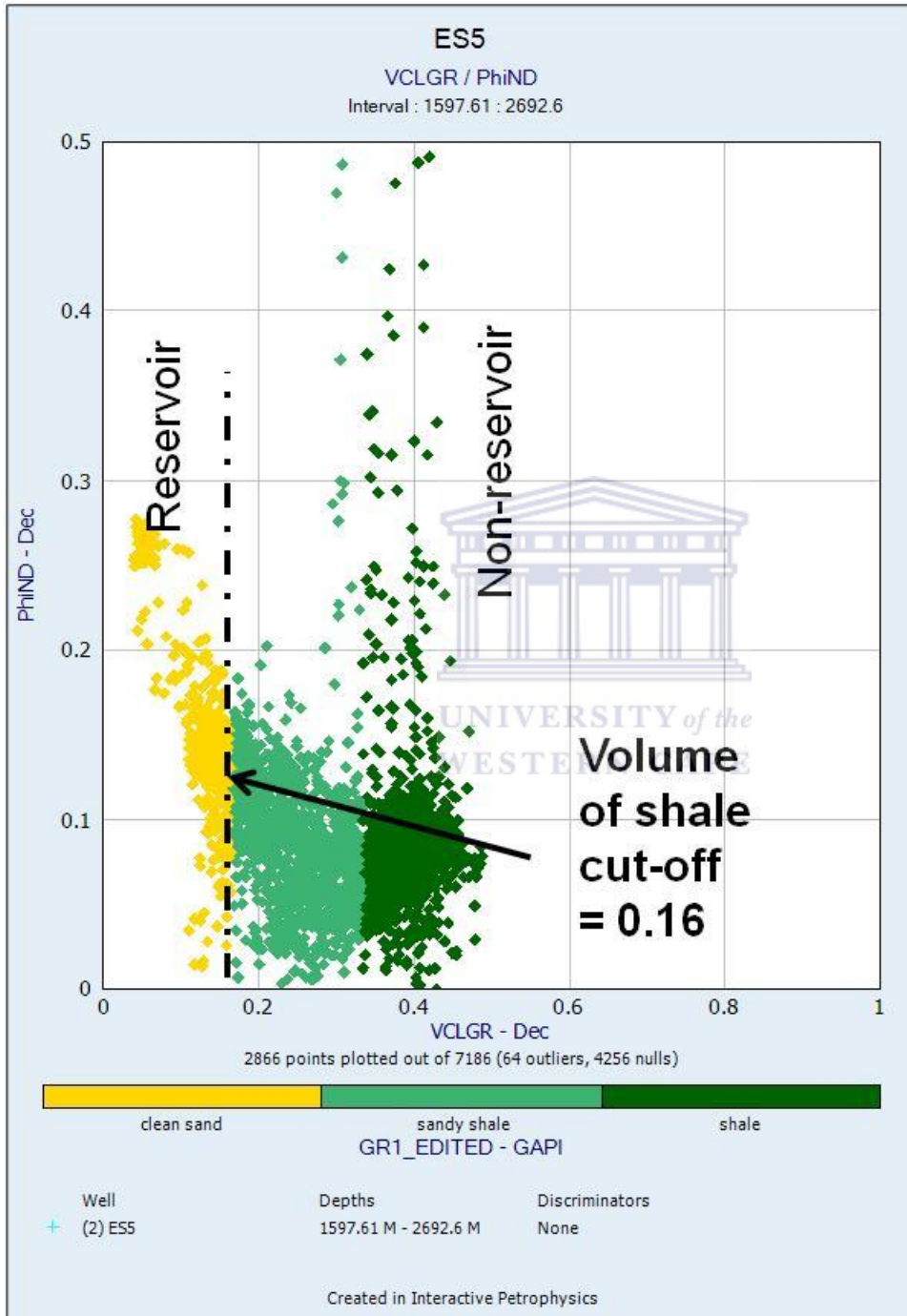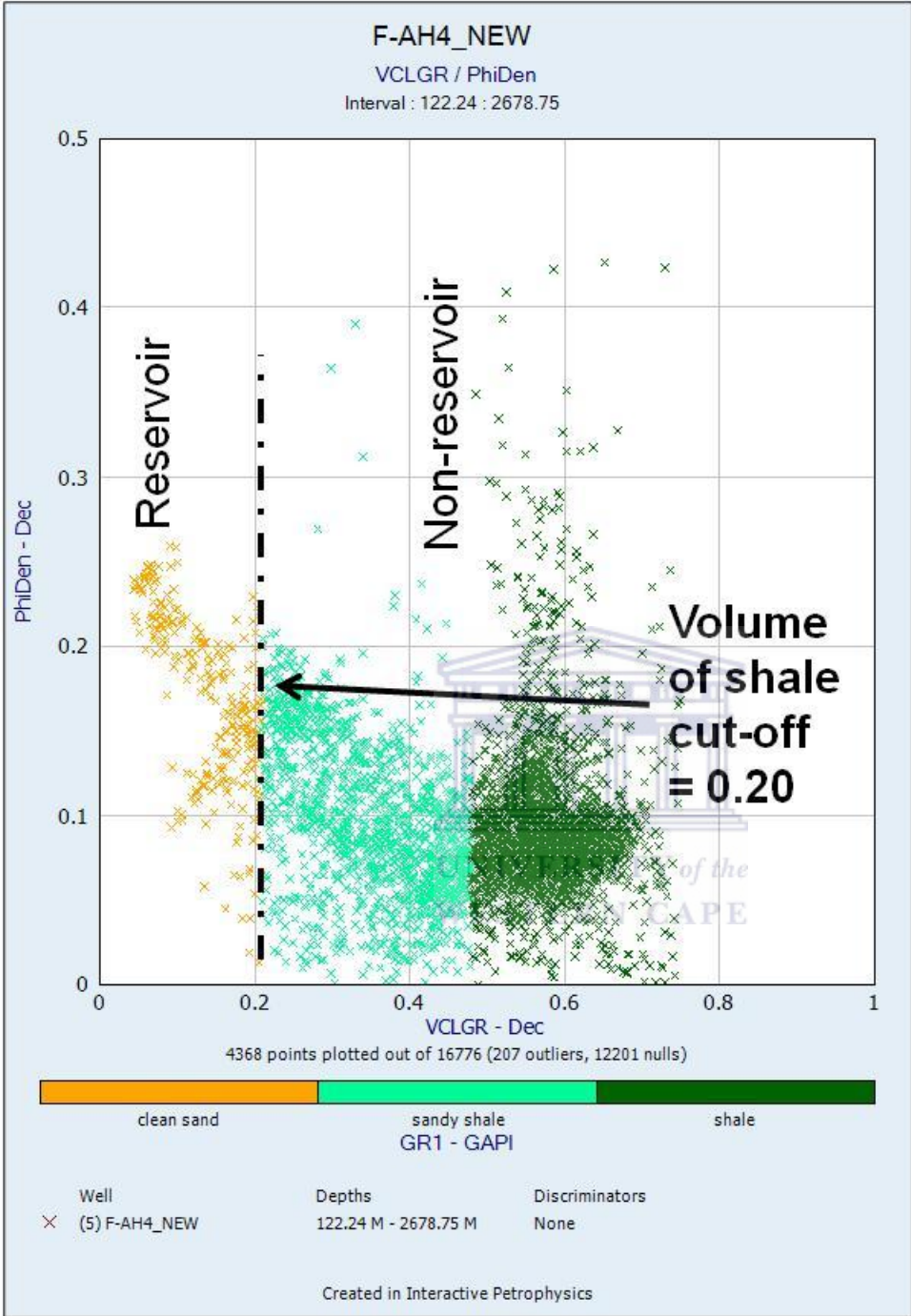
F-AH4_NEW

CORE POROSITY / CORE PERMEABIL
Interval : 122.24 : 2678.75

$Y=f(x): Log(CORE\ PERMEABIL) = -1.41973 + 23.2128 * CORE\ POROSITY\quad R2= 0.54$

27 points plotted out of 16776

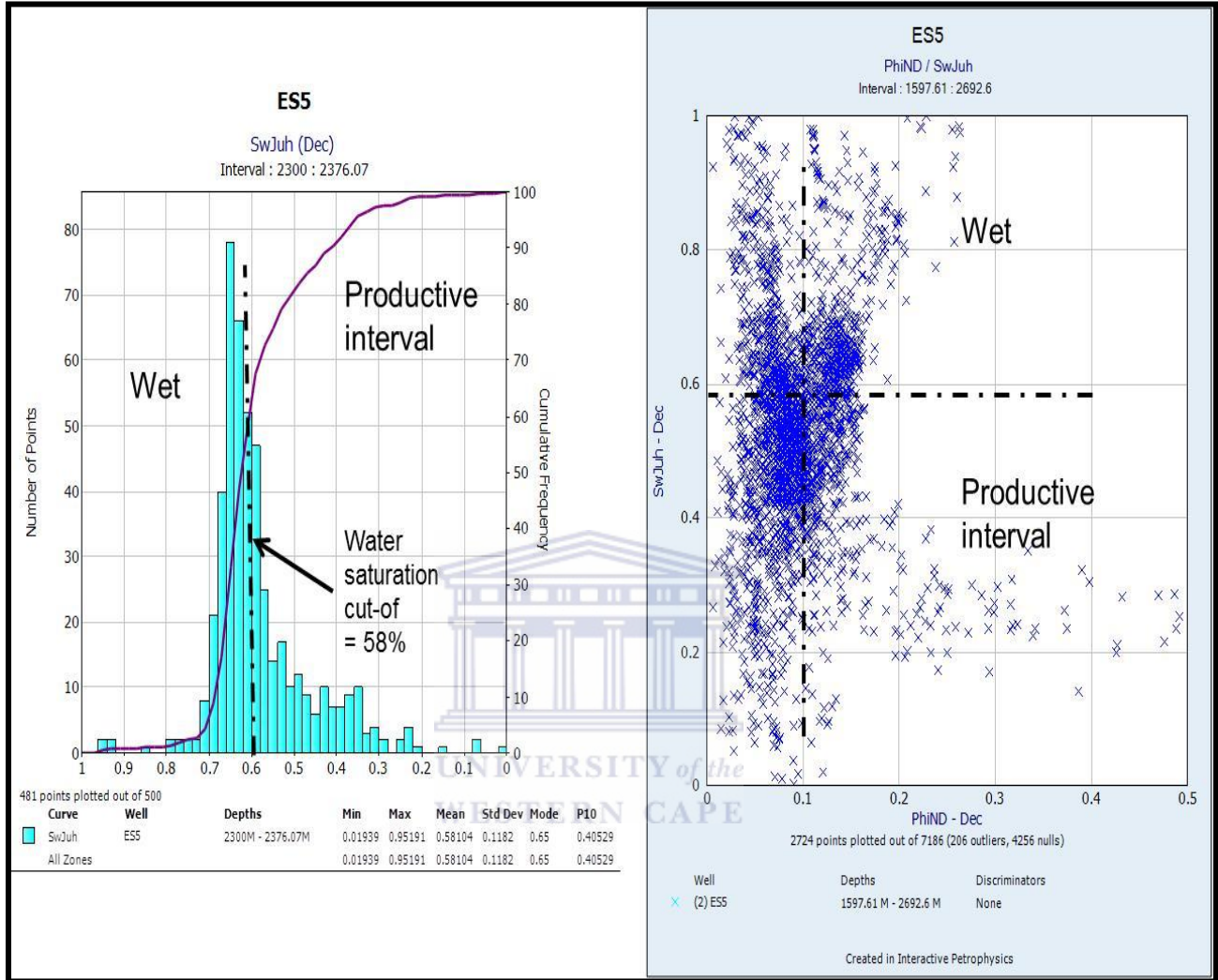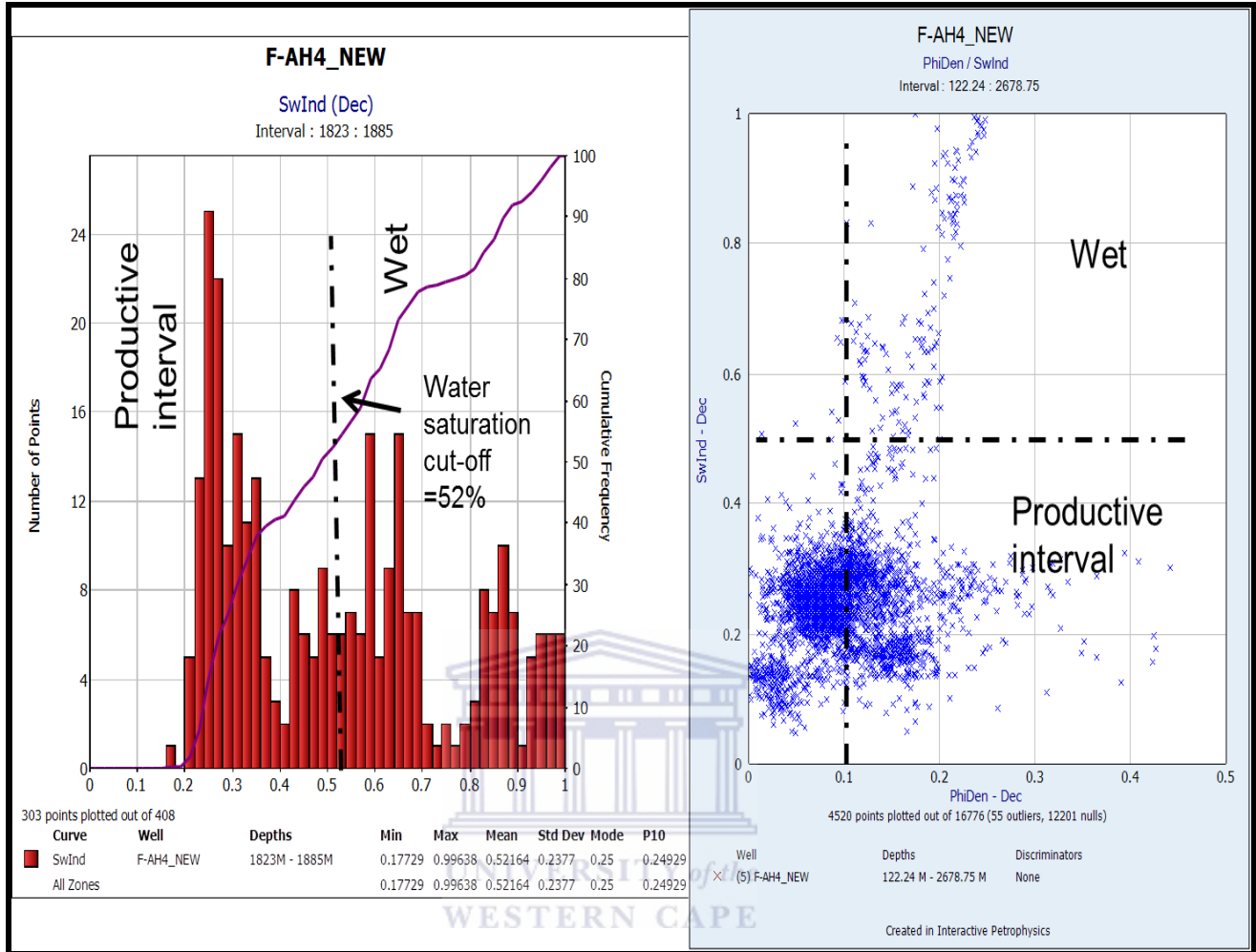| Well | Depths |
|---|---|
| (5) F-AH4_NEW | 122.24 M - 2678.75 M |
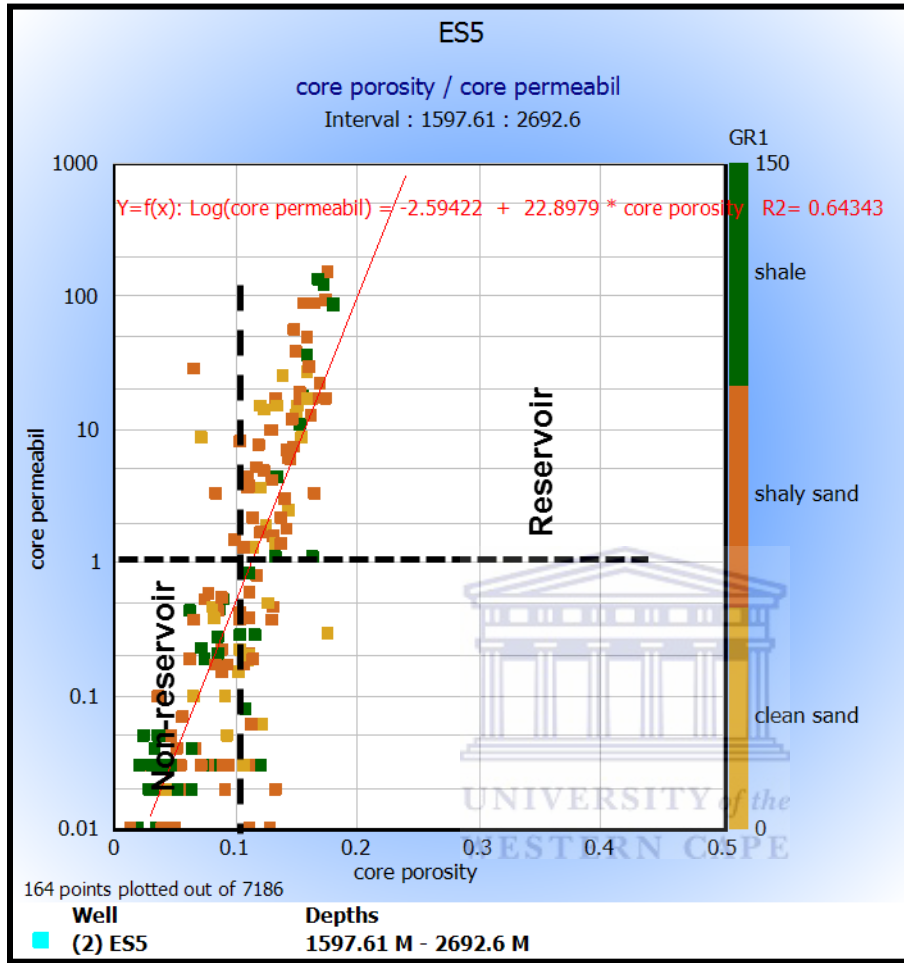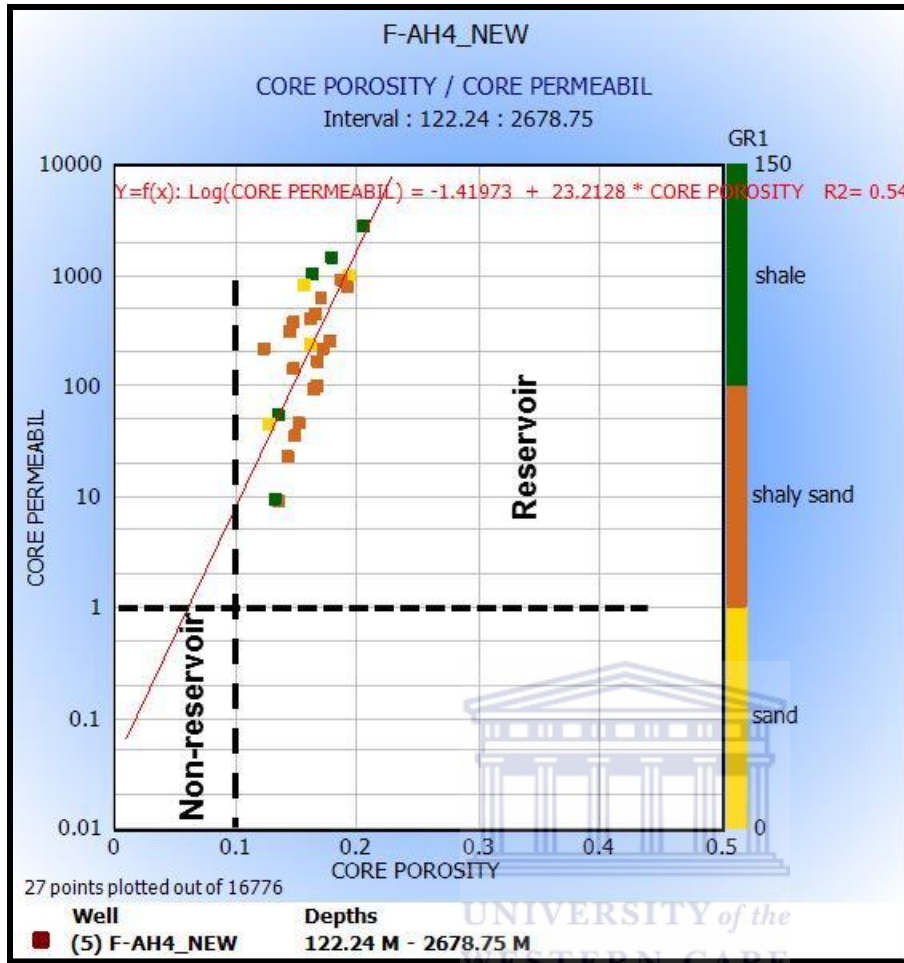
## APPENDIX 8: SCATTER PLOT OF VOLUME OF SHALE VS. POROSITY AND GAMMA RAY

# APPENDIX 9: HISTOGRAM AND SCATTER PLOT OF WATER SATURATION CUT-OFFS

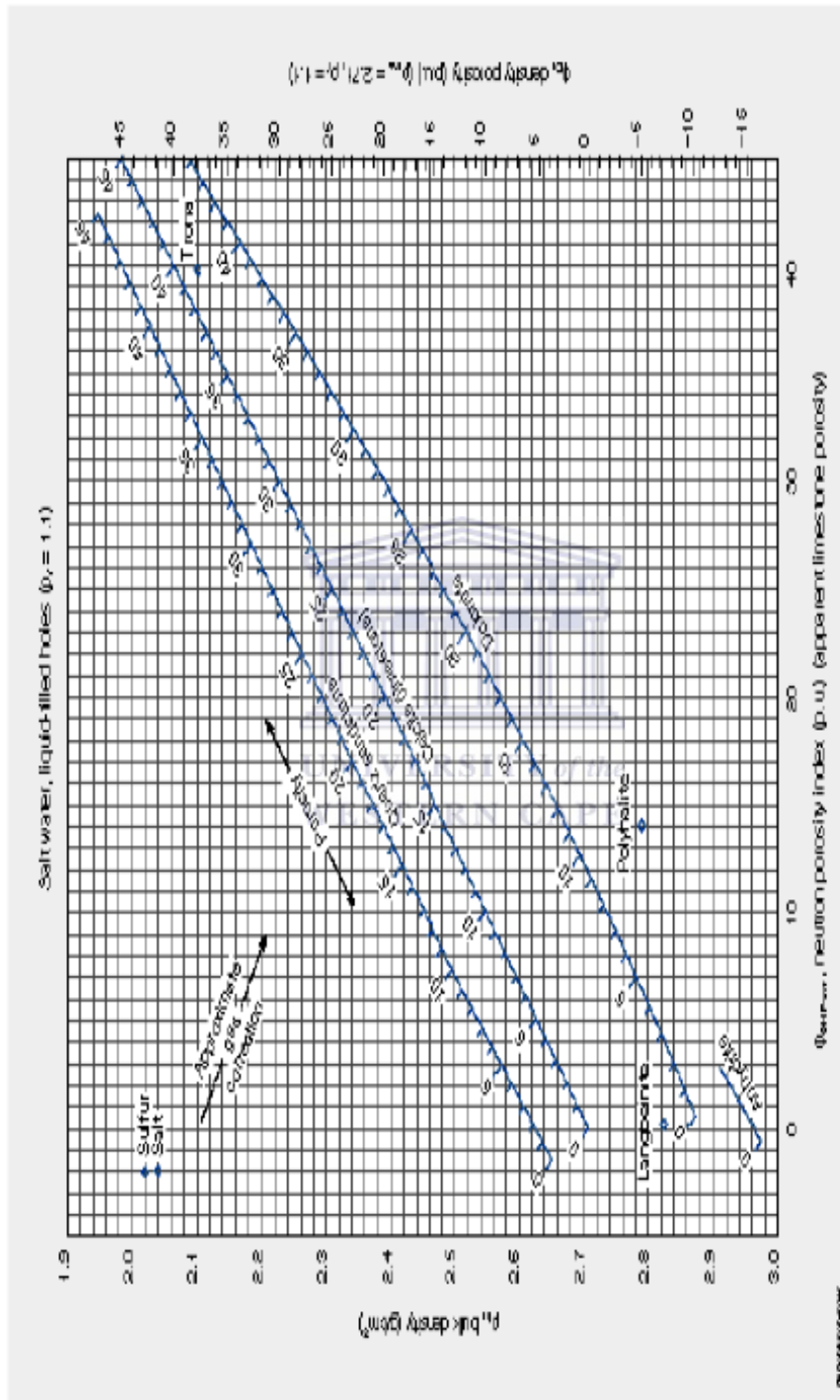## APPENDIX 10: DENSITY LOG AND NEUTRON LOG



Crossplots for Porosity, Lithology and Saturation

Porosity and Lithology Determination from Formation Density Log and SNP Sidewall Neutron Porosity Log